

Thiago Andrade Patente

Vias de Regulação Metabólicas em Células Dendríticas com Viés Tolerogênico

Tese apresentada ao Programa de
Pós-Graduação em Imunologia do
Instituto de Ciências Biomédicas da
Universidade de São Paulo para obtenção
do título de doutor em Ciências

SÃO PAULO
2020

Thiago Andrade Patente

Vias de Regulação Metabólicas em Células Dendríticas com Viés Tolerogênico

Tese apresentada ao Programa de Pós-Graduação em Imunologia do Instituto de Ciências Biomédicas da Universidade de São Paulo para obtenção do título de doutor em Ciências.

Área de Concentração: Imunologia

Orientador: José Alexandre Marzagão
Barbuto

Co-orientadora: Maria Lúcia Cardillo
Correa-Giannela

SÃO PAULO
2020

CATALOGAÇÃO NA PUBLICAÇÃO (CIP)
Serviço de Biblioteca e informação Biomédica
do Instituto de Ciências Biomédicas da Universidade de São Paulo

Ficha Catalográfica elaborada pelo(a) autor(a)

Patente, Thiago Andrade
Vias de Regulação Metabólicas em Células
Dendríticas com Viés Tolerogênico / Thiago Andrade
Patente; orientador Prof. Dr. José Alexandre
Marzagão Barbuto; coorientadora Prfa.Dra. Maria
Lucia Cardillo Corrêa Giannella. -- São Paulo, 2019.
181 p.

Tese (Doutorado) -- Universidade de São Paulo,
Instituto de Ciências Biomédicas.

1. Células Dendríticas. 2. Imunometabolismo. 3.
Diabetes Tipo 1. 4. AMPK. 5. Tolerância. I. Marzagão
Barbuto, Prof. Dr. José Alexandre, orientador. II.
Cardillo Corrêa Giannella, Prfa.Dra. Maria Lucia,
coorientador. III. Título.

UNIVERSIDADE DE SÃO PAULO
INSTITUTO DE CIÊNCIAS BIOMÉDICAS

Candidato (a): Thiago Andrade Patente

Título da Tese: Vias de Regulação Metabólicas em Células Dendríticas com Viés Tolerogênico

Orientador (a): Prof^o. Dr. José Alexandre Marzagão Barbuto

A Comissão Julgadora dos trabalhos de Defesa da Dissertação de Mestrado/Tese de Doutorado, em sessão pública realizada a/...../....., considerou o(a) candidato(a):

() **Aprovado(a)** () **Reprovado(a)**

Examinador(a): Assinatura:
Nome:
Instituição:

Examinador(a): Assinatura:
Nome:
Instituição:

Examinador(a): Assinatura:
Nome:
Instituição:

Presidente: Assinatura:
Nome:
Instituição:



UNIVERSIDADE DE SÃO PAULO
INSTITUTO DE CIÊNCIAS BIOMÉDICAS

Cidade Universitária "Armando de Salles Oliveira"
Av. Prof. Lineu Prestes, 2415 - cep. 05508-000 São Paulo, SP - Brasil
Telefone : (55) (11) 3091.7733 telefax : (55) (11) 3091-8405
e-mail: cep@icb.usp.br

São Paulo, 06 de março de 2015.

PARECER 1222/CEPSH

A Comissão de *Ética em Pesquisas em Seres Humanos* do ICB, nesta data, **APROVOU** o projeto intitulado: "*Efeito da glicose e da albumina glicada sobre células dendríticas derivadas de monócitos (mo-DCs) de doadores saudáveis e de pacientes portadores de diabetes mellitus tipo 1*" do pesquisador **José Alexandre Marzagão Barbuto** e aluno **Thiago Andrade Patente**.

Cabe aos pesquisadores elaborar e apresentar a este Comitê, relatórios anuais (parciais e final), de acordo com a Resolução nº 466/12, item II, II.19 e II.20, do Conselho Nacional de Saúde, conforme modelo constante no site: icb.usp.br.

Aos pesquisadores cabê também finalizar o processo junto à Plataforma Brasil quando do encerramento deste.

O primeiro relatório deverá ser encaminhado à Secretaria deste CEP em **23.01.2016**.

Atenciosamente,

Prof. Dr. PAOLO M.A. ZANOTTO
Coordenador da Comissão de Ética em
Pesquisas com Seres Humanos - ICB/USP

PARECER CONSUBSTANCIADO DO CEP

DADOS DO PROJETO DE PESQUISA

Título da Pesquisa: Efeito da glicose e da albumina glicada sobre células dendríticas derivadas de monócitos (mo-DCs) de doadores saudáveis e de pacientes portadores de diabetes mellitus tipo 1

Pesquisador: José Alexandre Marzagão Barbuto

Área Temática:

Versão: 2

CAAE: 41905015.0.0000.5467

Instituição Proponente: Universidade de São Paulo

Patrocinador Principal: FUNDACAO DE AMPARO A PESQUISA DO ESTADO DE SAO PAULO

DADOS DO PARECER

Número do Parecer: 975.982

Data da Relatoria: 09/03/2015

Apresentação do Projeto:

Título da Pesquisa: Efeito da glicose e da albumina glicada sobre células dendríticas derivadas de monócitos (mo-DCs) de doadores saudáveis e de pacientes portadores de diabetes mellitus tipo 1

Pesquisador: José Alexandre Marzagão Barbuto

Instituição Proponente: Universidade de São Paulo

Objetivo da Pesquisa:

Atendimento a pendências

Avaliação dos Riscos e Benefícios:

Sem alteração necessária

Comentários e Considerações sobre a Pesquisa:

O projeto, após análise, foi encaminhado com pendências sobre a caracterização da população de doadores bem como solicitação de substituição, no TCLE, de termos técnicos por termos de fácil entendimento por parte de leigos.

Os Pesquisadores atenderam de forma adequada a todas pendências

Considerações sobre os Termos de apresentação obrigatória:

Foi readequado.

Endereço: Av. Prof Lineu Prestes, 2415

Bairro: Cidade Universitária

CEP: 05.508-000

UF: SP

Município: SAO PAULO

Telefone: (11)3091-7733

Fax: (11)3091-8405

E-mail: cep@icb.usp.br

INSTITUTO DE CIÊNCIAS
BIOMÉDICAS DA
UNIVERSIDADE DE SÃO



Continuação do Parecer: 975.982

Recomendações:

Sem recomendações

Conclusões ou Pendências e Lista de Inadequações:

Sem pendências

Situação do Parecer:

Aprovado

Necessita Apreciação da CONEP:

Não

Considerações Finais a critério do CEP:

Cabe ao pesquisador elaborar e apresentar a este Comitê, relatórios anuais (parciais e final), de acordo com a Resolução nº 466/12, item II, II.19 e II.20, do Conselho Nacional de Saúde.

Em não havendo um biorrepositório e se houver retenção de material deverá ser solicitado o devido cadastro conforme modelo constante site do ICB.

Ao pesquisador cabe também finalizar o processo junto à Plataforma Brasil quando do encerramento deste.

SAO PAULO, 06 de Março de 2015

Assinado por:
Regina Scivoletto
(Coordenador)

Endereço: Av. Profº Lineu Prestes, 2415
Bairro: Cidade Universitária **CEP:** 05.508-000
UF: SP **Município:** SAO PAULO
Telefone: (11)3091-7733 **Fax:** (11)3091-8405 **E-mail:** cep@icb.usp.br

This project was developed at the Laboratory of Tumor Immunology at the Immunology Department of Immunology from the Biomedical Sciences Institute from the University of São Paulo in São Paulo, SP, Brazil, and received financial support from São Paulo Research Foundation (FAPESP) and Coordination of Superior Level Staff Improvement (CAPES).

Part of this project was developed at the Parasitology Department at the Leiden University Medical Center, Leiden The Netherlands, with financial support from São Paulo Research Foundation (FAPESP).

Dedico este trabalho aos meus pais, Clayton e Sônia, meu irmão, Lucas por todo o apoio, carinho e compreensão;

À minha companheira de vida Tamires, por sempre ter me incentivado e me acompanhado em todas as etapas.

AGRADECIMENTOS/AKNOWLEDGMENTS

Aos meus pais, Clayton e Sônia, pelo apoio incondicional durante, não apenas estes anos de doutorado, mas todo o meu processo de formação profissional desde a graduação. Muito obrigado, pelo amor, carinho, compreensão e tenham certeza que sem a ajuda de vocês nada disto teria sido possível.

Ao meu irmão Lucas pelos momentos divididos ao longo das nossas vidas. Muito obrigado por confiar em mim; sei que posso contar com você para tudo que eu precisar.

À minha companheira de vida Tamires, não há palavras que possam descrever meu agradecimento, meu amor e minha admiração. Agradeço por você sempre ter estado ao meu lado, por você sempre ter me ajudado, seja com palavras de apoio ou com broncas para que eu voltasse à realidade e, principalmente, agradeço por ter me acompanhado durante o ano em que ficamos fora do país. Você certamente fez esta jornada se tornar muito fácil. Obrigado e te amo.

Ao meu orientador José Alezandre Marzagão Barbuto por, primeiramente, ter me aceitado no laboratório. Sou eternamente grato por você sempre incentivar a busca por conhecimento, por sempre encarar a pesquisa com bom humor e por nunca nos desestimular, muito pelo contrário, quando um resultado não dá o que esperamos, o senhor sempre nos faz olhar o lado positivo do experimento. Sempre fazendo com que nossas pesquisas sejam “divertidas” e “quentes”. Meu muito obrigado. O senhor será sempre uma inspiração de como ser um formador de alunos.

À minha co-orientadora Maria Lúcia Cardillo Corrêa-Giannella por toda a ajuda desde o meu tempo de iniciação científica. Muito obrigado pela ajuda com a obtenção das amostras de pacientes pelos conselhos e conversas, que sempre foram muito além da ciência e, principalmente, pela preocupação com minha formação. Meu muito obrigado, serei eternamente grato.

À Patty por sempre estar ao meu lado dentro do laboratório e cuja preocupação sempre foi muito além das questões laboratoriais. Sempre foi uma preocupação de mãe, com muito carinho e sempre disposta a ajudar no que fosse preciso. Muito obrigado, de coração.

À Aline por ter sido a companheira de laboratório durante boa parte do meu doutorado, dividindo as frustrações e alegrias diárias. Muito obrigado e pode ter certeza que a rotina de experimentos foi muito mais fácil com a sua ajuda.

Aos “monstros” do meu coração Aline, Felipe, Raíssa e Rafael. Vocês estão e estarão para sempre comigo, amigos verdadeiros que a pós me deu e que dividiram viagens, churrascos e diversões e que tenho certeza estarão comigo sempre. O que a pós uniu, ninguém desune!

Aos companheiros do Laboratório de Imunologia de Tumores, especialmente Mariana, Sarah, Aline, Rodrigo, Karen, Cecília, Bella, Ana, Bruna, Roberto, Cris (*in memoriam*), Gabi, Beth, Nádia e Célia. Muito obrigado pela companhia e distrações diárias.

Ao João e, principalmente, à Eni por me aturarem nas minhas constantes idas à secretaria sempre me recebendo de braços abertos, seja para ouvir meus problemas ou para resolver todas as minhas dúvidas. Muito obrigado por tudo.

Ao Prof. Niels Olsen Saraiva Câmara e aos membros do seu laboratório, em especial a Meire, Paulo, Thiago, Ângela, Cris, Amanda e Fernanda pela ajuda nos experimentos de Seahorse e western blot.

Aos amigos especiais que fiz no departamento de Imunologia que sempre acompanharam no bom e velho “Ceará” ou Franboi: Aline, Felipe, Raíssa, Rafael, Maria, Nath, Jean, Carolzinha, Nágela, Lilian, Marília, Bruno (praticamente do ICB), Anna Cláudia, Anna Djay, João (Xu), Flávia, Gabi, Cainho, Elaine (Ploc), Thethe e Raposo (quase ICB também).

A todos do departamento que, em algum momento, me ajudaram ou estiveram presente para um café, uma conversa, especialmente, Paulo, Thiago, Tais, Letícia, Nátalli, Cris Naffah, Caio, Ildefonso, Franciane, Zé, Rogério, Áurea, Cidinha.

A todos os professores do departamento, em especial ao Prof^o Jean Pierre, Prof^o Niels Olsen, Prof^a Bruna Alencar, Prof^o Gustavo, Prof^o Lepique, Prof^o Alexandre Steiner e Prof^o Anderson pelas discussões científicas em congressos, corredores, festas ou churrascos e auxílio como supervisores PAE.

Ao grupo da sala de complicações da FMUSP: Gustavo, Tadashi, Sharon, Tati e Adriana, muito obrigado por me ajudarem na coleta das amostras dos pacientes e por me

permitirem acompanhar a rotina clínica com vocês! Podem ter certeza que foi muito enriquecedor para o meu conhecimento.

Às enfermeiras e auxiliares de enfermagem do ambulatório de Endocrinologia da FMUSP que sempre me ajudaram na coleta das amostras dos pacientes.

Aos eternos “Malunos” Bia, Dani, Gustavo, Sharon, Tati, Perez, Karine pelas discussões e momentos de descontração.

À Dr^a Marisa Passareli por ceder as amostras de albumina e albumina glicada para parte dos experimentos.

Aos amigos de colégio e faculdade, em especial Pri, Fe, Rah, Vitoka, Luan, Aka, Daniel, Daniela, Camila, Zizi, Amandinha, Libs, Murilo, Ju, Marininha, Jhonny, Bibi, Bahia, Paloma por todos os momentos de descontração fora do meu ambiente de trabalho.

À CAPESP pelo apoio financeiro.

À Fundação de Amparo a Pesquisa do Estado de São Paulo (FAPESP) pelo apoio financeiro por meio da bolsa de doutorado (processo FAPESP nº 2014/26437-9) e da bolsa BEPE (processo FAPESP nº 2018/00719-9).

À todos que direta ou indiretamente estiveram presente durante esta etapa da minha vida, meu muito obrigado.

To my supervisor at the Leiden University Medical Center (LUMC), Dr. Bart Everts, for receiving me as student in his laboratory and helping me with experiments, presentations, discussions and giving me the opportunity to work in a field that I'm really passionate about.

To Anna, Dominik, Olek and John, the most amazing family I could ever met in The Netherlands. Thank you all for making our lives at The Netherlands so much easy! I really don't know how to thank you enough for everything. For receiving us in your house in Poland during Christmas and New Year, for planning an amazing trip through Poland, for receiving us in your Dutch house so many times for drinks, poker, board games or just to watch the volleyball finals Brazil x Poland! Anna, thank, in special, for making my lab life easier, helping me with ELISA, sections, isolation of PBMC, discussions, coffe. Really, I have no words to thank you enough!

To Leonard who received me before I even start my internship, showed me the lab and the LUMC during a Saturday in which he was still making his presentation for a

conference. Thank you for the endless experiments, for the helping with mice procedures, which I had no idea how to perform, for the analysis and Flow Jo discussions, for the “borrels” and, off course, parties outside the lab. You are an inspiration!

To Eline, who was always with a smile in her face and available to help in the experiments. Thank you for the conversations, the experiments, the distractions, the sailing time, the cake (which was pretty good), my birthday present, which was the most amazing thing, and everything!

To Miriam and Erik for the conversations, the coffees and the good times we had outside the lab! You guys were really nice to us and helped us a lot!

To Tom for all the talks, the laughs (which were not few), the drinks, the days outside the lab, the board night, the dinner at Amsterdam! Thank you a lot man!

To Frank, Alwin, Arifa, Lonneke, Ruthger and Patrick for the help in all the experiments, without you guys I would not have had not even half of the results I obtained. Thank you very much!

To Joost for the help in qPCR experiments and for endless discussions about NFL. I wouldn't imagine I would find someone to discuss NFL with during my internship! Thanks for everything man!

To everyone who participate in my life during this year in such a positive way that I have no words to thank you enough: Paula, Marije, Astrid, Roos, Nikolas, Patrick, Mark, Alice Catherin, each one of you were important to me during this year and I will always have you guys with me.

To everyone from Aquarium, Catherin, Anna, Miriam, Chiara, Frank, Carola, Shinya, Beckley and Munisha, thank you for the conversations and Christmas' game!

To Bruno for all the discussion during the “borrels” and also outside the lab.

To all the professors from the Parasitology department, especially Hermelijn, Ron and Bruno for the suggestions during my presentations.

To Dr. Maria Yazdanbakhsh for accepting me in the department of Parasitology, for the scientific discussion during the meetings and for the help when I needed.

To everyone at the Parasitology Department at LUMC who I might have forgotten, thank you for everything,

*“O fracasso e o sucesso são impostores.
Ninguém fracassa tanto quanto imagina.
Ninguém tem tanto sucesso como imagina.”*

Rudyard Kipling

ABSTRACT

PATENTE, TA. **Metabolic Regulatory Pathways in Tolerogenic Bias Dendritic Cells.** 2019. 181 f. Ph.D. Thesis (Immunology Department) – Instituto de Ciências Biomédicas, Universidade de São Paulo, São Paulo, 2019.

Type 1 diabetes mellitus (T1D) is an autoimmune disease in which dendritic cells (DC) play a relevant role. DC are antigen presenting cells, central to CD4⁺ T cell differentiation, including regulatory T cells (Tregs). When the environment provides tolerogenic signals, DC fail to induce T lymphocyte proliferation and are prone to induce tolerance. Different stimuli, such as retinoic acid (RA), dexamethasone (Dex) and vitamin D3 (VitD3), are capable of generating tolerogenic DC (tolDC). Immunogenic DC and tolDC differ in expression of costimulatory molecules, proinflammatory cytokine secretion, ability to generate suppressive T lymphocytes and metabolic profile. While immunogenic DC rely on glycolysis and anabolic metabolism to support their activity, the metabolic pathways involved in the induction of Treg by tolDC are less well defined. AMPK is a metabolic sensor known to antagonize anabolic signals, promoting catabolism and studies suggest that tolDC are characterized by a catabolic profile. However, the role of AMPK signaling in regulating tolDC metabolism and function has not been addressed. Moreover, the presence of VitD3 during mo-DC differentiation induces an initial glucose-dependent metabolic reprogramming. Thus, the present study had two main objectives: (1) as hyperglycemia is the main characteristic of T1D, we aimed to evaluate how glucose availability would impact the differentiation of mo-DC treated with VitD3 (VitD DC); (2) to investigate how and if AMPK could control the differentiation of tolDC induced by VitD3, RA and Dex. Metabolically, VitD3 differently modulates controls mo-DC and patients, inducing tolDC in patients in a glucose-independent manner. In controls, VitD3 induced increase in glycolysis and OXPHOS, which were, at least partially, reduced in hyperglycemia, as well as CD86 expression, TNF- α secretion and lymphostimulatory capacity. In diabetic patients, while VitD3 reduced both CD86 expression and TNF- α secretion in hyperglycemia, cell metabolism was not affected, suggesting that VitD3-induced metabolic reprogramming may not rely on glycolysis in patients. In the second part of the project, we confirmed that VitD3, Dex and RA induced functional tolDCs, since these tolDC induced suppressor CD4⁺ T cells. Metabolically, however, each tolDC exhibited a distinct phenotype: VitD-DC had increased glycolysis and OXPHOS, RA-DC had reduced spare respiratory capacity and Dex-DC had reduced glycolysis. ACC phosphorylation, a direct downstream target of AMPK, was increased in VitD-DC and

RA-DC, suggesting increased AMPK activity. Consistently, AMPK silencing reverted the metabolic changes induced by VitD3 and RA, but not by Dex. When AMPK was silenced in human RA-DC, both ALDH activity (that was increased by RA treatment) and their tolerogenic capacity were lost. Mice with a deficiency in AMPK selectively in DC showed a reduction in ALDH activity and frequency of gut CD103⁺CD11b⁺ DC, considered to be the *in vivo* equivalent of RA-DC. This suggests that AMPK signaling is important for homeostasis of tolerogenic DC in the gut by promoting an anti-inflammatory status via regulation of ALDH activity specifically in CD103⁺CD11b⁺ DC. Taken together, these data point towards a key role for AMPK in regulating both the metabolic and tolerogenic properties of RA-DC and the homeostasis of the gut.

Keywords: Dendritic Cells. Immunometabolism. Type 1 Diabetes. AMPK. Tolerance.

RESUMO

PATENTE, TA. **Vias de Regulação Metabólicas em Células Dendríticas com Viés Tolerogênico**. 2019. 181 f. Tese (Doutorado em Imunologia) – Instituto de Ciências Biomédicas, Universidade de São Paulo, São Paulo, 2019.

O diabetes mellitus tipo 1 (DM1) é uma doença autoimune na qual células dendríticas (DC) desempenham um papel relevante. DC são células apresentadoras de antígenos, centrais para a diferenciação de células T CD4⁺, incluindo células T reguladoras (Tregs). Quando o ambiente fornece sinais tolerogênicos, DC falham em induzir a proliferação de linfócitos T tendendo a induzir tolerância. Diferentes estímulos, como ácido retinóico (RA), dexametasona (Dex) e vitamina D3 (VitD3), são capazes de gerar DC tolerogênicas (tolDC). DC imunogênicas e tolDC diferem em expressão de moléculas co-estimulatórias, secreção de citocinas pró-inflamatórias, capacidade de gerar linfócitos T supressivos e perfil metabólico. Enquanto DC imunogênicas dependem da glicólise e de metabolismo anabólico, as vias metabólicas envolvidas na indução de Treg pelas tolDC são menos detalhadas. AMPK é um sensor metabólico conhecido por antagonizar sinais anabólicos, promovendo catabolismo e estudos sugerem que tolDC sejam caracterizadas por um perfil catabólico. Entretanto, o papel da sinalização de AMPK na regulação metabólica e funcional de tolDC ainda não foi abordado. Ainda, a presença de VitD3 durante a diferenciação mo-DC, induz uma reprogramação metabólica inicial, dependente de glicose. Assim, o presente trabalho teve dois objetivos principais: (1) como a hiperglicemia é a principal característica do DM1, avaliou-se como a concentração de glicose afetaria a diferenciação de mo-DC tratadas com VitD3 (VitD-DC); (2) investigar como AMPK poderia controlar a diferenciação de tolDC induzida por VitD3, RA e Dex. Observou-se que, metabolicamente, VitD3 modula de maneira diferente mo-DC de controle e pacientes, induzindo tolDC em pacientes de maneira glicose independente. Em controles, VitD3 induziu aumento da glicólise e OXPHOS, que foram, pelo menos parcialmente, reduzidas em hiperglicemia, assim como a expressão de CD86, a secreção de TNF- α e a capacidade linfoestimulatória. Já em pacientes diabéticos, embora VitD3 reduziu tanto a expressão de CD86 quanto a secreção de TNF- α em hiperglicemia, o metabolismo das células não foi afetado, sugerindo que a reprogramação metabólica induzida pela VitD3 pode não depender da glicólise em pacientes. Na segunda parte do projeto, confirmamos que VitD3, Dex e RA induziram tolDC funcionais, já que estas tolDC diferenciaram células T CD4⁺ supressoras. Entretanto, metabolicamente, cada tolDC exibiu fenótipo distinto: VitD-DC aumentaram glicólise e OXPHOS, RA-DC

reduziram a capacidade respiratória sobressalente e Dex-DC reduziram glicólise. A fosforilação de ACC, um alvo direto de AMPK, aumentou em VitD-DC e RA-DC, sugerindo aumento da atividade de AMPK. Coerentemente, o silenciamento de AMPK reverteu as alterações metabólicas induzidas por VitD3 e RA, mas não por Dex. Quando AMPK foi silenciada em RA-DC humana, tanto a atividade de ALDH (induzida pelo RA) como sua capacidade tolerogênica foram perdidas. Camundongos com DC deficientes em AMPK, apresentaram redução na atividade de ALDH e na frequência de DC CD103⁺CD11b⁺ intestinal, consideradas o equivalente *in vivo* das RA-DC. Isso sugere uma importância da sinalização de AMPK para a homeostase de DC tolerogênicas intestinais, promovendo ambiente anti-inflamatório via atividade de ALDH em DC CD103⁺CD11b⁺. Sendo assim, estes dados sugerem um papel fundamental da AMPK na homeostase intestinal e na regulação das propriedades metabólicas e tolerogênicas de RA-DC.

Palavras-chave: Células Dendríticas. Imunometabolismo. Diabetes Tipo 1. AMPK. Tolerância.

FIGURE LIST

Figure 1: Dendritic cells activation.	36
Figure 2: Main characteristics and differences of cDC1, cDC2 and pDC.	37
Figure 3: Immunogenic DC vs tolerogenic DC.	39
Figure 4: Overview of metabolic pathways.	42
Figure 5: Metabolic characteristics of immunogenic and tolerogenic DC.	48
Figure 6: AMPK activation in mammalian cells.	50
Figure 7: Monocytes purity isolated by magnetic beads from PBMCs.	57
Figure 8: No significant alteration in blood populations of DC and circulating monocytes in diabetic patients.	72
Figure 9: Diabetic patients have a higher frequency of CD123^{lo}CD11c + blood DC expressing high levels of CD16.	74
Figure 10: Metabolic profile of blood cDC from healthy donors and diabetic patients.	75
Figure 11: Blood cDC and classical monocytes from diabetic patients secrete higher levels of TNF-α.	76
Figure 12: Phenotypic characterization of mo-DC generated from controls and differentiated type 1 diabetic patients at varying glucose concentrations.	78
Figure 13: Representative graphs of CD86 expression in two different experiments	79
Figure 14: Secretion of TNF-α, IL-10, IL-12p70 and IL-6 in supernatant from DC and VitD DC differentiated in the presence of 5.5 mM or 25 mM glucose.	82
Figure 15: DC and VitD DC lymphostimulatory capacity from healthy donors and diabetic patients, differentiated under various glucose concentrations and activated with 100 ng/mL of LPS.	84
Figure 16: Lower IL-2 concentration in supernatant from CD3⁺ T lymphocyte co-cultured with DC and VitD DC differentiated at different glucose concentrations.	85
Figure 17: Cytokine pattern secreted by T lymphocytes co-cultured with DC and VitD DC.	88
Figure 18: Metabolic profile of DC and VitD DC from healthy donors and diabetic patients.	90

Figure 19: Mo-DC and murine peritoneal macrophages from T1D subjects appears to be more glycolytic than those from controls.....	91
Figure 20: GLUT1 expression in mo-DC and monocytes and glucose uptake by DC and VitD DC from healthy donors and diabetic patients..	93
Figure 21: Analysis of the mitochondrial mass and membrane potential of DC and VitD DC from healthy donors and diabetic patients differentiated in the presence of either 5.5 mM or 25 mM glucose.....	95
Figure 22: Characterization of mo-DC rendered tolerogenic by VitD3, RA or Dex.	98
Figure 23: Metabolic profile from tolDC.	99
Figure 24: LPS activation induces a rapid increase in glycolytic metabolism in both control and tolerogenic DC.....	100
Figure 25: Quantitative PCR from tolDC treated with compounds at day 0.	102
Figure 26: Expression of elongases in tolDC treated with compounds at day 0..	103
Figure 27: Quantitative PCR from tolDC treated with compounds at day 5.	104
Figure 28: Expression of elongases in tolDC treated with compounds at day 5..	105
Figure 29: Lipidome analysis from tolDC treated with compounds at day 0.....	107
Figure 30: Lipidome analysis from tolDC treated with compounds at day 5.....	108
Figure 31: Lipidome analysis from tolDC treated with compounds at day 5 – graphic view..	109
Figure 32: Total neutral lipids content is increased in VitD DC and RA DC treated at day 0.....	109
Figure 33: Effect of glucose concentrations during the differentiation of mo-DC..	112
Figure 34: Metabolic characterization of tolDC. Monocytes were isolated from PBMC with CD14⁺ magnetic beads and differentiated in DC in the presence of either 1 mM, 5.5 mM or 25 mM of glucose.	114
Figure 35: Mitochondrial membrane potential and mass were not affected by glucose concentration. Monocytes were isolated from PBMC with CD14⁺ magnetic beads and differentiated in DC in the presence of either 1 mM, 5.5 mM or 25 mM of glucose.....	115
Figure 36: TolDC displayed altered AMP/ATP ratio.	116
Figure 37: AMPK activity is increased in VitD3- and RA-induced tolDC.....	117
Figure 38: Metabolic characterization of VitD DC.	118

Figure 39: Metabolic characterization of RA DC.....	118
Figure 40: Metabolic characterization of Dex DC.....	119
Figure 41: Suppressive ability of T cells primed by RA DC is dependent on AMPK.	121
Figure 42: ALDH activity in RA-induced DC might be controlled by AMPK.....	123
Figure 43: RA-induced GMDC recapitulate the phenotype of RA DC.....	125
Figure 44: Metabolic characterization of GMDC.	127
Figure 45: AMPK is important for RA-induced GMDC to limit the secretion of IFN-γ by T cells in vivo.....	129
Figure 46: ALDH activity in gut CD11b+CD103+ DC is partially dependent of AMPK.....	132
Figure 47: AMPK limits the expression of co-stimulatory molecules in cDC and helps to promote homeostasis in msLN..	133

TABLE LIST

Table 1 - Clinical Characteristics of diabetic patients.	56
Table 2 - Oligonucleotides used for qPCR amplification.....	66
Table 3 - Covariates associated with pDC in T1D patients	71

ABBREVIATION LIST

$\Delta\psi_m$ – mitochondrial membrane potential

2-DG – 2-deoxy- d-glucose

2-DG-P – 2-deoxyglucose-phosphate

2-NBDG – 2-(N-(7-Nitrobenz-2-oxa-1,3-diazol-4-yl)Amino)-2-Deoxyglucose

5-LOX – 5-lipoxygenase

AA – arachidonic acid

ACC - acetyl-CoA carboxylase

ACE – angiotensin converter enzyme

ADL – adrenoleukodystrophy

ADP – adenosine diphosphate

ALDH – aldehyde dehydrogenase

AM – alveolar macrophages

AMP – adenosine monophosphate

AMPK – AMP-activated protein kinase

ANCOVA – analysis of covariance

ANOVA – analysis of variance

APCs – antigen presenting cells

ATM – adipose tissue macrophages

ATP – adenosine triphosphate

Batf-3 - Basic Leucine Zipper ATF-Like Transcription Factor-3 ()

BDCA – blood dendritic cells antigens

BM – bone marrow

BMI – body mass index

BPTES - bis-2-(5-phenylacetamido-1,3,4-thiadiazol-2-yl)ethyl sulfide

CAMKK2 – calcium/calmodulin-dependent kinase kinase 2

CBA – cytometric bead assay

CCCP – carbonyl cyanide m-chlorophenylhydrazone

CCL - C-C motif ligand

CD – cluster of differentiation

CD11c ^{Δ AMPK α 1} – mouse with deletion of AMPK α 1 in CD11c cells

CD11c^{WT} – mouse without deletion of AMPK α 1 in CD11c cells

CDAI - Crohn's Disease Activity Index

cDC – conventional dendritic cells

CDEIS - Crohn's Disease Endoscopic Index of Severity
CFSE – 5,6-carboxy fluorescein diacetate succinimidyl ester
CoA - coenzyme A
COX – cyclooxygenase
CPT1 – carnitine palmitoyltransferase 1,
CSF-1 – colony stimulating factor-1
CTLA-4 – cytotoxic T-lymphocyte-associated antigen 4
CTP – citrate transport protein
CTV – cell trace violet
DAMP – damage-associated molecular patterns
DC – dendritic cells
DDA – 13-16-docosadienoic acid
DEAB – diethylaminobenzaldehyde
Dex – dexamethasone
Dex DC – mo-DC differentiated in the presence of dexamethasone
DHA – docosahexaenoic acid
DHAP - dihydroxyacetone phosphate
DM – diabetes mellitus
dMo – differentiating monocytes
DNA – deoxyribonucleic acid
ECAR – extracellular acidification rate
EDA – 11,14-eicosadienoic acid
EDTA – ethylenediamine tetraacetic acid
eEF2K – elongation factor 2 kinase
ELISA – enzyme-linked immunosorbent assay
ELOVL – elongation of very long chain fatty acids protein
ENO1 – enolase 1
EPA – eicosapentaenoic acid
F1,6biP - fructose 1,6 biphosphate
F5P - fructose 5 phosphate
F6P - fructose 6 phosphate
FACS – fluorescence-activated cell sorting
FADH₂ – flavin adenine dinucleotide
FAO – fatty acid oxidation
FAS – fatty acid synthesis

FAs – fatty acids
FASN - fatty acid synthase
FCCP – fluoro-carbonyl cyanide phenylhydrazone
FoxP3 – forkhead box P3
FSC – forward side scatter
G6P - glucose 6 phosphate
G6PDH - glucose 6 phosphate dehydrogenase
GA3P - glyceraldehyde 3 phosphate,
GAD – glutamic acid decarboxylase
GAPDH – glyceraldehyde-3-phosphate dehydrogenase
GC-MS – gas chromatography-mass spectrometry
GFR_e – estimated glomerular filtration rate
GLS – glutaminase
GLUT1 - glucose transporter 1
GM-CSF – granulocyte-macrophage colony stimulation factor
GMDC – GM-CSF bone marrow-derived dendritic cells
GWAS – genome-wide association studies
HbA1c – hemoglobin A1c
HBSS – hank's balance salt solution
HCA – hierarchical cluster analysis
HDAC5 – histone deacetylation 5
HDL – high-density lipoprotein
HIF1 α - hypoxia inducible factor 1alpha
HK-II - hexokinase 2
HRP – horseradish peroxidase
IA-2 – tyrosine phosphatase-like insulinoma antigen 2
ICA – islet cell antibodies
iDC – immature dendritic cells
IDH – isocitrate dehydrogenase
IDO – indoleamine 2,3-dioxygenase
IFN-g – interferon-gamma
IL – interleukin
ILT3 – immunoglobulin-like transcript 3
IM – interstitial macrophages
iNOS – inducible nitric oxide synthase

iTreg – induced regulatory T cells
LC – long chain
LCFA – long chain fatty acids
LDH - lactate dehydrogenase
LDL – low-density lipoprotein
LIN⁻ - lineage negative
LKB1 – liver kinase B1
LN – lymph nodes
LOX – lipoxygenase
LPS – lipopolysaccharide
LTB4 – leukotriene-B4
LTB5 – leukotriene-B5
mDC – mature dendritic cells
MDD – major depressive disorder
MFI – mean fluorescence intensity
MHC – major histocompatibility complex
mM – millimolar
Mo-DC – monocyte-derived dendritic cells
MPC1 - mitochondrial pyruvate carrier 1
MS – multiple sclerosis
msLN – mesenteric lymph nodes
mTOR – mechanistic target of rapamycin
MUFA – monounsaturated fatty acids
NADH - nicotinamide adenine dinucleotide
NADPH - nicotinamide adenine dinucleotide phosphate
NF- κ B - nuclear factor kappa B
NK – natural killer
NOD – non obese diabetic
OCR – oxygen consumption rate
OXPHOS – oxidative phosphorylation
PAMP – pathogen-associated molecular patterns
PBMC – peripheral blood mononuclear cells
PBS – phosphate buffer saline
PCA – principal component analysis
PD-L1 – programmed death-ligand 1

pDC – plasmacytoid dendritic cells
PDH - pyruvate dehydrogenase
PDK1-4 - pyruvate dehydrogenase kinase 1-4,
PEP - phosphoenolpyruvate
PFK1 - phosphofructokinase-1
PGE₂ – prostaglandin E₂
PKA – cyclic-AMP-dependent protein kinase
PKM2 - pyruvate kinase isozyme M2
PMA – phorbol 12-myristate 13-acetate
PP – Peyer's patch
PPAR- γ – peroxisome proliferator-activated receptor- γ
PPP – pentose phosphate pathway
PRPP - 5-phosphoribosyl-1-pyrophosphate
PRR – pattern recognition receptors
pTreg – peripheral regulatory T cells
PUFA – polyunsaturated fatty acids
qPCR – quantitative real-time polymerase chain reaction
R5P - ribose 5-phosphate
RA – retinoic acid
RA DC – mo-DC differentiated in the presence of retinoic acid
Raptor – regulatory-associated protein of mTOR
RNA – ribonucleic acid
RPMI – Roswell Park Memorial Institute
RT – room temperature
RvE1 – resolvin E1
SCFA – short chain fatty acids
SD – standard deviation
SDH - succinate dehydrogenase
SDHA – succinate dehydrogenase A
SEM – standard error mean
siLP – small intestine lamina propria
siRNA – short interference ribonucleic acid
SIRT1 – sirtuin 1
SLC1A5 – sodium-dependent neutral amino acid transporter type 2
SPF – specific-pathogen-free

SRC – spare respiratory capacity
SSC – side scatter
T1D – type 1 diabetes
T2D – type 2 diabetes
TBC1D1 – TBC1 domain family member 1
TCA – tricarboxylic acid
TGF- β – transforming growth factor beta (
Th – helper T cells
TLRs – toll like receptors
TMRE – tetramethylrodamine ethyl ester ester
TNF- α – tumor necrosis factor alpha
TOFA - 5-(Tetradecyloxy)-2-furoic acid
tolDC – tolerogenic dendritic cells
Tregs – regulatory T cells
TSC2 – tuberous sclerosis 2
TXA₂ – thromboxane A₂
TXB₃ – thromboxane B₃
TXNIP – thioredoxin interacting protein
UC – ulcerative colitis
VitD DC – mo-DC differentiated in the presence of VitD3
VitD3 – metabolic active form of vitamin D3 (1,25-dihydroxicholecalciferol)
VLCFA – very long chain fatty acids
WNT – Wingless-related integration site
WT – wild type
 α KGDH – α -ketoglutarate dehydrogenase
 μ M – micromolar

TABLE OF CONTENT

ABSTRACT	15
RESUMO	15
FIGURE LIST	19
TABLE LIST	22
ABBREVIATION LIST	23
1. INTRODUCTION	32
1.1. DIABETES	32
1.2. DENDRITIC CELLS	34
1.3. IMMUNOGENIC VS TOLEROGENIC DC	38
1.4. OVERVIEW OF METABOLIC PATHWAYS	41
1.5. METABOLIC PATHWAYS IN DC	45
1.6. AMPK: ONE METABOLIC SENSOR OF THE CELLS	48
2. OBJECTIVES	53
2.1. GENERAL OBJECTIVE	53
2.2. SPECIFIC OBJECTIVES	53
3. MATERIAL AND METHODS	55
3.1. PATIENTS	55
3.2. MICE	55
3.3. DIFFERENTIATION OF HUMAN MONOCYTE-DERIVED DENDRITIC CELLS (MO-DC) – RESULTS PART I	57
3.4. DIFFERENTIATION OF HUMAN MO-DC – RESULTS PART II	58
3.5. DIFFERENTIATION OF MOUSE BONE MARROW-DERIVED DENDRITIC CELLS (GMDC)	58
3.6. IMMUNOLOGICAL CHARACTERIZATION OF DC BY FLOW CYTOMETRY	59
3.7. MITOCHONDRIAL MASS AND MEMBRANE POTENTIAL ANALYSIS	59
3.8. GLUCOSE UPTAKE AND NEUTRAL LIPIDS ANALYSIS	60
3.9. RETINALDEHYDE DEHYDROGENASE ACTIVITY	60
3.10. INTRACELLULAR CYTOKINE DETECTION ON GMDC	60
3.11. COCULTURE OF MO-DC WITH J558 CD40L-EXPRESSING B CELLS	61
3.12. HUMAN T CELL PROLIFERATION ASSAY	61
3.13. CYTOMETRIC BEADS ASSAY (CBA)	61
3.14. HUMAN T-CELL CULTURE AND ANALYSIS OF T-CELL POLARIZATION	61
3.15. HUMAN FOXP3 INTRACELLULAR DETECTION	62
3.16. T-CELL SUPPRESSION ASSAY	62
3.17. IN VITRO MOUSE T CELL PRIMING ASSAY	63
3.18. IN VIVO MOUSE T CELL PRIMING FOLLOWING DC IMMUNIZATION	63
3.19. CYTOKINE DETECTION BY ELISA	64
3.20. METABOLIC PROFILE OF DC	64
3.21. LIPIDOMIC ANALYSIS	64
3.22. QUANTITATIVE REAL-TIME PCR	65
3.23. SMALL INTERFERING RNA (siRNA) ELECTROPORATION	66
3.24. LYMPH NODE AND PEYER’S PATCH ISOLATION	66
3.25. SMALL INTESTINE LAMINA PROPRIA ISOLATION	67
3.26. LUNG CELLS ISOLATION	67
3.27. STATISTICAL ANALYSIS	68
4. RESULTS	70
PART I - CHARACTERIZATION OF TOLDC FROM T1D PATIENTS AND HEALTHY DONORS	70
4.1. <i>Characterization of monocytes and blood DC subpopulations in healthy donors and type 1 diabetic patients</i>	70
4.2. <i>Characterization of surface markers in DC and VitD DC generated at different glucose concentrations</i>	76
4.3. <i>Quantification of cytokines secreted by DC and VitD DC generated at different glucose concentrations</i>	80
4.4. <i>Evaluation of lymphostimulatory capacity of mo-DC generated at different glucose concentrations</i>	83
4.5. <i>IL-2 quantification in supernatants of allogeneic T lymphocytes co-cultured with mo-DC generated at different glucose concentrations</i>	85
4.6. <i>Intracellular quantification of cytokines produced by T lymphocytes co-cultured with DC and VitD DC generated at different glucose concentrations</i>	86
4.7. <i>Extracellular flux analysis</i>	89
4.8. <i>Glucose uptake by DC and VitD DC from healthy donors and T1D patients</i>	92
4.9. <i>Mitochondrial mass and potential membrane analysis in mo-DC and VitD DC from healthy donors and T1D patients</i> ..	94
PART II – THE ROLE OF AMPK IN THE TOLEROGENIC PROPERTIES OF DC	96
4.10. CHARACTERIZATION OF TOLDC	96
4.10.1. <i>RA DC, VitD DC and Dex DC differ in many characteristics, but are equally suppressive</i>	96
4.10.2. <i>Elongation of very long-chain fatty acids family member 6 (ELOVL6) is increased in RA DC and Dex DC</i>	100
4.10.3. <i>Long chain fatty acid pathway is differently affected in RA DC, VitD DC and Dex DC</i>	106
4.11. GLUCOSE EFFECTS DURING DIFFERENTIATION OF TOLDC	110
4.12. ROLE OF AMPK IN THE FUNCTION OF TOLEROGENIC DC	115
4.12.1. <i>AMPK activity is increased in RA-DC and VitD DC</i>	115

4.12.2.	<i>AMPK^{KD} restores spare respiratory capacity in RA-DC</i>	117
4.12.3.	<i>AMPK^{KD} decreases induction of suppressive T cells by RA DC</i>	120
4.12.4.	<i>AMPK^{KD} restored ALDH activity in RA-DC</i>	122
4.12.5.	<i>Mouse RA GMDC mimic human RA-DC</i>	123
4.12.6.	<i>CD11c^{AMPK^{Kal}} RA GMDC failed to decrease polyclonal IFN-γ secretion by T cells in cell transfer experiment.</i>	127
4.12.7.	<i>CD11c^{AMPK^{Kal}} gut CD11b⁻CD103⁺ DC have low ALDH activity.</i>	130
5.	DISCUSSION	136
6.	CONCLUSIONS	152
7.	REFERENCES	154
8.	APPENDIXES	174

1. INTRODUCTION

1. INTRODUCTION

1.1. Diabetes

Diabetes mellitus (DM) is a syndrome characterized by hyperglycemia resulting from defects in insulin secretion associated or not with resistance to the action of this hormone. DM is one of the most common endocrine diseases in all populations, and its prevalence varies according to ethnic group and geographic region (FORLENZA; REWERS, 2011). According to the Multicenter Study on Prevalence of DM in Brazil (MALERBI; FRANCO, 1992), conducted from June 1986 to July 1988, the age-adjusted prevalence rate of DM in the Brazilian population aged 30 to 69 years ranged from 5.22% in Brasilia to 9.66% in São Paulo, with a national average of 7.66%. A study conducted between September 1996 and November 1997 in the city of Ribeirão Preto, with the same age range used in the multicenter study, showed that 12.1% of the resident population in this city (approximately 27,739 people) had DM and about 25% of them were diagnosed during the study (TORQUATO et al., 2003). Another study, conducted between February 2005 and June 2007, also at Ribeirão Preto, found an increased prevalence of diabetes, 15.02%, and about 15% of the subjects were diagnosed during the study (MORAES; FREITAS; GIMENO, 2010). According to data from the Ministry of Health (DATASUS), during 2011, the mortality rate from DM in Brazil was 30.1/100,000 inhabitants, representing 57,876 individuals who died specifically from this disease. More recent data from the United States, revealed that the prevalence of diabetes was 9.7% in 2016 and 2017 being more prevalent in men (XU et al., 2018).

In 2004, Wild et al. developed a study in which the prevalence of DM for the year 2000 and 2030 was estimated. For this, only populations diagnosed in studies that used the criteria used by the World Health Organization (blood glucose levels higher than 200 mg/dL two hours after ingestion of 75g of glucose) were used. In this study, it was estimated that about 171 million people would have DM in 2000 and about 366 million in 2030 (WILD et al., 2004). However, in 2015, the global number of adults with DM was estimated in 415 million, with projected increase to 642 million by 2040 (OGURTSOVA et al., 2017).

The clinical manifestations extremes and the pathogenesis are the basis for the classification in type 1 DM (T1D, an autoimmune disease with exuberant clinical manifestations resulting from almost complete insulin deficiency) and type 2 DM (T2D, oligo or asymptomatic patients whose insulin deficiency coexists with insulin resistance). The elevated blood glucose observed in the disease may be accompanied by other

biochemical changes and clinical manifestations whose severity depends on the degree of insulin deficit, environmental conditions and the evolution of chronic blood vessel complications (diabetic micro and macroangiopathy).

T1D corresponds to approximately 10% of DM cases and it is a complex autoimmune disease that by the time of diagnosis, has already affected most of the pancreatic islets (KLINKE, 2008). Although the most important associated HLA class II haplotypes have been known for decades (NERUP et al., 1974), the concordance rates between monozygotic twins suggests that other factors also play an important role in the pathogenesis of T1D (REDONDO et al., 2001). With the advent of genome wide association studies (GWAS) more than 60 different loci could be associated with the development and or progression of T1D (BAKAY et al., 2019), which highlights how complex this disease is. As an autoimmune disease, environmental factors, such as virus infections and diet habits, can also contribute to the initiation of T1D (PASCHOU et al., 2018). Yet, immunological factors involving both CD8⁺ and CD4⁺ T cells, as well as dendritic cells (DC) and other innate immune cells are also important and an extensive data is available describing how these mechanisms can influence islets beta cells destruction (LEHUEN et al., 2010). However, the precise mechanisms that trigger the initiation of T1D are not easy to unravel and are not completely understood. Endogenous ligands from programmed cell death of the pancreatic β cells, as well as infection with certain types of viruses, may initiate the process of insulinitis, which generates more β -cell apoptosis, increased exposure of self-antigens and, by recruiting antigen presenting cells (APCs), such as DC, creates sensitization conditions of the immune system against islets (DOGUSAN et al., 2008; LIU, 2001; RASSCHAERT et al., 2003; 2005). In this context, it is believed that self-antigens from β -cell apoptosis are captured by DC that would migrate to the lymph node, where they would present these antigens to CD4⁺ T lymphocytes, initiating the autoimmune adaptive immune response (CALDERON; CARRERO; UNANUE, 2014; TURLEY et al., 2003).

Data from the literature suggest that the development of T1D requires the collaboration of both CD4⁺ and CD8⁺T lymphocytes, since the transfer of only one of these cell subtypes from nonobese diabetic mice (NOD), was unable to induce disease in immunocompromised mice (PHILLIPS et al., 2009). CD4⁺ T lymphocytes may promote macrophage migration to the pancreatic islets through the production of chemokine C-C motif ligand 1 and 2 (CCL1 and CCL2, respectively) (CANTOR; HASKINS, 2007; MARTIN et al., 2008). In addition, CD4⁺ T lymphocytes activate both B lymphocytes

and CD8⁺ T lymphocytes, either by direct cytokine production (such as interleukin (IL) - 21 (SUTHERLAND et al., 2009)), or by licensing APCs which promotes CD8⁺ T cell activation during disease onset (BALASA et al., 1997). In this licensing, the interaction between CD40L-CD40 promotes an increased IL-7 production, which appears to be important for activation of CD8⁺ T cells (CARRENO; BECKER-HAPAK; LINETTE, 2008) which, in turn, would lead to β cells death, recognized for exposing, in the context of class I molecules encoded by the major histocompatibility complex (MHC I), the antigens recognized by such effector cells.

DC and macrophages seem to be important for the onset of T1D. Macrophages comprise the most frequent myeloid cells present in the pancreatic islet (CARRERO et al., 2013) and macrophage's depletion by treatment with an antibody against the colony stimulating factor-1 (CSF-1) could prevent the diabetes onset if administered either at earlier time point (2-3 weeks of age) or later time point (10 weeks of age) (CARRERO et al., 2017). DC also seem to play a pivotal role in T1D onset since the ablation of conventional DC (cDC) (specifically CD11b⁺ DC) in nonobese diabetic (NOD) mice prevented the development of insulinitis and subsequent T1D. Interestingly, while cDC were important in the induction of T1D, once the insulinitis process is established, plasmacytoid DC (pDC) seem to be important to limit the progression of the disease, since the addition of pDC but not cDC, to mice with ongoing insulinitis limited the progression of the disease (SAXENA et al., 2007). A role for the other subset of cDC (the CD103⁺ DC) was also observed in NOD mice. The frequencies of CD103⁺ DC was increase in NOD mice from 4-6 weeks of age and, concomitantly, the frequencies of intraislets CD3⁺ T cells were also increased. The diabetes onset and the frequencies of intraislets CD3⁺ T cells were abolished in mice lacking the Basic Leucine Zipper ATF-Like Transcription Factor-3 (Batf-3), the main transcription factor of CD103⁺ DC, suggesting that this subset of cDC is also essential for the onset of T1D (FERRIS et al., 2014). It is still unclear which cell type is more important for the disease onset, if there is time-dependent process in which macrophages could be more prejudicial at the earlier stages while DC would be required once the insulinitis process is starting or, yet, if macrophages and DC cooperate to initiate the recruitment of diabetogenic T cells into pancreatic islets.

1.2. Dendritic Cells

DC are specialized in capture, processing and presentation of antigens to T lymphocytes and are believed to be the most effective in activating naïve T lymphocytes (CROFT; BRADLEY; SWAIN, 1994). In general, DC have been functionally divided into immature DC (iDC) and mature DC (mDC) (BANCHEREAU et al., 2000; GUERMONPREZ et al., 2002). Since iDC are rich in molecules associated with antigen capture, they are normally located within various tissues, efficiently capturing antigens, and, once an homeostatic state is present within this tissue, they present these antigens to T lymphocytes inducing tolerance to them (ITANO; JENKINS, 2003). Thus, iDC contribute to the maintenance or establishment of a tolerant state by presenting self or non-self antigens to T lymphocytes (WALLET; TISCH, 2006), without, at the same time, providing the necessary costimulatory signals, usually dependent on molecules such as B7.1 (CD80) and B7.2 (CD86). Such presentation may lead to a condition called clonal anergy in T lymphocytes (LUTZ; SCHULER, 2002), or even to the differentiation of T lymphocytes into regulatory cells (Tregs) (TAI et al., 2011).

At this stage of maturation, DC have a high density of receptors for immunocomplexes, cytokines and pattern recognition receptors (PRR), capable of recognizing pathogen-associated (PAMP) and damage-associated molecular patterns (DAMP) (STEINMAN et al., 2000). This set of receptors allows effective detection of homeostatic imbalances and their engagement leads DC to functional changes, characterized as maturation (MADDUR et al., 2010). DC maturation, thus, is triggered by the rupture of tissue homeostasis (CERBONI; GENTILI; MANEL, 2013; HEMMI; AKIRA, 2005) and turns on different metabolic, cellular, and gene transcription programs, allowing DC to migrate from peripheral tissues to T-dependent areas in secondary lymphoid organs, where T lymphocyte-activating antigen presentation may occur (ALVAREZ; VOLLMANN; ANDRIAN, 2008; DONG; BULLOCK, 2014; FRIEDL; GUNZER, 2001; HENDERSON; WATKINS; FLYNN, 1997; IMAI; YAMAKAWA; KASAJIMA, 1998; RANDOLPH; ANGELI; SWARTZ, 2005) (Figure 1).

Dendritic cells can be, also, anatomically divided into resident lymphoid tissue DC and migratory non-lymphoid tissue DC (HANIFFA; COLLIN; GINHOUX, 2013). They comprise heterogeneous populations with different subsets that can be distinguished by phenotypical markers and genetic profile. The first identification of a different population of DC arose from the observation that CD8 expression occurred on a subset of mouse resident splenic and thymic DC (VREMEC, 1992). While the identification of

mouse DC subpopulations is well advanced (MERAD et al., 2013; MILDNER; JUNG, 2014), mostly due to the facility of accessing a variety of tissues, the same is not true for human DC, where most studies that identified such subpopulations were performed in peripheral blood or skin. It is worth noting that recent studies have also characterized DC subpopulations in the human lung (GUILLIAMS et al., 2016) and intestine (GRANOT et al., 2017)

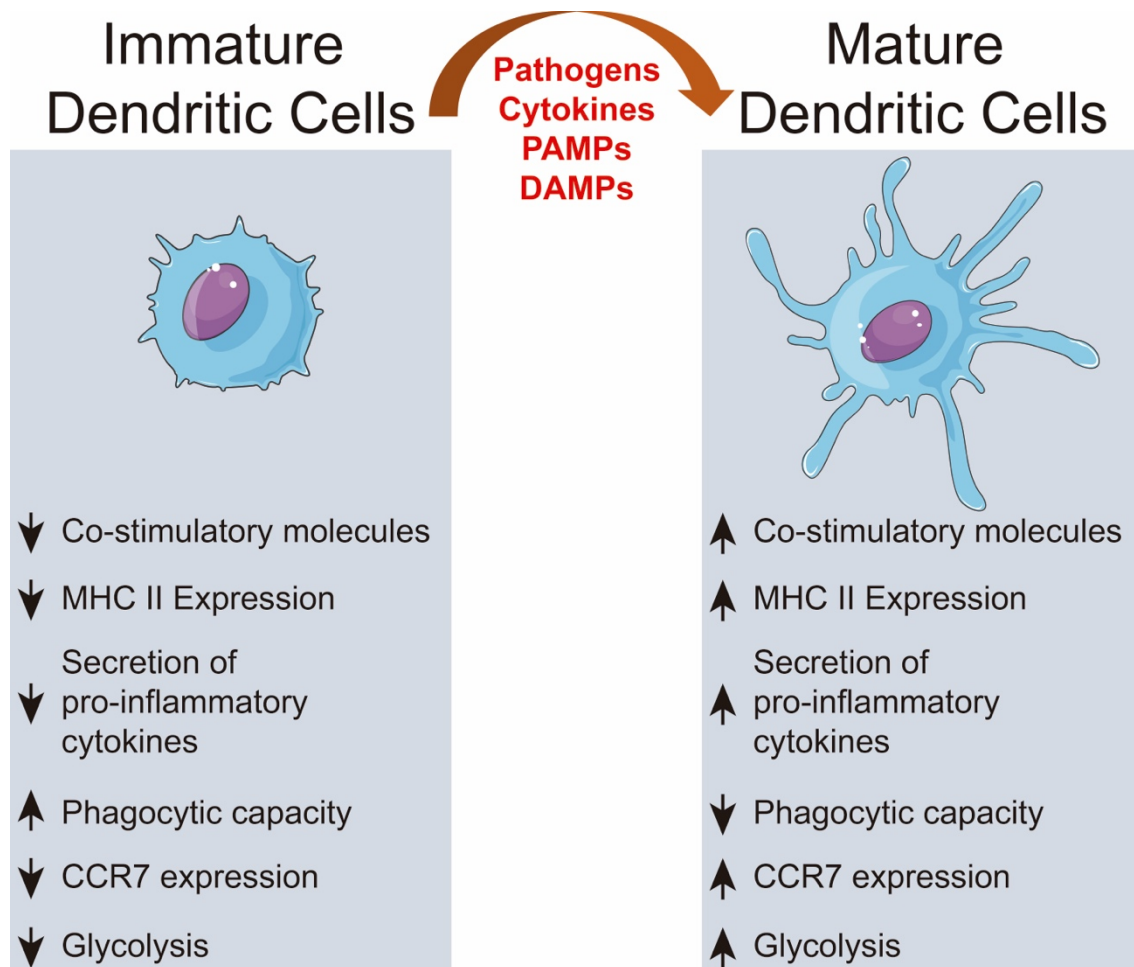


Figure 1: Dendritic cells activation. Extracellular signals, such as PAMPs or DAMPs, trigger alterations on immature DC leading to significant changes on surface proteins, intracellular pathways and metabolic activity. Adapted from Patente et. al, Front Immunol. 2019 Jan 21;9:3176.

In human blood, DC constitute a rare cell population that can be broadly divided into two subtypes: pDC and cDC. These subpopulations of DC can basically be distinguished by the expression of CD123 and CD11c, since pDC are CD123⁺CD11c⁻ and cDC are CD123⁻CD11c⁺ (BOLTJES; VAN WIJK, 2014; MERAD et al., 2013; O'KEEFFE; MOK; RADFORD, 2015; PATENTE et al., 2018). Additionally, cDC, can be further subdivided into two other subsets of DC, namely cDC1 and cDC2 DC

(GUILLIAMS et al., 2014). These subsets of cDC can be identified by the expression of CD141 in cDC1 and by the expression of CD1c in cDC2 (Figure 2). Genomic studies with emphasis on the subpopulations of monocytes and DC, could align the human peripheral blood CD1c⁺ DC with the mouse CD11b⁺DC and the human peripheral blood CD141⁺ DC with the mouse CD8 α ⁺/CD103⁺ DC respectively (ROBBINS et al., 2008; WATCHMAKER et al., 2013). New markers expressed by both human and mice DC could better define those subsets and the expression of XCR1 and CD172a are more commonly used to define cDC1 and cDC2, respectively. Nowadays, the nomenclature of cDC1 and cDC2 is well established and with new techniques, such as single cell RNA sequencing, new populations of DC (VILLANI et al., 2017), a better understanding of DC ontogeny (SEE et al., 2017), on how those subsets behave themselves in healthy and disease (DUTERTRE et al., 2019) and how specific transcription factors dictate the fate of each subset (DURAI et al., 2019) are starting to be unveiled.

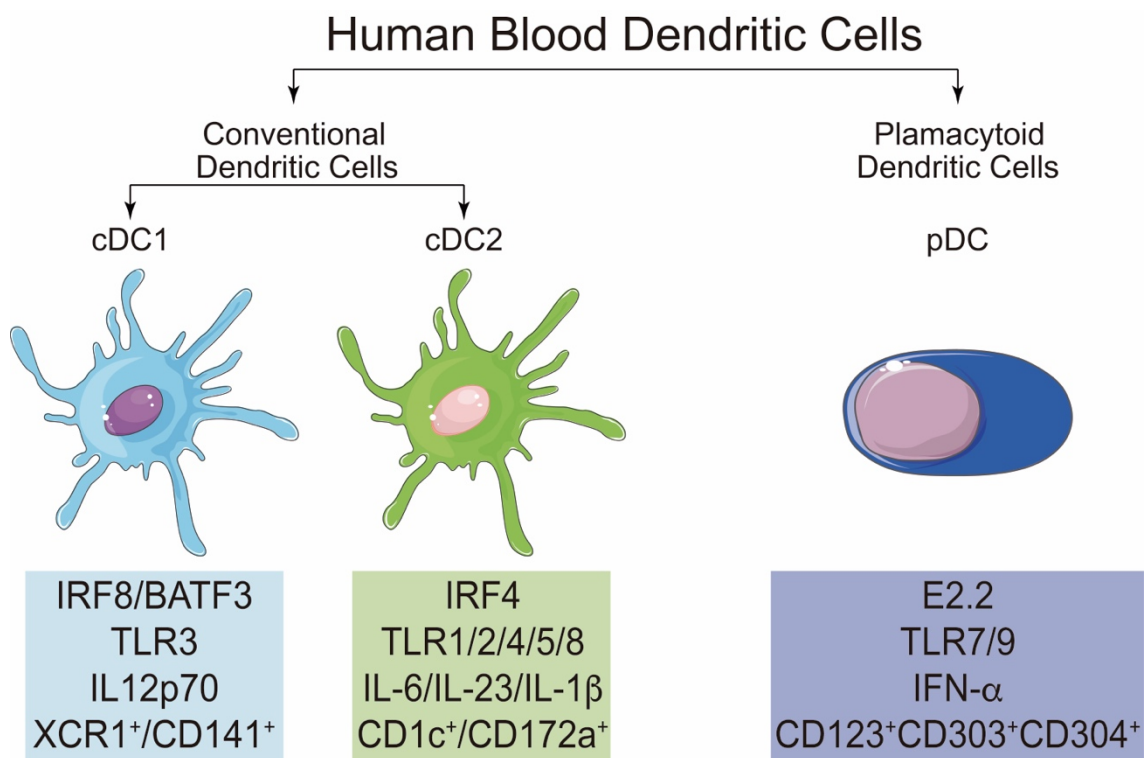


Figure 2: Main characteristics and differences of cDC1, cDC2 and pDC. In human blood, it is possible to find two main populations of DC: conventional DC (cDC) and plasmacytoid DC (pDC). cDC can be further subdivided in cDC1 and cDC2. Each subset of DC is characterized by its own transcription factors, functions and surface markers that helps to properly identify them in both mice and human. Adapted from Patente et. al, Front Immunol. 2019 Jan 21;9:3176.

Much of our understanding about human DC biology was possible due to *in vitro* experiments, in which monocytes isolated from the blood were differentiated to DC, the so called monocyte-derived DC (mo-DC), with the use of GM-CSF and IL-

4(SALLUSTO; LANZAVECCHIA, 1994). However, they do not seem to be equivalent to the cDC we can find in the blood, since they arise from different precursors (GEISSMANN et al., 2010). It is still unclear to which subpopulation of DC, mo-DC are more closely related, but DC ontogeny data suggest that mo-DC are similar to the inflammatory DC (REYNOLDS; HANIFFA, 2015). Inflammatory DC are a heterogeneous subpopulation of DC, expressing higher levels of CD11c and MHCII. The first reports about inflammatory DC, were observed in the skin of atopic dermatitis patients (WOLLENBERG et al., 1996) and in the spleen of *Listeria* monocytogenes-infected mice (SERBINA et al., 2003). Recently, by gene signature analysis, inflammatory DC were more closely related to *in vitro* generated mo-DC than macrophages, cDC2, CD16⁺ monocytes and CD14⁺ monocytes, suggesting that inflammatory DC could be the counterparts of mo-DC (SEGURA et al., 2013).

1.3. Immunogenic vs tolerogenic DC

Initially, DC function was largely associated with its capacity to capture, process and present antigens to T cells in order to initiate T-cell mediated immunity (STEINMAN, 1991; STEINMAN; WITMER, 1978). However, it was soon becoming clear that those cells not only were important for the induction of immune response, but also for the induction of tolerance, either in the thymus, by helping to negatively select autoreactive T cells (BROCKER; RIEDINGER; KARJALAINEN, 1997), or in the periphery by probably inducing T cell anergy or deletion (FÖRSTER; LIEBERAM, 1996; KURTS, 1996). The balance between immunogenic and tolerogenic DC (tolDC) is crucial for the maintenance of tissue homeostasis helping to promote immunity or tolerance depending on the environment.

TolDC express less co-stimulatory molecules, secrete less proinflammatory cytokines and upregulate the expression of inhibitory molecules, such as programmed death-ligand 1 (PD-L1) and cytotoxic T-lymphocyte-associated antigen 4 (CTLA-4) (GROHMANN et al., 2002; MANICASSAMY; PULENDRAN, 2011; MORELLI; THOMSON, 2007; SAKAGUCHI et al., 2010). Additionally, they are able to secrete anti-inflammatory cytokines (like IL-10) and are essential to prevent responses against healthy tissues (HAWIGER et al., 2001; IDOYAGA et al., 2013; MAHNKE et al., 2003; STEINMAN et al., 2003; YATES et al., 2007; YOGEV et al., 2012). Among the numerous stimuli capable of generating tolDC, cytokines and interactions with other cell types (like mastocytes via PD-L1/PD-L2) seem to be important to induction of this state

in DC (RODRIGUES et al., 2016; SVAJGER; ROZMAN, 2014). Among cytokines, IL-10, IL-6 and transforming growth factor beta (TGF- β) (TORRES-AGUILAR et al., 2010) have been described as capable of producing tolerogenic DC, with low expression of costimulatory molecules and MHC II, but capable of secrete high amounts of IL-10(LAN et al., 2006). Also, vitamin D3 (VitD3) (ADORINI, 2003; BAKDASH et al., 2014; FERREIRA et al., 2012; 2014; 2015), retinoic acid (RA) (BAKDASH et al., 2015), butyrate (KAISAR et al., 2017) and dexamethasone (Dex) (DÁŇOVÁ et al., 2015; MAGGI et al., 2016; NAVARRO-BARRIUSO et al., 2018) has been described as capable of inducing such condition, at least in vitro, on DC (Figure 3) and has been explored in animal models as a tool for the treatment of autoimmune diseases and prevention of transplant rejection (KLEIJWEGT et al., 2013; LAN et al., 2006).

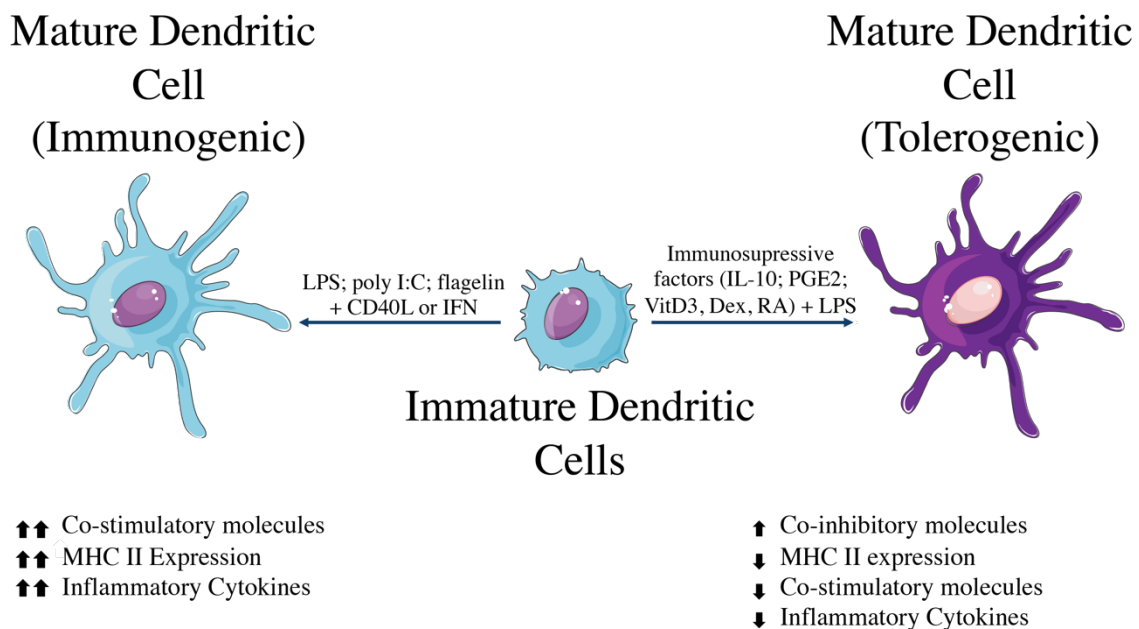


Figure 3: Immunogenic DC vs tolerogenic DC. Different stimuli can engage differentiation of immature DC toward immunogenic or tolerogenic profile. Immunogenic DC are characterized by the ability to induce activation of T cells in order to stimulate an inflammatory response. On the other hand, tolerogenic DC can induce the differentiation of regulatory T cell (Tregs) in order to control inflammatory environments.

The use of tolDC to prevent the development or to treat autoimmune disease is a particular interesting research field. Clinical trials have already been performed for T1D (GIANNOUKAKIS et al, 2011), rheumatoid arthritis (BELL et al., 2017; BENHAM et al., 2015), multiple sclerosis (MS) (clinicaltrials.gov identifier: NCT02283671 and NCT02618902) and Crohn's disease (JAUREGUI-AMEZAGA et al., 2015). The first phase I clinical trial with tolDC was performed by Giannoukakis et al. (GIANNOUKAKIS et al, 2011) in patients with T1D. In this trial, autologous DC were

treated with antisense oligonucleotides for CD40, CD80 and CD86. And, even though no clinical improvement was reported, infusion of these tolDC was safe and well tolerated with no adverse effects reported by the patients. A second phase I study with tolerogenic DC was performed by Benham et al. in patients with rheumatoid arthritis in which tolDC were generated by the use of “signal inhibitor” of the nuclear factor kappa B (NF- κ B) transcription factor (BENHAM et al., 2015). In this study, tolDC were pulsed with four citrullinated peptides, called Rheumavax, and reduction in effector T cell frequency with concomitant increase in Tregs frequency were observed. In the study performed by Jauregui-Amezaga et al., tolDC were administered intraperitoneally to Crohn’s disease patients in different doses and time points. Again, no adverse effects were observed in the patients and decrease in the Crohn’s Disease Activity Index (CDAI), Crohn’s Disease Endoscopic Index of Severity (CDEIS) with increase in the numbers of circulating Tregs were observed.

Before the use in clinical trials tolDC have been studied in mouse models to prevent the onset of, for example, T1D in NOD mice (FERREIRA et al., 2014; MA et al., 2003; TAI et al., 2011). Both, genetically modified mice, expressing HLA-DQ8 on antigen-presenting cells and the human co-stimulatory molecule B7.1 on the islet-beta cells, which develop spontaneous diabetes and NOD mice, when treated with bone marrow-derived DC (BMDC) differentiated in the presence of IL-10, displayed reduced insulinitis, increased numbers of Tregs in the spleen, suppression of diabetogenic T lymphocytes and did not develop T1D (TAI et al., 2011). It is worth noting that other treatments can also drive DC to a tolerogenic phenotype: immature GMDC from NOD mice, which have been shown to have higher CD80 and CD86 content compared to wild-type mouse BMDC, when treated with VitD3 displayed immunosuppressive properties (FERREIRA et al., 2014).

Although different methods were used for the generation of tolDC in the clinical trials tested so far, no adverse effects were observed, what, by itself, is already a positive observation. Thus, it is so far unclear, to what extent differences in methodology can change the effectiveness of the cells or can potentiate their beneficial effects. A common feature that seems to be shared by most of the tolDC tested is their ability to increase Tregs frequencies in the peripheral blood of the patients. However, each disease has its own course, and this needs to be taken into consideration. For example, the window to treat T1D patients is tight and difficult to reach, since, normally, by the time of diagnosis,

about 80% of the pancreatic islets have been already destroyed (KLINKE, 2008) and the tolDC-based therapy would not restore pancreatic islets.

Perhaps, the use of tolDC-based therapy in T1D would be more beneficial to prevent islet rejection, in the context of therapeutic transplantation. Although many studies in rodents have shown promising results with transfusion of modified tolerogenic DC in pancreatic islet transplantation models (HUANG et al., 2010; SUN et al., 2012; THOMAS et al., 2013; YANG et al., 2008), to date, no clinical trial results have been reported describing the effectiveness of tolDC in pancreatic islet transplantation or any other transplantation in humans. A study in primates, however, was able to demonstrate a significant increase in mean graft survival when VitD3 and IL-10 modified tolDC were administered seven days prior to kidney transplantation together with CTLA4-Ig (CD80/CD86 inhibitor), administered for a period of 2 or 9 weeks (EZZELARAB et al., 2013). These and other data in the literature highlight the potential of tolDC, both in transplantation and for the treatment of autoimmune diseases (OCHANDO et al., 2019).

1.4. Overview of metabolic pathways

Energy is necessary to execute any function, either in a complex organism or at a cellular level. Cells are constantly breaking down molecules to produce energy (a process called catabolism) or synthesizing molecules to either be stored or used immediately (a process called anabolism). Energy inside the cell is stored, mainly, in the form of adenosine triphosphate (ATP), which is constantly produced by the cell, mostly via two metabolic pathways: glycolysis and oxidative phosphorylation (OXPHOS). Glycolysis produces a limited amount of ATP but, in the presence of oxygen, it can fuel OXPHOS, via the tricarboxylic acid (TCA) cycle (MOOKERJEE et al., 2017), thus generating many more ATP molecules. The TCA cycle generates the reducing molecules, nicotinamide adenine dinucleotide (NADH) and flavin adenine dinucleotide (FADH₂), which serve as electron donors to the electron transport chain, fueling OXPHOS (PEARCE; PEARCE, 2013). Glycolysis is, of course, not the only metabolic pathway capable of fueling the TCA cycle. Other catabolic pathways like fatty acid oxidation (FAO) and glutaminolysis are also able to do so. Apart from catabolic pathways, anabolic pathways, like glycogenolysis, fatty acid synthesis and pentose phosphate pathway (PPP) are also important in cells to regulate the bioenergetic status manage nutrients (O'NEILL; KISHTON; RATHMELL, 2016) (Figure 4).

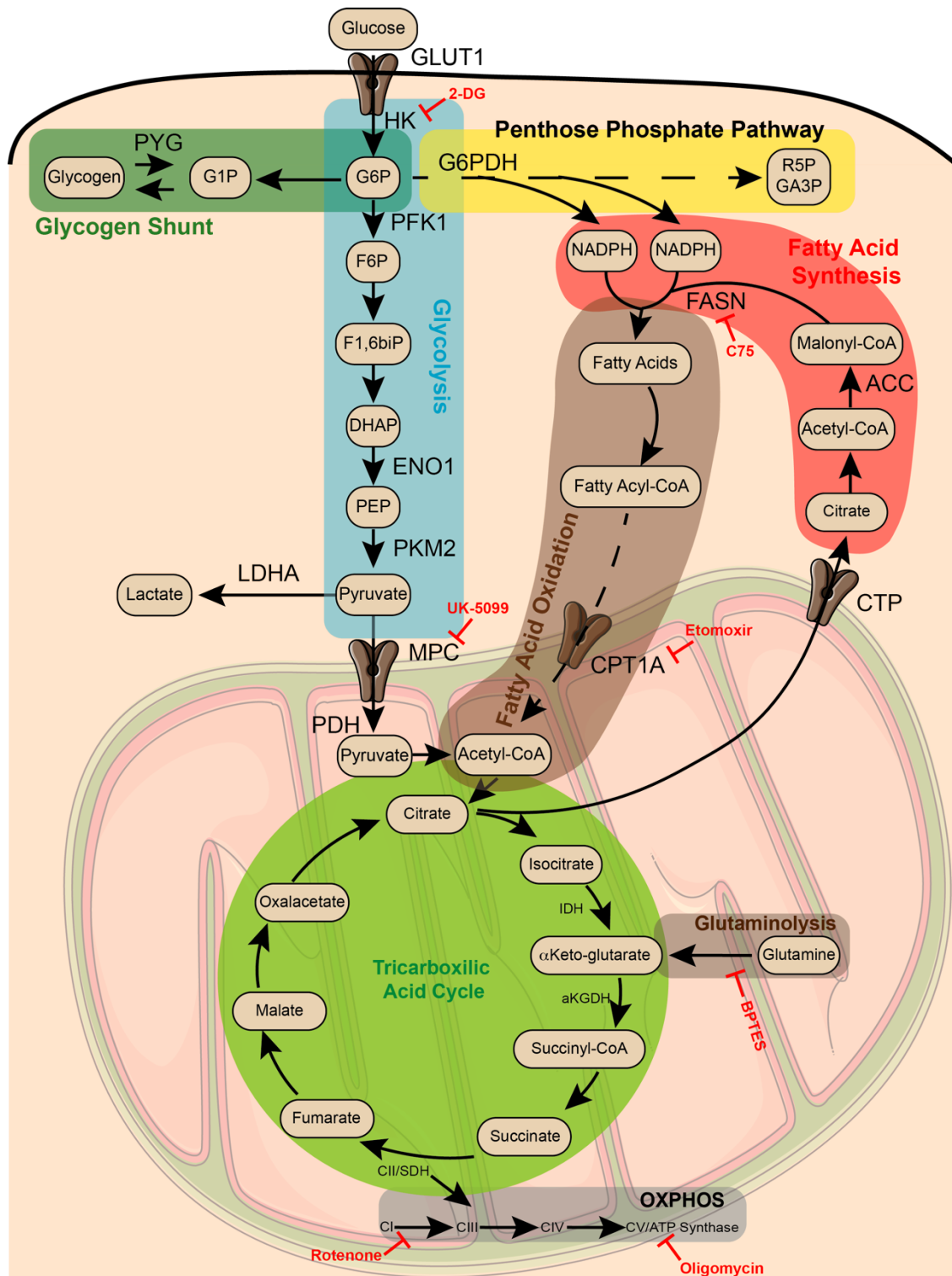


Figure 4: Overview of metabolic pathways. Frequently used metabolic inhibitors are indicated in red. 2-DG, 2-deoxy-D-glucose; ACC, acetyl-CoA carboxylase; α KGDH, α -ketoglutarate dehydrogenase; CoA, coenzyme A; CPT1, carnitine palmitoyltransferase 1; CTP, citrate transport protein; DHAP, dihydroxyacetone phosphate; DON, 6-Diazo-5-oxo-L-norleucine; ENO1, enolase 1; F1,6biP, fructose 1,6 biphosphate; F5P, fructose 5 phosphate; F6P, fructose 6 phosphate; FASN, fatty acid synthase; G6P, glucose 6 phosphate; G6PDH, glucose 6 phosphate dehydrogenase; GA3P, glyceraldehyde 3 phosphate; GLUT1, glucose transporter 1; HK-II, hexokinase 2; IDH, isocitrate dehydrogenase; LDHA, lactate dehydrogenase A; MPC1, mitochondrial pyruvate carrier 1; NADPH, nicotinamide adenine dinucleotide phosphate; PDH, pyruvate dehydrogenase PDK1-4, pyruvate dehydrogenase kinase 1-4; PEP, phosphoenolpyruvate; PFK1, phosphofructokinase-1; PKM2, pyruvate kinase isozyme M2; R5P, ribose 5-phosphate; SDH, succinate dehydrogenase; TOFA, 5-(Tetradecyloxy)-2-furoic acid.

Glycolysis starts with the uptake of glucose from the extracellular space via specific glucose transporters (GLUT) that can be found in many isoforms, among which, GLUT1 is the main isoform expressed by immune cells (KNOTT; FORRESTER, 1995). Once inside the cells, glucose is rapidly phosphorylated into glucose 6-phosphate (G6P), a process catalyzed by hexokinase (HK) that consumes ATP instead of producing it. A series of enzymatic reactions takes place in the cytosol to break down G6P and, ultimately, produce pyruvate that can either be reduced to lactate by lactate dehydrogenase (LDH) or carried into the mitochondria, by mitochondrial pyruvate carrier (MPC). Inside the mitochondria, pyruvate is converted to Acetyl-CoA that fuels the TCA. Glycolysis is a relatively poor pathway, for the production of ATP, since it produces only two molecules of ATP for each molecule of glucose. However, glycolysis is important to: (1) reduce NAD^+ to NADH, which is a cofactor for a series of enzymes; (2) provide biosynthetic intermediates, like G6P, for nucleotides (via PPP), 3-phosphoglycerate, for aminoacids (via the serine biosynthetic pathway) and citrate, derived from pyruvate in the TCA cycle, for fatty acids (DOMÍNGUEZ-AMOROCHO et al., 2019; O'NEILL; KISHTON; RATHMELL, 2016).

Experimentally, it is possible to inhibit glycolysis with 2-deoxy-d-glucose (2-DG) which is an analogous of glucose that is phosphorylated by HK, but whose end product, 2-deoxyglucose-phosphate (2-DG-P) cannot be used in the following steps of glycolysis, resulting in accumulation of 2-DG-P and inhibition of HK (SEO; CROCHET; LEE, 2013). The oxidation of glucose can be also blocked by a compound called UK-5099, which inhibits the activity of MPC, thus preventing the entrance of glucose-derived pyruvate into the mitochondria.

The PPP is a metabolic pathway that takes place in the cytosol and it is an offshoot of glycolysis. In the first step of PPP, G6P is dehydrogenated by glucose-6-phosphate dehydrogenase, generating 6-phosphogluconolactone. This molecule enters an oxidative branch of PPP that generates 2 equivalents of nicotinamide adenine dinucleotide phosphate (NADPH), which can be used for FAS, and ribulose-5-phosphate. This latter molecule may enter the non-oxidative branch of PPP, that starts with its conversion to ribose-5-phosphate (R5P), by the ribose-5-phosphate isomerase. R5P can serve as substrate for the generation of 5-phosphoribosyl-1-pyrophosphate (PRPP) a key intermediate in the nucleotide biosynthesis, required for *de novo* synthesis of purine and pyrimidine nucleotides (BHAGAVAN; HA, 2015). Additionally, when G5P is in excess,

ribulose-5-phosphate can be converted to glyceraldehyde-3-phosphate (GA3P) or fructose-6-phosphate (F6P), refueling glycolysis.

In the FAO pathway fatty acids are converted into Acetyl-CoA that can be used, in the TCA, to generate NADH and FADH₂. The FAO pathway can be divided into two steps: the first one is the activation of the fatty acids that occurs in the cytosol; the second step is the β -oxidation and occurs inside the mitochondria. The activation step is the formation of a fatty acyl-CoA, a reaction catalyzed by acyl-CoA synthases, located in the outer membrane of the mitochondria. Short-chain fatty acyl-CoA, defined as having less than six carbons in the aliphatic tail, can diffuse into the mitochondria, while medium and long chain fatty acyl-CoA need to be conjugated with carnitine by the action of carnitine palmitoyl transferase I (CPT1). Once carnitine-conjugated fatty acyl-CoA are inside the mitochondrial matrix, CPT2 is responsible for the removal of carnitine, which is transferred back to the cytosol via carnitine-acylcarnitine translocase. The next step in FAO is the oxidation of the acyl-CoA located at the β carbon of the molecule, the so called β -oxidation. This step involves the sequential action of 4 enzymes: acyl-CoA dehydrogenase, enoyl-CoA hydratase, β -hydroxyacyl-CoA dehydrogenase and 3-ketoacyl-CoA thiolase culminating with the production of acetyl-CoA, which can, now, fuel the TCA cycle to generate NADH and FADH₂, electron donors in the electron transport chain of OXPHOS (BHAGAVAN; HA, 2010; O'NEILL; KISHTON; RATHMELL, 2016). Experimentally, FAO can be partially blocked with etomoxir, a molecule that binds irreversibly to CPT1, thus preventing the entrance of fatty acyl-CoA in the mitochondria.

Cells synthesize lipids by the FAS pathway, generating lipids needed for cell growth and proliferation. *De novo* synthesis of fatty acids takes place in the cytosol and has as the rate limiting enzyme the acetyl-CoA carboxylase (ACC). ACC is the enzyme responsible for the conversion of acetyl-CoA into malonyl-CoA. In this process, an important regulator of the ACC is citrate, that is deviated from the TCA to the cytosol via the mitochondria citrate transport (CTP) protein. Citrate is important for the FAS pathway for two reasons: (1) it binds to ACC promoting the assembly of its active polymeric form from its inactive protomer; (2) it provides carbon atoms for the FAS pathway by the cytosolic generation of acetyl-CoA (citrate shuttle). The cytosolic acetyl-CoA is originated from the cleavage of citrate into acetyl-CoA and oxaloacetate by the action of ATP citrate lyase. The citrate shuttle is the main provider of cytosolic acetyl-CoA, since

it cannot be transported from the mitochondria. After citrate is converted to acetyl-CoA in the cytosol, the polymeric ACC, whose assembly also depends on citrate, catalyzes the conversion of acetyl-CoA into malonyl-CoA which is then elongated by fatty acid synthetase (FASN), in a NADPH-dependent manner, producing mainly palmitate, a C₁₆ fatty acid. Elongation of palmitate can occur in endoplasmic reticulum or in the mitochondria to generate long-chain fatty acids (LCFA) with C₁₈, C₂₀, C₂₂ and C₂₄ molecules. LCFA can be classified as monounsaturated (MUFA) or polyunsaturated (PUFA), depending on the number of double bonds between their carbon atoms. Malonyl-CoA is also an inhibitor of CPT1, a phenomenon that balances FAO and FAS in the cell. FAS can be blocked using a compound called C75, which inhibits FASN activity, thus preventing the synthesis of fatty acids from malonyl-CoA (BHAGAVAN; HA, 2010; BLANCO, 2017; O'NEILL; KISHTON; RATHMELL, 2016)

Another way cells can fuel the TCA cycle is via glutaminolysis, the process by which cells convert glutamine into TCA cycle metabolites. Initially glutamine is converted in glutamate, catalyzed by the enzyme glutaminase (GLS). Glutamate is, then, converted to α -ketoglutarate by the action of glutamate dehydrogenase enzyme and α -ketoglutarate can serve as an anaplerotic source to TCA cycle (YANG; VENNETI; NAGRATH, 2017). Glutaminolysis can be prevented by treating cells with a GLS inhibitor, like Bis-2-(5-phenylacetamido-1,3,4-thiadiazol-2-yl)ethyl sulfide (BPTES). Glutamine metabolism seems to be especially important in tumor cells because they undergo a metabolic reprogramming that renders them highly dependent on glutaminolysis, believed to be mainly via the activation of the proto-oncogene *c-MYC* that increases the expression of high-affinity glutamine importers, like sodium-dependent neutral amino acid transporter type 2 (SLC1A5) (WISE et al., 2008).

1.5. Metabolic pathways in DC

While in the late 1920s, Otto Warburg described a mechanism present in tumor cells that became known as the Warburg effect, in which cells, even in the presence of oxygen to perform oxidative phosphorylation, "preferred" to use the glycolytic pathway to generate ATP (WARBURG; WIND; NEGELEIN, 1927), the influence of metabolism on immune cell function has only recently began to be investigated in depth. The first reports of how metabolism could affect the immune cells functions date from the late 50's (ALONSO; NUNGESTER, 1956) and early 60's (OREN et al., 1963) showing differences in the metabolism of polymorphonuclear cells, basically by measurement of

gas change in Warburg flasks or enzymatic activity. More recently, with advantage of more innovative techniques, it was possible to study in deep the changes orchestrated by metabolism in the function of immune cells.

A large data in the literature has focused in the metabolic changes that occurs in immunogenic DC, leading to the consensus that activation of immunogenic DC is accompanied by, and dependent on, a switch from OXPHOS to glycolysis (BASIT et al., 2018; EVERTS et al., 2012; 2014b; FLIESSER et al., 2015; JANTSCH et al., 2008; KRAWCZYK et al., 2010; MCKEITHEN et al., 2017; PANTEL et al., 2014; RYANS et al., 2017; THWE et al., 2017). It is becoming increasingly clear that immune cell activation and function, including that of DC, is coupled to, and underpinned by, profound changes in cellular metabolism (BUCK et al., 2017; O'NEILL; KISHTON; RATHMELL, 2016). Immature DC predominantly use OXPHOS to obtain energy; however, when stimulated by Toll-like Receptor ligands (TLRs), such as LPS, these cells rapidly increase the glycolytic pathway by consuming more glucose, which acts to fuel the TCA. Increased glucose flow, in fact, provides TCA intermediates, especially citrate and isocitrate, which are diverted to other pathways (such as FAS) (EVERTS et al., 2014b; KRAWCZYK et al., 2010). Recently, it was demonstrated that glycogen-derived carbon is used during this initial increase in the glycolytic pathway for citrate synthesis and that much of the extracellular glucose captured by DC is rapidly converted to glycogen (THWE et al., 2017). These modulations that occur in LPS-activated DC appear to be at least partially dependent on hypoxia inducible factor 1- α (HIF1 α), since the silencing of this transcription factor was able to decrease the expression of the glucose transporters, such as GLUT-1, CD86 and the ability of these cells to stimulate the proliferation of T lymphocytes (JANTSCH et al., 2008). Additionally, long term LPS stimulation, increased the expression of mechanistic target of rapamycin (mTOR) which demonstrated to be important to stabilize HIF1 α and sustain glycolytic activity in DC, with significant increasing expression of MHC II, CD80, CD86 and CD40 (GUAK et al., 2018).

While the metabolic basis of immunogenic DC is being largely explored, the metabolic alterations that drives tolerogenicity in DC are just starting to be unveiled (Figure 5). The generation of tolDC from monocytes in the presence of rapamycin, a mTORC1 inhibitor (FISCHER et al., 2009), provided one of the first indications that blocking anabolic metabolism could favor acquisition of a tolerogenic phenotype in DC. Supporting this information, two recent studies aimed to characterize the metabolic

properties of human mo-DC rendered tolerogenic with VitD3 alone (FERREIRA et al., 2015) or together with Dex (MALINARICH et al., 2015), and reported increased mitochondrial activity evidenced by heightened OXPHOS. In the latter study acquisition of tolerogenic phenotype by the DC was partly dependent on increased FAO (MALINARICH et al., 2015). Interestingly, VitD3-DC displayed increased mTOR/HIF1 α -dependent glycolysis (FERREIRA et al., 2015) and this increased glycolysis was functionally relevant, since several markers of a tolerogenic phenotype (i.e. reduced expression of costimulatory molecules CD86 and CD80 and increased production of IL-10) was lost by VitD3-DC treated with 2-DG (FERREIRA et al., 2015). Additionally, glycolysis inhibition limited their ability to suppress CD4⁺ T cell proliferation. These cells showed an increased AMP-activated protein kinase (AMPK) activation (FERREIRA et al., 2015) and elevated glucose carbon tracing into the TCA cycle (VANHERWEGEN et al., 2018), suggesting that this increased glycolytic flux, in contrast to immunogenic DC, may primarily serve a catabolic role by fueling mitochondrial OXPHOS.

Consistent with these human DC data, a *in vivo* study focusing on the metabolic properties of DC in tumors (ZHAO et al., 2018), a microenvironment that is well-known to promote tolDC (RAMOS et al., 2012), revealed that these cells displayed increased FAO-dependent OXPHOS. This metabolic shift as well as IDO activity was driven by tumor cell-derived Wnt5a and it was dependent on β -catenin and peroxisome proliferator-activated receptor- γ (PPAR- γ) signaling. Importantly, blocking FAO in DC, abolished the increased Wnt5a-enhanced IDO activity as well as the induction of FoxP3⁺ peripheral Treg (pTreg) differentiation leading to enhanced anti-tumor immunity *in vivo*. Interestingly, a similar β -catenin-PPAR- γ dependent pathway is required for the maintenance of tolDC in visceral adipose tissue (MACDOUGALL et al., 2018). This, together with the findings that tolDC in mucosal tissues depend on PPAR- γ signaling for ALDH expression and activity (HOUSLEY et al., 2009; KHARE et al., 2015), points towards a crucial role for PPAR- γ in supporting tolerogenic properties of DC. However, to what extent these PPAR- γ -driven effects are mediated by controlling lipid metabolism remains to be determined.

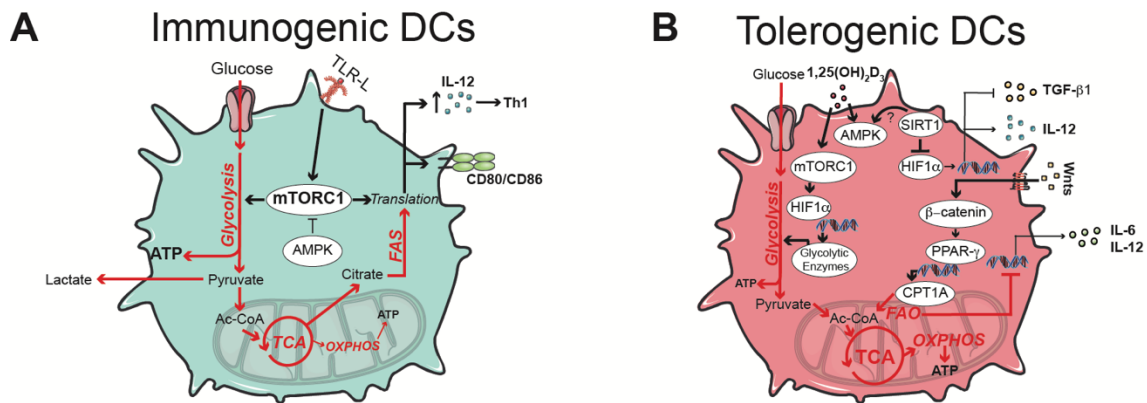


Figure 5: Metabolic characteristics of immunogenic and tolerogenic DC. Metabolic pathways and upstream signaling pathways regulating immunogenic (A) and tolerogenic (B) responses are indicated in red and black, respectively. Adenosine triphosphate (ATP); AMP-activated protein kinase (AMPK); carnitine palmitoyl transferase 1A (CPT1A); fatty oxidation (FAO); fatty synthesis (FAS); hypoxia inducible factor 1- α (HIF1 α); mechanistic target of rapamycin complex 1 (mTORC1); oxidative phosphorylation (OXPHOS); peroxisome proliferator-activated receptor- γ (PPAR- γ); tricarboxylic acid (TCA); sirtuin-1 (SIRT1). Adapted from Patente et al. 2019.

A switch from OXPHOS towards aerobic glycolysis was observed in sirtuin-1 (SIRT1)-deficient DC by stabilization of HIF1 α . As consequence, peripheral Treg (pTreg) differentiation was redirected towards Th1 priming T cells by enhanced IL-12 production and reduced TGF- β secretion by DC (LIU et al., 2015), providing further support for a key role in catabolic/oxidative metabolism in pTreg induction by DC. AMPK has a key role in promoting this type of metabolism and one could speculate that this kinase might be important in DC-driven induced Treg (iTreg) and pTreg polarization. The fact that SIRT1 can promote the activation of AMPK, through deacetylation of liver kinase B1 (LKB1) (CHEN et al., 2015), and that VitD3-treated human DC showed increased AMPK activation (FERREIRA et al., 2015), would be consistent with this idea and warrants a more direct assessment of the role of AMPK signaling in regulating the tolerogenic properties in DC.

1.6. AMPK: one metabolic sensor of the cells

Inside the cells, energy is measured by the levels of ATP produced, mainly, within the mitochondria. If ATP levels are low, catabolic process are triggered in order to break down molecules and uptake nutrients to restore the intracellular levels of ATP. In this sense, a protein that senses when ATP is low is crucial for the maintenance of cellular functions and homeostasis. The main sensor of cellular energy status, is AMPK which has the ability to sense increases in the AMP:ATP or ADP:ATP ratios and restores energy homeostasis by inhibiting anabolic pathways that consumes ATP and promoting catabolic

pathways that will have as end consequence the generation of ATP (GARCIA; SHAW, 2017).

AMPK is a heterotrimeric protein composed by an α -subunit, with catalytic activity, and a β - and γ -subunits with regulatory functions. All the subunits have more than one isoforms: (1) α 1 and α 2 subunits, encoded by the genes *PRKAA1* and *PRKAA2*; (2) β 1 and β 2 subunit, encoded by the genes *PRKAB1* and *PRKAB2* (THORNTON; SNOWDEN; CARLING, 1998); γ 1, γ 2 and γ 3 subunits, encoded by the genes *PRKAG1* and *PRKAG2* and *PRKAG3* (CHEUNG et al., 2000). The AMPK complex is composed of one subunit of each and all the combinations can be found. The α -subunit is the most important one, since it contains the kinase domain and a threonine 172 (Thr172) residue that can be phosphorylated by LKB1 (HAWLEY et al., 2003) and calcium/calmodulin-dependent kinase kinase 2 (CAMKK2) (HAWLEY et al., 2005), the two main upstream kinases that activates AMPK.

The activation of AMPK can be regulated by a canonical nucleotide-dependent and a non-canonical nucleotide-independent mechanism (GARCIA; SHAW, 2017; HARDIE; ROSS; HAWLEY, 2012). In the canonical nucleotide-dependent regulation process, changes in AMP:ATP or ADP:ATP ratio promotes the binding of AMP or ADP to the γ -subunit of AMPK, which by itself promotes an allosteric activation of AMPK, especially the binding of AMP (GOWANS et al., 2013). AMP or ADP binding to the γ -subunit of AMPK also induces the phosphorylation of Thr172 by LKB1 (HAWLEY et al., 2003) and drives a conformational change in AMPK, protecting it from phosphatases actions, thus creating an activation loop (GOWANS et al., 2013; XIAO et al., 2011). On the other hand, the non-canonical nucleotide-independent regulation involves a series of cellular alterations that culminates with the phosphorylation of AMPK. Hormones and stress can induce increased levels in intracellular Ca^{2+} which induce the phosphorylation of Thr172 in AMPK by CAMKK2 (HAWLEY et al., 2005). Other mechanisms have been reported to also induce the activation of AMPK such as: (1) phosphorylation of AMPK in different sites by other kinases, like phosphorylation of Ser485 by cyclic-AMP-dependent protein kinase (PKA) in AMPK α 1; (2) the localization of AMPK to the cellular membrane; (3) indirect (by increasing AMP levels) or direct activation by reactive oxygen species (ROS) and (4) DNA-damaging drugs that activate AMPK in a LKB1-independent manner (revised in (GARCIA; SHAW, 2017; HARDIE; ROSS; HAWLEY, 2012)).

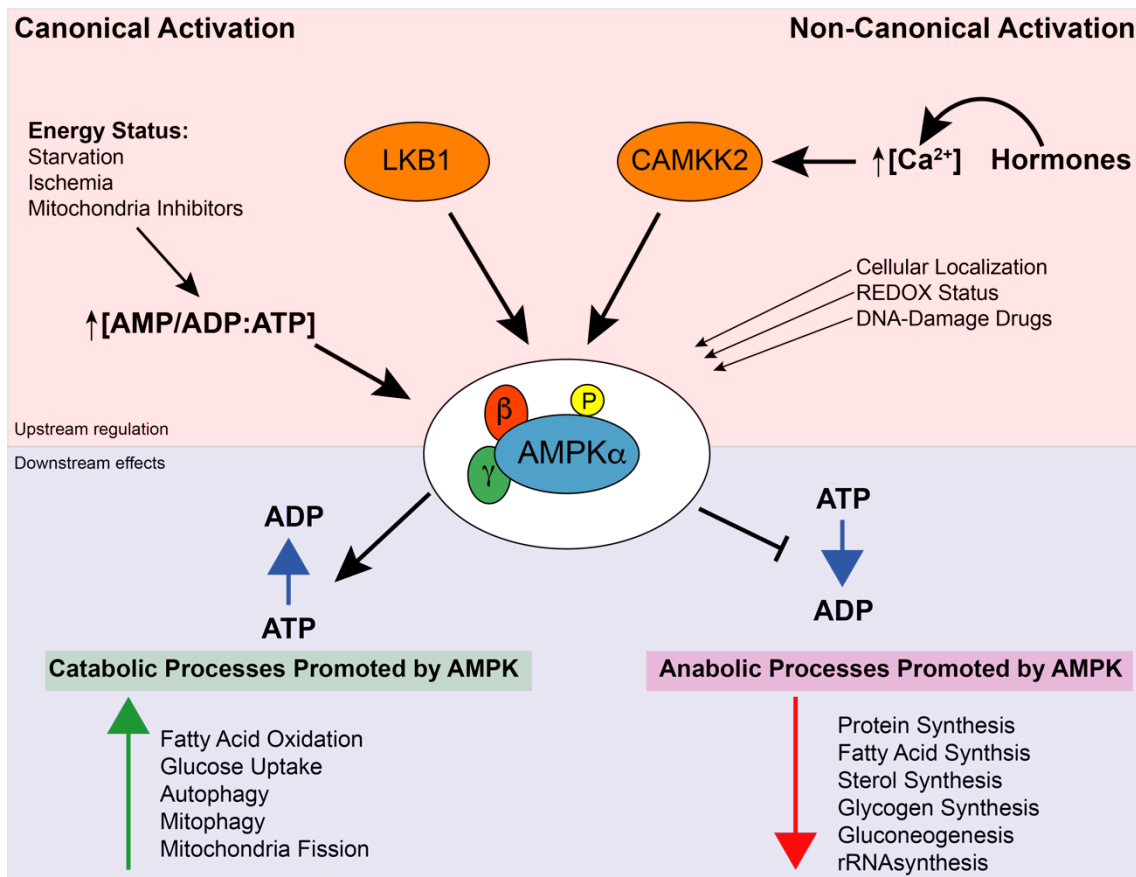


Figure 6: AMPK activation in mammalian cells. Canonical and non-canonical pathways can activate AMPK, mainly altering the AMP/ADP:ATP ratio. However, increases in Ca^{2+} concentration, localization of AMPK within the cells, redox status and DNA-damage drugs might activate AMPK that has as main characteristic the activation of catabolic processes while inhibiting anabolic processes. Adapted from Garcia, D. and Shaw, R.J., *Molecular Cell*, 2017

As already discussed, AMPK activation has as main goal, the restoration of energy homeostasis, by promoting the generation of ATP, via catabolic pathways, and preventing the consumption of ATP by inhibiting anabolic pathways. As consequence, AMPK activation has a direct impact in the overall cellular metabolism affecting lipid, glucose and protein metabolism. Additionally, AMPK activation has an important role in regulating mitochondria dynamics: promoting mitochondrial biogenesis, fission and mitophagy. This apparently contradictory effects of AMPK, promoting mitophagy and mitochondrial fission while promoting, also, mitochondrial biogenesis, suggests that AMPK favors the segregation of damaged and dysfunctional mitochondria and, at the same time, induces the synthesis of new mitochondria to replace the mitochondrial mass, lost by mitophagy (GARCIA; SHAW, 2017; HARDIE; ROSS; HAWLEY, 2012).

AMPK promotes glucose uptake by phosphorylating the thioredoxin interacting protein (TXNIP) (WU et al., 2013a), TBC1 domain family member 1 (TBC1D1)

(PEHMØLLER et al., 2009) and histone deacetylase 5 (HDAC5) (MCGEE et al., 2008) and therefore, by different mechanisms, increasing GLUT1 (TXNIP) and GLUT4 (TBC1D1 and HDAC5) translocation to the membrane, and, thus, glucose uptake, leading to the normalization of AMP:ATP ratio (WU et al., 2013b). AMPK is also a central regulator of lipid metabolism, since it promotes the phosphorylation of ACC1 and ACC2 leading to inhibition of FAS and promotion FAO by an indirect activation of CPT1, since the production of malonyl-CoA, inhibitor of CPT1, is reduced (O'NEILL; KISHTON; RATHMELL, 2016; PEARCE; PEARCE, 2017; WANG et al., 2016). Protein metabolism, which is largely regulated by mTOR, especially mTORC1 (JONES; PEARCE, 2017), is also affected by AMPK, since it can inhibit mTORC1 activity by two different mechanisms: (1) phosphorylation and activation of upstream mTORC1 inhibitor tuberous sclerosis 2 (TSC2) (INOKI; ZHU; GUAN, 2003) and (2) phosphorylation with consequent inhibition of the regulatory-associated protein of mTOR (Raptor) (GWINN et al., 2008), a scaffold subunit of mTORC1 that recruits downstream substrates. AMPK has also been linked with the direct phosphorylation of eukaryotic elongation factor 2 kinase (eEF2K) (LEPRIVIER et al., 2013), a negative protein elongator that is inhibited by mTORC1 (FALLER et al., 2014), reinforcing the importance of correct balance of these two important metabolic sensors and further demonstrating how these two proteins work, counteracting the actions of each other.

2. OBJECTIVES

2. OBJECTIVES

2.1. General Objective

This project had mainly two objectives: (1) to investigate how glucose levels modulate the metabolism and functional properties of human mo-DC, rendered tolerogenic in the presence of VitD3 in healthy donors and in type 1 diabetic patients; (2) to investigate the role AMPK in the tolerogenic properties of tolDC induced by RA, Dex and VitD3 treatments.

2.2. Specific Objectives

- Part I: Characterization of tolDC from type 1 diabetic patients and healthy donors
 - Compare metabolic and immunological properties of mo-DC from healthy donors and type 1 diabetic patients differentiated either in the presence or absence of VitD3;
 - Establish the role of extracellular glucose levels on mo-DC phenotype and functions.
- Part II: The role of AMPK in the tolerogenic properties of DC
 - Compare metabolic and immunological properties of human and mouse DC rendered tolerogenic by VitD3, RA and Dex
 - Establish role of extracellular glucose levels on human tolDC phenotype and function
 - Establish the role of AMPK in the tolerogenic function of human and mouse DC

3. MATERIAL AND METHODS

3. MATERIAL AND METHODS

3.1. Patients

The study comprises 26 healthy donors with no history of T1D or T2D in the family and 37 patients with T1D for over 10 years were recruited from the diabetes/endocrinology department of the university hospital from University of São Paulo. T1D was diagnosed following hyperglycemia, positive autoantibodies (islet cell antibodies [ICA], glutamic acid decarboxylase [GAD] or tyrosine phosphatase-like insulinoma antigen 2 [IA-2]) and undetectable C-peptide or ketoacidosis. All patients are under permanent insulin treatment initiated at diagnosis or within 6 months of diagnosis. HbA1c data are the average of the last 3 examinations performed by patients at the HC-FMUSP outpatient clinic.

The clinical characteristics of the patients are shown in Table 1. The average age of the patients was 37 years old with approximately 25 years of disease, 58.3% of them being female. It can be observed that these are poorly controlled patients, since the average HbA1c was 8.19% (ideal HbA1c value for T1D patients is approximately 7.5%) (REWERS et al., 2014).

More than half of the patients did not present any microvascular complication, 11.1% of the patients presented one complication, while 33.3% of the patients presented two complications.

3.2. Mice

Itgax^{cre} Prkaal^{fl/fl} (AMPKa1) (21124450) mice, transgenic mice with OVA-specific CD4⁺ T cells (OT-II) and WT mice, all on a C57BL/6 background were purchased from The Jackson Laboratory and crossed, housed and bred at the LUMC, Leiden, The Netherlands, under SPF conditions. All animal experiments were performed in accordance with local government regulations and the EU Directive 2010/63EU and Recommendation 2007/526/EC regarding the protection of animals used for experimental and other scientific purposes as well as approved by the Dutch Central Authority for Scientific Procedures on Animals (CCD) (animal license number AVD116002015253).

Table 1 - Clinical Characteristics of diabetic patients.

Characteristics	Controls	Patients	p-value
N	26	37	
Sex			0.74
Female (%)	53.8	62.2	
Male (%)	46.1	37.8	
Age (years)	29 ± 5	38 ± 11	0.005
Age at diabetes onset (years)	-	13 + 10	
Duration of diabetes (years)	-	25 ± 9	
HbA1c (%)	-	8.08 ± 1.19	
Glycemia (mg/dL)	-	218 ± 123	
25 Hydroxyvitamin D (ng/mL)	-	27 ± 6	
Systolic blood pressure (mmHg)	-	120 ± 16	
Diastolic blood pressure (mmHg)	-	76 ± 10	
HDL Cholesterol (mg/dL)	-	60 ± 17	
LDL Cholesterol (mg/dL)	-	100 ± 27	
Triglycerides (mg/dL)	-	85 ± 44	
Total Cholesterol (mg/dL)	-	179 ± 29	
ACE inhibitor treatment (%)	-	9	
GFR _e	-	92 ± 27	
Diabetic nephropathy stages (%)			
Absence	-	84.4	
Incipient	-	6.2	
Established	-	9.4	
Diabetic retinopathy stages (%)			
Absence	-	56.2	
Non-Proliferative	-	31.3	
Proliferative	-	12.5	
Arterial Hypertension (%)	-	24.2	
Cardiovascular autonomic neuropathy (%)			
Absence	-	79.4	
Incipient	-	8.8	
Established	-	11.8	
Peripheral neuropathy (%)			
Absence	-	93.9	
Present	-	6.1	

Results expressed as means ± SD.

Statistics of quantitative parameters are student's T test.

Statistics of qualitative parameters are Chi Square test

Arterial hypertension: systolic blood pressure (SBP) >140 mmHg and/or diastolic blood pressure (DBP) >90 mmHg or presence of antihypertensive medication and history of hypertension. ACE: angiotensin conversion enzyme; GFR_e: estimated glomerular filtration rate; p≤0.05 is significant.

3.3. Differentiation of human monocyte-derived dendritic cells (mo-DC) – Results

Part I

Monocytes were isolated from venous blood and differentiated into mo-DC. In brief, blood was diluted 1: 2 in phosphate buffer saline (PBS) and placed on 12 mL of Ficoll to obtain mononuclear cells. The solution was centrifuged at 900 x g for 30 minutes at 18 ° C, without braking. Subsequently, the formed mononuclear cell layer was removed, placed in a new tube containing PBS, for further centrifugation at 300 x g for 10 min. The cells were washed 2 more times at 250 x g for 10 min and monocytes were isolated using CD14 MACS beads (Miltenyi) according to the manufacturer's recommendations, routinely resulting in a monocyte purity of >95% (Figure 7). Subsequently, 3×10^5 /well of monocytes were cultured in 24 well plate in RPMI medium supplemented with 10% FCS, 100 U/mL of penicillin, 100 µg/mL streptomycin, 2 mM of glutamine and either 5.5 mM of glucose and 25 mM of glucose, equivalent to a normoglycemia (99mg/dL) or a hyperglycemia (450mg/dL). Cells were differentiated in the presence of 50 ng/mL human granulocyte macrophage-colony stimulation factor (GM-CSF – Peprotech USA) and 50 ng/mL of human interleukin-4 (IL-4 – Peprotech USA) to differentiate them into a homogeneous population of immature mo-DC; or cells were differentiated in the presence of 50 ng/mL GM-CSF, 50 ng/mL of IL-4 and 10^{-8} M of VitD3 (VitD DC). On day 6, immature DC were either stimulated with 100 ng/mL ultrapure LPS (mDC) or left untreated (iDC).

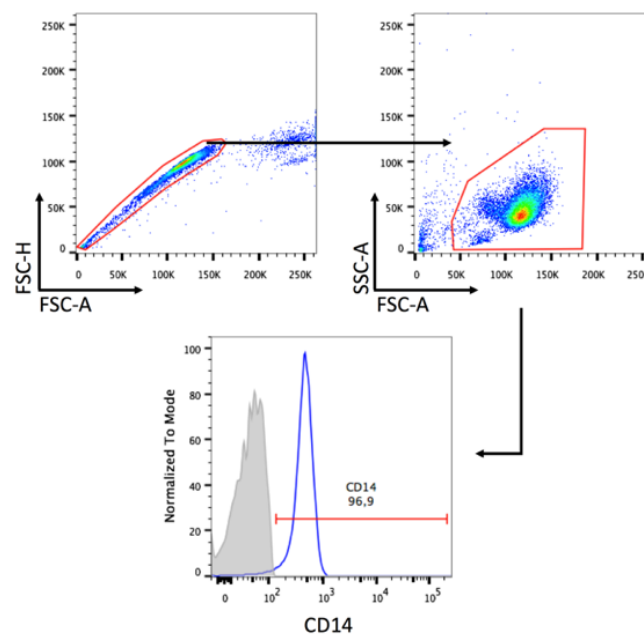


Figure 7: Monocytes purity isolated by magnetic beads from PBMCs.

3.4. Differentiation of human mo-DC – Results Part II

Monocytes were isolated from venous blood or buffy coat and differentiated into mo-DC. In brief, blood was diluted 1: 2 in Hanks' Balanced Salt Solution (HBSS) and placed on 13 mL of Ficoll to obtain mononuclear cells. The solution was centrifuged at 600 x g for 30 minutes at 18 ° C, without braking. Subsequently, the formed mononuclear cell layer was removed, placed in a new tube containing HBSS, for further centrifugation at 1000 rpm for 20 min. The cells were washed 2 more times at 1000 rpm for 20 min and monocytes were isolated using CD14 MACS beads (Miltenyi) according to the manufacturer's recommendations, routinely resulting in a monocyte purity of >95%. Subsequently, 2x10⁶/well of monocytes were cultured in 6 well plate in RPMI medium supplemented with 10% FCS, 100 U/mL of penicillin, 100 µg/mL streptomycin, 2 mM of glutamine, 10 ng/mL human rGM-CSF (Invitrogen) and 0.86ng/mL of human rIL4 (R&D Systems) to differentiate them into a homogeneous population of CD14 low, CD1a⁺ mo-DC. On day 2/3 of the differentiation process, media was refreshed, and the same concentration of cytokines was added to the cells. On day 5, immature DC were either treated with 10⁻⁸ M of VitD3 (VitD DC), 1 µM of retinoic acid (RA DC), 1µM of dexamethasone (Dex DC) or left untreated. In some experiments, the tolerogenic compounds were added on day 0 and refreshed together with the cytokines on day 2/3. On day 6, immature DC were stimulated with 100 ng/mL ultrapure LPS (*E. coli* 0111 B4 strain, InvivoGen, San Diego). In some experiments, at day 5, mo-DC were treated with 10 µM ALDH inhibitor diethylaminobenzaldehyde (DEAB) (Stem Cell Technologies) 30 minutes before treatment with RA.

For a different set of experiments, mo-DC were generated as described before but with different glucose concentration in the medium, as stated in the Results section.

3.5. Differentiation of mouse bone marrow-derived dendritic cells (GMDC)

BM cells were flushed from femurs and the cells were differentiated in 20 ng/mL of GM-CSF (PeproTech) in media comprised of RPMI-1640 (Gibco) supplemented with 5% FCS (Gibco), 25 nM β-mercaptoethanol (Sigma), 100 U/mL penicillin (Eureco-pharma) and 100 µg/mL streptomycin (Sigma), for 8 days in 6-well plate wells, with a medium change on day 4. At day 6, GMDC were either treated with 10⁻⁸M of VitD3, 1 µM of RA or left untreated. At day 7, GMDC were either left untreated or activated with 100 ng/mL of LPS (ultrapure, InvivoGen). In some experiments, at day 7 GMDC were

pulsed with 100 µg/ml OVA (InvivoGen) and 100 ng/ml LPS (ultrapure, InvivoGen) for 24 hours for further experiments.

3.6. Immunological characterization of DC by flow cytometry

After differentiation and maturation of DC under different conditions, both mo-DC and GMDC were measured by flow cytometer to analyze the expression of surface markers. Approximately 1×10^5 cells were placed in 96 V bottom plates and centrifuged for 5 min at 1500 rpm at 4 °C. Each well then received specific antibodies at concentrations predetermined by titration experiments for the markers of interest: (1) for human mo-DC: anti-CD80, anti-CD83, anti-CD86, anti-CD40, anti-HLA-DR, anti-PD-L1, anti-ILT-3, anti-CD103, anti-CD14, anti-LAP and Fixable Aqua Dead Cell Stain Kit (Invitrogen) (2) for GMDC: CD11c, CD11b, CD80, CD83, CD86, CD40, PD-L1 and Fixable Aqua Dead Cell Stain Kit (Invitrogen), The plate was then incubated for 20 min at 4 °C and centrifuged. The cells were washed once with 200 µL of FACS buffer (PBS - phosphate buffered saline, pH = 7.2, 0.5% BSA, 2mM EDTA). After washing, the cells were resuspended in 30 µL of FACS buffer and analyzed by flow cytometer (FACS Canto II or FACS LSR) using FlowJo vX.0.7 software for analysis. For the detection of phosphorylated ACC Ser79 (pACC), cells were left to rest for 1 hour at 37 °C and then immediately fixed for 10 minutes at RT using a 4% methanol-free formaldehyde solution (Polysciences). Then, cells were stained for 30min at 4 °C. The second round of staining included goat anti-rabbit-AF647 to detect the unconjugated rabbit anti-pACC Ser79. All samples were run on a FACSCanto II or BD LSR II and analyses using FlowJo (Version vX.0.7 TreeStar).

3.7. Mitochondrial mass and membrane potential analysis

After obtaining mo-DC, cells were removed from the plate and centrifuged at 300 x g for 10 minutes and a control group was incubated at 37 °C for 30 minutes with 100 µM carbonyl cyanide m-chlorophenylhydrazone (CCCP). Then, all groups were incubated with 200 nM tetramethylrodamine ethyl ester ester (TMRE) and 200 nM MitoTracker Deep Red probe (Invitrogen) at 37 °C for 30 minutes. In some experiments for mitochondrial mass, cells were incubated with 20 nM of MitoTracker Green (Invitrogen). After the incubation period, cells were centrifuged at 300 x g for 10 minutes and resuspended in PBS buffer. Cells were measured in FACS Canto II BD flow cytometer and analyzed in FlowJo vX.0.7 software.

3.8. Glucose uptake and neutral lipids analysis

Cells were centrifuged at 300 x g for 10 minutes and incubated in RPMI for 30 min at 37 ° C with 50 nM of 2-(N-(7-Nitrobenz-2-oxa-1,3-diazol-4-yl)Amino)-2-Deoxyglucose (2-NBDG - Invitrogen) for the analysis of glucose uptake. Additionally, cells were incubated in PBS for 30 min at 37 ° C with 200 nM of bodipy (Invitrogen) for the analysis of neutral lipids content. After the incubation period, cells were centrifuged at 300 x g for 10 minutes, resuspended in PBS buffer and measured in FACS Canto II BD flow cytometer and analyzed in FlowJo vX.0.7 software.

3.9. Retinaldehyde dehydrogenase Activity

The ALDH activity was performed with Aldefluor kit (Stemcell Technologies) according to manufacturer's protocol. Briefly, cells were harvested, transferred to a V bottom 96 well plate, washed in PBS, stained with Fixable Aqua Dead Cell Stain Kit (Invitrogen) for 15 min at RT and then resuspended in 200 µL of assay buffer. 3 µL (end concentration of 45 µM) of ALDH inhibitor DEAB was added to an empty well. Next, 1 µL (1.83 µM) of aldefluor reagent was added to the well with the cells and immediately homogenized and transferred to the well containing DEAB. Samples were incubated for 30 min at 37o C. In some experiments, after the staining with aldefluor, samples were stained with mix of antibodies diluted in assay buffer and kept in assay buffer until the measurement. All samples were run on a FACSCanto II or BD LSR II and analyzed using FlowJo (Version vX.0.7 TreeStar).

3.10. Intracellular cytokine detection on GMDC

After 8 day of differentiation, approximately 1×10^5 immature GMDC were plated in a 96 well flat bottom plate and activated for 6 hours with 100 ng/mL of LPS (ultrapure, InvivoGen) in the presence of brefeldin A. Subsequently, cells were stained with Fixable Aqua Dead Cell Stain Kit (Invitrogen) for 15 min at RT, fixed with 1.9% formaldehyde (Sigma-Aldrich), permeabilized with permeabilization buffer (eBioscience) and stained with anti-IL-6, anti-IL-12, anti-IL-10. Approximately 1×10^5 GMDC activated with LPS for 24 hours were also fixed with 1.9% paraformaldehyde (Sigma-Aldrich), permeabilized with permeabilization buffer (eBioscience) and stained with anti-iNOS. All samples were run on a FACSCanto II or BD LSR II and analyzed using FlowJo (Version vX.0.7 TreeStar).

3.11. Coculture of mo-DC with J558 CD40L-expressing B cells

After harvesting and counting of mo-DC, 1×10^4 cells were cocultured with 1×10^4 CD40L-expressing J558 cells and supernatants were collected after 24 hours to detect the presence of IL-10 and IL12p70 by ELISA (both by BD Bioscience).

3.12. Human T cell proliferation assay

CD3⁺ T lymphocytes were isolated by negative selection using magnetic beads (Miltenyi Biotec Inc.) from PBMCs obtained from healthy donors. After isolation, lymphocytes were incubated in PBS buffer containing 0.5% BSA and 10 μ M of carboxyfluorescein succinimidyl ester (CFSE). Incubation was performed at 37 ° C in the dark for 15 min. Cells were then washed 2 times with PBS and T lymphocytes (at a concentration of 1×10^5 /well) were co-cultured with allogeneic mo-DC for a period of 5 days at a ratio of 30 (LT): 1 (DC). At the end of the co-culture period, lymphocytes were labeled with anti-CD3, anti-CD4, anti-CD8, anti-CD25 fluorescent antibodies. Cells were measured on a FACS LSR FortessaX20 BD and analyzed using the FlowJo vX.0.7 software for analysis.

3.13. Cytometric beads assay (CBA)

Supernatants from mo-DC cultures were evaluated for the presence of cytokines IL-8, IL-1 β , IL-6, TNF- α , IL-12p70 and IL-10 by CBA (BD cat # 551811). Briefly, supernatants and cytokine standards from the commercial kit were incubated with capture microspheres coated with specific antibodies for the respective cytokines and phycoerythrin (PE) labeled detection antibody. After 3h of incubation in the dark at room temperature, 1 mL of the wash solution was added, and the material was centrifuged for 5 min at 200 x g. The supernatants were discarded, and the pellet resuspended in 300 μ L of wash solution. Cytokine detection was performed using a flow cytometer (FACSCanto II) and results were analyzed using the software BD FCAP Array v3.0.1.

3.14. Human T-cell culture and analysis of T-cell polarization

For analysis of T-cell polarization, mo-DC were cultured with allogeneic naive CD4⁺ T cells for 7 days in the presence of staphylococcal enterotoxin B (10 pg/mL). On day 7, cells were harvested and transferred to a 24 well plate and cultured in the presence of rhuIL-2 (10 U/mL, R&D System) to expand the T cells. Two days later, 2x concentrated rhuIL-2 was added to the well and cells were divided into 2 wells. Then, 2/3

days later, intracellular cytokine production was analyzed after restimulation with 100 ng/mL phorbol myristate acetate (PMA) and 1 µg/mL ionomycin for a total 6h; 10 µg/mL brefeldin A was added during the last 4 h. Subsequently, the cells were stained with Fixable Aqua Dead Cell Stain Kit (Invitrogen) for 15 min at RT, fixed with 1.9% formaldehyde (Sigma-Aldrich), permeabilized with permeabilization buffer (eBioscience) and stained with anti-IL-4, anti-IL-13, anti-IL-10, anti-IL-17A, anti-IFN-γ for 20 min at 4 °C. All samples were run on a FACSCanto II or BD LSR II and analyzed using FlowJo (Version vX.0.7 TreeStar).

Alternatively, 1×10^5 T cells were restimulated using anti-CD3 and anti-CD28 (both BD Biosciences). 24 h after restimulation, supernatants were collected, and IL-10 production by T cells was measured by ELISA (BD Bioscience).

3.15. Human FoxP3 intracellular detection

For analysis of human FoxP3 T cells, mo-DC were cultured with allogenic naive CD4⁺ T cells for 11 days in the presence of staphylococcal enterotoxin B (10 pg/mL). On day 6 and 8, rhuIL-2 (10 U/mL, R&D System) was added to expand the T cells. Cells were stained with Fixable Aqua Dead Cell Stain Kit (Invitrogen) for 15 min at RT, fixed with FoxP3/Transcription Factor Staining Buffer Set (Invitrogen, for FoxP3 detection) for 1 hour at 4 °C. Then, cells were washed twice with permeabilization buffer (eBioscience) and stained with anti-CD3, anti-CD4, anti-CD25, anti-CD127, anti-FoxP3, anti-CTLA4, anti-LAP. All samples were run on a FACSCanto II or BD LSR II and analyzed using FlowJo (Version vX.0.7 TreeStar).

3.16. T-cell suppression assay

For analysis of suppression of proliferation of bystander T cells by test T cells, 5×10^4 DC were cocultured with 5×10^5 naive CD4⁺ T cells for 6 days. These T cells (test T cells) were harvested, washed, counted and irradiated (3000 RAD) to prevent expansion. Bystander target T cells (responder T cells), which were allogeneic memory T cells from the same donor as the test T cells, were labeled with 0.5 µM cell tracking dye 5,6-carboxy fluorescein diacetate succinimidyl ester (CFSE). Subsequently, 5×10^4 test T cells, 2.5×10^4 responder T cells, and 1×10^3 LPS-stimulated DC were cocultured for additional 6 days. Proliferation was determined by flow cytometry, by co-staining with CD3, CD4 and CD25 APC. All samples were run on a FACSCanto II or BD LSR II and analyzed using FlowJo (Version vX.0.7 TreeStar).

3.17. In vitro mouse T cell priming assay

OT-II cells were negatively isolated with a CD4⁺ T cell Isolation Kit (Miltenyi) and 1×10^5 CTV-labeled OT II cells were plated in 100 μ L of media together with 100 μ L of media containing either 1×10^4 or 2×10^3 GMDC. After 4 days, cells were harvested and analyzed for proliferation by assessing CTV dilution. For cytokine production, cells were left for 6 days and then 100 μ L of media was removed and replaced with 100 μ L of media containing PMA/Ionomycin (both from Sigma) in the presence of Brefeldin A (Sigma) for 4 hours. Then, cells were stained with Fixable Aqua Dead Cell Stain Kit (Invitrogen) for 15 min at RT, fixed with FoxP3/Transcription Factor Staining Buffer Set (Invitrogen, for FoxP3 detection) for 1 hour at 4 °C, permeabilized with permeabilization buffer (eBioscience) and stained for anti-CD3, anti-CD4, anti-IFN- γ , anti-IL-10, anti-IL-17A, anti-FoxP3 and anti-CD25. All samples were run on a FACSCanto II or BD LSR II and analyzed using FlowJo (Version vX.0.7 TreeStar).

3.18. In vivo mouse T cell priming following DC immunization

In vitro-cultured GMDC were either treated with RA or left untreated and then pulsed with 100 μ g/ml OVA (InvivoGen) and 100 ng/ml LPS (ultrapure, InvivoGen) for 24 hours, after which cells were washed and used for subcutaneous immunization into the hind footpads of mice (5×10^5 DC/footpad). Seven days later, draining popliteal LNs were harvested and OVA-specific CD8⁺ T cell responses was determined by flow cytometry after staining cells with H-2Kb/OVA (SIINFEKL) MHC Tetramer. CD4⁺ and CD8⁺ T cell cytokine production was determined by flow cytometry after incubating the cells in PMA/Ionomycin (both from Sigma) in the presence of Brefeldin A (Sigma) for 4 hours. Then cell were stained with Fixable Aqua Dead Cell Stain Kit (Invitrogen) for 15 min at RT, fixed with 1.9% formaldehyde (Sigma-Aldrich), permeabilized with permeabilization buffer (eBioscience) and stained with anti-IL-4, anti-IL-10, anti-IL-17A, anti-IFN- γ , anti-CD3, anti-CD4 and anti-CD44 for 20 min at 4 °C. For FoxP3+ analysis, cells were stained with Fixable Aqua Dead Cell Stain Kit (Invitrogen) for 15 min at RT, fixed with FoxP3/Transcription Factor Staining Buffer Set (Invitrogen, for FoxP3 detection) for 1 hour at 4 °C, permeabilized with permeabilization buffer (eBioscience) and stained for anti-CD3, anti-CD4, anti-CD25, anti-FoxP3, anti-CTLA4 and anti-GITR. All samples were run on a FACSCanto II or BD LSR II and analyzed using FlowJo (Version vX.0.7 TreeStar).

3.19. Cytokine detection by ELISA

For the detection of IL-10 and IL12p70, BD OptEIA kits were used. Briefly, 96 well half area plates were coated with 50 μ L of capture antibody, diluted in coating buffer (0.1 M Na-carbonaat buffer, pH 9.6) and incubated overnight at 4o C. Then, wells were washed 3 times with 260 μ L of wash buffer (PBS with 0.05% Tween-20) and blocked with 100 μ L of assay diluent (PBS 10% FCS) for 1 hour at room temperature (RT). After 3 washes, 50 μ L of samples and standards were added and plates were incubated for additional 2 hours at RT. Then, plates were washed 5 times and 50 μ L of working detector (detection antibody + SAV-HRP reagent) were added to the wells and plates were incubated for 1 hour at RT. After 7 washes, 50 μ L of substrate solution (tetramethylbenzidine - TMB - and hydrogen peroxide) was added for 30 min at RT followed by 25 uL of stop solution (2N H₂SO₄). Absorbance was read by 450 nm and 570 nM by spectrophotometer. 570 nm absorbance was subtracted by 450 nm and 4 parameters logistic curve was used for calculations.

3.20. Metabolic profile of DC

The metabolic characteristics of mo-DC were analyzed using a Seahorse XFe96 Extracellular Flux Analyzer (Seahorse Bioscience). In brief, 5x10⁴ mo-DC or 7.5x10⁴ GMDC were plated in unbuffered, glucose-free RPMI supplemented with 5% FCS and left to rest 1 hour at 37o C before the assay in an CO₂ free incubator. Subsequently extracellular acidification rate (ECAR) and oxygen consumption rate (OCR) were analyzed in response to glucose (10 mM; port A), oligomycin (1 μ M; port B), fluoro-carbonyl cyanide phenylhydrazone (3 μ M; port C), and rotenone/antimycin A (1/1 μ M; port D) (all Sigma-Aldrich).

3.21. Lipidomic analysis

Lipids quantification were performed by gas chromatography-mass spectrometry (GC-MS). Briefly, DC were differentiated from CD14⁺ monocytes as described in sections 3.3.and 3.4 and on the fifth day cells were harvested and washed twice with PBS. After the second wash, pellet was resuspended in 100% methanol and stored in -80 °C until the moment of the analysis. Methanol extracts were transferred to a glass autosampler vial followed by a consecutively methanol and isopropanol extract of the cells. These cell extracts were combined and dried under nitrogen. Then the dried extracts

were reconstituted in 250 μ L acetone, hydrolyzed and further processed as described before (HOVING et al., 2018).

3.22. Quantitative real-time PCR

RNA was extracted from snap-frozen mo-DC. The isolation of mRNA was performed using Tripure method. Briefly, 500 μ L of Tripure reagent (Sigma) and 1 μ L of RNase-free glycogen (Invitrogen) were added to the pellet of samples. Samples were then vortexed and incubated at RT for 5 min. After this step, 100 μ L of RNase-free chlorophorm was added and samples were inverted vigorously for 30 seconds. Samples were then centrifuged for 12000 x g for 15 min at 4o C and the upper aqueous phase was transferred to a new RNase-free 1.5 mL tube. Then, 250 μ L of 2-isopropanol was added to each tube and after 5 min of incubation samples were centrifuged for 12000 x g for 15 min at 4o C. Next, 500 μ L of 75% ethanol was added, tubes were vortexed and centrifuged for 12000 x g for 15 min at 4o C. As much as possible of ethanol was removed and 30 μ L of RNase-free milliQ water was added to the tubes that were incubated for 10 minutes at 55o C. After this, RNA samples were quantified with NanoDrop (Invitrogen). cDNA was synthesized with reverse transcriptase kit (Promega) using the same amount of RNA for all the samples (settled by the sample with the lowest concentration of RNA). PCR amplification was performed by the SYBR Green method using CFX (Biorad). GAPDH mRNA levels was used as internal control. Specific primers for detected genes are listed in the table below. Relative expression was determined using the $2^{\Delta\Delta C_t}$ method.

Table 2 - Oligonucleotides used for qPCR amplification

Gene	Forward 5'-3'	Reverse 5'-3'
β2-microglobulin	GCCTGCCGTGTGAACCAT	TTACATGTCTCGATCCCACTTAACTAT
RALDH1	TGGCTTATCAGCAGGAGTGT	ACCGTACTCTCCAGTTCTCTTC
RALDH2	GAGCAGGGTCCCCAGATTGA	CCCAGTCCTTTGCCTCCACA
CPT1α	GCGCACTACAAGGACATGGGCA	CACCATGGCCCCGCACGAAGT
GLUT1	ATCGCCCAGGTGTTCCGGCCT	GGCCCCGGTTCTCCTCGTTGC
HK1	GGCGCCATCTTGAACCGCCT	CGCCGGGAATACTGTGGGTGC
HIF-1α	TGGCAGCAACGACACAGAAACT	TTGGCGTTTCAGCGGTGGGT
HK2	CACCGTGCCCGCCAGAAGAC	TCCCCTTTCTCTGTGCCGTCCG
PPARγ	CTCATATCCGAGGGCCAA	TGCCAAGTCGCTGTCATC
PGC1α	ACTGCAGGCCTAACTCCACCCA	ACTCGGATTGCTCCGGCCCT
AMPKα1	TCGGCAAAGTGAAGGTTGGCA	TCCTACCACATCAAGGCTCCGAA
PFKFB3	GAAGGACCTGCGCGTGTGGA	ACAGACGCCCGCGTCGATCTC
IDO	GGTCTGGTGTATGAAGGGTTCTG	GAGGAACTGAGCAGCATGTCTT
ELOVL1	AGCTCCGTGGCTTCATGATT	CGCCAGGTATAGGTGCTCAG
ELOVL2	CTTCTCTCCGCGTACATGCT	CGGATGTCAGCTTCCCCTG
ELOVL3	CCTCTGGTCCTTCTGCCTTG	CACACGGTTTGCTTTAGGCC
ELOVL4	AGATGCGTCTAGTGCTCATTATCT	TCCCACTCTGGCAAATATAGCT
ELOVL5	TTCTTCTGTCAGGGCACACG	GGTGTCTCTGCGCAGGATG
ELOVL6	GGAAGCCATTAGTGCTCTGGT	TGCTTCAGGCCTTTGGTCAT
ELOVL7	CCCTTTGAACTCAAGAAAGCAA	ACCTATACCCCAGCCAGACA
PPARα	TGTGAAGGCTGCAAGGGCTTCT	AGCTGCGGTTCGCACTTGTC
PPARδ	GGTGAAGGGCTTCTCCGTCG	TCCGGCATCCGACAAAACGG
GAPDH	CAGCCTCAAGATCATCAGCA	TGTGGTCATGAGTCCCTCCA
GSK3A	GGGTGAAGCTGGGCCGTGACA	AGCCGTGCCTGGTACACGAC
SIRT1	GGTGCCAGCTGATGAACCGC	GCACTTCATGGGGTATGGAAGTGG
SDHA	TGCTGCCGTGTTCCGTGTGG	ACCATCCCCGGTCGAACGTCT
LKB1	CTGAGGAGGTTACGGCACAA	AGCTGACAGAAGTACCCGTG

3.23. Small interfering RNA (siRNA) electroporation

On day 4 of the DC culture, the cells were harvested and transfected with either 20 nM non-target control siRNA or 20 nM AMPK α 1 siRNA (both Dharmacon) using Neon Transfection System (Invitrogen) with the following setting: 1.600 V, 20 ms width, one pulse. Following electroporation, 1.2×10^6 cells were seeded per well in to a 6-well plate containing RPMI media without antibiotics. After 24 h, culture medium (RPMI) supplemented with 10% FCS, rIL4 (0.86 ng/mL, R&D system) and rGM-CSF (10 ng/mL, Invitrogen) was added. AMPK α 1 silencing efficiency was determined by qPCR and the transfection efficiency was greater than 90%.

3.24. Lymph node and peyer's patch isolation

Lymph nodes (LNs) and peyer's patch (PP) were extracted and collected in 500 μ L of HBSS. Tissues were smashed with the back of a syringe and incubated with digestion buffer (1 μ g/mL of Collagenase D and 2000U/mL of RNase) for 20 minutes at

37 °C. Next, samples were smashed on top of a 100 µm cell strainer and washed 3 times with MACS buffer (PBS - phosphate buffered saline, pH = 7.2, 0.5% BSA, 2mM EDTA). Cells were centrifuged at 1500 rpm for 5 minutes at 4°C, counted and plated for further experiments.

3.25. Small intestine lamina propria isolation

Small intestine was collected, and fat tissues and Peyer's patch were manually removed. Small intestine was opened longitudinally and feces and mucus were removed using PBS and tissues were cut in small pieces of approximately 2 cm and transferred to a 50 mL tube with complete RPMI Glutamax (RPMI Glutamax [Gibco] supplemented with 3% FCS, 100 U/mL of penicillin, 100 µg/mL streptomycin and 20 mM of HEPES) + 5 mM of EDTA. Next, guts were manually shaken for 30 seconds, poured into a sieve, transferred back to 50 mL tubes containing 10 mL of pre-warmed complete RPMI Glutamax + 5 mM EDTA + 1 mM DTT (Invitrogen) and placed in an orbital shaker at 200 rpm for 20 min at 37°C. After that, guts were poured into a sieve and placed back to the 50 mL with 10 mL of complete RPMI Glutamax without FCS. Guts were shaken for 30 seconds and poured back into sieve three times and after the third shaking guts were placed in small plastic cups containing 1 mL of 5x digestion buffer (complete RPMI Glutamax without FCS with 0.3 mg/mL of Liberase LT [Sigma] and 100000U/mL of DNase [Sigma]). Guts were minced, transferred back to the 50 mL tubes and 4 mL of complete RPMI without FCS were added to the samples. Guts were then incubated for 30 min at 37°C shaking for 200 rpm. After digestion, 10 mL of complete RPMI Glutamax were added to the samples and placed in a 100 µm cell strainer on top of a new 50 mL tube. Guts were smashed in the cell strainer and washed with 20 mL of complete RPMI Glutamax. Then, samples were centrifuged at 450 x g for 5 min, resuspended in 10 mL of complete RPMI Glutamax, placed in a 40 µm cell strainer, washed with 10 mL of complete RPMI Glutamax and centrifuged at 450 x g for 5 minutes. Samples were then counted and used for further experiments.

3.26. Lung cells isolation

Lungs were perfused, collected in a 24 well plate and placed on ice. Next, lungs were minced and transferred to a well containing 500 µL of plain RPMI Glutamax. After all lungs were minced, 500 µL of 2x digestion buffer (plain RPMI Glutamax with 200 U/mL of collagenase III [Worthington] and 4000 U/mL of DNase I [Sigma]) were added

to the samples and plate were placed in water bath for 25 minutes. After that, 1 mL of 1x digestion buffer were added to the samples and incubation procedure was repeated. After digestion, homogenates were transferred onto 100 μ m cell strainer on top of a 50 mL tube, washed with MACS buffer and smashed. After 3 washes samples were centrifuged at 400 x g for 10 min at 4o C. Red blood cell were lysate with 2 mL of RBC lysis (0.15 M NH₄Cl, 1 mM KHCO₃, 0.1 mM Na₂EDTA) for 2 minutes and 10 mL of MACS buffer were added to stop reaction. Then, cells were centrifuged as before, counted and plated for further experiments.

3.27. Statistical analysis

Results are expressed as mean \pm standard error mean (SEM) except where stated otherwise. Continuous variables were log-transformed for the analyses when the normality of the distribution was rejected by the Shapiro-Wilk W test and in case of a new normality test failure, the nonparametric alternative was used for the analysis. Comparisons of pDC frequencies (ANCOVA) were adjusted for sex, BMI, mHbA1c, glycemia and duration of diabetes. Differences between groups were analyzed by two-way ANOVA or Kruskal-Wallis (non-parametric analysis) with Tukey HSD or Sidak post-test. If there were only two groups, unpaired Student's t-test or Mann-Whitney test (non-parametric analysis) were used. Statistical analyzes were performed using GraphPad Prism v.8.0 and JMP v9

For the qPCR and lipidome analysis, samples were analyzed using R software. Volcano plots were generated using the fold change data (for both lipidome and qPCR) with the package “metabolomics”. The hierarchical clustering analysis (HCA) and principal component analysis (PCA) plots were generated with the package “pcaMethods”. For the generation of heatmaps data were first rescaled with “scales” package and then scaled data were used to generate the heatmap with “metabolomics” package.

4. RESULTS

4. RESULTS

Part I - Characterization of tolDC from T1D patients and healthy donors

4.1. Characterization of monocytes and blood DC subpopulations in healthy donors and type 1 diabetic patients.

Initially, it was decided to evaluate the frequency of monocyte and DC subpopulations in PBMCs from healthy donors and type 1 diabetic patients. To this end, approximately 1×10^6 PBMCs were separated and labeled with anti-CD3/anti-CD19/anti-CD56 antibodies (called Lineage negative - LIN⁻), anti-CD14, anti-CD16, anti-HLA-DR, anti-CD11c, anti-CD123, anti-CD1c, and anti-CD141.

Supplementary figure 1 (Sup Fig1) shows the gating strategy used to identify DC populations and monocytes. Basically, for the identification of DC, debris and doublets were excluded, and LIN⁻/HLA-DR⁺ followed by HLA-DR⁺/CD14⁻ cells were selected. In these cells one can identify the two major populations of blood DC: CD123⁺CD11c⁻ pDC and classic CD123⁻CD11c⁺ DC cDC. Within the cDC, two additional subpopulations can still be identified, population expressing CD141 (BDCA-3, here called cDC1) and the population expressing CD1c (BDCA-1, called here cDC2). For the identification of monocyte subpopulations, after debris and doublets were excluded, monocytes were gated based on size and granularity, followed by the exclusion of LIN⁺ and HLA-DR⁻CD14⁻ cells. Within this population, it was possible to identify the 3 monocyte populations named: classical monocytes (CD14⁺CD16⁺), intermediate monocytes (CD14⁺CD16⁺) and non-classical monocytes (CD14⁻CD16⁺).

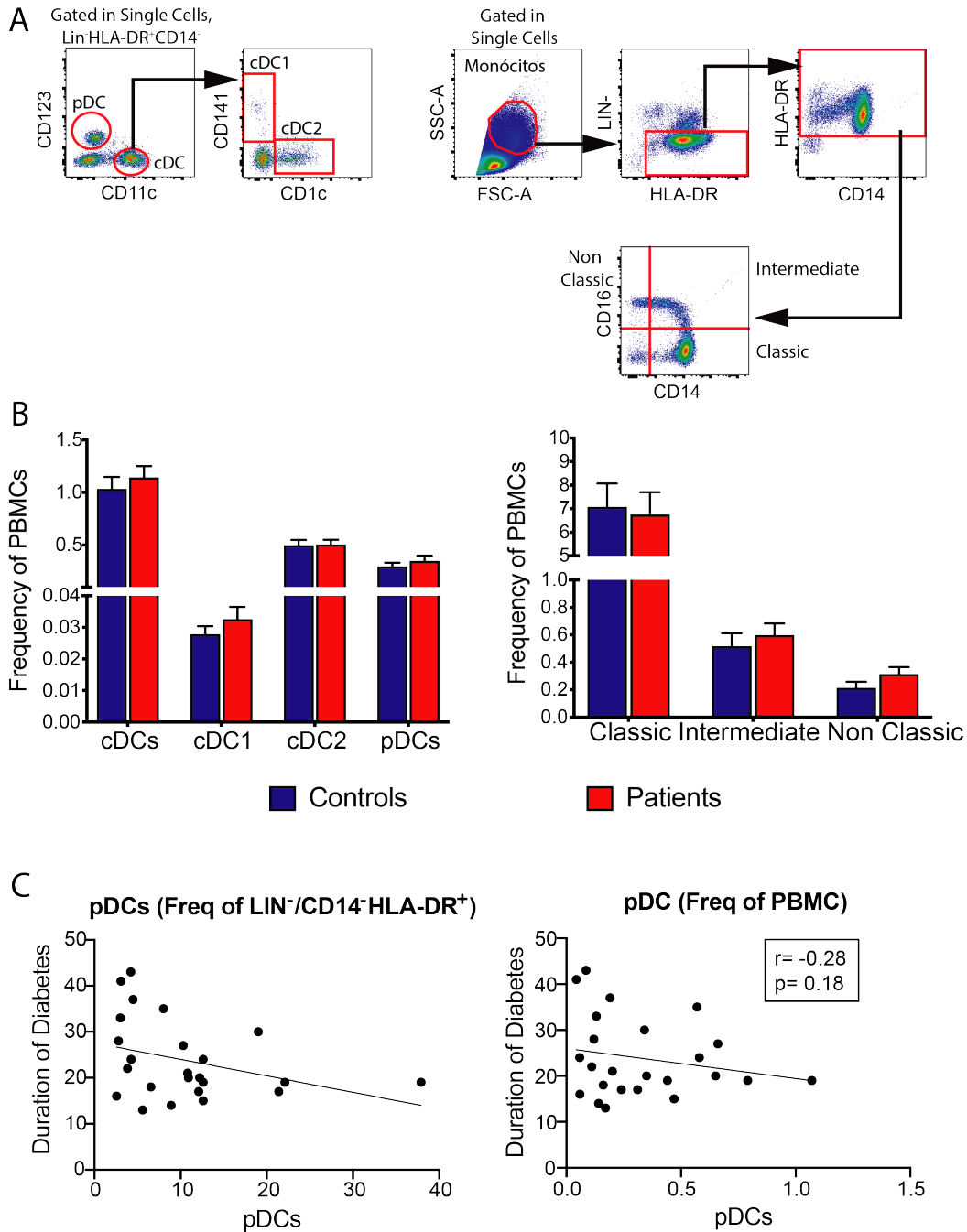
No significant changes were observed in frequencies of DC or monocyte subpopulations when comparing patients with healthy donors (Figure 8B). However, simple correlation analysis showed that frequency of pDC (related to PBMC) tended to be inverse associated with duration of diabetes. Considering the frequency of parental gate (LIN⁻CD14⁺HLA-DR⁺), a significantly inverse correlation was observed between pDC and duration of diabetes (Figure 8C). Interestingly, an ANCOVA analysis adjusted by sex, HbA1c, glycemia and BMI actually showed a significantly inverse correlation between these two parameters (Table 2), suggesting a time-related association between pDC and T1D.

Table 3 - Covariates associated with pDC in T1D patients

	β Coefficient	95% C.I.	p-value
<i>Frequency of PBMC</i>			
Sex (Female)	0.06	-0.373 – 0.497	0.77
BMI	0.14	0.003 – 0.287	0.04
mHbA1c	-0.06	-0.462 – 0.344	0.76
Glycemia	0.00	-0.003 – 0.005	0.52
Duration of Diabetes	-0.05	-0.108 – -0.001	0.04
<i>Frequency of Parent</i>			
Sex (Female)	0.09	-0.223 – 0.421	0.53
BMI	3.29	0.501 – 6.084	0.02
mHbA1c	0.62	-1.68 – 2.299	0.57
Glycemia	0.07	-0.543 – 0.693	0.80
Duration of Diabetes	-1.61	-2.664 – -0.574	0.005

ANCOVA analysis adjusted by Sex, mean HbA1c (mHbA1c), glycemia and duration of diabetes. Statistical analyses test the probability for the independent variable effect (β Coefficient) to be different from zero.

During the analyzes, we observed the presence of a CD123^{lo}CD11c⁺ population, which initially was thought to be present only in diabetic patients. However, this population was also seen in some healthy donors (Figure 9A). The frequency of this population was extremely heterogenous and even absent in some donors or patients. The CD123^{lo}CD11c⁺ population displayed elevated levels of CD16 and, in most cases, it was completely CD16⁺, while the CD123^{hi}CD11c⁺ population, the cDC, had a CD16⁺ and a CD16⁻ population (Figure 9B). As the CD16 marker can be expressed by neutrophils, even starting from PBMC samples, eventual contamination by this cell type could be causing the emergence of such population. However, when comparing the cell distribution by SSC-A x FSC-A (Figure 9C), it was clear that samples both with high or low frequency of CD123^{lo}CD11c⁺ population had similar size and granularity, with no events compatible with neutrophils. NK lymphocytes also express CD16 (COOPER et al., 2001), but we do not believe it to be a contamination with NK cells, which also express high levels of CD56 (marker included in our LIN⁻) and do not express HLA-DR. It is also noteworthy that this population is also not compatible with the populations of cDC1 and cDC2, which express CD141 and CD1c, respectively (Sup Fig2).



By analyzing CD16 expression within the cDC and CD123^{lo}CD11c⁺ populations, it was observed that the CD123^{lo}CD11c⁺ population expressed higher levels of this marker compared to the cDC population (2164 ± 483 vs 465 ± 102 , mean \pm SEM; $p=0.001$) and that this pattern is independent of diabetes (Figure 9D). However, although CD16 expression does not differ between controls and diabetic patients, this population was more frequent among diabetic patients when compared to controls (Figure 9F), and the more defined the CD123^{lo}CD11c⁺ and CD123-CD11c⁺ populations were, the more the dichotomy of CD16 expression is perceived (Figure 9E).

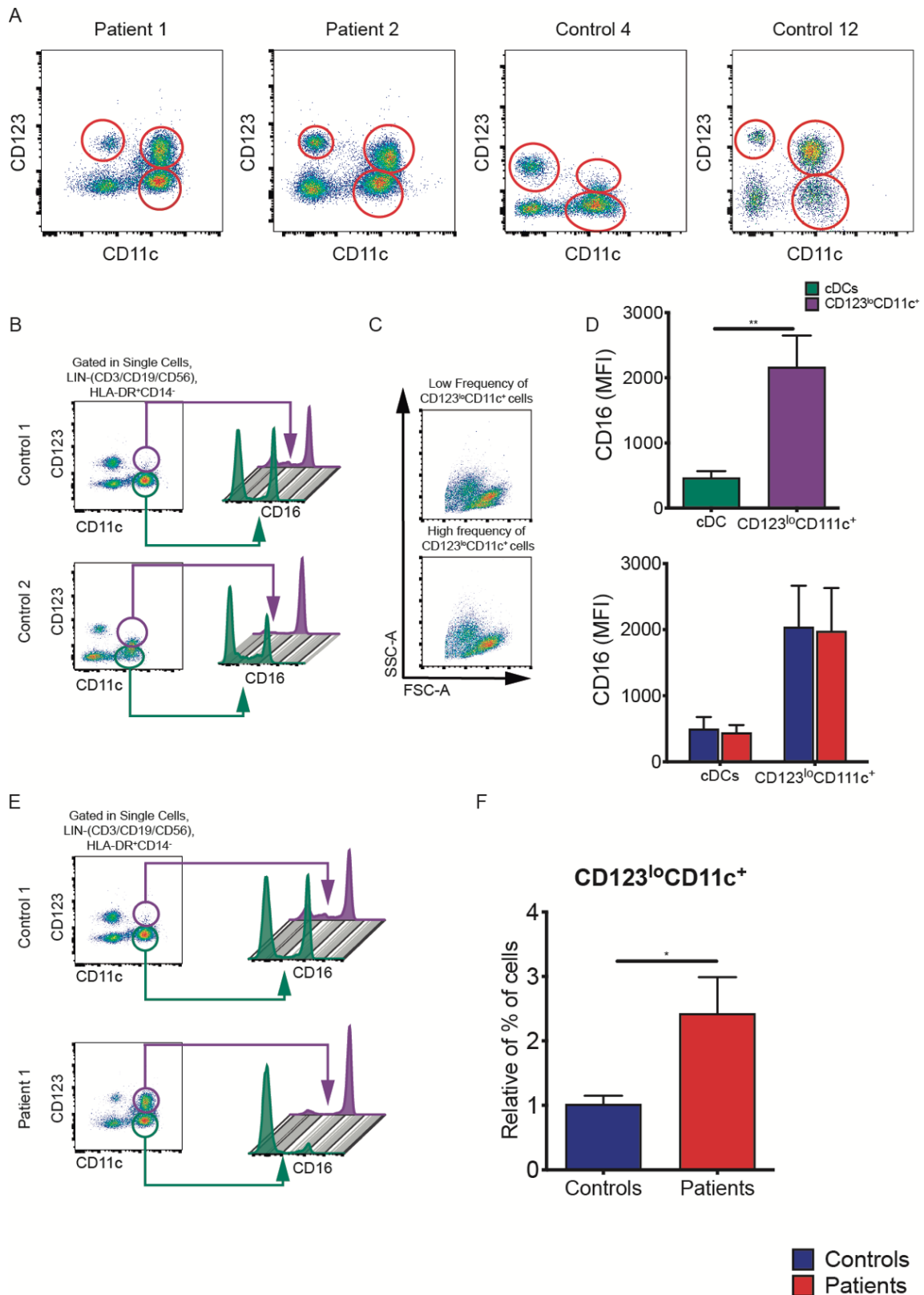


Figure 9: Diabetic patients have a higher frequency of CD123^{lo}CD11c⁺ + blood DC expressing high levels of CD16. (A) Dotplots from four different individuals (2 controls and 2 patients), in which it is possible to identify CD123^{lo}CD11c⁺ population. (B) CD123^{lo}CD11c⁺ cells are mostly CD16⁺ whereas CD123^{hi}CD11c⁺ cells have reduced levels of CD16. (C) Cells with a high or low presence of CD123^{lo}CD11c⁺ population are similar in size, and without signs of neutrophil contamination. (D) The CD123^{lo}CD11c⁺ population expresses higher levels of CD16, and this effect occurs in both controls and diabetic patients. (E) The better the resolution of CD123^{lo}CD11c⁺ cells, the more evident the dichotomy of CD16 expression. (F) The CD123^{lo}CD11c⁺ population was more prevalent in type 1 diabetic patients. Statistics were made with unpaired T test. **** (p < 0.0001), *** (P < 0.001), ** (p < 0.01), * (P < 0.05); n=22-26.

Next we aimed to evaluate the metabolic profile of blood DC. For that purpose, cDC were FACS sorted, plated in the extracellular flux plate (XF plate) and glycolytic test was performed with sequential injections of glucose, oligomycin and 2-DG. Figure 10 shows the metabolic profile of cDC from healthy donors and diabetic patients. It was possible to observe that cDC from diabetic patients tended to have higher glycolysis (Figure 10 B), with a dramatically decrease in glycolytic reserve (Figure 10C), suggesting these cells are already operating at their maximum glycolytic potential right after glucose injection. They also displayed increased levels of basal OXPHOS (Figure 10E), which was unexpected given their glycolytic potential, but might suggest that the mitochondrial from these cells could be oxidizing the glucose in order to produce energy.

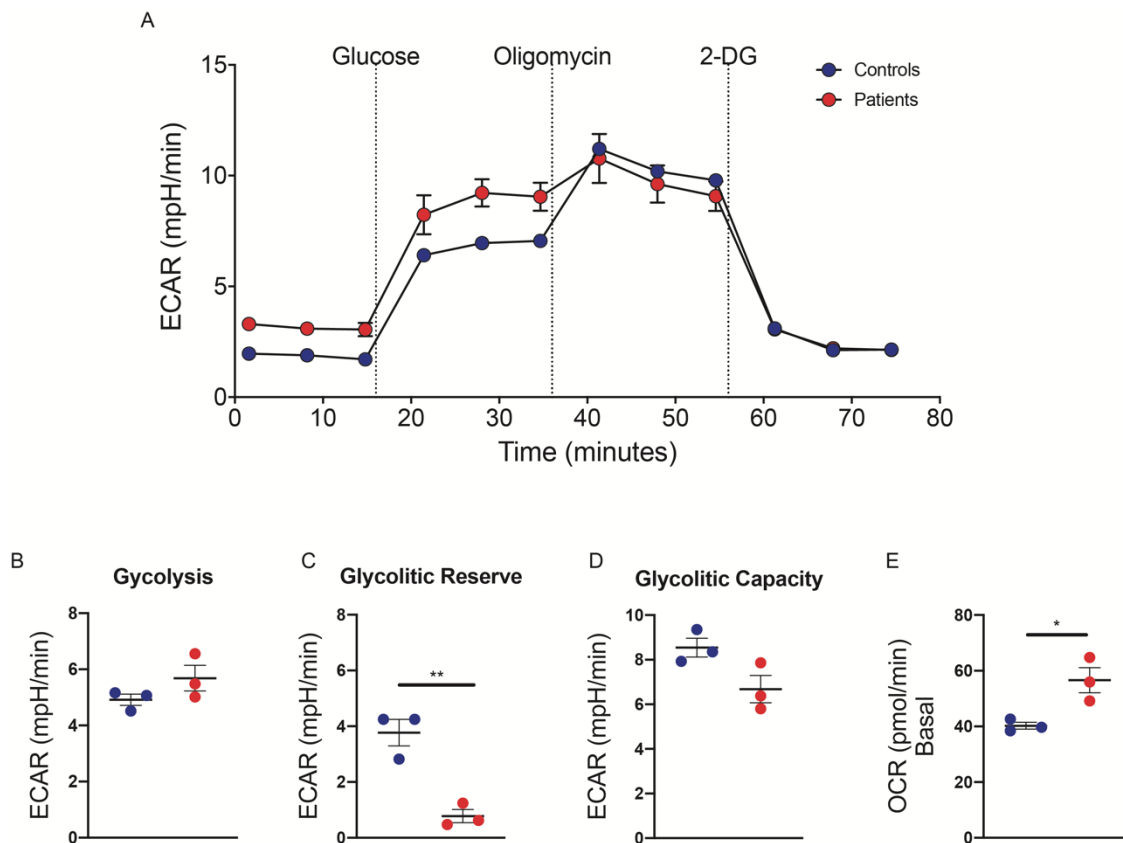


Figure 10: Metabolic profile of blood cDC from healthy donors and diabetic patients. After PBMCs isolation, cDC were FACS sorted and plated (70000 cells) in a XF plate. Then cells received sequential injections of glucose, oligomycin and 2-deoxy-D-glucose (2-DG) to evaluate their glycolytic profile (A) ECAR (B), glycolysis (C), glycolytic reserve (D), glycolytic capacity (E) and baseline levels of OCR measured in cDC from healthy donors and diabetic patients (A E) Data are from 1 experiment. Statistics are unpaired T test. Data shown as mean \pm SEM; * $p < 0.05$, ** $p < 0.01$, *** $p < 0.001$, **** $p < 0.0001$.

Surprisingly, however, cDC from diabetic patients, uptake less glucose and displayed reduced mitochondrial potential membrane. Interestingly, these features were also shared with pDC and classical monocytes. Increased glycolysis and reduced

glycolytic reserve were already associated with LPS activated DC (MALINARICH et al., 2015) and cDC, and even more pronounced classical monocytes, from diabetic patients secreted more TNF- α than cDC and classical monocytes from healthy donors, suggesting these cells could be more activated and in a more inflamed status (Figure 11D)

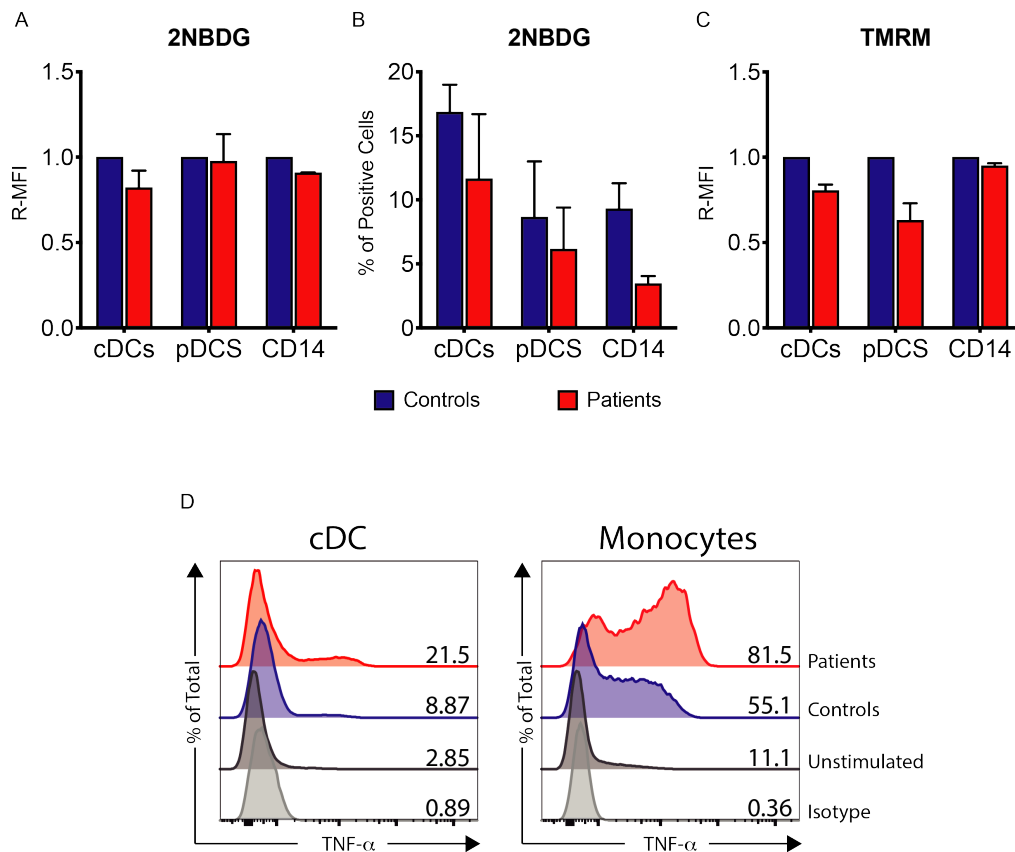


Figure 11: Blood cDC and classical monocytes from diabetic patients secrete higher levels of TNF- α . PBMCs were isolated from healthy donors and diabetic patients and (A;B) stained with 2-NBDG or (C) TMRM for 30 min at 37 °C followed by FACS measuring of the samples to evaluate the uptake of glucose and the mitochondrial potential membrane, respectively. (D) PBMCs were isolated from healthy donors and diabetic patients and stimulated with resiquimod (R848) in the presence of brefeldin-A for 6 hours. Then cells were harvested and intracellularly stained for TNF- α detection. Data are from (A - C) 2 and (D) 1 independent experiment.

4.2. Characterization of surface markers in DC and VitD DC generated at different glucose concentrations

Figure 12 shows data obtained for the expression of CD80, CD86, CD83, CD40, PD-L1 and HLA-DR markers in DC and VitD DC generated in the presence of either 5.5 mM or 25 mM glucose. It was possible to observe that glucose seemed to be important in modulate CD86 expression. When comparing VitD DC and DC, a significant reduction in R-MFI (median relative fluorescence intensity - in this case relative to 5.5 mM DC) of CD86 was observed when cells were cultured in the presence of 25 mM glucose but not when cells were cultured in the presence of 5.5 mM glucose. This reduction was observed

in both patients and controls. Furthermore, it was possible to observe significant differences in CD86 expression, both in controls and patients, when comparing VitD DC differentiated at 25 mM and 5.5 mM of glucose, supporting the idea that glucose concentration is important for the VitD3-limiting expression of CD86 in mo-DC. It was not possible to observe differences in CD86 expression between controls and patients in any of the evaluated conditions.

Especially regarding CD86 expression, it was initially thought that the modulation provided by VitD3 at 25 mM of glucose was limited to controls and not to diabetic patients. Figure 13 shows the expression of CD86 in two healthy donors and two diabetic patients, performed in two independent experiments. In “Experiment 01”, left graph, it is possible to observe an intense reduction on CD86 expression in the healthy donor (approximately 76%), while this reduction was only modest in patient (approximately 35%). However, in “Experiment 02”, the observed phenomenon was switched. While healthy donor displayed a weak reduction (approximately 10%), diabetic patient displayed an intense reduction (approximately 54%). It was not possible to observe an association between the reduction intensity of CD86 expression and patients' blood glucose or HbA1c data. These data suggest that the modulation of CD86 expression by VitD3 might rely on parameters that have not been evaluated/determined in our study.

Although VitD3 was able to decrease the expression of CD80 in a glucose independent manner, both in controls and patients, there was a trend for a stronger modulation in VitD DC from healthy donors differentiated into 25 mM glucose. When comparing the modulation provided by VitD3 in controls, it was possible to observe a trend towards reduction in CD80 expression in VitD DC differentiated at 25 mM glucose compared to VitD DC differentiated at 5.5 mM glucose (0.37 ± 0.10 vs 0.51 ± 0.12 ; mean \pm SD; $p = 0.11$). This does not seem to be so clear in VitD DC of patients (0.27 ± 0.09 vs 0.35 ± 0.12 ; mean \pm SD; $p = 0.55$). It is noteworthy that CD80 expression was reduced in DC from patients when compared to DC from healthy donors and that this reduction was observed at both 5.5 mM of glucose and 25 mM of glucose.

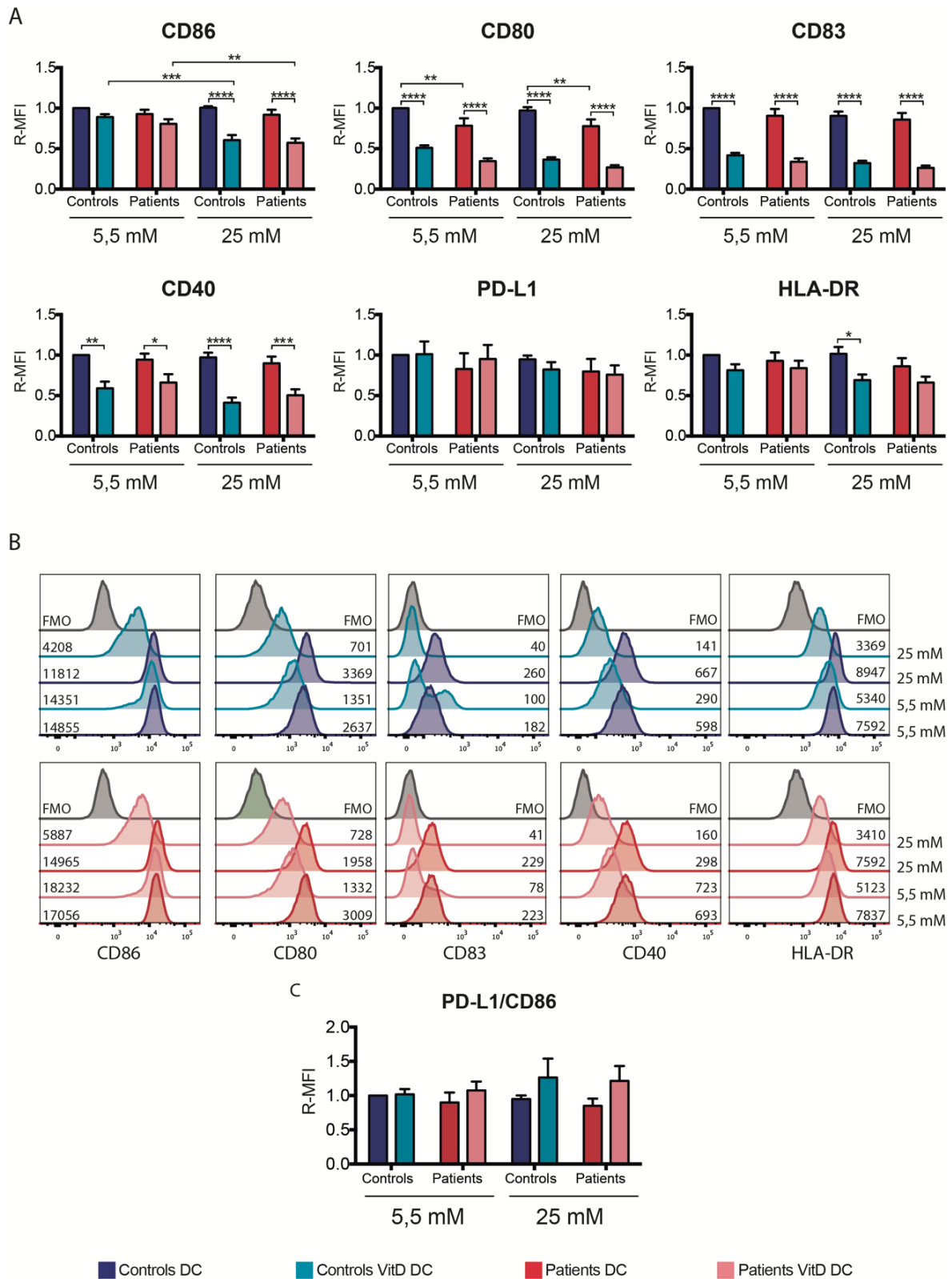


Figure 12: Phenotypic characterization of mo-DC generated from controls and differentiated type 1 diabetic patients at varying glucose concentrations. Mo-DC were differentiated in the presence of 5.5mM or 25mM glucose with GM-CSF and IL-4 (DC) or GM-CSF, IL-4 and VitD3 (VitD DC) and activated on day six with 100 ng/ml LPS. On the seventh day the cells were harvested and stained for flow cytometer analysis. (A) Analysis of relative mean fluorescence intensity (R-MFI) (which is calculated as the ratio of the target MFI group divided by the MFI from DC differentiated in 5.5mM of glucose from healthy donor) for CD80, CD86, CD83, PD-L1, CD40 and HLA-DR. (B) Representative histograms of PD-L1, CD86, CD80 and CD83 markers with the MFI values of one experiment. (C) PD-L1/CD86 Ratio. Statistics were made with two-way ANOVA with Tukey post-test. **** (p < 0.0001), *** (P < 0.001), ** (p < 0.01), * (P < 0.05); n = 14.

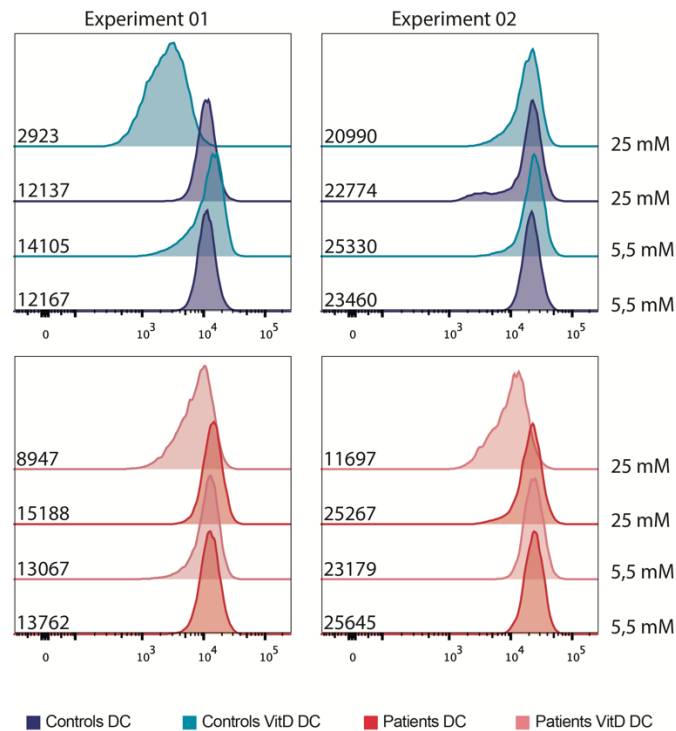


Figure 13: Representative graphs of CD86 expression in two different experiments. Mo-DC were differentiated into 5.5mM or 25mM glucose with GM-CSF and IL-4 (DC) or GM-CSF, IL-4 and VitD3 (VitD DC) and activated on day six with 100 ng/ml LPS. On the seventh day the cells were harvested and stained for flow cytometer analysis.

Although discreet, HLA-DR expression also appeared to be modulated by VitD3 in a glucose-dependent manner in healthy donors. Reduction expression of this marker could be observed when comparing VitD DC with DC differentiated in the presence of 25 mM glucose, but not at 5.5 mM of glucose. It is noteworthy that although VitD3 modulated HLA-DR expression, approximately 99% of the cells remained positive for this marker, suggesting that these cells were still able to present antigens in the context of the major histocompatibility complex class II (MHC-II). The expression of CD83 and CD40 molecules was significantly reduced by VitD3, in both patients and controls, independently of glucose and it was not modulated by T1D. Although expression of PD-L1 was not affected by VitD3, it could be observed that PD-L1/CD86 ratio in these cells was slightly increased, although without significantly statistical differences (Figure 12C).

Taken together, these data suggest that VitD3 seems to induce the differentiation of potentially tolerogenic mo-DC in a glucose-dependent manner and that this effect is even more prominent in healthy donors than in T1D patients.

4.3. Quantification of cytokines secreted by DC and VitD DC generated at different glucose concentrations

Next, secretion of cytokines by mo-DC differentiated in the presence of 5.5 mM or 25 mM glucose was verified. The secretion of TNF- α , IL-10, IL-12p70, IL-6, IL-1 β and IL-8 were evaluated by CBA. No major differences were observed for IL-1 β secretion in none of the groups (Figure 14E). IL-8 could not be evaluated because concentration values for IL-8 were above the curve and were therefore disregarded.

TNF- α secretion was reduced in VitD DC compared with DC group in both controls and patients, only at high glucose concentration, showing that TNF- α secretion followed the same trend observed for CD86 expression. On the other hand, extracellular levels of glucose tended to increase the concentration of TNF- α in both patients and healthy donors when analyzing mo-DC not treated with VitD3. This suggests that while VitD3 is reducing the secretion of TNF- α in a glucose-dependent manner glucose itself is increasing the secretion of TNF- α in non treated mo-DC (Figure 14A).

VitD3 reduced the secretion of IL12p70 in both controls and patients in a glucose-independent manner, although statistical significance could only be observed at high glucose concentration (Figure 14C). In addition, glucose was able to induce IL-12p70 secretion in the DC groups from both healthy donors and diabetic patients and, as observed for TNF- α , glucose-induced increases in IL12p70 secretion was stronger among patients than in healthy donors. However, differently from TNF- α , VitD3 seems to be inducing reduction secretion of IL-12p70 regardless of glucose concentration or disease state.

The only positively modulated cytokine by VitD3 was IL-6 (Figure 14D). Comparing IL-6 secretion between VitD DC and DC groups, in both healthy donors and diabetic patients, it could be observed that VitD DC secreted more IL-6 than DC, when cells were differentiated in the presence of 5.5 mM, especially in patients. Concordantly, when cells were differentiated in the presence of 25 mM glucose, it is also possible to observe an upward trend in IL-6 secretion by VitD DC group, suggesting that VitD3 induces secretion of IL-6, regardless of glucose concentration.

No statistical differences were observed for IL-10, however, it was possible to observe a clear trend in increase IL-10 secretion by mo-DC from diabetic patients. Also, only in diabetic patients, VitD3 was able to induce IL-10 secretion (Figure 14B). This might suggest that either mo-DC from diabetic patients present a more suppressive

profile, being even more susceptible to become tolerogenic after treatment with VitD3 or that mo-DC from diabetic patients are more prone to secrete IL-10 as a negative feedback mechanism to limit a pro-inflammatory status in mo-DC. This hypothesis could be supported by the fact that patients' mo-DC tended to secrete more IL-6 in normoglycemia and also by the fact that both TNF- α and IL-12p70 were positively regulated by glucose.

The IL-10/IL-12p70 ratio followed the same trend as observed in IL-10 secretion. VitD DC, from diabetic patients, had higher IL-10/IL-12p70 ratios and glucose did not significantly modulate this ratio. Although more discreet, and not statistically significant, VitD DC from healthy donors also displayed higher IL-10/IL-12p70 ratio. However, differently from diabetic patients, in which glucose did not affect this ratio, VitD DC from healthy donors differentiated in high glucose levels displayed higher IL-10/IL-12p70 ratio when compared to VitD DC from healthy donors differentiated in higher glucose concentrations (25.74 ± 7.76 vs 9.25 ± 2.83 ; mean \pm SEM; $p=0.01$ when analyzed healthy donors separately) (Figure 14F).

Taken together these data might suggest that glucose has limited role for VitD3 effects on mo-DC cytokine secretion, perhaps being important in reducing TNF- α secretion and increasing IL-10/IL-12p70 ration (only in healthy donors). On the other hand, chronic exposition to high glucose concentration (as in T1D patients) might induce the secretion of important inflammatory cytokines, like TNF- α , IL-6 and IL-12p70 rendering mo-DC perhaps in a low-grade inflammatory status.

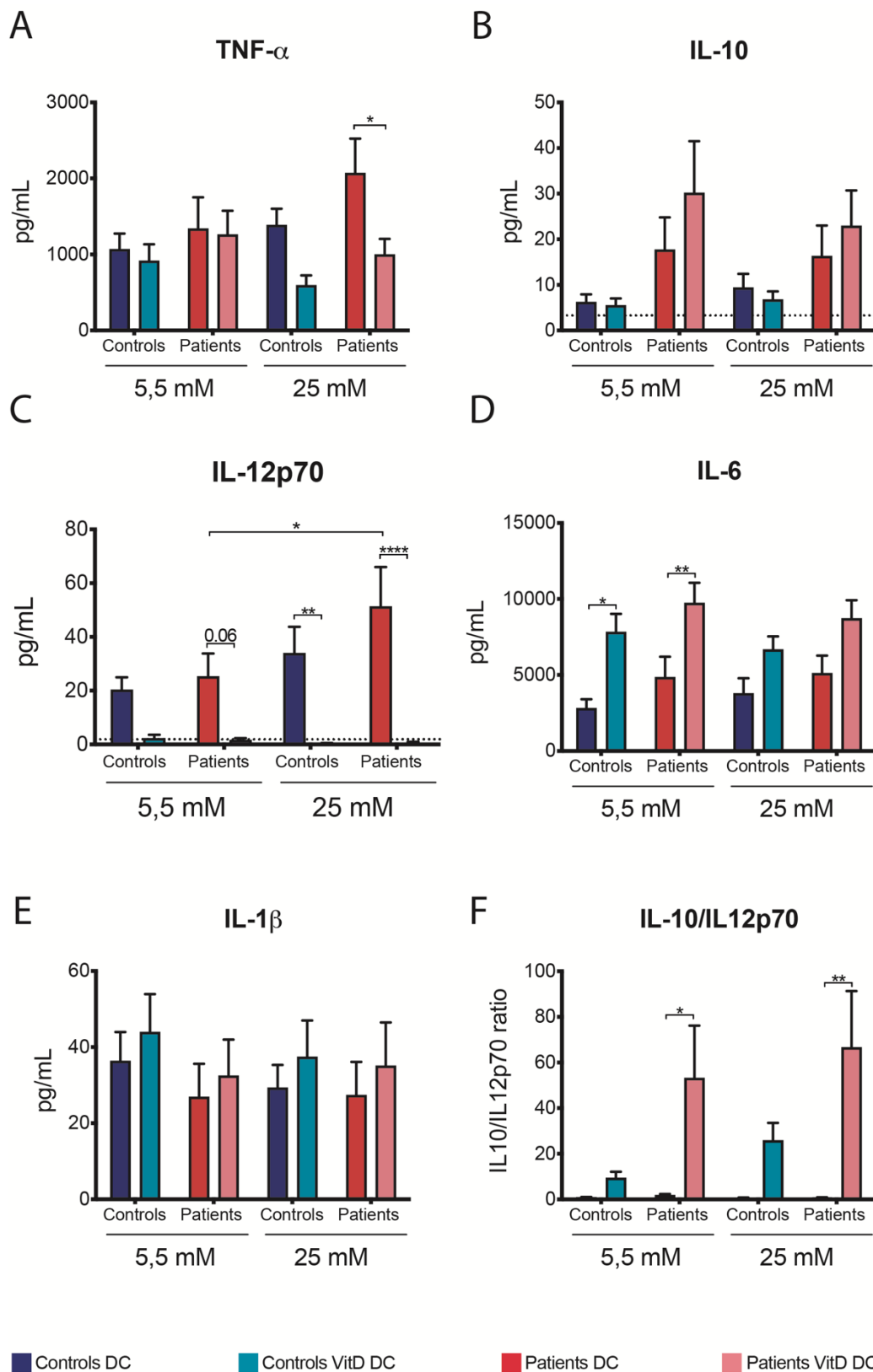


Figure 14: Secretion of TNF- α , IL-10, IL-12p70 and IL-6 in supernatant from DC and VitD DC differentiated in the presence of 5.5 mM or 25 mM glucose. Mo-DC were differentiated in the presence of 5.5mM or 25mM glucose with GM-CSF and IL-4 (DC) or GM-CSF, IL-4 and VitD3 (VitD DC) and activated on day six with 100 ng/ml LPS. On the seventh day the cells were harvested, and the supernatant was frozen to be evaluated by CBA methodology. (A) TNF- α secretion, (B) IL-10 secretion, (C) IL12p70 secretion, (D) IL-6 secretion, (E) IL-1 β and (F) IL-10/IL-12p70 ratio. Two-way ANOVA statistics with Tukey post-test. **** (p < 0.0001), *** (P < 0.001), ** (p < 0.01), * (P < 0.05); n = 14-17.

4.4. Evaluation of lymphostimulatory capacity of mo-DC generated at different glucose concentrations

Next, we aimed to evaluate the functional capacity of mo-DC from controls and diabetic patients by analyzing their capacity to induce proliferation of allogeneic T lymphocytes. To this end, CD3⁺ T lymphocytes from healthy donors were immunomagnetically isolated, stained with CFSE and co-cultured with either LPS-activated DC or LPS-activated VitD DC in a U-bottom 96 plate at a ratio of 1 DC : 30 LT.

It was observed that VitD3 was able to limit lymphostimulatory capacity of mo-DC from both healthy donors and diabetic patients at the two glucose concentrations evaluated (Figure 15). Decreased lymphostimulatory capacity of VitD DC was observed for both CD4⁺ T lymphocytes (Figure 15B) and for CD8⁺ T lymphocyte (Figure 15C). Although without statistically significant difference, glucose appears to modulate VitD DC lymphostimulatory capacity in healthy donors while this was not the case for T1D patients. It could be observed that VitD DC trend to be less efficient in inducing CD4⁺ T lymphocyte proliferation when they were differentiated in the presence of 25 mM of glucose (0.54 ± 0.17 vs 0.72 ± 0.13 ; mean \pm SD; $p = 0.23$). However, this trend did not seem to exist when we analyze the same data on VitD DC from diabetic patients (0.46 ± 0.21 vs 0.53 ± 0.22 ; mean \pm SD; $p = 0.88$). In line with these data, it was also observed a trend for VitD DC from healthy donors to be more efficient in inducing CD4⁺ T lymphocyte proliferation when differentiated in the presence of 5.5 mM glucose than VitD DC from patients differentiated under the same conditions (0.90 ± 0.23 vs 0.53 ± 0.23 ; mean \pm SD; $p = 0.18$). These differences are evident when analyzing data from controls and diabetic patients separately (Figure 15D). Although statistically incorrect, this analysis serves to demonstrate the effects mentioned above. When analyzing only the data from healthy donors, a significant reduction in lymphostimulatory capacity of VitD DC differentiated in the presence of 25 mM glucose was observed when compared to VitD DC differentiated in the presence of 5.5 mM glucose (0.54 ± 0.17 vs 0.72 ± 0.13 ; mean \pm SD; $p = 0.02$). The same analysis, even if performed alone in diabetic patients, did not result in any significant differences (0.46 ± 0.21 vs 0.53 ± 0.22 ; mean \pm SD; $p = 0.98$).

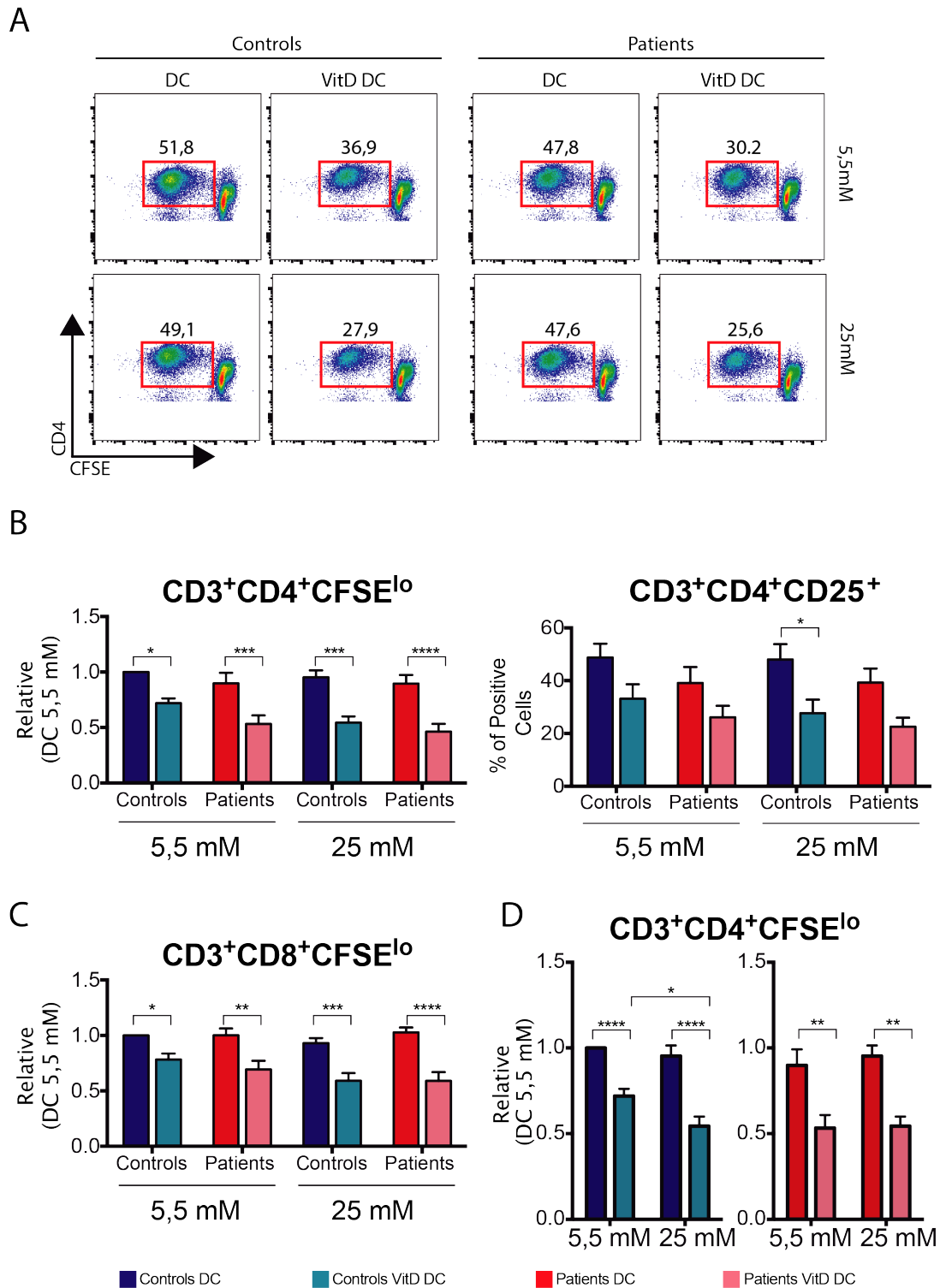


Figure 15: DC and VitD DC lymphostimulatory capacity from healthy donors and diabetic patients, differentiated under various glucose concentrations and activated with 100 ng/mL of LPS. Allogeneic CD3⁺ T lymphocytes were previously stained with CFSE and incubated with DC and VitD DC at a ratio of 1 DC: 30 LT. (A) Representative Dot plot of the lymphostimulatory capacity of mo-DC, in which the abscissa expresses the CFSE fluorescence and in the ordered the expression of CD4. (B) Relative plots (relative to healthy donor's DC differentiated at 5.5mM glucose) of CD3⁺CD4⁺CFSE^{lo} cell proliferation and percentage of CD3⁺CD4⁺CD25⁺ cells. (C) Relative plots (relative to healthy donor's DC differentiated at 5.5mM glucose) of CD3⁺CD8⁺CFSE^{lo} cell proliferation. (D) Relative plots (relative to healthy donor's DC differentiated at 5.5mM glucose) of CD3⁺CD4⁺CFSE^{lo} cell proliferation from controls (left panel) and diabetic patients (right panel). Statistics were performed with two-way ANOVA with Tukey post-test. **** (p < 0.0001), *** (P < 0.001), ** (p < 0.01), * (P < 0.05); n = 9.

4.5. IL-2 quantification in supernatants of allogeneic T lymphocytes co-cultured with mo-DC generated at different glucose concentrations

The IL-2 concentration present in the supernatants of mo-DC and allogeneic T lymphocytes co-cultures was also verified. It was found that co-cultures with VitD DC had lower IL-2 content, regardless of the glucose concentration at which mo-DC were differentiated (Figure 16). This finding, coupled with the fact that VitD DC are less efficient in stimulating the proliferation of allogeneic T lymphocytes, suggests that this is a consequence of the lower proliferation of these lymphocytes, which would result in lower IL-2 secretion in the supernatant; however, this may also indicate that lymphocyte-secreted IL-2 is being consumed by regulatory T cells, characterized by the expression of high levels of CD25 (IL-2 high affinity receptor α chain), the expression FoxP3 transcription factor, to not produce high amount of IL-2 and to have low proliferation rates (RUDENSKY, 2011; SAKAGUCHI et al., 2010). We could observe a trend towards increased Tregs when cells were treated with VitD3 in both controls and patients and regardless of glucose concentration. However, this tendency was not statistically significant and the reduction in IL-2 secretion can actually be a consequence of both reduced IL-2 secretion by T cells with the concomitant consumption of the few IL-2 that is produced by Tregs. (Figure 16B).

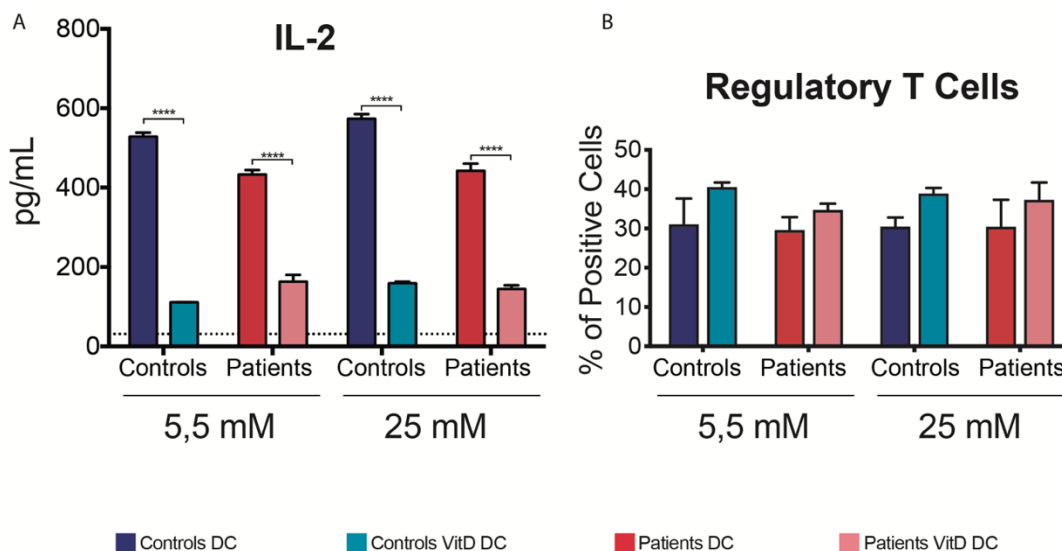


Figure 16: Lower IL-2 concentration in supernatant from CD3⁺ T lymphocyte co-cultured with DC and VitD DC differentiated at different glucose concentrations. Allogeneic CD3⁺ T lymphocytes were incubated with DC and VitD DC at a ratio of 1 DC: 30 LT and after five days of co-cultivation cells were harvested the supernatant was collected and used for IL-2 quantification. (A) Representative chart of IL-2 quantification by ELISA; (B) Frequency of regulatory T cells determined by FACS as CD3⁺CD4⁺CD25^{hi}CD127^{lo}FoxP3⁺ cells. Statistics were performed with two-way ANOVA with Tukey post-test. **** (p < 0.0001), *** (P < 0.001), ** (p < 0.01), * (P < 0.05); n = 1 out of 3 independent experiments (A); n=2 (B).

4.6. Intracellular quantification of cytokines produced by T lymphocytes co-cultured with DC and VitD DC generated at different glucose concentrations

In addition to IL-2 quantification by ELISA, intracellular staining for IFN- γ , IL-4, IL-17 and IL-10 cytokines were also verified. These cytokines are commonly associated with the Th profile induced by DC. Therefore, after seven days of co-culture between mo-DC and allogeneic T lymphocytes, the cells received a second stimulus with 10 ng/mL of PMA and 1.0 μ g/mL of ionomycin in the presence of 1 μ l/mL of brefeldin-A (BD GolgiPlug TM) for 16 hours. Then cells were extracellularly labeled with viability dye, anti-CD4 and anti-CD8, fixed, permeabilized and intracellularly labeled with anti-CD3, anti-IFN- γ , anti-IL-4, anti-IL-17 and anti-IL-10.

No statistically significant differences were observed regarding CD4⁺IFN- γ ⁺, CD4⁺IL-4⁺, CD4⁺IL10⁺, CD4⁺IL-17⁺ and CD4⁺IFN- γ ⁺IL17⁺ cells (Figure 17A and Figure 17B - upper right graph). However, it was possible to observe a trend for reduction of IL-17 positive cells and for IFN- γ and IL-17 double positive cells. No differences were observed in the percentage of CD4⁺IL-10⁺ cells and although this data disagree with many studies in the literature showing that T-lymphocytes co-cultured with mo-DC generated in the presence of VitD3, secrete higher levels of IL-10 (BAKDASH et al., 2014; FERREIRA et al., 2014), a recent work has shown that DC generated in the presence of Dex (added alone or in combination with VitD3 during the mo-DC differentiation), although they were efficient in inducing hypo-response in CD4⁺ T lymphocytes, they were neither able to stimulate increased Tregs cell frequencies nor to stimulate IL-10 production in autologous T lymphocytes (MAGGI et al., 2016).

Although no difference was observed regarding the frequency of IFN- γ positive lymphocytes in any of the conditions evaluated, when analyzing MFI of CD4⁺IFN- γ ⁺ cells, a trend toward the reduction of IFN- γ R-MFI (relative to DC differentiated in the presence of 5.5 mM from healthy donor) was observed when lymphocytes were co-cultured with VitD DC from healthy donors differentiated in the presence of both 5.5 mM (0.71 ± 0.22 vs 1.00 ± 0.00 ; mean \pm SD; $p = 0.24$) and 25 mM glucose (0.64 ± 0.20 vs 0.93 ± 0.15 ; mean \pm SD; $p = 0.24$). This reduction was not observed when analyzing IFN- γ R-MFI from CD4⁺IFN- γ ⁺ cells that were co-cultured with VitD DC from diabetic patients who were able to induce not only the same percentage of CD4⁺IFN⁺ cells but the same amount of IFN- γ .

When analyzing IFN- γ production by CD8⁺ cells, as observed for CD4⁺ cells, no differences were observed regarding the frequencies of CD8⁺IFN- γ ⁺ cells (Figure 17C) in both healthy and diabetic patients. However, unlike what it was observed for CD4⁺IFN- γ ⁺ cells, there was no modulation in IFN- γ R-MFI in CD8⁺IFN- γ ⁺ cells co-cultured with VitD DC from healthy donors.

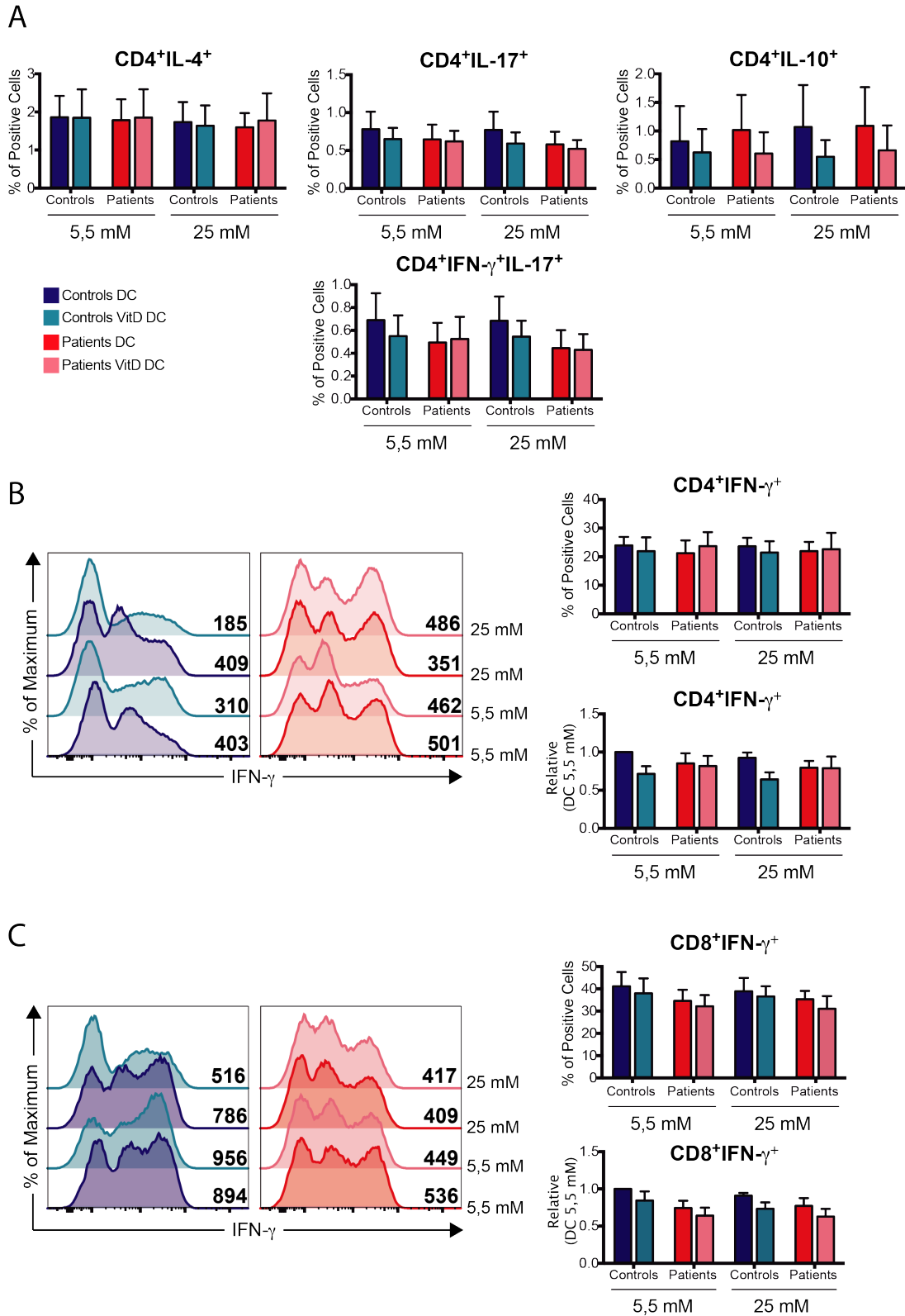


Figure 17: Cytokine pattern secreted by T lymphocytes co-cultured with DC and VitD DC. Allogeneic CD3⁺ T lymphocytes were incubated with DC and VitD DC at a ratio of 1 DC: 30 LT and after five days of co-culture T cells were re-stimulated with PMA/ionomycin in the presence of brefeldin A for 16 hours. Then, cells were harvested and labeled intracellularly for IFN- γ , IL-17, IL-4 and IL-10. (A) Percentage graphs of cells expressing IL-4, IL-17, IL-10, IFN- γ and IFN- γ and IL-17. (B and C) Representative histograms, percent and relative graphs (relative to DC from controls differentiated in the presence of 5.5 mM) of IFN- γ MFI secretion in CD4⁺ (B) and CD8⁺ (C) cells. Statistics were performed with two-way ANOVA with Tukey post-test. **** (p < 0.0001), *** (P < 0.001), ** (p < 0.01), * (P < 0.05); n = 6

4.7. Extracellular flux analysis

Recently, extracellular flux analysis technique has been widely used to determine the bioenergetic state of cells (ANGELIN et al., 2017; EVERTS et al., 2012; EVERTS; PEARCE, 2014). By this technique it is possible to infer whether a cell is preferentially compromised with glycolysis or OXPHOS pathway or if both pathways are being used at the same time. For this purpose, extracellular acidification (a measured called ECAR - Extracellular Acidification Rate) and oxygen consumption (a measured called OCR - Oxygen Consumption Rate) are evaluated in real time. In general, cells with a glycolytic profile, secrete larger amounts of lactate, which is accompanied by the proton H^+ , providing acidification of the medium. For this reason, ECAR measurement is used to determine the glycolytic profile of the cell. On the other hand, cells with OXPHOS profile consume larger amounts of O_2 to feed the production of ATP inside the mitochondria. Thus, the OCR measurement is used as an indicator of the mitochondrial respiration levels of the cell. In addition, it is possible to determine the OCR/ECAR ratio to evaluate which metabolic pathway is preferably used by the cells.

Figure 18 shows the analysis of metabolic profile from DC and VitD DC groups generated at different glucose concentrations from both healthy donors and type 1 diabetic patients. It could be observed that mo-DC from healthy donors generated in the presence of VitD3 showed an increase in both glycolysis and OXPHOS when compared to mo-DC generated only in the presence of GM-CSF and IL-4 (Figure 18B and Figure 18C, respectively). The increase in both metabolic profiles, although observed in the two glucose concentrations, seemed to have been influenced, at least partially, by glucose concentration. Among healthy donors, it was observed that baseline OCR values in VitD DC group were significantly reduced as glucose concentration increased during the period of cell differentiation (Figure 18C).

Also, among healthy donors, it was possible to observe an increase in glycolysis in VitD DC group when compared to DC group when cells were differentiated in the presence of 5.5 mM. However, this phenomenon was not observed when VitD DC were differentiated in the presence of 25 mM glucose (Figure 18B). Interestingly, VitD DC that were differentiated in the presence of 25 mM glucose had reduced glycolysis when compared to the VitD DC differentiated in the presence of 5.5 mM (Figure 18B).

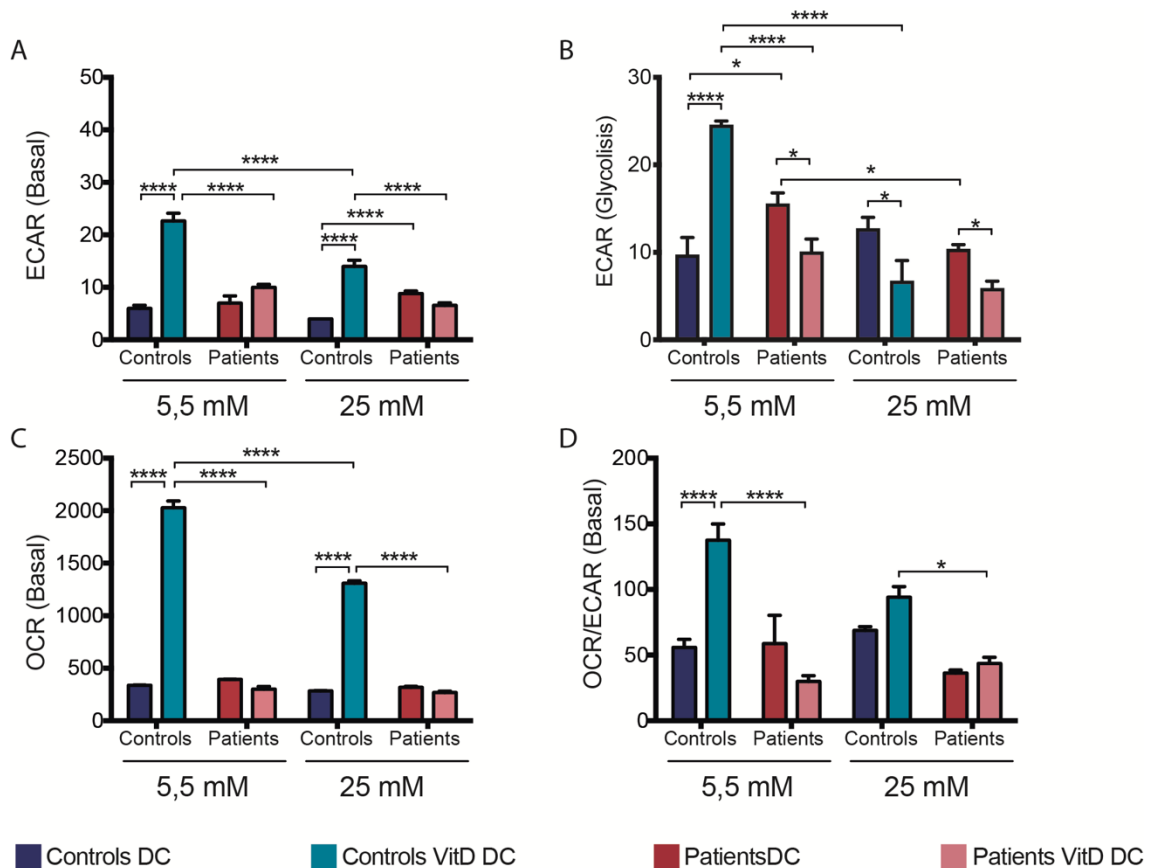


Figure 18: Metabolic profile of DC and VitD DC from healthy donors and diabetic patients. mo-DC were differentiated in the presence of 5.5 mM or 25 mM glucose with GM-CSF and IL-4 (DC) or GM-CSF, IL-4 and VitD3 (VitD DC) and activated on day six with 100 ng/mL LPS. On the seventh day cells were removed, counted and plated on poly-D-lysine pre-treated XF24 plate (90000-140000 cells per well) and allowed to adhere to for one hour in a CO₂-free incubator. Cells were then taken to the XF24 Analyzer for quantification of ECAR and OCR values. (A) Mean ECAR baseline values for DC and VitD DC from healthy donors and patients. (B) Glycolysis in DC and VitD DC from healthy donors and patients. (C) Mean baseline OCR values for DC and VitD DC from healthy donors and patients. (D) OCR/ECAR ratio for DC and VitD DC from healthy donors and patients. Statistics were performed with two-way ANOVA with Tukey post-test. **** (p < 0.0001), *** (P < 0.001), ** (p < 0.01), * (P < 0.05); data are representative of 1 out of 2 independent experiments (A, C, D) or 1 independent experiment (B).

When analyzing the cells from patients with T1D, it was observed that VitD DC had lower glycolytic profile and OXPHOS when compared to VitD DC from healthy donors (Figure 18A, Figure 18B and Figure 18C). Interestingly, VitD DC from diabetic patients had reduced glycolysis (regardless of glucose concentration) when compared to DC group, a characteristic that was also observed in healthy donors differentiated at high glucose concentration (Figure 18B). It was also observed that in diabetic patients, the oxygen consumption of VitD DC is similar to the oxygen consumption of DC, a fact that was not observed in healthy donors (Figure 18C). While OXPHOS in diabetic patients was not affected by the glucose concentration to which the cells were subjected during the differentiation period, that was not the case for glycolysis, which was slightly reduced at higher glucose concentration, especially when cells were not treated with VitD3 (Figure 18B and Figure 18C). Also, when comparing mo-DC not treated with VitD3, glycolysis

was increased in diabetic patients differentiated under normoglycemia, but that was not the case for cells differentiated under hyperglycemia (Figure 18B and Figure 19A). Peritoneal macrophages from diabetic mice also displayed increased glycolytic rates than controls (RAMALHO et al., 2019; Davanso et al. unpublished data presented in Figure 19B with authorization). This might suggest that under normoglycemic situation, cells from diabetic patients consume higher amounts of glucose, perhaps by increased expression of glucose transporters, which would facilitate the increased intracellular glucose track. However, when glucose availability increases, these cells start to undergo to metabolic adaptations leading, perhaps, to a “exhaustion” state causing decrease in the consumption of glucose.

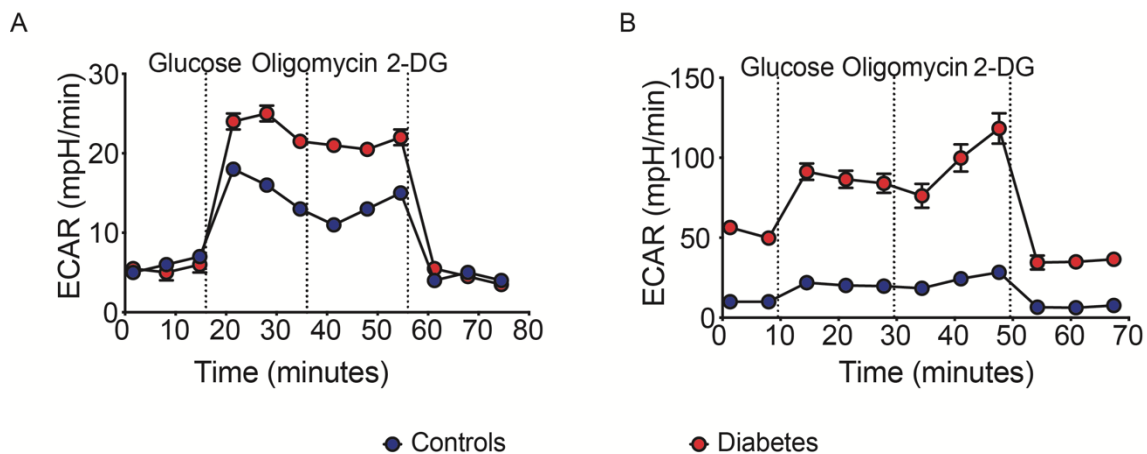


Figure 19: Mo-DC and murine peritoneal macrophages from T1D subjects appears to be more glycolytic than those from controls. (A) ECAR values from mo-DC from T1D patient or control subject. mo-DC were differentiated in the presence of 5.5 mM glucose with GM-CSF and IL-4 and activated on day six with 100 ng/mL LPS. On the seventh day cells were removed, counted and plated on poly-D-lysine pre-treated XF24 plate (90000-140000 cells per well) and allowed to adhere to for one hour in a CO₂-free incubator. Cells were then taken to the XF24 Analyzer for quantification of ECAR values. (B) ECAR values from peritoneal macrophages isolated from mice either treated with streptozotocin (STZ) or left untreated. The peritoneal cells were plated (1×10^5 per well) on XF96 plates, and after 2 hours for adhesion to the plate, were washed to obtain peritoneal macrophages. One hour prior to the assay, cells were left at 37 ° C in the absence of CO₂ and then taken to the XF96 Analyzer for the quantification of ECAR values

Taken together these data suggest that the metabolic reprogramming induced by VitD3 in healthy donor monocytes may not occur in the same way as in diabetic patients' monocytes. The fact that VitD DC from diabetic patients differentiated under higher glucose concentration were not affect neither in glycolysis nor in OXPHOS while in healthy donors both glycolysis and OXPHOS were impaired, might suggest that, in healthy donors, these cells could be using glucose to fuel TCA cycle while the same might not be true for diabetic patients.

4.8. Glucose uptake by DC and VitD DC from healthy donors and T1D patients

When the cell's glycolytic energy demand increases, so does glucose consumption. As an example, to support biosynthesis of fatty acids for the expansion of endoplasmic reticulum and Golgi, rapidly after activation with LPS, DC shift from OXPHOS to glycolysis with consequent increase in glucose consumption (EVERTS et al., 2014a; PEARCE; EVERTS, 2015) and GLUT1 expression (KRAWCZYK et al., 2010). The results obtained in the seahorse experiment are consistent with literature data in which VitD DC have increased glycolysis, suggesting also increased glucose consumption. Based on this, the expression of GLUT1 in mo-DC and VitD DC from controls and diabetic patients differentiated at different glucose concentrations was evaluated (Figure 20).

Although not statistically different, when analyzing GLUT1 R-MFI, it was possible to observe a trend in VitD DC, from both diabetic patients and healthy donors, to increase membrane GLUT1 expression when differentiated in the presence of 5.5 mM glucose. This trend was not observed when cells were differentiated in the presence of 25 mM glucose (Figure 20A). These results might suggest that VitD DC differentiated in the presence of 5.5 mM of glucose have a greater ability to increase membrane GLUT1 expression, which would be consistent with Seahorse data, suggesting that, at least in healthy donors, not only the increase in glycolysis, but also GLUT1 expression and, potentially, the glucose uptake, would be dependent on glucose concentration in VitD DC. Because mo-DC from diabetic patients displayed higher glycolysis at normoglycemia, we would expect that the expression of GLUT1 to also be increased in these cells. However, it was observed that both DC and VitD DC from diabetic patients had lower R-MFI values when compared to DC and VitD DC from healthy donors, regardless of the glucose concentration in which these cells were differentiated (Figure 20A).

As DC and VitD DC from healthy donors showed higher expression of the transporter membrane GLUT1 after activation with LPS, we hypothesized that this increase in GLUT1 could lead to higher glucose uptake by healthy donors. To this end, glucose uptake was evaluated by flow cytometry using 2-NBDG (a glucose-like fluorescent compound widely used in the literature to study glucose uptake by cells (BUCK et al., 2016; EVERTS et al., 2014b; IP et al., 2017)). Therefore, DC and VitD DC from healthy donors and diabetic patients were differentiated in the presence of either 5.5 mM or 25 mM glucose and activated with LPS for 24 hours. After this time, cells

were harvested and incubated with 50 nM of 2-NBDG in PBS at 37 °C for 1 hour and measured by flow cytometer. Surprisingly, as can be seen in Figure 20B, no differences between healthy donors and patients were observed in none of the groups, which could suggest that some other glucose transporter may be compensating the reduced expression of GLUT1 observed in diabetic patients. However, VitD DC from healthy donors and diabetic patients were able to uptake more glucose than DC, independently of glucose concentration

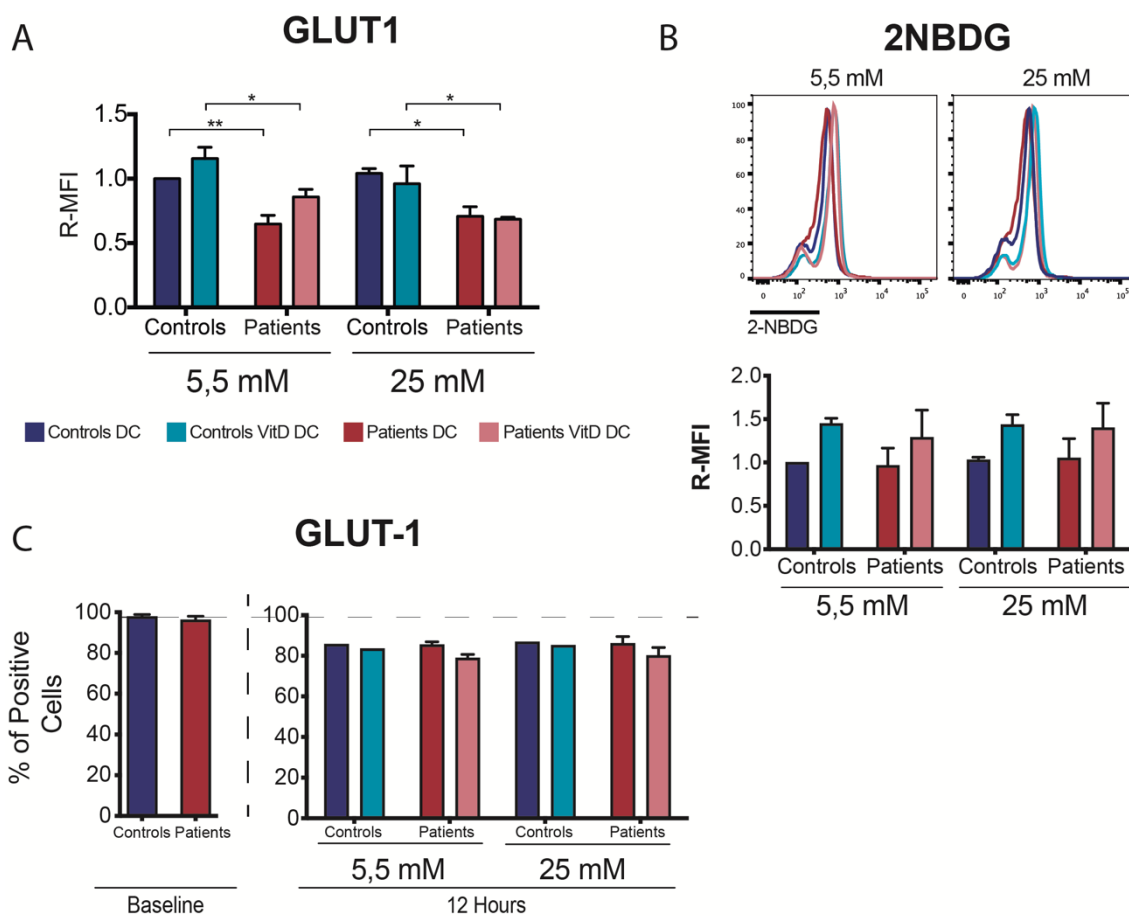


Figure 20: GLUT1 expression in mo-DC and monocytes and glucose uptake by DC and VitD DC from healthy donors and diabetic patients. mo-DC were differentiated in the presence of either 5.5 mM or 25 mM glucose with GM-CSF and IL-4 (DC) or GM-CSF, IL-4 and VitD3 (VitD DC) and activated on day six with 100 ng/ml of LPS for 24 hour in which cells were harvested and GLUT1 expression and glucose uptake were evaluated. (A) R-MFI graph (relative to DC from healthy donors differentiated in the presence of 5.5 mM glucose) from GLUT1 expression. (B) Representative histograms and R-MFI (relative to DC from healthy donors differentiated in the presence of 5.5 mM glucose) plot of 2-NBDG uptake by DC and VitD DC. (C) Expression of GLUT1 in monocytes and dMo 12 hours after receiving stimulus for differentiation in DC or VitD DC. Statistics were performed with two-way ANOVA with Tukey post-test. **** (p < 0.0001), *** (P < 0.001), ** (p < 0.01), * (P < 0.05); n = 6 (Figure 11A); n = 4 (Figure 11B); n = 2-6 (Figure 11C).

In order to better understand the effects regarding GLUT1 expression and glucose uptake in mo-DC from healthy donors and diabetic patients, GLUT1 expression was evaluated in fresh CD14⁺ monocytes isolated from PBMC as well as in differentiating

monocytes 12 hours after monocytes were stimulated with GM-CSF and IL-4 or GM-CSF, IL-4 and VitD3 (these monocytes will be called dMo). There were no differences in GLUT1 expression when analyzing fresh CD14⁺ monocytes from healthy donors and diabetic patients isolated from PBMCs (Figure 20C). It was observed that 12 hours after the differentiation, dMo showed reduction in membrane GLUT1 expression, which could indicate that these cells internalized this transporter to capture the glucose present in the culture medium. No significant differences could be observed in GLUT1 membrane expression in dMo. However, it was possible to observe a trend for VitD3 to decrease membrane GLUT1 expression in dMo of diabetic patients, suggesting that these dMo would be capturing more glucose than dMo who did not receive VitD3.

Taken together these data suggest that after activation with LPS, VitD3 appears to increase GLUT1 expression when mo-DC are differentiated at low glucose concentrations, without, however, affecting the glucose consumption by the cells. Yet, because we measured the surface expression of GLUT1, other modulations induced by the internalization of this molecule might have occurred that were missed by us (better discussed in the Discussion section)

4.9. Mitochondrial mass and potential membrane analysis in mo-DC and VitD DC from healthy donors and T1D patients

In addition to increased glycolysis, VitD DC from healthy donors also displayed increase values of basal OCR when VitD DC were differentiated in the presence of 5.5 mM glucose. Additionally, these cells displayed higher OCR/ECAR ratio, suggesting a predominance of OXPHOS over glycolysis. It has been shown that effector T lymphocytes, which have a predominantly aerobic respiration metabolic profile, when becoming memory T lymphocytes, change their metabolism toward OXPHOS and FAO (BUCK et al., 2016). This change is characterized by increased OCR/ECAR ratio with predominance of OXPHOS over glycolysis (BUCK et al., 2016). The same work demonstrated that this change was provided by altered fission/fusion balance in mitochondria, with effector cells having fissioned mitochondria while memory T cells had fused mitochondria. Since VitD DC from healthy donors had a similar profile, with higher baseline OCR values and OXPHOS predominance over glycolysis, we hypothesized that VitD3 could also modulate mitochondrial fitness.

For this purpose, mitochondrial mass and membrane potential ($\Delta\psi_m$) were evaluated using TMRE and MitoTracker Deep Red probes, respectively. In mitochondrial

membrane potential experiments, a control group was added to which 100 μM of CCCP (a compound with the ability to decouple mitochondria inducing loss of membrane potential) was added. Figure 21 shows the results obtained for membrane potential (Figure 21A), mitochondrial mass (Figure 21B) in addition to the OCR (Figure 21C) and OCR/ECAR (Figure 21D) data observed in the Seahorse experiment. It could be observed that even with a marked increase in oxygen consumption by VitD DC from healthy donors, surprisingly no changes were observed regarding mitochondrial membrane potential or mitochondrial mass in none of the groups evaluated. These data suggest that VitD3 is not changing mitochondrial mass or membrane potential; however, the increased OCR values observed might, yet, be a consequence of VitD3-induced increase fusion/fission ratio leading to more functional mitochondria without necessarily affecting its mass or membrane potential.

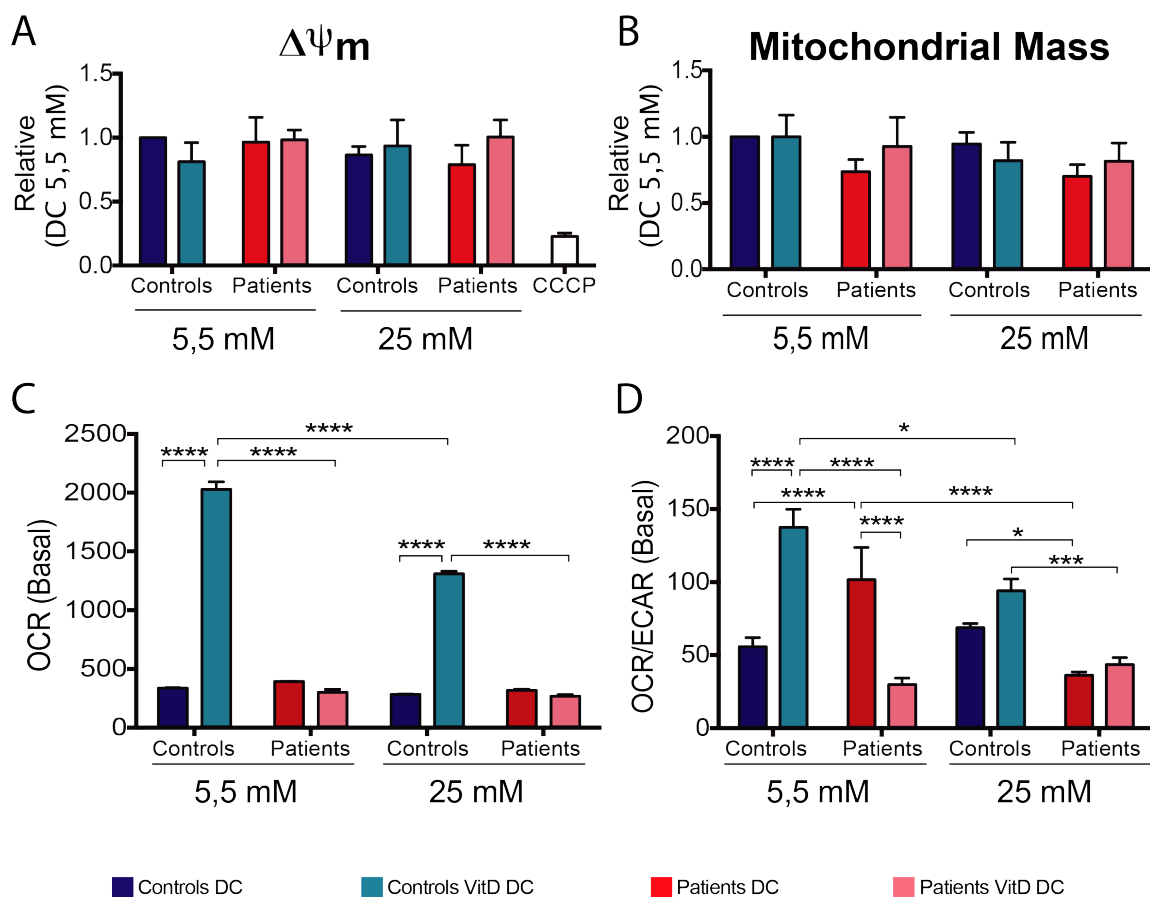


Figure 21: Analysis of the mitochondrial mass and membrane potential of DC and VitD DC from healthy donors and diabetic patients differentiated in the presence of either 5.5 mM or 25 mM glucose. mo-DC were differentiated in the presence of either 5.5 mM or 25 mM glucose with GM-CSF and IL-4 (DC) or GM-CSF, IL-4 and VitD3 (VitD DC) and activated on the sixth day with 100 ng/mL of LPS for 24 hour, in which cells were harvested and incubated with TMRE or MitoTracker Deep Red. (A) Mitochondrial membrane potential graph ($\Delta\psi_m$) and (B) mitochondrial mass of DC and VitD DC. (C) OCR and (D) OCR/ECAR data from DC and VitD DC. Statistics were performed with two-way ANOVA with Tukey post-test. **** (p < 0.0001), *** (P < 0.001), ** (p < 0.01), * (P < 0.05); n = 6 (A and B); n = 2 (C and D).

Part II – The role of AMPK in the tolerogenic properties of DC

4.10. Characterization of tolDC

4.10.1. RA DC, VitD DC and Dex DC differ in many characteristics, but are equally suppressive

We decided to select VitD3, RA and Dex as tolerogenic compounds since a large data in literature confirm their ability to induce tolDC either alone or in combination (BAKDASH et al., 2015; FERREIRA et al., 2014; 2015; MAGGI et al., 2016; MALINARICH et al., 2015; VANHERWEGEN et al., 2018). However, none of these studies compared the metabolic properties of each one of these induced tolDC. First, we aimed to confirm that VitD3, RA and Dex were indeed capable of generating tolerogenic mo-DC and results are shown in Figure 22. CD14⁺ monocytes were treated with GM-CSF and IL-4 plus either VitD3, RA or Dex on day 0. Tolerogenic compounds were on refreshed together with the cytokines on day 2/3 and on day 6, mo-DC were activated with 100 ng/mL of LPS for 24 hours. In the first experiment, two concentrations of each compounds were tested 0.01 μ M and 0.1 μ M of VitD3, 0.1 μ M and 1.0 μ M of RA and Dex. Since the results were similar, the dose of 0.01 μ M of VitD3 and 1.0 μ M of RA and Dex were selected. Those doses were the ones already being used in Brazil, in the case of VitD3 and the doses of RA and Dex previously used in the lab of Dr. Bart Everts.

Both VitD3 and Dex were able to decrease the expression of important co-stimulatory molecules, such as CD80, CD86, CD83 (Figure 22A), increase the secretion of IL-10 and decrease the secretion of IL12p70 (Figure 22B). RA did not decrease the expression of co-stimulatory molecules on mo-DC and also had no effect on the secretion of IL-10 and IL-12p70 by mo-DC; however, the expression of important inhibitory molecules such as PD-L1 and ILT3 was significantly increased (Figure 22A). It is worth noting that the expression of CD103 was significantly increased by RA. CD103 is an α E integrin commonly associated with mucosal sites, specially the intestine, where epithelial cells are able to metabolize the dietary vitamin A into RA, that in turn, instructs the differentiation of tolDC (ILIEV et al., 2009; LAMPEN et al., 2000). Increased expression of CD103 had already been shown as a consequence of RA treatment, generating functionally tolDC (BAKDASH et al., 2015; SWAIN et al., 2018).

We also functionally analyzed the tolDC by investigating the properties of T cells primed by these DC (Figure 22C, Figure 22D and Figure 22E). The secretion of IFN- γ was significantly decrease when T cells were primed with all 3 types of tolDC. On the

other hand, the secretion of IL-10 by T cells, was significantly increased when T cells were primed by RA DC and we could also observe a trend in increase the secretion of IL-10 when T cells were primed by Dex DC when compared with control DC (2.66 ± 1.6 vs 1.0 ± 0.0 , $p=0.55$). The most important characteristic of a tolDC, is to induce T cells that are functionally able to suppress the proliferation of bystander T cells. As observed in Figure 22E, DC primed with all the tolerogenic compounds were efficient in generating tolerogenic T cells as evidenced by their capacity to suppress the proliferation of autologous memory T cells.

We also analyzed the metabolic profile of tolDC and could observe that VitD DC are the tolDC that present the most striking metabolic differences, compared to the untreated DC (Figure 23). It was possible to observe that VitD DC were metabolic more active than all the other DC; they had higher basal values of OCR (Figure 23B) and maximal respiration (Figure 23C) and were highly glycolytic as well (Figure 23E). Those results are in agreement to the results observed for us in Brazil, reinforcing the highly metabolic profile of those cells. In addition to understanding how changed in glucose concentrations could affect tolDC phenotype, we aimed to find some common metabolic mechanisms that could potentially be important for the function of tolerogenic DC. A common feature of DC is the ability of those cells to rapidly switch from OXPHOS to glycolysis after the engagement of TLR ligands (EVERTS et al., 2014a; GUAK et al., 2018). We were interested to know if tolerogenic DC are also able to promote this rapid switch towards glycolysis. As depicted in Figure 24A, all the tolerogenic DC were able to induce a rapid glycolytic metabolism after LPS stimulation, as observed in the control DC. However, different from what we can see in the control group, the increased glycolytic metabolism is also accompanied by an increase in OCR values, especially in the VitD DC group, but this pattern could be observed in all tolerogenic DC (Figure 24B).

The concomitant increase in OXPHOS with glycolytic metabolism in response to the LPS might suggest that glucose in tolerogenic DC is being oxidized in the mitochondria to increase OXPHOS to support production of ATP. Taken together these results suggest that all three tolerogenic compounds were able to induce functionally tolDC, even though differences could be observed among them regarding surface markers, IL-10 and IL-12p70 secretion and metabolic profile.

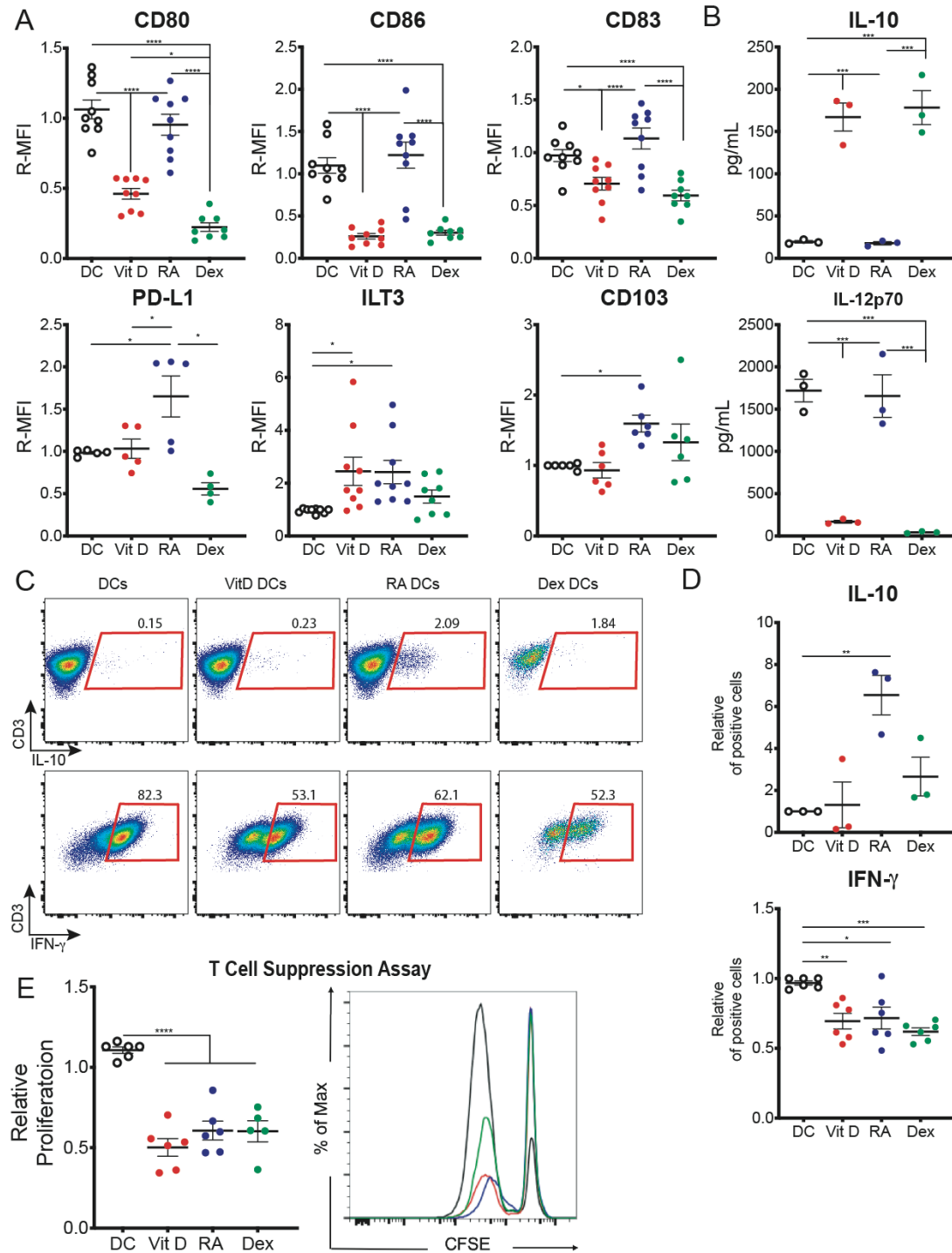


Figure 22: Characterization of mo-DC rendered tolerogenic by VitD3, RA or Dex. Monocytes were isolated from PBMC with CD14⁺ magnetic beads and differentiated in DC in the presence of GM-CSF + IL-4 and either VitD3, RA or Dex were added on day 0. On the 6th day, 100 ng/mL of LPS were added and mo-DC were used for further experiments. (A) Characterization of surface markers of tolDC by flow cytometry. (B) mo-DC were co-cultured with CD40L-expressing cell line (J558) for 24 hours and supernatants were collected, and cytokines were measured by ELISA. (C-E) mo-DC were co-cultured with allogeneic naïve T cells as described in “material and methods” section and (C,D) intracellular cytokines levels were measured by flow cytometry or (D) T cell suppression assay was performed. (C) Representative plots of ICS for IL-10 and IFN- γ ; (D) Quantification of Of cytokines measured by ICS. (E) Quantification (left chart) and representative graphic (right chart) of T suppression assay. Data are pooled from 4-9 (A) independent experiments, representative of 1 out 3 independent experiments (B) and pooled from 2-3 independent experiments (C-E) with one to two donors. Statistics are One-Way Anova with Tukey HSD post-test. Data shown as mean \pm SEM; * p < 0.05, ** p < 0.01, *** p < 0.001, **** p < 0.0001.

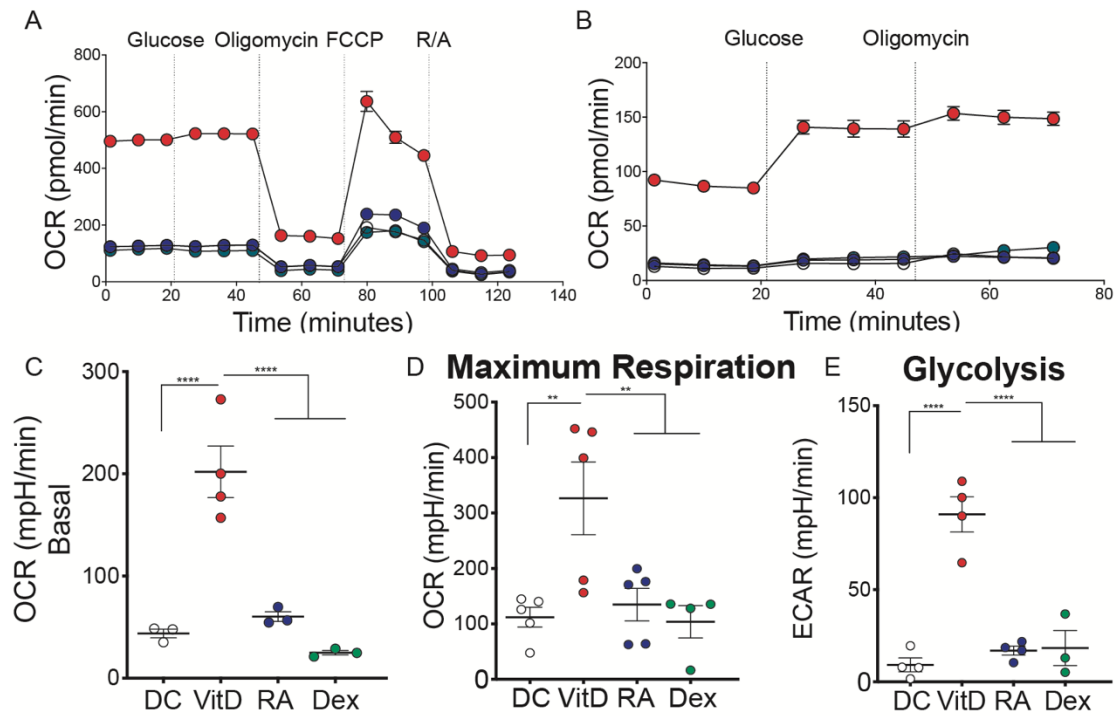


Figure 23: Metabolic profile from tolDC. Monocytes were isolated from PBMC with CD14⁺ magnetic beads and differentiated in DC in the presence of GM-CSF + IL-4 and either VitD3, RA or Dex were added on day 0. On the 6th day, 100 ng/mL of LPS were added and mo-DC were used for further experiments. Extracellular flux analysis ECAR (A) and OCR (B) of tolDC and quantification of basal levels of OCR (C), maximal respiration (D) and glycolysis (E). Data are pooled from from 2-3 independent experiments with one to two donors. Statistics are One-Way Anova with Tukey HSD post-test. Data shown as mean \pm SEM; * $p < 0.05$, ** $p < 0.01$, *** $p < 0.001$, **** $p < 0.0001$.

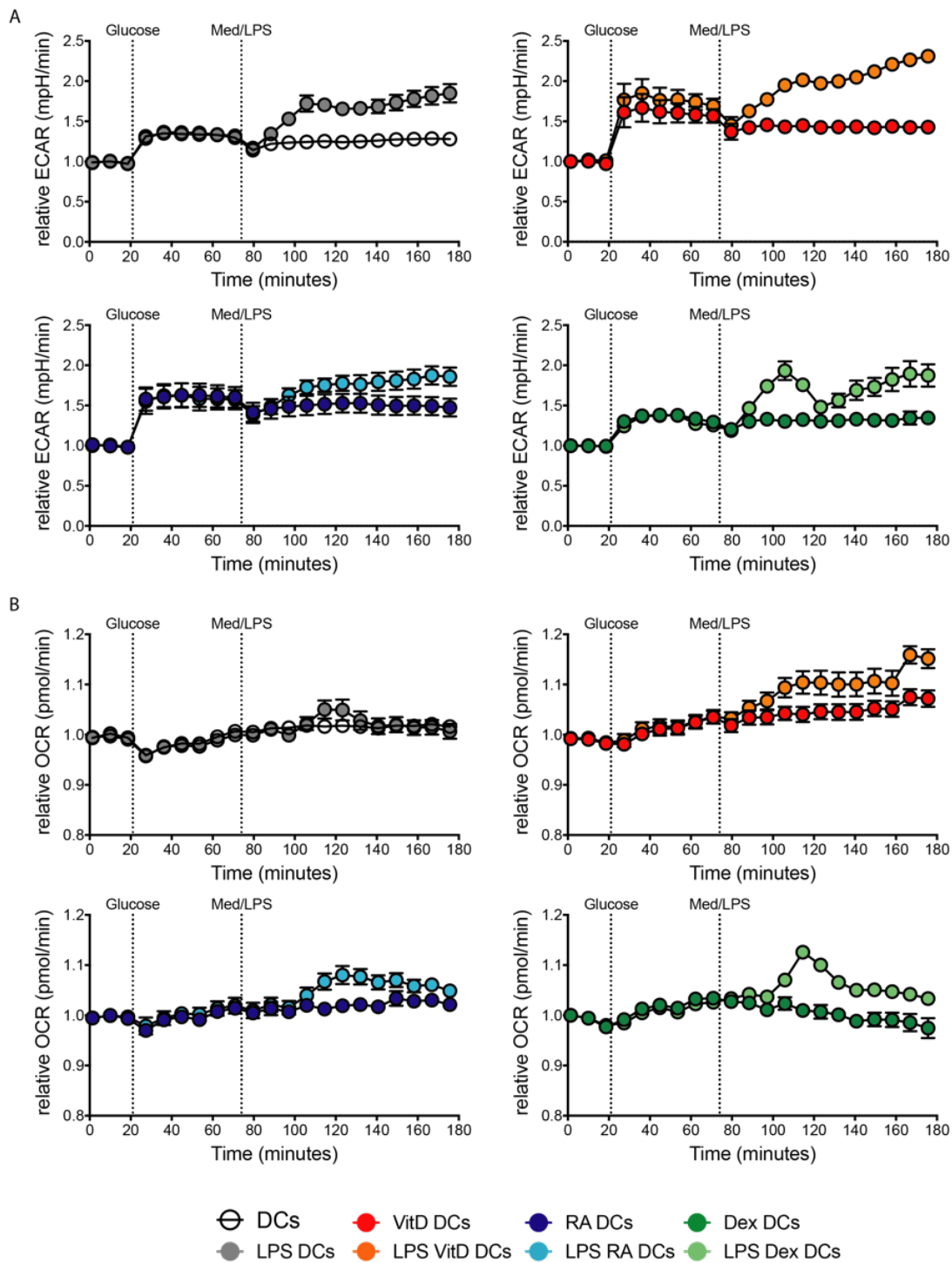


Figure 24: LPS activation induces a rapid increase in glycolytic metabolism in both control and tolerogenic DC. Real-time changes in the ECAR (A) and OCR (B) of mo-DC left untreated or treated with LPS. The second dot line indicate the moment in which LPS was inject in the cells. Data are pooled from 3 donors from 3 independent experiments.

4.10.2. Elongation of very long-chain fatty acids family member 6 (*ELOVL6*) is increased in RA DC and Dex DC.

To better understand the metabolic pathways involved in tolDC features, we performed a qPCR to address the expression of several metabolic-related enzymes in mo-

DC treated with tolerogenic compounds either at day 0 or at day 5. To exclude the LPS-induced effects in the metabolic pathways, iDC were used in the experiments. Figure 25 and Figure 26 show the results for tolDC treated at day 0 and at day5, respectively.

Several metabolic-associated genes were modulated when tolDC were treated with compounds at day 0 and, interestingly, even though PCA could not clear separate VitD DC and RA DC from each other (different from what it was observed for Dex DC – Figure 25C), HCA could still identify the three different cluster related to each one of the tolDC groups (Figure 25B), which suggests intrinsic differences between the groups. Surprisingly, HK1 and 6-phosphofructo-2-kinase/fructose-2,6- biphosphatase 3 (PFKFB3), important glycolytic enzymes, were downregulated in VitD DC, which displayed the higher glycolytic metabolism among all of the tolDC. RA DC displayed reduced levels of CPT1A, which might suggest that FAO is not important for RA DC immunosuppressive capacity. VitD DC and RA DC shared some common features, since most of the significantly modulated protein were downregulated and some proteins behaved in the same way for both conditions, like LKB1 and SIRT1. Some proteins had different patterns, as it is the case for the succinyl dehydrogenase subunit A (SDHA), the complex II in the electron transport chain and also an enzyme responsible for the oxidation of succinyl (LAMPROPOULOU et al., 2016; MILLS et al., 2016). While SDHA was downregulated in RA DC it was upregulated in Dex DC.

The most interesting observation was the modulation observed on the elongase of very long-chain fatty acids (ELOVL) family genes. ELOVL family is a set of protein that consists of 7 different proteins (ELOVL1-7) and each one of them have distinct tissue distribution and preferences for different fatty acid substrate (JAKOBSSON; WESTERBERG; JACOBSSON, 2006). ELOVL1 is associated with the elongate of FA up to C₂₆ (CASTRO; TOCHER; MONROIG, 2016); ELOVL2 and ELOVL5 are the elongases capable to act on PUFA, however ELOVL2 is capable to elongate C₂₀ and C₂₂ PUFA while ELOVL5 only elongates C₁₈ and C₂₀, with no activity over C₂₂ PUFA; ELOVL3 is thought to control the elongation of FA up to C₂₄ (CASTRO; TOCHER; MONROIG, 2016); ELOVL4 is the only elongase capable of elongate both PUFA and saturated FA as well (CASTRO; TOCHER; MONROIG, 2016); ELOVL6 is the main elongase capable to elongate C₁₂₋₁₆ saturated fatty acids up to C₁₈, but cannot elongate FA beyond this (INAGAKI et al., 2002; MOON et al., 2001) and ELOVL7 seems to be involved in the elongation of saturated FA up to C₂₄ (TAMURA et al., 2009). Among the genes modulated in tolDC, at least one member of the ELOVL family was either up or

downregulated in all tolDC groups (Figure 25A). In VitD DC ELOVL1 and ELOVL4 tended to be downregulated and ELOVL5 and ELOVL7 were significantly downregulated, while ELOVL3 and ELOVL6 tended to be upregulated (Figure 25B and Figure 26). RA DC displayed an overall increase in ELOVL member, with ELOVL3, ELOVL4 and ELOVL5 tending to be upregulated while ELOVL6 was significantly upregulated. On the other hand, ELOVL1 tended to be downregulated and ELOVL7 was significantly downregulated (Figure 25A and Figure 26). Dex DC displayed decreased expression of ELOVL7 and increased expression of ELOVL6 while ELOVL3 and ELOVL4 were not amplified, which could be either due to lack of expression of these genes or some technical issue (Figure 25A, Figure 25B and Figure 26).

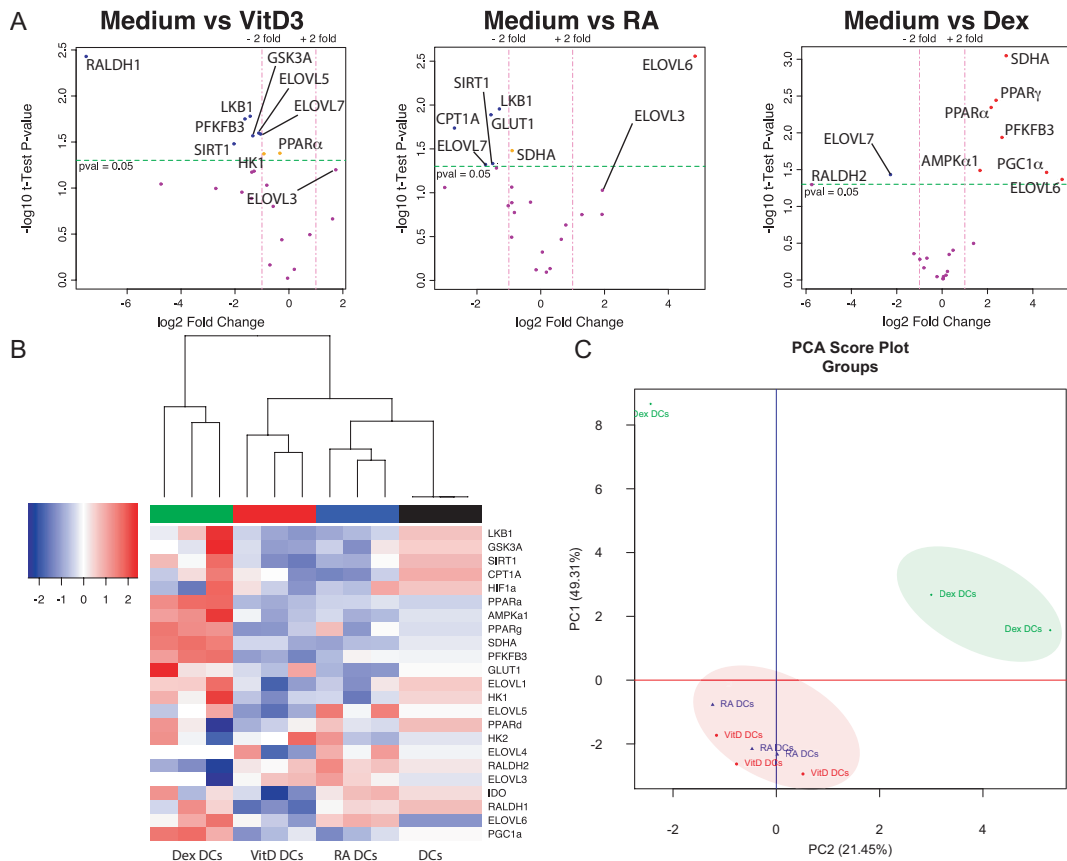


Figure 25: Quantitative PCR from tolDC treated with compounds at day 0. Monocytes were isolated from PBMC with CD14⁺ magnetic beads and differentiated in mo-DC in the presence of GM-CSF + IL-4 and either VitD3, RA or Dex were added at day 0. On the 7th day, mo-DC were harvested, washed in PBS and snap frozen in liquid nitrogen until qPCR evaluation. (A) Volcano plot of VitD DC (upper left), RA DC (upper middle) and Dex DC (upper right) vs DC group. (B) hierarchical cluster analysis (HCA) and heatmap displaying different genes expressed by tolDC. (C) PCA score plot from PCA analysis performed in tolDC. The cluster highlighted in red represents VitD DC and RA DC that could not be completely isolated and in green is the cluster from Dex DC. Data are pooled from 3 independent experiments with one donor each. Statistics in (A) are student's T test performed with log-transformed data and $p < 0.05$ was considered significant.

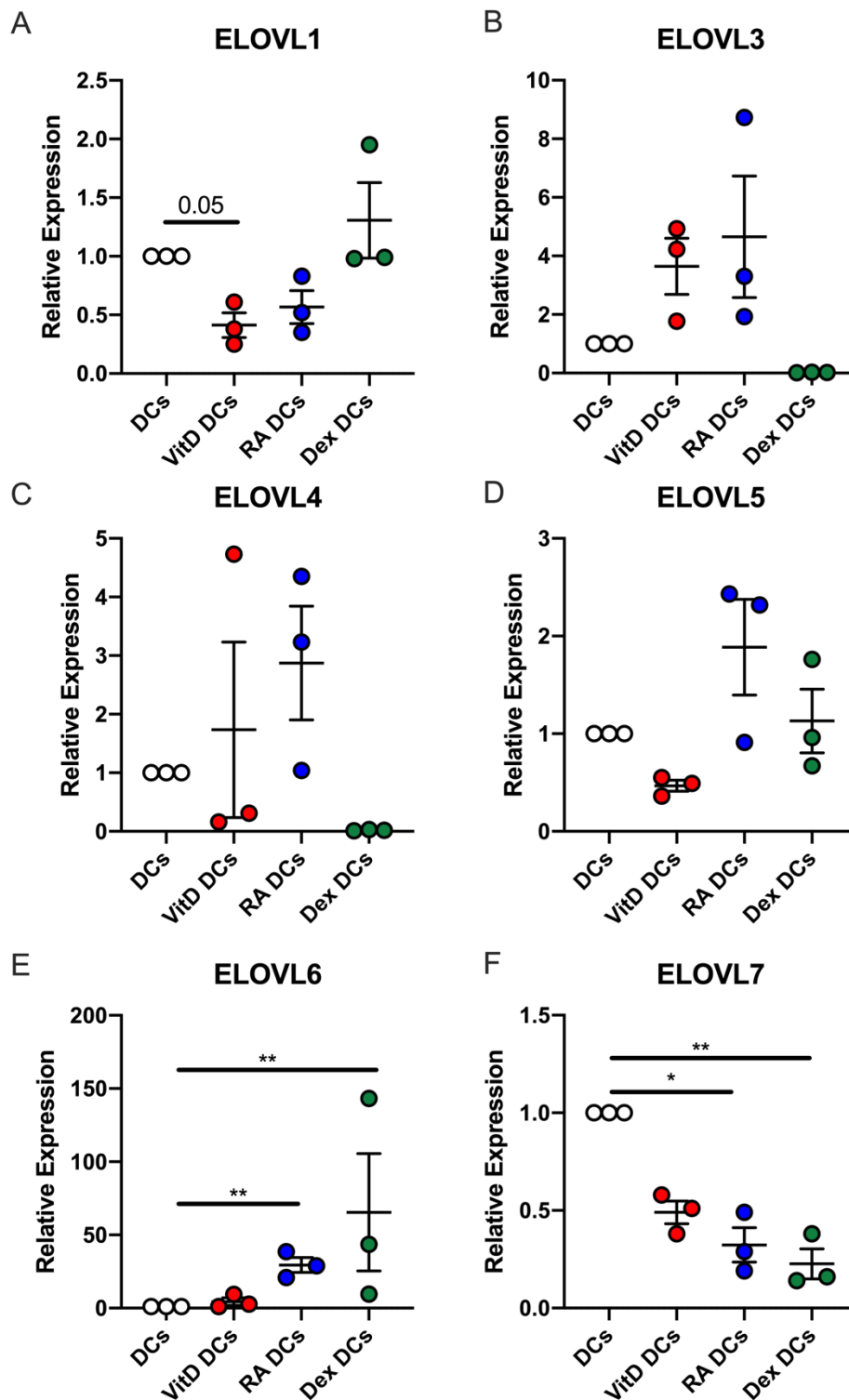


Figure 26: Expression of elongases in tolDC treated with compounds at day 0. Monocytes were isolated from PBMC with CD14+ magnetic beads and differentiated in mo-DC in the presence of GM-CSF + IL-4 and either VitD3, RA or Dex were added at day 0. On the 7th day, mo-DC were harvested, washed in PBS and snap frozen in liquid nitrogen until qPCR evaluation. Data are pooled from 3 independent experiments with one donor each. Statistics are Two-Way Anova with Tukey post-test or Kruskal-Wallis with Tukey post test. Data shown as mean ± SEM; *p < 0.05, **p < 0.01, ***p < 0.001, ****p < 0.0001.

In tolDC treated at day 5, PCA analysis could better identify the clusters for each tolDC (Figure 27C) and this was confirmed by the HCA analysis (Figure 27B). When

analyzing the genes expressed by these cells, the modulation of ELOVL family members was again clearly displayed in all tolDC. In VitD DC ELOVL1 tended to be downregulated and ELOVL4 and ELOVL5 were significantly downregulated (Figure 27A) while ELOVL3 and ELOVL6 tended to be upregulated and ELOVL7 was significantly upregulated (Figure 27A and Figure 28). RA DC also displayed an overall increase in ELOVL member, with ELOVL3, ELOVL4, ELOVL5 and especially ELOVL6 being significantly upregulated while only ELOVL7 tended to be downregulated (Figure 27A and Figure 28). Dex DC displayed a trend for decreased expression of ELOVL4 and ELOVL7 and increased expression of ELOVL3 and ELOVL6 (Figure 27A and Figure 28).

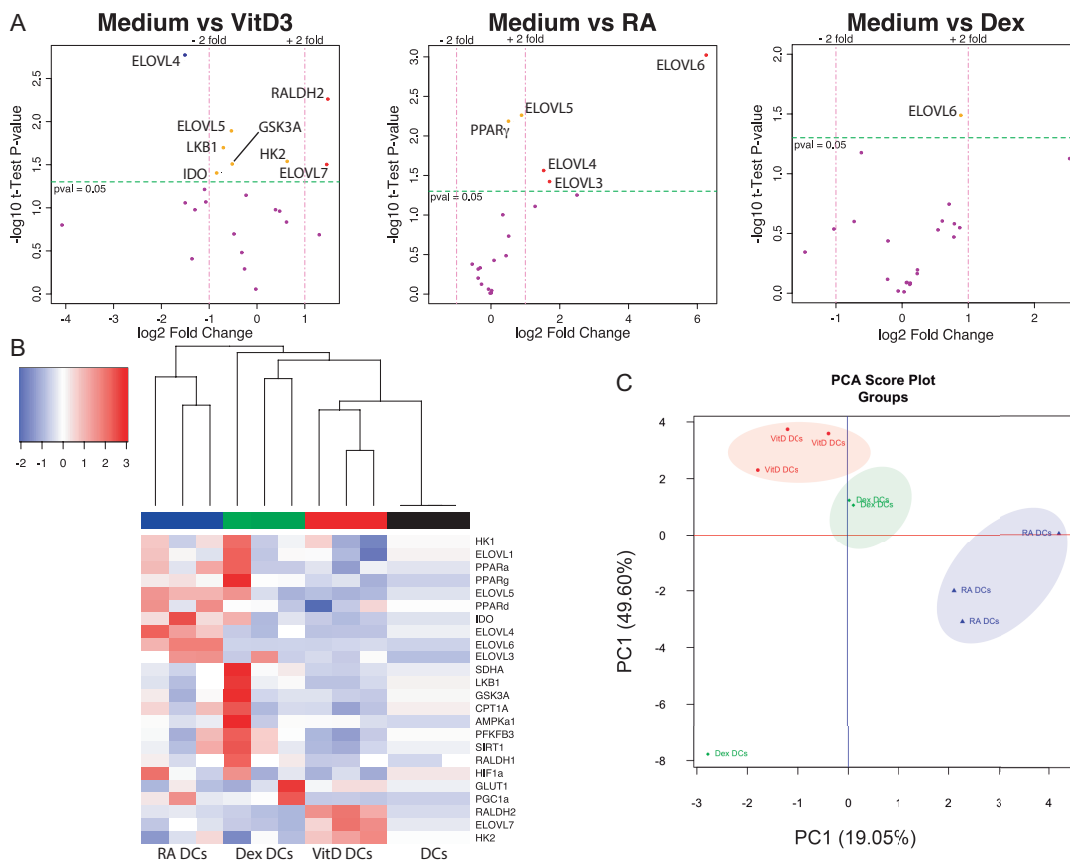


Figure 27: Quantitative PCR from tolDC treated with compounds at day 5. Monocytes were isolated from PBMC with CD14⁺ magnetic beads and differentiated in DC in the presence of GM-CSF + IL-4 and either VitD3, RA or Dex were added at day 5. On the 7th day, mo-DC were harvested, washed in PBS and stored at -80 °C until the moment of GC-MS analysis. (A) Volcano plot of VitD DC (upper left), RA DC (upper middle) and Dex DC (upper right) vs DC group. (B) hierarchical cluster analysis (HCA) and heatmap displaying different genes expressed by tolDC. (C) PCA score plot from PCA analysis performed in tolDC. The clusters highlighted in red (VitD DC), blue (RA DC) and green (Dex DC) are displayed in the figure. Data are pooled from 3 independent experiments with one donor each. Statistics in (A) are student's T test performed with log-transformed data and $p < 0.05$ was considered significant.

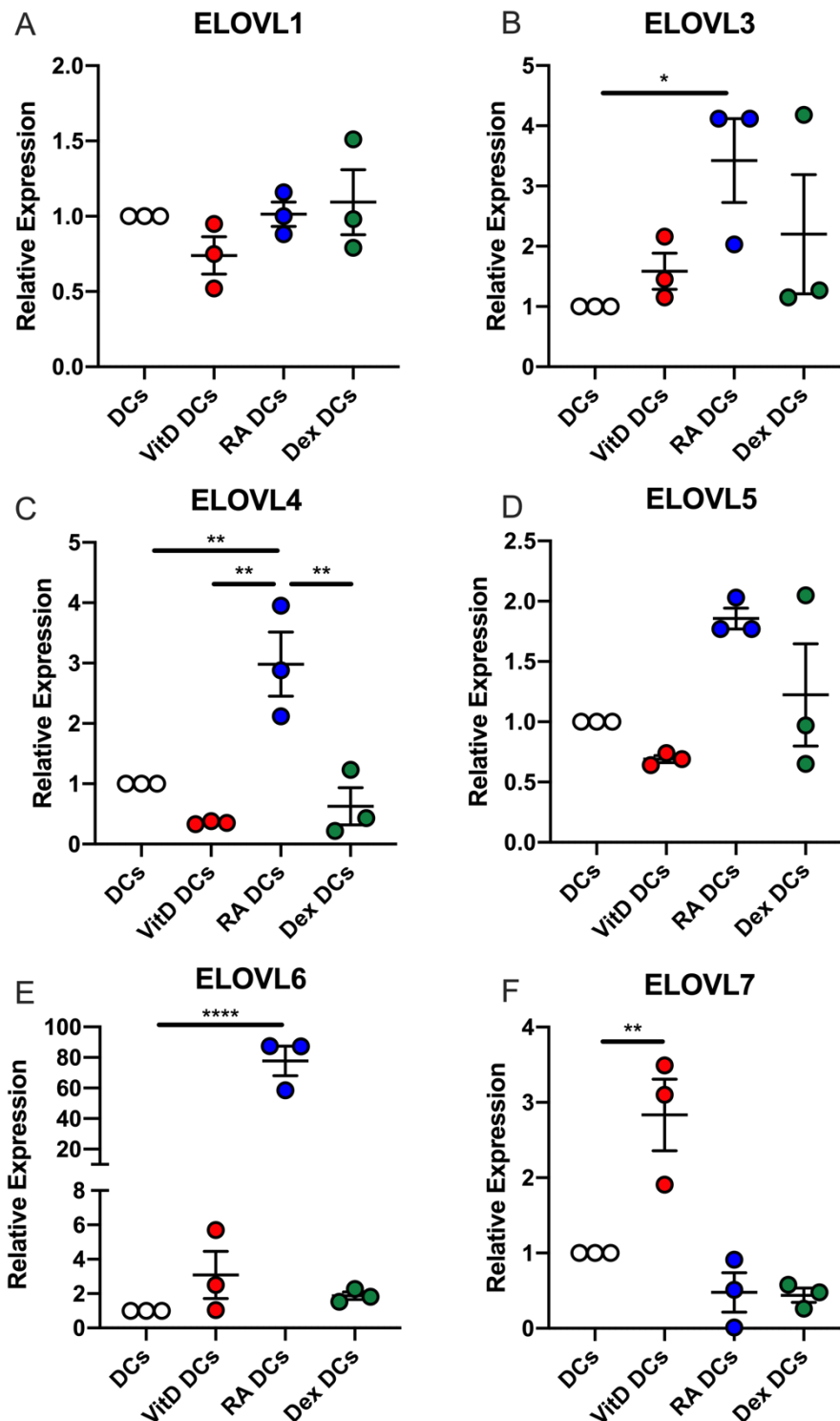


Figure 28: Expression of elongases in tolDC treated with compounds at day 5. Monocytes were isolated from PBMC with CD14⁺ magnetic beads and differentiated in mo-DC in the presence of GM-CSF + IL-4 and either VitD3, RA or Dex were added at day 5. On the 7th day, mo-DC were harvested, washed in PBS and snap frozen in liquid nitrogen until qPCR evaluation. Data are pooled from 3 independent experiments with one donor each. Statistics are Two-Way Anova with Tukey post-test or Kruskal-Wallis with Tukey post-test. Data shown as mean ± SEM; *p < 0.05, **p < 0.01, ***p < 0.001, ****p < 0.0001.

Even though cells treated at day 5 seem to have a more pronounced modulation of ELOVL genes, these genes were modulated similar in tolDC, regardless if they were treated at day 0 or at day 5. In summary, while RA DC displayed an overall upregulation of ELOVL genes, VitD DC displayed an overall downregulation and Dex DC displayed few alterations. Taken together, data suggest that, among the tolDC evaluated, RA DC might have an increase in LCFAs as consequence of an increased expression of elongases.

4.10.3. Long chain fatty acid pathway is differently affected in RA DC, VitD DC and Dex DC.

To better understand the data observed in the qPCR analysis, we hypothesized that the increase in ELOVLs proteins could be accompanied by an increase in LCFAs in tolDC and to test this, we performed a lipidomic analysis in tolDC treated with tolerogenic compounds either at day 0 (Figure 29) or at day 5 (Figure 30). Previous data from the laboratory already pointed towards an increase in PUFAs pathway in tolDC. PUFAs are fatty acids that contains more than two bonds between carbon atoms and mainly two types of PUFA can be found: omega 3-fatty acids and omega 6-fatty acids. Omega-6 linoleic acid and omega-3 α -linoleic acid are the most common PUFAs and they are both essentials FAs, which means they cannot be synthesized, and need to be acquired from the diet, which is not the case for MUFA (DOMINGUEZ; BARBAGALLO, 2017).

The analysis performed for cells treated at day 0 showed that, even though each group clustered separately from each other in PCA, VitD DC and RA DC were more closely related to each other than they were from Dex DC (Figure 29C). This is even more evident when analyzing the heatmap and HCA (Figure 29B). It is possible to observe that the distance of Dex DC cluster from RA DC and VitD DC is higher, suggesting the lipids profile of Dex DC is not similar to the one observed in RA DC and VitD DC. Additionally, heatmap and volcano plot clearly showed that while VitD DC and RA DC had increase in LCFA, Dex DC had decrease amounts of these lipids. RA DC displayed the most striking increasing in LCFA with increases of both MUFA (elaidic acid, nervonic acid, erucic acid and 11-eicosenoic acid) and omega-6 family PUFAs [11,14-eicosadienoic acid (EDA), 13-16-docosadienoic acid (DDA)]. On the other hand, VitD DC displayed increases in omega-3 family PUFA [eicosapentaenoic acid (EPA)], omega-6 family PUFA (arachidonic acid - AA) as well as MUFA (elaidic acid). Interestingly,

although a massive reduction in LCFAs, Dex DC displayed increases in EPA, as it was also observed for VitD DC.

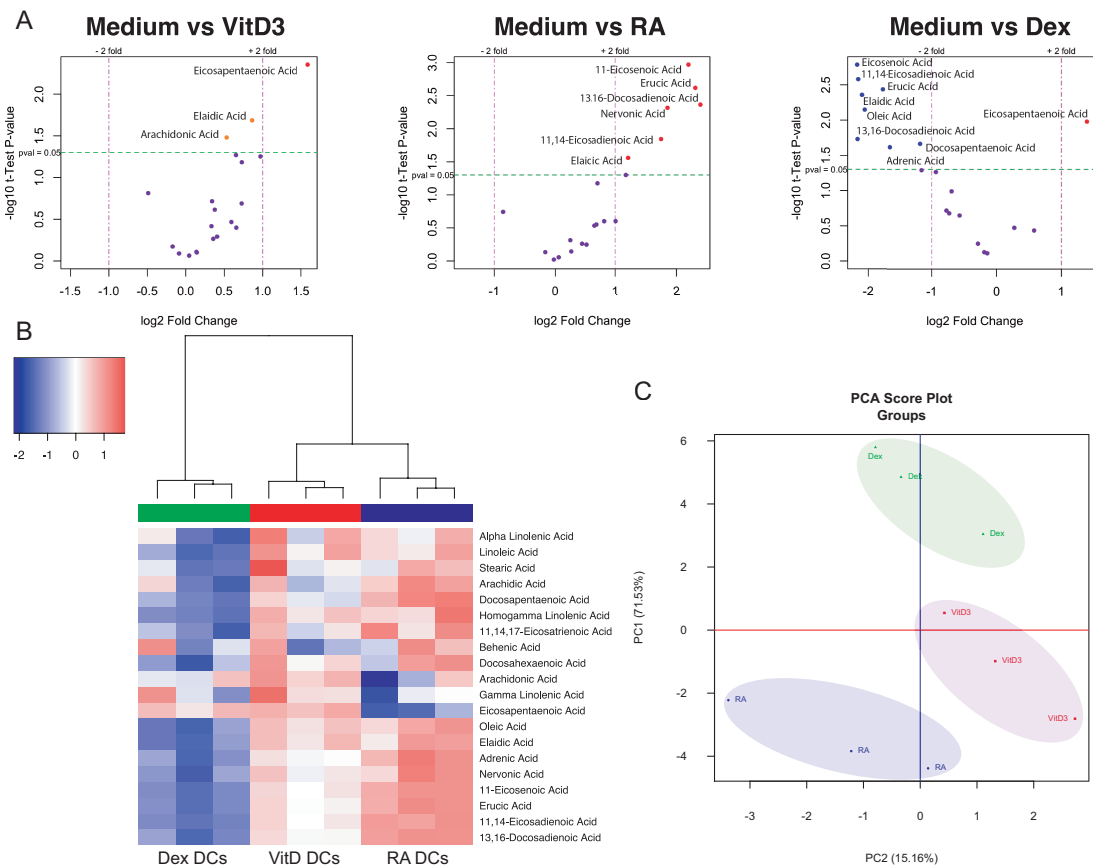


Figure 29: Lipidome analysis from tolDC treated with compounds at day 0. Monocytes were isolated from PBMC with CD14⁺ magnetic beads and differentiated in DC in the presence of GM-CSF + IL-4 and either VitD3, RA or Dex were added at day 0. On the 5th day, mo-DC were harvested, washed in PBS and stored at -80 °C until the moment of GC-MS analysis. (A) Volcano plot of VitD DC (upper left), RA DC (upper middle) and Dex DC (upper right) vs DC group. (B) hierarchical cluster analysis (HCA) and heatmap displaying lipids expressed by tolDC. (C) PCA score plot from PCA analysis performed in tolDC. The cluster observed in the dendrogram from item (B) are highlighted in red (VitD DC), blue (RA DC) and green (Dex DC). Data are pooled from 3 independent experiments with one donor each. Statistics in (A) are student's T test performed with log-transformed data and $p < 0.05$ was considered significant.

Surprisingly, since the major alterations in ELOVL genes were observed in cells treated at day 5, these cells displayed less intensive lipid alterations but they were, at some level, closely related to the ones observed when cells were treated at day 0, especially for Dex DC, which were the only cells clustered separately in the PCA analysis (Figure 30C). VitD DC and RA DC were distributed in two separate clusters containing donors from both groups. This is also evident analyzing the heatmap graph which shows a non-uniform pattern in this two groups (Figure 30B). However, similar to what was observed for cells treated at day 0, a globally reduction in LCFA with a small increase in EPA could also be observed for Dex DC. The LCFA reduced in Dex DC were elaidic

acid, erucic acid, oleic acid and 11-eicosenoic acid, all LC MUFA (Figure 30A) that were also reduced when cells were treated at day 0.

It is worth noting that VitD DC and RA DC treated at day 5 also shared some common features with the cells treated at day 0. Although less prominent, it was also possible to observe a trend for increasing 11-eicosenoic acid, EDA, DDA and erucic acid for RA DC and EPA for VitD DC (Figure 31), all of them strongly increased when cells were treated at day 0.

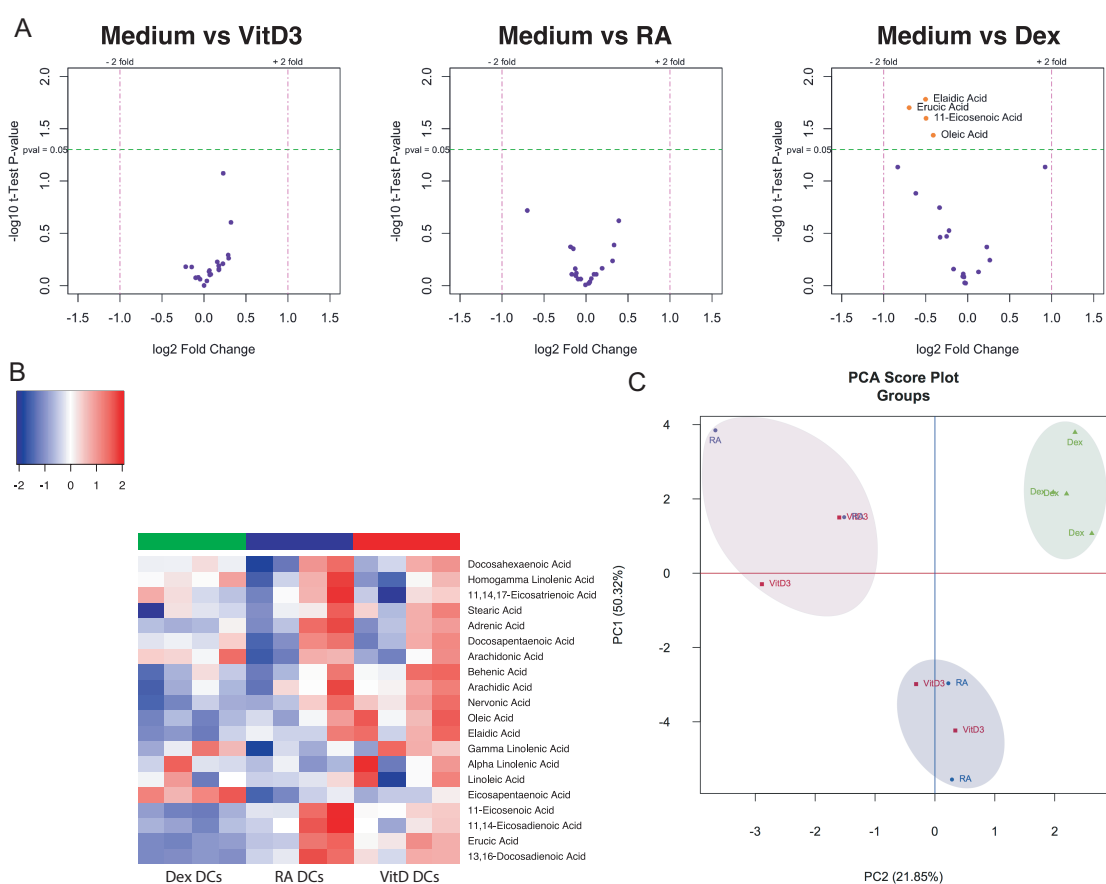


Figure 30: Lipidome analysis from tolDC treated with compounds at day 5. Monocytes were isolated from PBMC with CD14⁺ magnetic beads and differentiated in DC in the presence of GM-CSF + IL-4 and either VitD3, RA or Dex were added at day 5. On the 5th day, mo-DC were harvested, washed in PBS and stored at -80 °C until the moment of GC-MS analysis. (A) Volcano plot of VitD DC (upper left), RA DC (upper middle) and Dex DC (upper right) vs DC group. (B) hierarchical cluster analysis (HCA) and heatmap displaying lipids expressed by tolDC. (C) PCA score plot from PCA analysis performed in tolDC. The cluster highlighted in red and blue represent VitD DC and RA DC that could not be completely isolated and in green is the cluster from Dex DC. Data are pooled from 4 independent experiments with one donor each. Statistics in (A) are student's T test performed with log-transformed data and $p < 0.05$ was considered significant.

This increased lipid content, especially for cells treated at day 0 was also confirmed by the quantification of neutral lipids with the bodipy dye (Figure 32). We could observe a clear increase in neutral lipids for VitD DC and RA DC when cells were treated at day 0, but this was not the case for cells treated at day 5. It is worth to note,

however, that the bодipy staining accounts for the total neutral lipids inside the cells and does not distinguish between LCFA, short chain fatty acid (SCFA) or even triglycerides and total cholesterol.

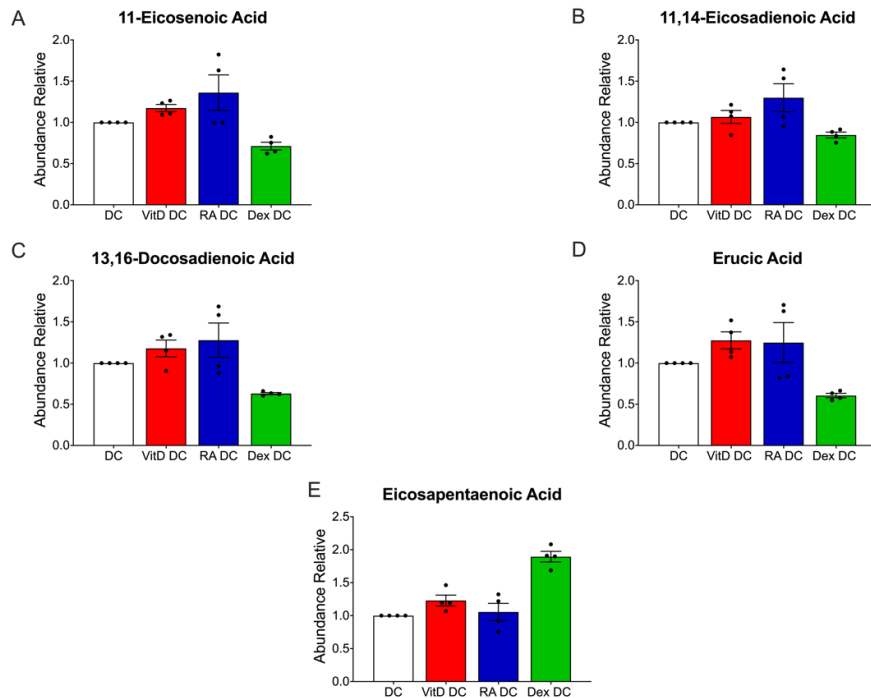


Figure 31: Lipidome analysis from tolDC treated with compounds at day 5 - graphic view. Monocytes were isolated from PBMC with CD14⁺ magnetic beads and differentiated in DC in the presence of GM-CSF + IL-4 and either VitD3, RA or Dex were added at day 5. On the 5th day, mo-DC were harvested, washed in PBS and stored at -80 °C until the moment of GC-MS analysis. Bar graphic representation of (A) 11-Eicosenoic acid, (B) 11,14-Eicosadienoic acid, (C) 13,16-Docosadienoic acid, (D) erucic acid and (E) EPA observed in Figure 26. Statistics are Two-Way Anova with Tukey post-test or Kruskal-Wallis with Tukey post-test. Data shown as mean ± SEM; *p < 0.05, **p < 0.01, ***p < 0.001, ****p < 0.0001. Data are pooled from 4 independent experiments with one donor each.

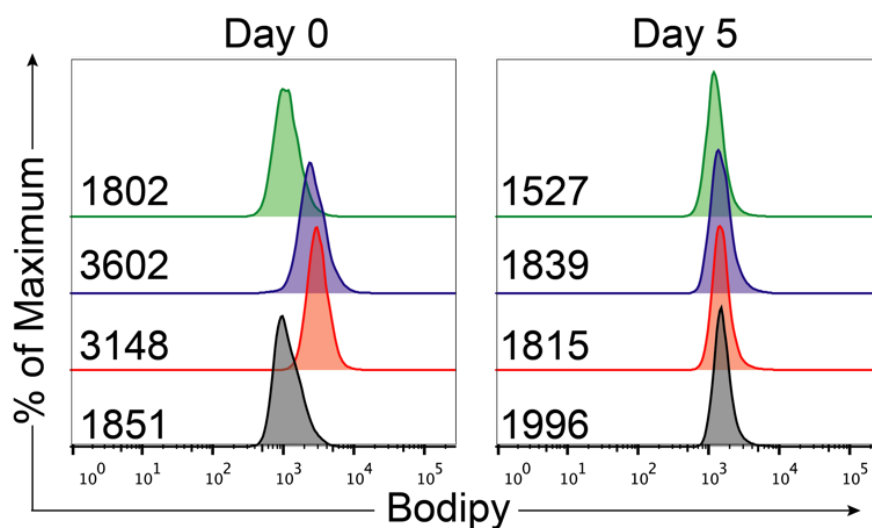


Figure 32: Total neutral lipids content is increased in VitD DC and RA DC treated at day 0. Monocytes were isolated from PBMC with CD14⁺ magnetic beads and differentiated in DC in the presence of GM-CSF + IL-4 and either VitD3, RA or Dex were added on day 0. On the 6th day, 100 ng/mL of LPS were added and mo-DC were stained with bодipy and FACS measured. Data are mean from 2 independent experiments.

Taken together, these data suggest that LCFA pathway might be a common feature in tolDC with, however, different lipids being associated with different tolDC, since increasing in EPA seemed to be the main characteristic for VitD DC and, especially Dex DC, while increasing in low-inflammatory LCFA, as erucic acid and EDA, seemed to be the characteristic for RA DC.

4.11. Glucose effects during differentiation of tolDC

After characterizing tolDC, we aimed to investigate the effects of glucose concentration during the differentiation of tolDC. For that, CD14⁺ monocytes were isolated, and mo-DC were generated in the presence of GM-CSF + IL-4 or GM-CSF + IL-4 and tolerogenic compounds. The differentiation was performed in either 1 mM, 5.5 mM or 25 mM (which resembles the situation of hypoglycemia, normoglycemia and hyperglycemia respectively) of glucose with media, cytokines, tolerogenic compounds and glucose being replenished at day 2/3 of the differentiation.

The Figure 33A shows the expression of the surface markers from tolDC differentiated in different glucose concentrations. It could be observed that for RA DC and Dex DC glucose does not seem to be important for the modulation of any surface markers evaluated. However, for VitD DC the expression of CD86 and, to a lesser extent, CD83, were further reduced when glucose concentration in the media was increased. Also, the PD-L1/CD86 ratio was increased suggesting that VitD DC differentiated in high glucose concentration could be more tolerogenic. As well as it had already been observed in Brazil, and different from what has been previously published (FERREIRA et al., 2015), the expression of CD80 and HLA-DR were hardly affected by the glucose concentration in the media.

Because previous data from the literature, and also our own, suggested that glucose concentration was important for the tolerogenic functions of VitD DC, one could hypothesize that while the expression of CD86 was decreased, the expression of inhibitory markers such as ILT-3 and PD-L1 would be increased. However, the ILT-3 expression was trend to decrease when glucose concentration was increased. It is worth noting, however, that VitD3 induced the expression of ILT-3 in all conditions, suggesting that VitD3 induced expression of this tolerogenic marker was independent from glucose levels. PD-L1 expression, was little affected in normal and high glucose concentration. However, surprisingly, low glucose concentration induced the expression of PD-L1. One possible explanation for this phenomenon is that in the absence of glucose, cells rely in a

different metabolic pathway to survive, as for example glutaminolysis (O'NEILL; KISHTON; RATHMELL, 2016). In bladder cancer cells, glucose deprivation stimulated glutaminolysis and the IFN- γ -dependent expression of PD-L1 was abolished when glutaminolysis was blocked (WANG et al., 2018). VitD DC differentiated in low glucose media might also rely on glutaminolysis for their survival which might favor the expression of VitD3-induced PD-L1.

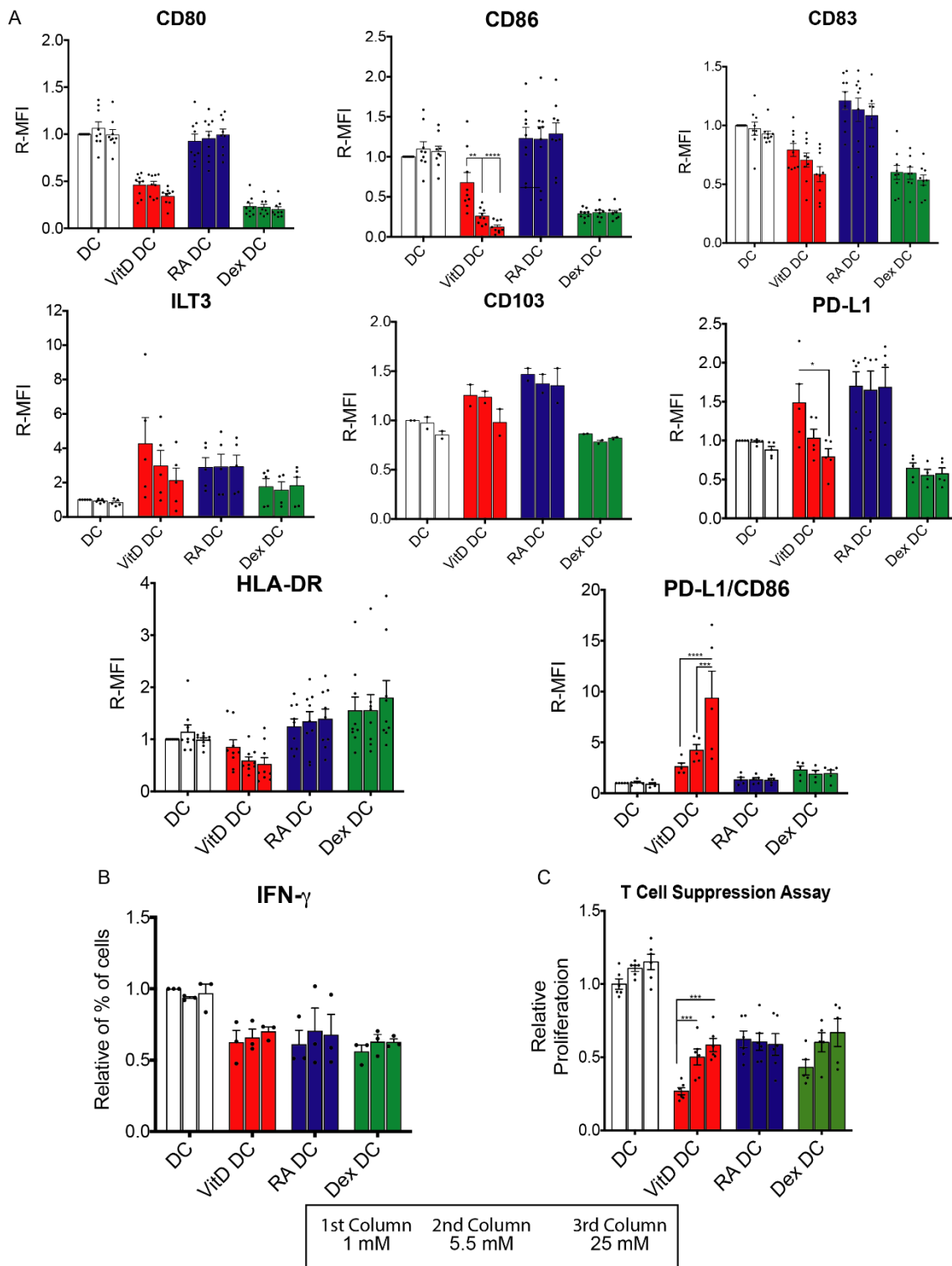


Figure 33: Effect of glucose concentrations during the differentiation of mo-DC. Monocytes were isolated from PBMC with CD14⁺ magnetic beads and differentiated in DC in the presence of either 1 mM, 5.5 mM or 25 mM of glucose. GM-CSF + IL-4 and either VitD3, RA or Dex were added on day 0 and on the 6th day, 100 ng/mL of LPS were added and mo-DC were used for further experiments. (A) Characterization of surface markers of mo-DC by flow cytometry. (B,C) mo-DC were co-cultured with allogeneic naïve T cells as described in “material and methods” section and (C) intracellular cytokines levels were measured by flow cytometry or (D) T cell suppression assay was performed. Data (A-C) are pooled from 4-9 independent experiments (A), 2-3 independent experiments with one to two donors. Statistics are Two-Way Anova with Sidak’s post-test. Data shown as mean \pm SEM; * $p < 0.05$, ** $p < 0.01$, *** $p < 0.001$, **** $p < 0.0001$.

Next, we evaluated the functional properties of tolDC by analyzing the cytokines produced by T cells primed with tolDC and also the ability of those T cells to suppress the proliferation of bystander T cells. It could be observed in Figure 33B that IFN- γ secretion by T cells was not modulated by the glucose concentration in which mo-DC were differentiated. All tolDC in all glucose concentrations were still able to limit the IFN- γ secretion by T cells.

The ability to generate tolerogenic T cells, were also tested by the T suppression assay, in which T cells that were primed by DC were co-culture with autologous memory T cells. It was possible to observe that RA DC suffered no influence from the glucose concentration while Dex DC and specially VitD DC became less tolerogenic when differentiated in high glucose concentration (Figure 33C). This was surprising, because the alterations observed in surface markers, the results observe in Brazil and data from literature pointed toward an inverse relationship between glucose concentration and tolerogenicity of VitD DC.

After having explored the function and characteristics of tolerogenic mo-DC, we also tried to explore the metabolic profile of tolDC, differentiated under various glucose concentrations. As observed for other parameters, the most important difference related to glucose concentration was observed in the VitD DC. Those cells presented lower values of basal OCR and glycolysis when differentiated in low glucose concentration, but it was still higher than all the other mo-DC (Figure 34).

The increase in glycolysis and OXPHOS from 1 mM of glucose to 5.5 mM of glucose in VitD DC was also observed in Brazil. Here we could also observe a trend to decrease glycolysis when VitD DC were differentiated in high glucose concentration, similar as we had observed in Brazil (Figure 34C); however, that was not the case for OXPHOS (Figure 34B and Figure 34D). Interesting, RA DC were more glycolytic when differentiated at low glucose levels and went back to the same level as control DC when differentiated at normoglycemia or hyperglycemia (Figure 34C).

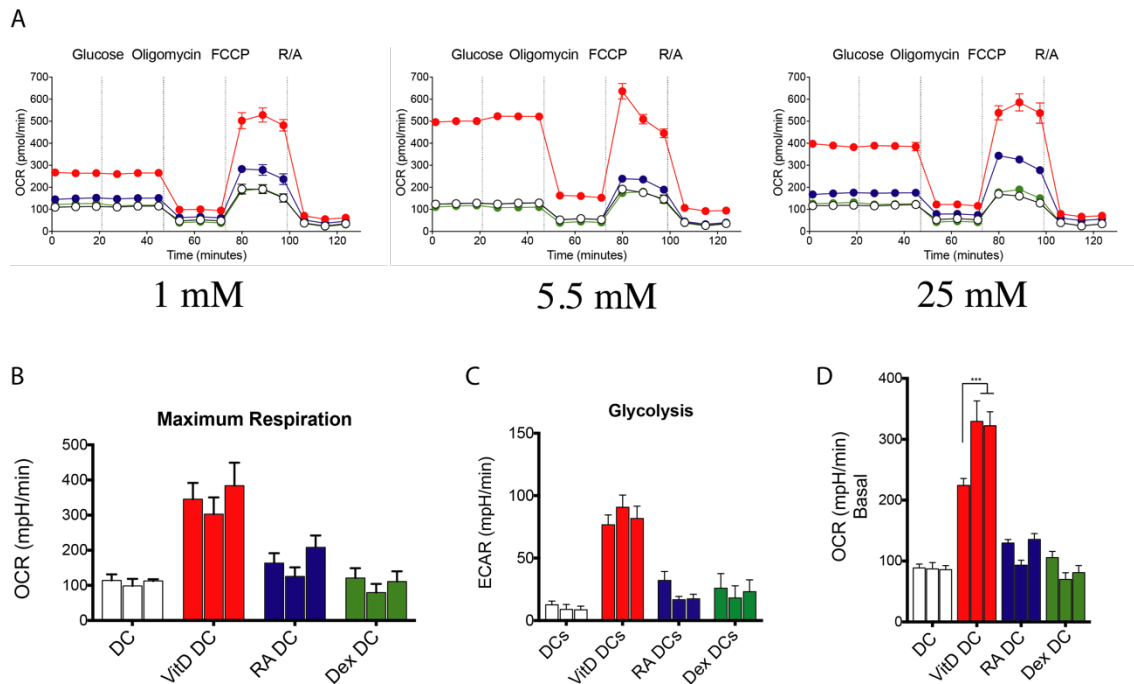


Figure 34: Metabolic characterization of tolDC. Monocytes were isolated from PBMC with CD14⁺ magnetic beads and differentiated in DC in the presence of either 1 mM, 5.5 mM or 25 mM of glucose. GM-CSF + IL-4 and either VitD3, RA or Dex were added on day 0 and on the 6th day, 100 ng/mL of LPS were added and mo-DC were used to measure extracellular flux acidification rate (ECAR) and oxygen consumption rate (OCR). Graphics are quantification of maximum respiration (bottom left), glycolysis (bottom middle) and basal levels of OCR (bottom right). Data are pooled from 3 independent experiments one to two donors. Statistics are Two-Way Anova with Sidak's post-test. Data shown as mean \pm SEM; * p < 0.05, ** p < 0.01, *** p < 0.001, **** p < 0.0001.

Because OXPHOS and maximum respiration were very high in VitD DC, we investigated the mitochondrial membrane potential and mitochondrial mass in tolDC, to see if the increase in OXPHOS was also accompanied by an increase in mitochondrial activity. However, mitochondrial membrane potential and mitochondrial mass were not changed neither in unstimulated DC (Figure 35A) nor in LPS-stimulated DC (Figure 35B). These observations further support the idea that in VitD DC glycolysis is being used to fuel the mitochondria to support the high metabolic activity of those cells.

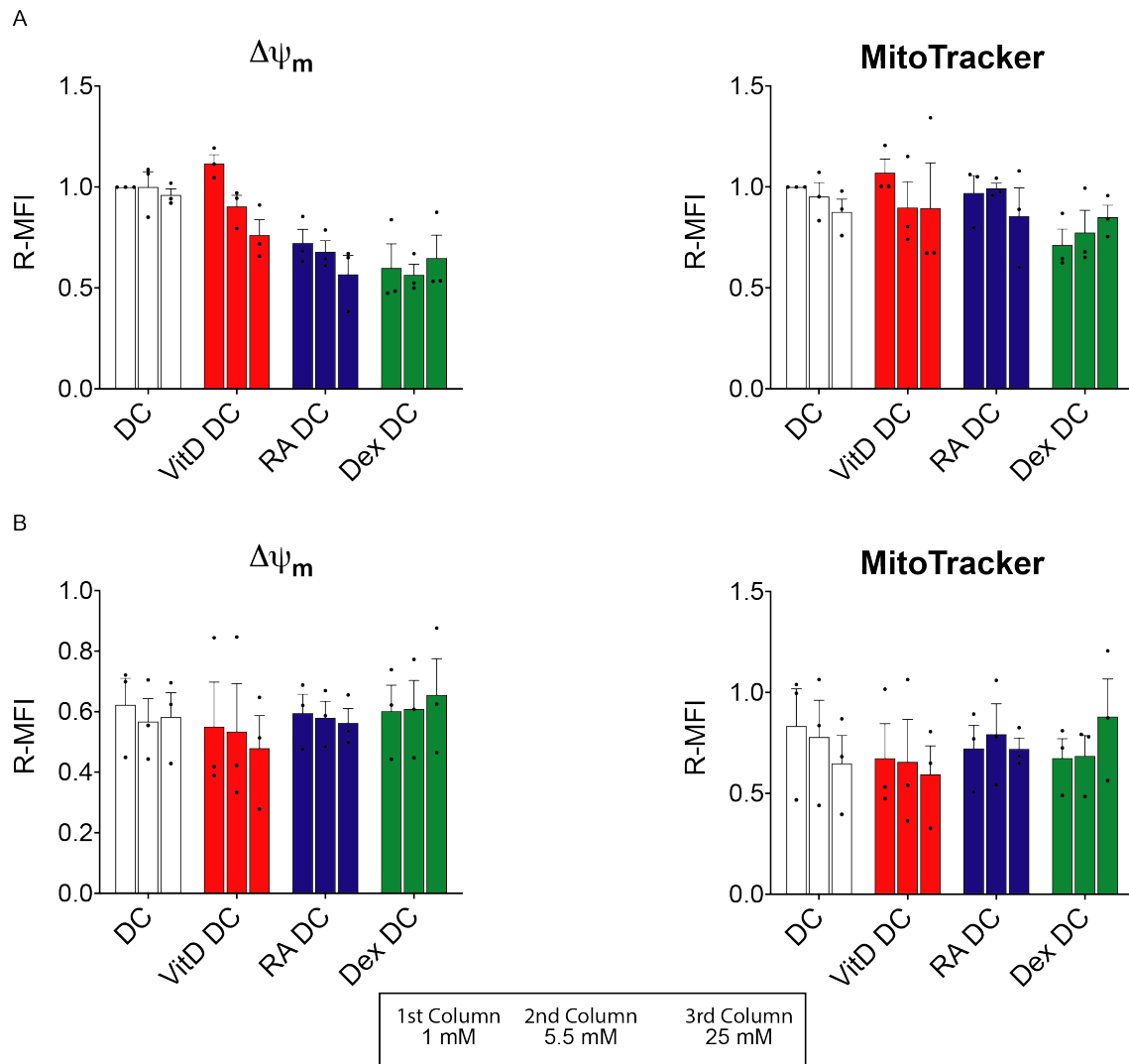


Figure 35: Mitochondrial membrane potential and mass were not affected by glucose concentration. Monocytes were isolated from PBMC with CD14⁺ magnetic beads and differentiated in DC in the presence of either 1 mM, 5.5 mM or 25 mM of glucose. GM-CSF + IL-4 and either VitD3, RA or Dex were added on day 0 and on the 6th day, 100 ng/mL of LPS were added and mo-DC were stained with Tetramethylrhodamine, Methyl Ester, Perchlorate (TMRM) (A) or MitoTracker green (B) for the analysis of mitochondrial mass and mitochondrial membrane potential, respectively. Data are pooled from 3 independent experiments one donor each. Statistics are Two-Way Anova with Sidak's post-test. Data shown as mean \pm SEM; * p < 0.05, ** p < 0.01, *** p < 0.001, **** p < 0.0001.

In conclusion, changes glucose levels only had an effect on the functional properties of VitD3 treated DC which is largely in line with the strongly glycolytic phenotype of these but not the other tolDC.

4.12. Role of AMPK in the function of tolerogenic DC

4.12.1. AMPK activity is increased in RA-DC and VitD DC

In previous experiments from the laboratory it was found that that the AMP/ATP ratio in both VitD3, RA and Dex DC was increased when compared to untreated DC (Figure 36). One of the main metabolic sensors in our cells and activated upon increases in AMP/ATP ratio is AMPK, a heterotrimeric protein, formed by a catalytic α -subunit

and two regulatory subunits: β and γ (HARDIE; ROSS; HAWLEY, 2012). The oxidation of glucose is often linked to AMPK activation, since the fate of the glucose is catabolism to generate ATP inside the mitochondria. The increase in OCR in response to LPS together with the increased AMP/ATP ratio previously observed, prompted us to assess the role of AMPK in the biology of these tolDC.

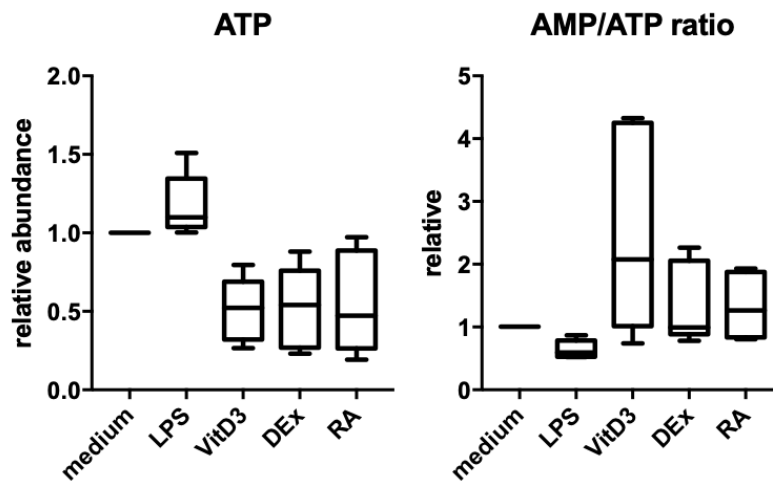


Figure 36: TolDC displayed altered AMP/ATP ratio. Previous data from the laboratory showed that AMP/ATP ratio was increased in tolDC.

First to evaluate the activation status of AMPK in the tolDC, we checked the phosphorylation of Ser79 in ACC, a main protein downstream of AMPK signaling pathway. As it can be observed in Figure 37, there was a significant increase in ACC phosphorylation in VitD DC and RA DC providing a first hint that AMPK activation might be important for tolDC functions.

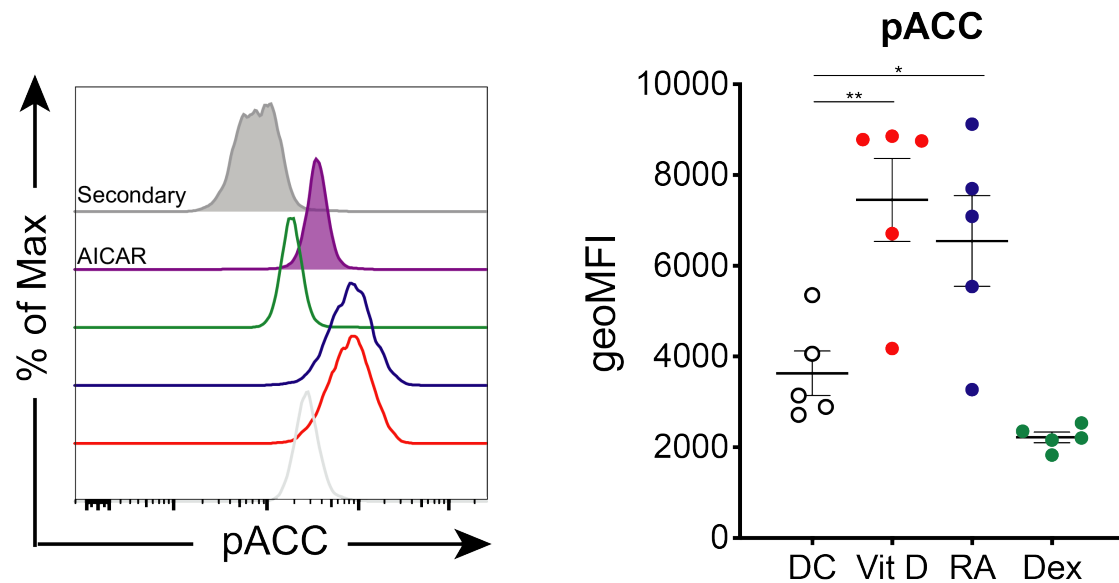


Figure 37: AMPK activity is increased in VitD3- and RA-induced tolDC. Monocytes were isolated from PBMC with CD14⁺ magnetic beads and differentiated in DC in the presence of GM-CSF + IL-4 and either VitD3, RA or Dex were added on day 0. On the 6th day, 100 ng/mL of LPS were added and mo-DC were used for further experiments. Data are pooled from 3 independent experiments with one to two donors. Statistics are One-Way Anova with Tukey HSD post-test. Data shown as mean \pm SEM; * p < 0.05, ** p < 0.01, *** p < 0.001, **** p < 0.0001.

4.12.2. *AMPK^{KD} restores spare respiratory capacity in RA-DC*

Next we wanted to explore the role of AMPK in regulating the properties of these tolDC. To this end, we decided to silence the expression of AMPK in tolerogenic DC to properly address the function of this protein. To silence the expression of AMPK in mo-DC, the protocol of differentiation of the cells was slightly modified. Monocytes were differentiated in mo-DC in the presence of GM-CSF and IL-4 and media and cytokines were replenished at day 2 of the differentiation. On the fourth day, cells were transfected with siRNA for either control or AMPK α 1 gene, that encodes the catalytic subunit of AMPK and is the only isoform expressed by myeloid cells (QUENTIN et al., 2011). On the fifth day, cells were either treated with VitD3, RA, Dex or left untreated. Then, in the sixth day cells were activated with LPS for 24 hours and then harvested for the experiments.

We hypothesized that AMPK could be involved in controlling the metabolic profile of tolDC. Figure 38, Figure 39 and Figure 40 shows the metabolic profile of VitD DC, RA DC and Dex DC, respectively.

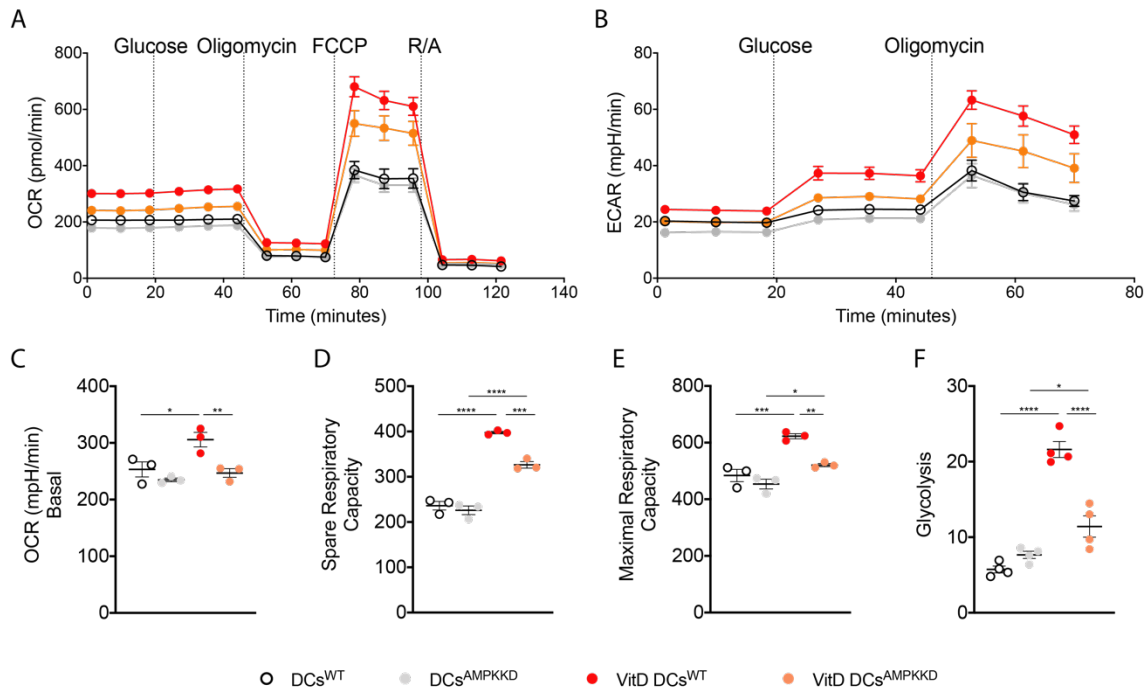


Figure 38: Metabolic characterization of VitD DC. Monocytes were isolated from PBMC with CD14⁺ magnetic beads and differentiated in DC in the presence of GM-CSF + IL-4. On day 4 cells were harvested and silenced with either control siRNA or AMPK α 1 siRNA. On day 5 cells were treated with either VitD3, RA or Dex. On the 6th day, 100 ng/mL of LPS were added and mo-DC were used for further experiments. OCR (A) and ECAR (B), baseline levels of OCR (C), Mitochondrial spare respiratory capacity (SRC) (D), mitochondrial maximal respiratory capacity (E) and glycolysis (F) measured in control or AMPK α 1 silenced DC and VitD DC. (A,B) Data are from 3 independent experiments with one donor each. (C, D, E, F) Data are representative of 1 out of 3 independent experiments. Statistics are Two-Way Anova with Sidak's post-test. Data shown as mean \pm SEM; *p < 0.05, **p < 0.01, ***p < 0.001, ****p < 0.0001.

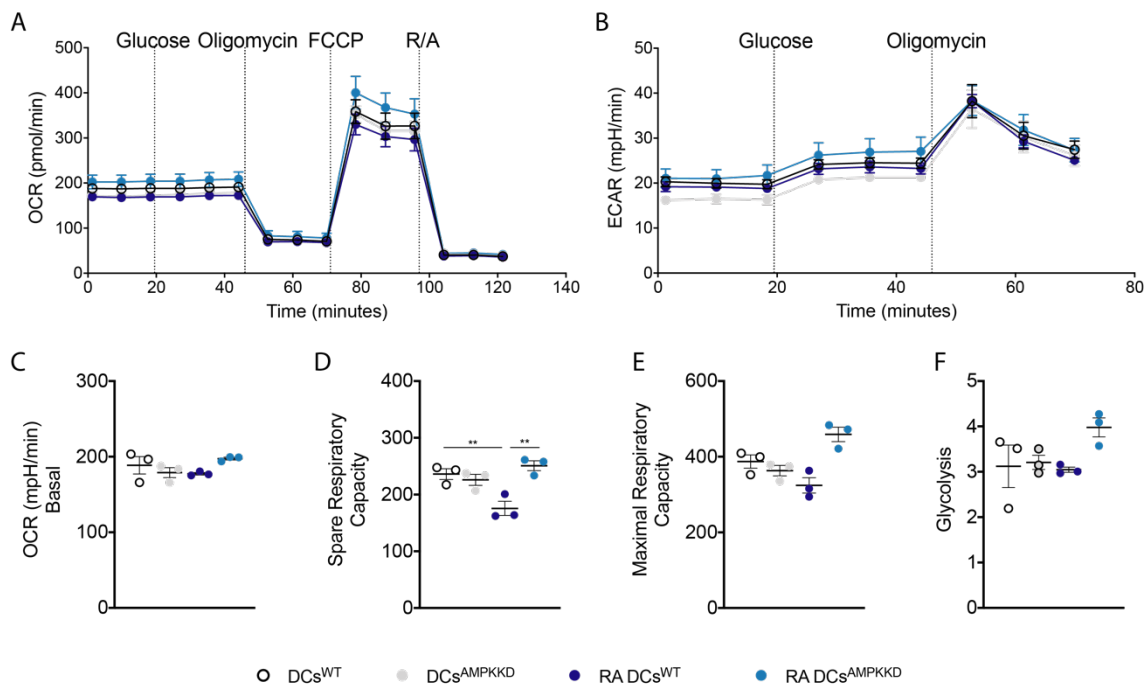


Figure 39: Metabolic characterization of RA DC. Monocytes were isolated from PBMC with CD14⁺ magnetic beads and differentiated in DC in the presence of GM-CSF + IL-4. On day 4 cells were harvested and silenced with either control siRNA or AMPK α 1 siRNA. On day 5 cells were treated with either VitD3, RA or Dex. On the 6th day, 100 ng/mL of LPS were added and mo-DC were used for further experiments. OCR (A) and ECAR (B), baseline levels of OCR (C), Mitochondrial spare respiratory capacity (SRC) (D), mitochondrial maximal respiratory capacity (E) and glycolysis (F) measured in control or AMPK α 1 silenced DC and RA DC. (A,B) Data are from 3 independent experiments with one donor each. (C, D, E, F) Data are representative of 1 out of 3 independent experiments. Statistics are Two-Way Anova with Sidak's post-test. Data shown as mean \pm SEM; *p < 0.05, **p < 0.01, ***p < 0.001, ****p < 0.0001.

glycolysis (F) measured in control or AMPK α 1 silenced DC and RA DC. (A,B) Data are pooled from 3 independent experiments with one donor each. (C, D, E, F) Data are representative of 1 out of 3 independent experiments. Statistics are Two-Way Anova with Sidak's post-test. Data shown as mean \pm SEM; * $p < 0.05$, ** $p < 0.01$, *** $p < 0.001$, **** $p < 0.0001$.

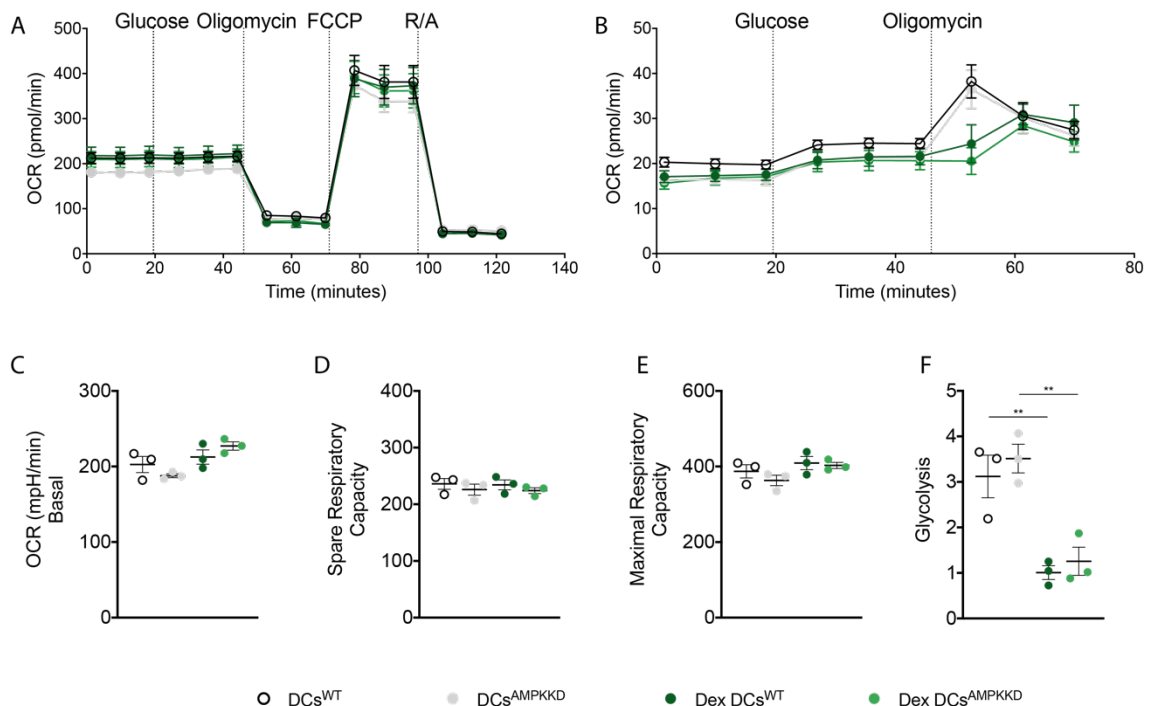


Figure 40: Metabolic characterization of Dex DC. Monocytes were isolated from PBMC with CD14⁺ magnetic beads and differentiated in DC in the presence of GM-CSF + IL-4. On day 4 cells were harvested and silenced with either control siRNA or AMPK α 1 siRNA. On day 5 cells were treated with either VitD3, RA or Dex. On the 6th day, 100 ng/mL of LPS were added and mo-DC were used for further experiments. OCR (A) and ECAR (B), baseline levels of OCR (C), Mitochondrial spare respiratory capacity (SRC) (D), mitochondrial maximal respiratory capacity (E) and glycolysis (F) measured in control or AMPK α 1 silenced DC and Dex DC. (A,B) Data are pooled from 3 independent experiments with one donor each. (C, D, E, F) Data are representative of 1 out of 3 independent experiments. Statistics are Two-Way Anova with Sidak's post-test. Data shown as mean \pm SEM; * $p < 0.05$, ** $p < 0.01$, *** $p < 0.001$, **** $p < 0.0001$.

Loss of AMPK largely reverted, the VitD3-induced metabolic alterations, especially glycolysis and basal levels of mitochondrial OCR (Figure 38).

Differently from what we observed in VitD DC, in which mitochondria seem to be highly active, RA DC had reduced SRC that was restored in the absence of AMPK (Figure 39D). A similar trend could be observed in the maximal respiratory capacity of those cells. Finally, consistent with the absence of AMPK activation in Dex-DC no major alterations were observed in the metabolic profile of Dex DC, in absence of AMPK (Figure 40). Taken together these data suggest that AMPK is important for VitD3 and RA-induced metabolic changes in tolDC.

4.12.3. *AMPK^{KD} decreases induction of suppressive T cells by RA DC*

As it can be observed in Figure 41A, knockdown of AMPK α 1 mRNA expression was higher than 90% and cells that were silenced for AMPK could not properly phosphorylate ACC when treated with AICAR. Interesting, none of the costimulatory markers (Figure 41B) or the cytokines secreted by tolDC (Figure 41C) were affected by lack of AMPK. However, there was a clear trend towards reduced expression of CD103, the main marker associated with RA DC differentiation, in the absence of AMPK, suggesting that AMPK might be important for the differentiation process of these tolDC (Figure 41B).

Next we aimed to analyze the cytokines secreted by naïve T cells primed by tolDC as well as their ability to induce the differentiation of FoxP3 Treg. The T cells ability to secrete IFN- γ was not affected by the lack of AMPK, since all tolDC were still able to decrease the ability of T cells to secrete this cytokine. However, it could be observed that the ability of RA DC to induce IL-10-secreting T cells was slightly reduced when RA DC were silenced for AMPK (4.00 ± 1.23 vs 6.54 ± 1.63 ; mean \pm SD; $p=0.35$) (Figure 11D). Regarding the generation of Treg, surprisingly, VitD DC did not induce the gene (KAISAR et al., 2017) (Figure 11E). RA-DC and Dex DC most likely induce Tr1 Treg, characterized by the secretion of IL-10. The lack of AMPK did not affect the FoxP3⁺ generation by any of the tolDC.

So far, the data had suggested the lack of AMPK was not important for the tolerogenic properties of VitD DC nor Dex DC. However, several pieces of data pointed out that AMPK has an impact in the RA DC, since the expression of CD103 and the ability to promote IL-10 secretion by T cells were impaired in the absence of AMPK. Concordantly, the ability to generate functional suppressor T cells by RA DC was completely abrogated when AMPK was silenced in these cells (Figure 41F). To further corroborate these findings we cultured murine GM-CSF bone marrow-derived dendritic cells (GMDC) from CD11c^{WT} and CD11c ^{Δ AMPK α 1} mice in the presence of RA. Interestingly, while RA conditioned GMDC displayed reduced ability to promote OT-II CD4⁺ T cell proliferation, this was not observed in GMDC lacking AMPK (Figure 41G). Taken together, these data suggest that RA depends on AMPK to promote tolDC with the ability to induce functional suppressive IL-10-secreting T cells.

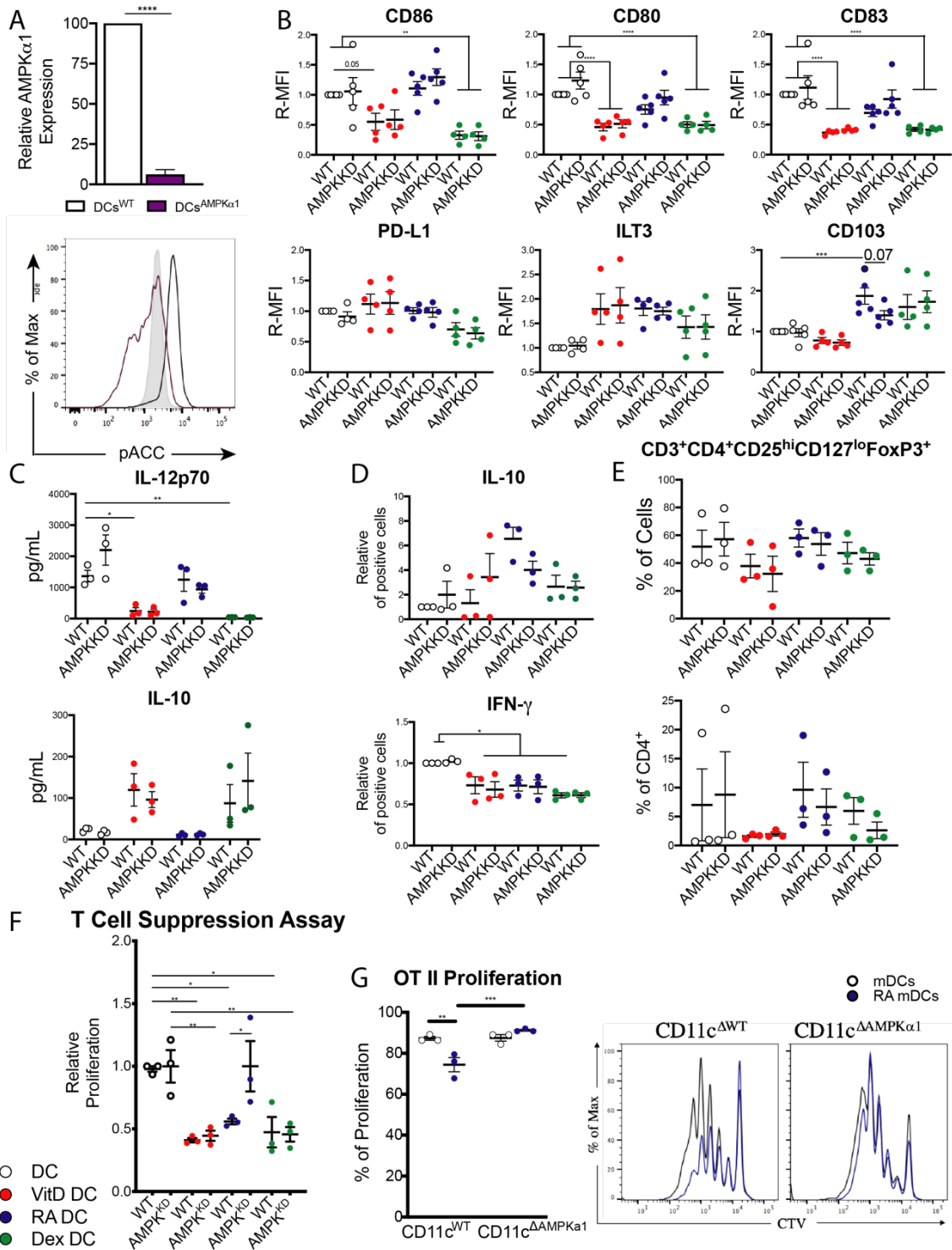


Figure 41: Suppressive ability of T cells primed by RA DC is dependent on AMPK. Monocytes were isolated from PBMC with CD14⁺ magnetic beads and differentiated in DC in the presence of GM-CSF + IL-4. On day 4 cells were harvested and silenced with either control siRNA or AMPK α 1 siRNA. On day 5 cells were treated with either VitD3, RA or Dex. On the 6th day, 100 ng/mL of LPS were added and mo-DC were used for further experiments. (A) fold change of AMPK α 1 expression by mo-DC (B) Characterization of surface markers of tolDC by flow cytometry. (C) mo-DC were co-cultured with CD40L-expressing cell line (J558) for 24 hours and supernatants were collected, and cytokines were measured by ELISA. (D, E, F) mo-DC were co-cultured with allogeneic naive T cells as described in “material and methods” section and (E) intracellular cytokines levels were measured by flow cytometry, (F) FoxP3 expression was analyzed by flow cytometry or (E) T cell suppression assay was performed. (G) Bone marrow cells were isolated from CD11c^{WT} and CD11c Δ AMPK α 1 mice and cultured in the presence of murine GM-CSF for 8 days. On day 6, cells were either treated with RA or left untreated and on the 7th day GMDC were pulsed with OVA + LPS for

24 hours. On day 8, MACS-isolated CTV-labelled OVA-specific OT-II T cells were co-cultured with GMDC. 4 days later, proliferation of OT-II T cells was evaluated by CTV dilution. (A-G) Data are pooled from 3-4 independent experiments with one donor each. Statistics are Two-Way Anova with Sidak's post-test. Data shown as mean \pm SEM; * $p < 0.05$, ** $p < 0.01$, *** $p < 0.001$, **** $p < 0.0001$.

4.12.4. *AMPK^{KD} restored ALDH activity in RA-DC*

One of the main characteristics of RA DC is the expression of the αE integrin CD103. Moreover, DC differentiated in the presence of RA have been shown to express ALDH2, encoded by the *aldh1a2* gene, which is responsible for metabolizing vitamin A to RA (BAKDASH et al., 2015). In the gut CD103⁺ DC are also characterized by the expression of ALDH2 and production of RA, which has been linked to their ability to prime and recruit Tregs (COOMBES et al., 2007; ESTERHÁZY et al., 2019). Because of this we decided to evaluate the expression and activity of ALDH in RA DC and test if AMPK would affect this.

The activity of ALDH is, as expected, significantly increased in RA DC, and in some extent in Dex DC and VitD DC as well (Figure 42A). To try to better understand if the increased ALDH activity could be important for the tolerogenic properties of RA DC, mo-DC were incubated with DEAB (an inhibitor of ALDH activity) for 30 minutes, treated with RA then on the next day cells were activated with LPS for 24 hours (48 hours of RA treatment in total). The treatment with DEAB did not affect the ALDH activity (Figure 42B) nor the ability of RA DC to generate functional suppressive T cells (Figure 42C), suggesting that there was no proper inhibition of the enzyme.

To try to better understand the ALDH function in RA DC, we hypothesized that AMPK could be involved in the RA-induced ALDH activity and to test this we analyzed the ALDH activity in RA DC lacking AMPK. We could observe that in iDC the RA treatment itself had little impact in the ALDH activity and, as a consequence, AMPK had no significant impact in the activity of this protein (Figure 42D). However, when RA DC were activated with LPS we could see that the increased RA-induced ALDH activity was completely abolished in the absence of AMPK (Figure 42E). Taken together these data suggest that RA-induced ALDH activity in LPS-stimulated DC might be dependent on AMPK.

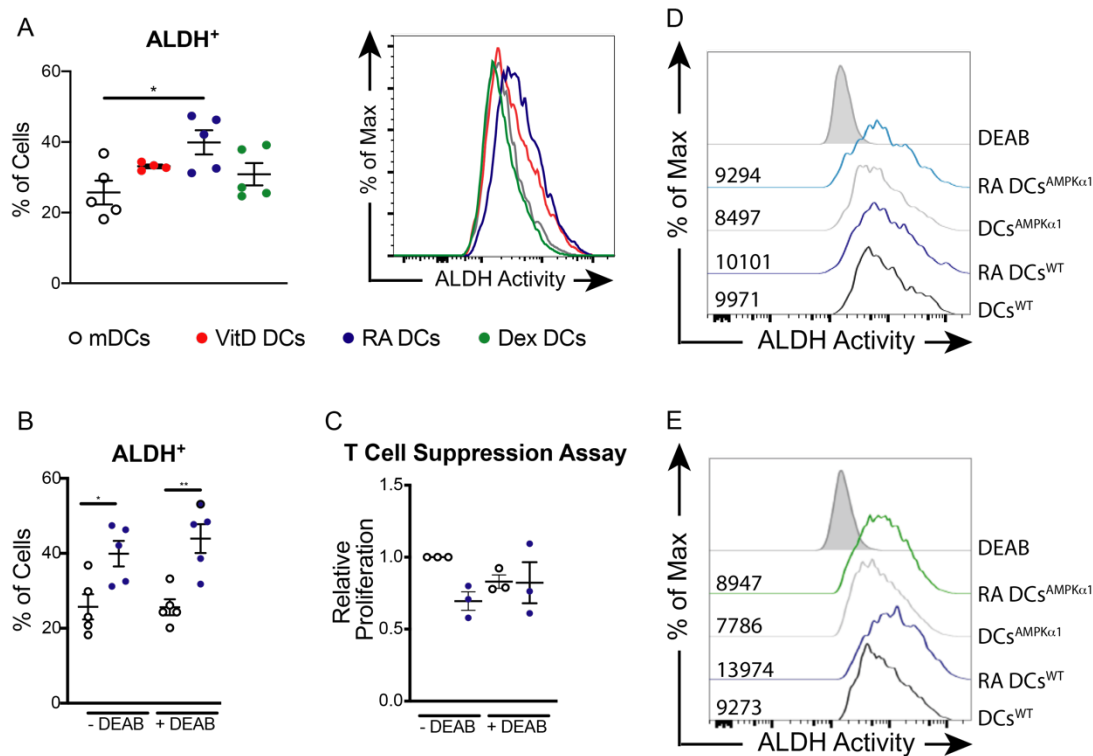


Figure 42: ALDH activity in RA-induced DC might be controlled by AMPK. (A) Monocytes were isolated from PBMC with CD14⁺ magnetic beads and differentiated in DC in the presence of GM-CSF + IL-4. On day 5 cells were treated with either VitD3, RA or Dex. On the 6th day, 100 ng/mL of LPS were added and ALDH activity was measured by flow cytometry. (B,C) Monocytes were isolated from PBMC with CD14⁺ magnetic beads and differentiated in DC in the presence of GM-CSF + IL-4. On day 5 cells were either treated with N,N-diethylaminobenzaldehyde (DEAB) or left untreated and 30 minutes later cells were treated with RA. On the 6th day, 100 ng/mL of LPS were added and ALDH activity was measured by flow cytometry (B) or mo-DC were co-cultured with allogeneic naïve T cells for T cell suppression assay as described in “material and methods” section (C). (D,E) Monocytes were isolated from PBMC with CD14⁺ magnetic beads and differentiated in DC in the presence of GM-CSF + IL-4. On day 4 cells were harvested and silenced with either control siRNA or AMPK α 1 siRNA. On day 5 cells were treated with either treated with RA or left untreated. On the 6th day, cells were left untreated (D) or treated with 100 ng/mL of LPS (E) and ALDH activity was measured by flow cytometry. Data are pooled from 2 independent experiments with 2 and 3 donors (A,B) or 1 experiment with 3 donors (C) or 1 experiment with 1 donor (D,E). Statistics are One-Way Anova with Tukey HSD post test (A) or Two-Way Anova with Sidak’s post-test (B,C). Data shown as mean \pm SEM; *p < 0.05, **p < 0.01, ***p < 0.001, ****p < 0.0001.

4.12.5. Mouse RA GMDC mimic human RA-DC

We had already observed that RA GMDC were also dependent on AMPK to inhibit the proliferation of OT-II CD4⁺ T cells (Figure 41G). Next we aimed to investigate the whole profile of GMDC treated with RA. First of all, we observed that indeed the AMPK α 1 was knocked out of CD11c cells, since the levels of pACC were reduced in CD11c ^{Δ AMPK α 1} when compared to CD11c^{WT} (Figure 43A). Although without statistical significance, the expression of CD80 and CD86 tended to be reduced in RA GMDC in an AMPK-independent manner while no differences were observed regarding PD-L1 expression (Figure 43B). The secretion of IL-12p70 was also reduced by RA GMDC independently from AMPK (Figure 43C). These results were different from the ones we observed in mo-DC, since the expression of co-stimulatory markers were not affected as

well as the secretion of IL-12p70. However, even with those differences, RA GMDC relied on AMPK to inhibit the proliferation of (Figure 43D). The secretion of IFN- γ was reduced when OT-II CD4⁺ T cells were co-culture with RA GMDC (0.69 ± 0.07 vs 1.00 ± 0.00 ; mean \pm SEM; $p= 0.09$), but this reduction was independent on AMPK (Figure13E). Interestingly, while RA mo-DC could not induce FoxP3⁺ Treg, RA GMDC not only were able to induce those cells as this ability was reversed in CD11c ^{Δ AMPK α 1} GMDC (Figure 43E). Interestingly, in GMDC the inhibition of ALDH with DEAB was effective in restore the ability of GMDC to induce the proliferation of OT II CD4⁺ T cells and the increased of FoxP3⁺ cells trend to reduce. Taken together the data suggests that, in the mice system, RA also depends on AMPK to generate suppressive DC, via ALDH activity that, instead of generating IL-10-secreting T cells, are now able to induce FoxP3⁺ Treg.

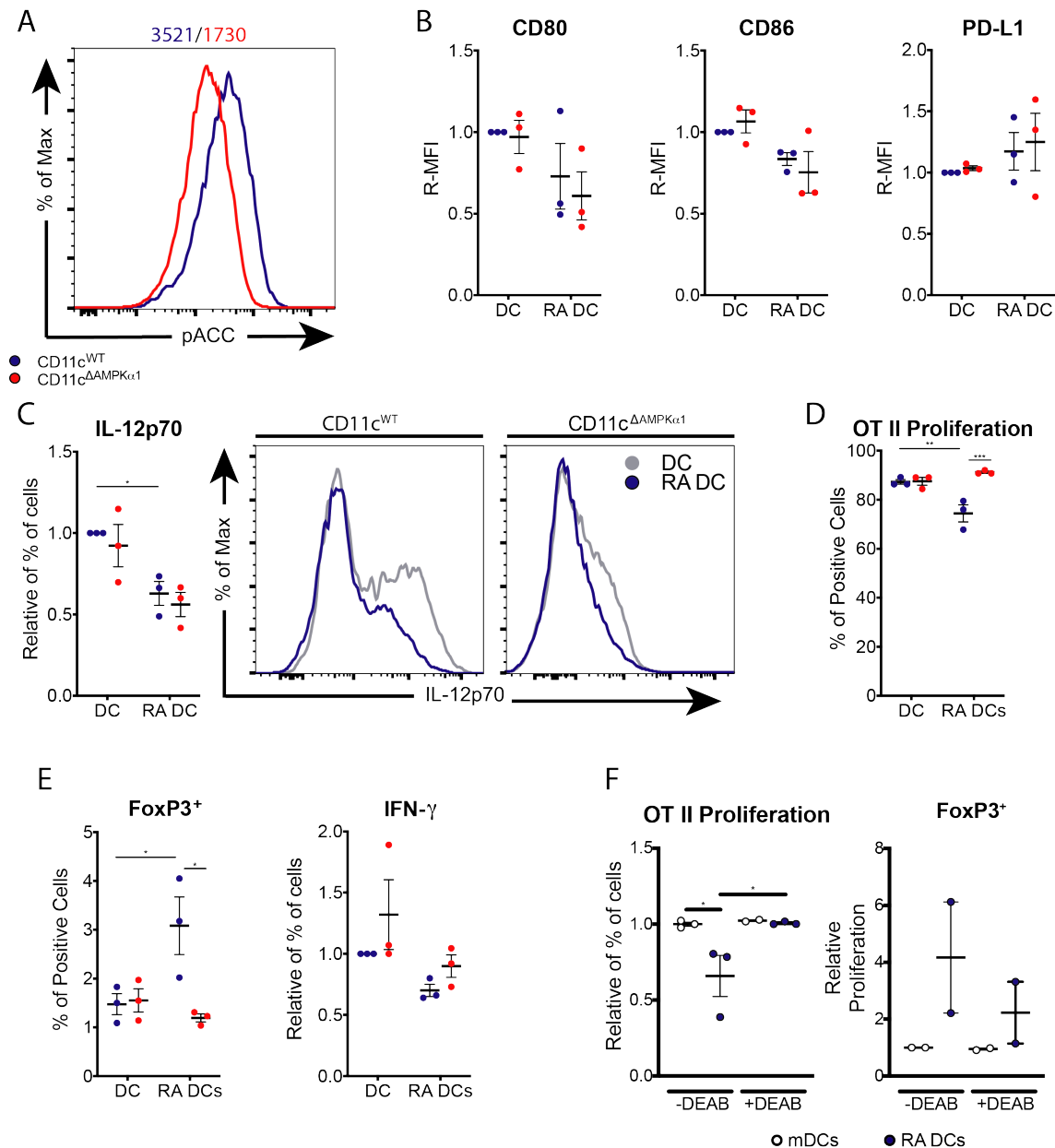


Figure 43: RA-induced GMDC recapitulate the phenotype of RA DC. Bone marrow cells were isolated from CD11c^{WT} and CD11c^{ΔAMPKα1} mice and cultured in the presence of murine GM-CSF for 8 days. On day 6, cells were either treated with RA or left untreated and on the 7th day GMDC were pulsed with OVA + LPS for 24 hours. (A) phosphorylation levels of acetyl-coA acetylase (pACC) measured by flow cytometry. (B) Surface markers expressed by GMDC. (C) GMDC that were not treated with LPS on day 7 were treated with LPS in the presence of brefediln A. Six hours later cells were harvested and fixed with 1.9% of formaldehyde and then permeabilized with ebioscience permubuffer and stained for IL12p70 secretion. (D,E) On day 8, MACS-isolated CTV-labelled OVA-specific OT-II T cells were co-cultured with GMDC. 4 days later, proliferation of OT-II T cells was evaluated by CTV dilution (D) and 6 days later the T cell expression of FoxP3 and cytokines were evaluated (E). (F) Bone marrow cells were isolated from CD11c^{WT} and CD11c^{ΔAMPKα1} mice and cultured in the presence of murine GM-CSF for 8 days. On day 6, cells were either treated with RA or left untreated and on the 7th day GMDC were either treated with N,N-diethylaminobenzaldehyde (DEAB) or left untreated and 30 minutes and then pulsed with OVA + LPS for 24 hours. On day 8, MACS-isolated CTV-labelled OVA-specific OT-II T cells were co-cultured with GMDC. 4 days later, proliferation of OT-II T cells was evaluated by CTV dilution (left panel) and 6 days later the T cell expression of FoxP3 was evaluated (right panel). (A-F) Data are pooled from 2/3 independent experiments with one mouse from each genotype in each experiment. Statistics are Two-Way Anova with Sidak's post-test. Data shown as mean ± SEM; *p < 0.05, **p < 0.01, ***p < 0.001, ****p < 0.0001.

Next we evaluated the metabolic profile of immature GMDC and similar to what we had observed in the mo-DC, VitD GMDC had an overall increase in the metabolic activity, with increased levels of both glycolysis and OXPHOS that were also dependent on AMPK (Figure 44A and Figure 44D). It is interesting to note that RA GMDC also showed reduced SRC, as it could be observed in RA mo-DC. However, the absence of AMPK did not completely restore the mitochondrial fitness that was still impaired (Figure 44B). The basal respiration of both tolDC was completely abrogated in the absence of AMPK (Figure 44D), which might suggest that AMPK is important for the mitochondrial function of tolerogenic GMDC in a more extensive way than it is for the mo-DC. Glycolysis was slightly, but not significantly increased in VitD and RA GMDC, but AMPK was important for the glycolytic activity of all GMDC (Figure 44C and Figure 44D). Interesting, the absence of AMPK in control GMDC did not only affect glycolysis, but SRC and most striking the maximal respiratory capacity were also reduced. Taken together, the data suggest that AMPK is important for the metabolic function of GMDC in a more extensive manner than it was for the mo-DC and that tolerogenic GMDC relies on AMPK for glycolysis.

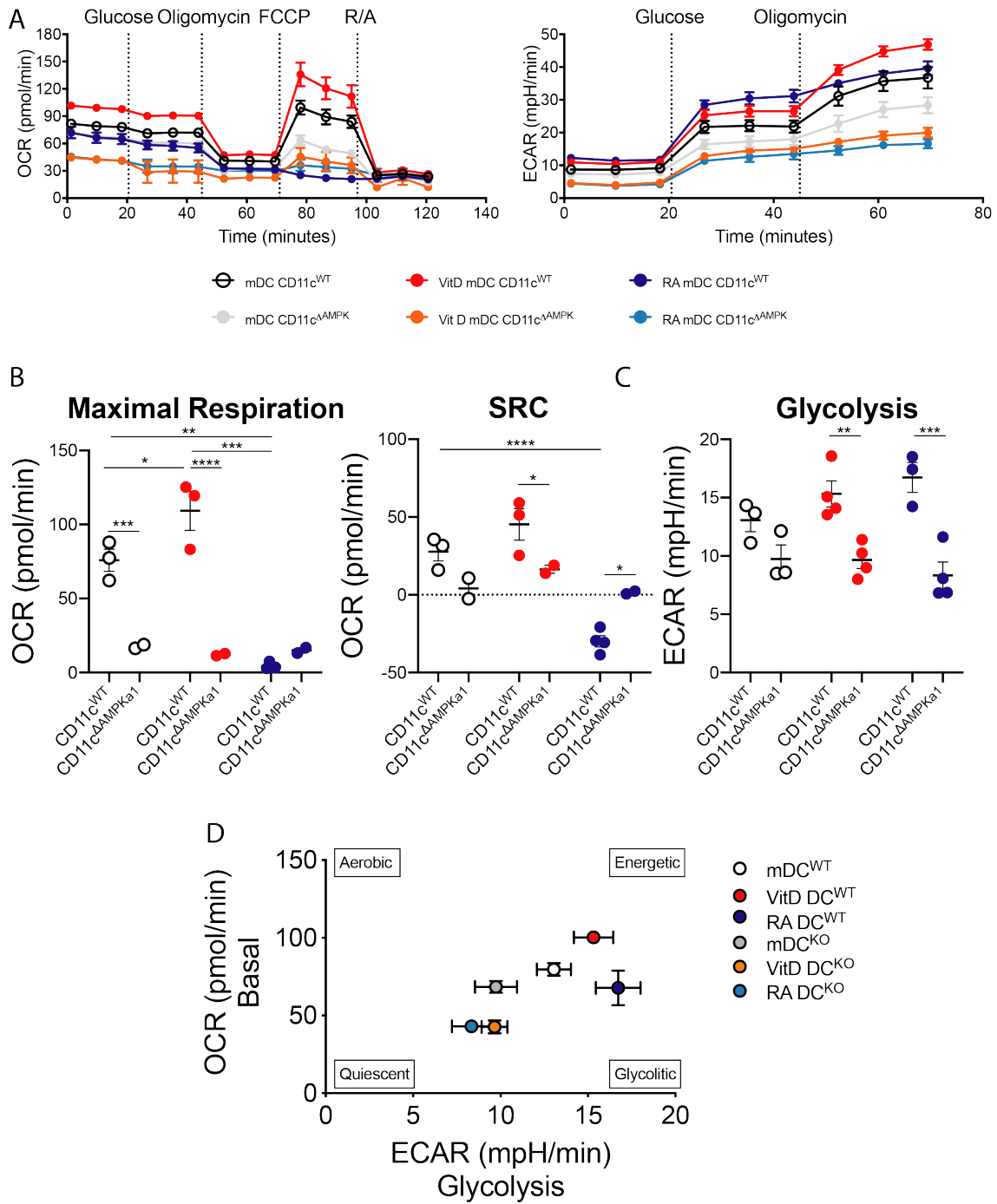


Figure 44: Metabolic characterization of GMDC. Bone marrow cells were isolated from CD11c^{WT} and CD11c^{AMPKα1} mice and cultured in the presence of murine GM-CSF for 8 days. On day 6, cells were either treated with VitD, RA or left untreated and cells were harvested on the 8th day. (A) OCR and ECAR values from GMDC. (B) Quantification of maximal respiration (left panel) and spare respiratory capacity (SRC) (right panel) from GMDC. (C) Quantification of glycolysis from GMDC. (D) Energetic graphic showing the baseline levels of OCR vs glycolysis levels from GMDC. Data are representative from one out of 3 independent experiments with one mouse from each genotype in each experiment. Statistics are Two-Way Anova with Sidak's post-test. Data shown as mean ± SEM; *p < 0.05, **p < 0.01, ***p < 0.001, ****p < 0.0001.

4.12.6. CD11c^{AMPKα1} RA GMDC failed to decrease polyclonal IFN- γ secretion by T cells in cell transfer experiment.

After having established that RA GMDC also relied on AMPK activity for their tolerogenic properties, we aimed to address how the loss of AMPK would affect the T

cell-priming capacities of DC *in vivo*. To this end we adoptively transferred GMDC derived from either CD11c^{WT} or CD11c^{ΔAMPKα1} mice, treated or not with RA and pulsed *in vitro* with OVA and LPS into footpads of recipient mice and analyzed the T cell response in the draining LNs 7 days later (Figure 45A). Compared to WT GM-DC, the immunization with AMPK-deficient GMDC did not affect the frequencies of CD4⁺CD44⁺ nor the frequencies of CD8⁺CD44⁺ T cell. On the other hand, the frequency of effector CD44⁺CD62L⁻CD8⁺ T cells (Figure 45B) and OVA-specific CD8⁺ T cells (Figure 45C) were significantly increased. The immunization with WT RA GMDC did not affect the priming of OVA-specific CD8⁺ T cells nor reduced the frequencies of effector CD4⁺ or CD8⁺ T cells. However, the immunization with WT RA GMDC decreased the frequencies of both IFN-γ and IL-17A-secreting CD4⁺ T cells (Figure 45D and Figure 45E, respectively), but only the secretion of IFN-γ could be rescued when AMPK-deficient RA GMDC were transfected (Figure 45D). No differences were observed in the secretion of IL-10 and IL-4 by CD4⁺ T cells neither the secretion of IFN-γ by CD8⁺ T cells (Figure 45F). Surprisingly, no differences were observed neither on the frequencies of CD4⁺FoxP3⁺ T cells nor on the expression of CTLA-4 by FoxP3⁺ Treg (Figure 45G).

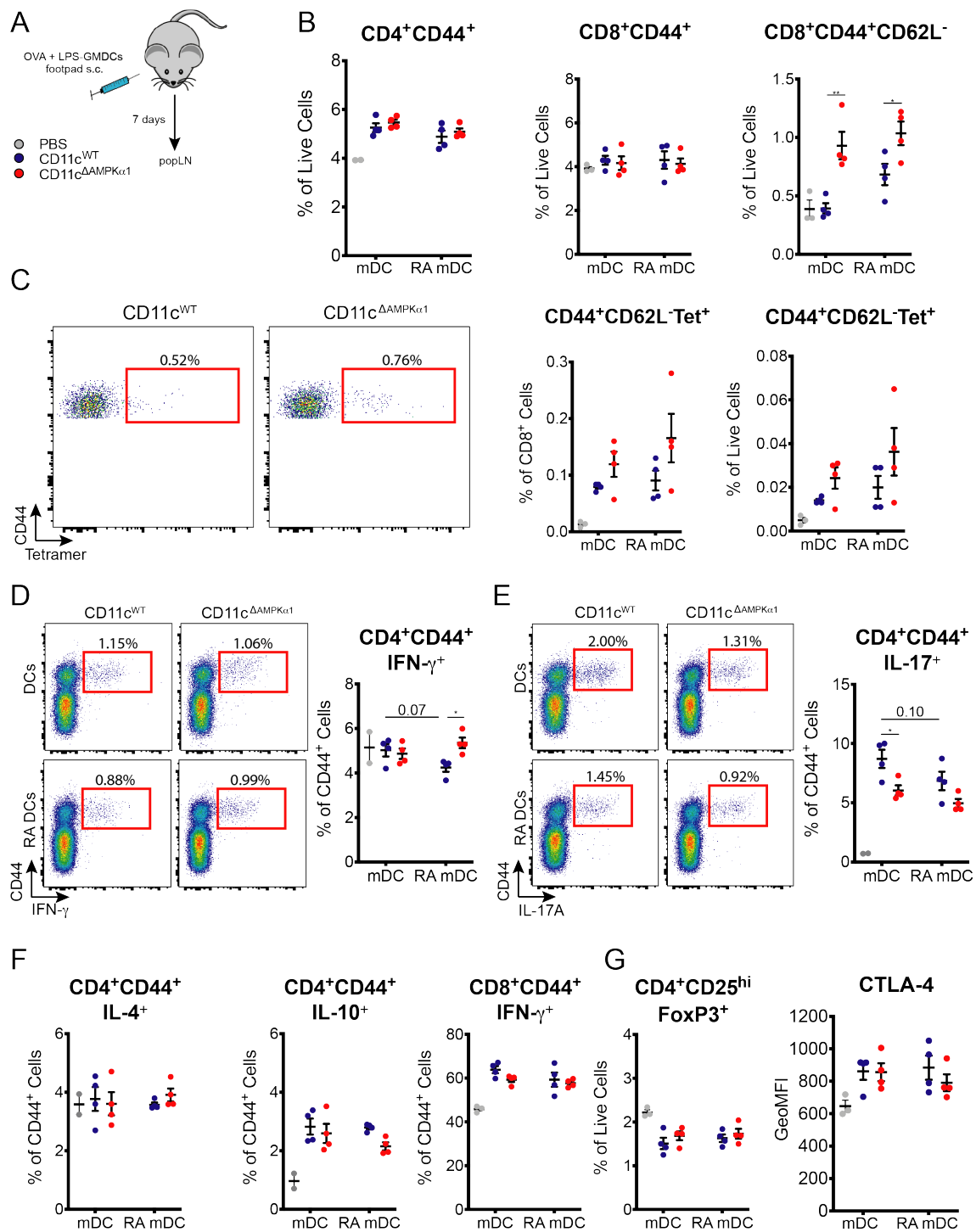


Figure 45: AMPK is important for RA-induced GMDC to limit the secretion of IFN- γ by T cells in vivo. GMDC were stimulated for 24hours with OVA and LPS and then injected into footpads of WT mice. Seven days later, T cell responses were evaluated in draining popliteal LNs (popLN) by flow cytometry (A-G). (B) Frequencies of CD4⁺CD44⁺ cells (left panel), CD8⁺CD44⁺ cells (middle panel) and CD8⁺CD44⁺CD62L⁻ effector CD8⁺ and CD4⁺ T cells. (C) Frequencies of CD8⁺CD44⁺CD62L⁻ OVA-specific CD8⁺ T cells, based on K^bOva tetramer, are shown in representative flow cytometry plots (left) and frequencies of CD8⁺ (middle) and live cells (right). (D-G) popLN cells were stimulated with PMA/Ionomycin in the presence of Brefeldin A and CD4⁺ T cells were analyzed for expression of IFN- γ (D) and IL-17A (E) as shown in representative flow cytometry plots (left) and frequencies of live cells (right). CD4⁺ popLN cells were also analyzed for the expression of IL4 (F left), IL-10 (F middle) and CD8⁺ T cells were analyzed for the expression of IFN- γ (F right) as shown in frequencies of live cells. CD4⁺ popliteal LN cells were also analyzed for the expression of FoxP3 (G left) and FoxP3⁺ cells were analyzed for the expression of CTLA-4 (G right). Data are from one experiment with four lymph nodes per condition. Statistics are Two-Way Anova with Sidak's post-test. Data shown as mean \pm SEM; * p < 0.05, ** p < 0.01, *** p < 0.001, **** p < 0.0001.

4.12.7. *CD11c^{AMPK α 1} gut CD11b⁺CD103⁺ DC have low ALDH activity.*

To further explore the *in vivo* importance of AMPK for the tolerogenic properties of DC, we next aimed to investigate how AMPK could modulate the function of DC *in vivo* in the two main suppressive tissues: the gut and the lungs. For that, we extracted small intestine lamina propria (siLP) together with mesenteric lymph nodes (msLN) and Peyer's patch as well as lungs from CD11c^{WT} and CD11c ^{Δ AMPK α 1} mice.

In the gut and msLN, we can identify three main subsets of cDC: CD103⁺CD11b⁻ (CD103⁺ DC), CD103⁺CD11b⁺ (CD103⁺CD11b⁺ DC) and CD103⁻CD11b⁺ (CD11b⁺ DC). In CD11c ^{Δ AMPK α 1} mice the frequency of CD103⁺CD11b⁺ DC tended to be reduced when compared to the cells presented in the gut of CD11c^{WT} (Figure 46A) and the frequencies of other myeloid subsets such as cDC2, pDC, CD11c⁺ macrophages and CD11c⁻ macrophages also tended to be reduced (Figure 46C). Interestingly, the ALDH activity was reduced only on CD103⁺CD11b⁺ DC (Figure 46B). At steady state, no differences were observed in the frequency of regulatory FoxP3⁺ T cells (Figure 46D) nor in the expression of co-stimulatory molecules in any of the gut subtypes of cDC (Figure 46E). Analysis of the lungs of CD11c ^{Δ AMPK α 1} mice showed no differences in the frequencies of CD103⁺ or CD11b⁺, alveolar macrophages or interstitial macrophages (Figure 46F). Interestingly, also in the lungs, the ALDH activity of CD103⁺ DC was reduced (Figure 46G). In naïve mice with AMPK deficiency in CD11c⁺ cells, no differences in frequency of FoxP3⁺ T cells were observed in the lungs, although the expression of the immune-suppressor marker CTLA-4 was increased in FoxP3⁺ T cells in the lungs (Figure 46F). Concordantly, reduced frequency of effector CD4⁺CD44⁺ T cells, as well as reduced frequencies of IFN- γ and IL-10-secreting CD4⁺ T cells were observed, suggesting AMPK is important for cDC to mount T cell response in lungs (Figure 46G).

CD11c ^{Δ AMPK α 1} mice had normal frequencies of migratory, resident and the three main DC subtypes in the msLN (Figure 47A). ALDH activity of cDC was not affected as well in none of the subtypes of DC (Figure 47B) and, an overall increase of several activation markers could be observed in all cDC, specially CD103⁺CD11b⁺ and CD11b⁺ DC (Figure 47C). All though no differences were observed in the frequencies or activation status of FoxP3⁺ Tregs at steady state (Figure 47E), CD11c ^{Δ AMPK α 1} mice displayed enhanced production of IFN- γ and IL-10 by CD4⁺ T cells in msLNs (Figure

17D). The increase in IL-10 production by T cells might be a negative feedback mechanism, triggered by a possible inflammatory status in the msLN.

Interestingly, we could observe that ALDH activity, was higher in CD11b⁺CD103⁺ cDC in the gut while in the msLN, the subtype with higher ALDH activity was CD103⁺CD11b⁻ cDC (Figure 17F). This might suggest that in the siLP, the main suppressive subset of cDC would be the CD11b⁺CD103⁺ cDC instead of CD103⁺CD11b⁻ cDC, which was claimed to have this function in the msLN (ESTERHÁZY et al., 2019). Collectively, the data suggest that AMPK signaling in DC might control gut and msLN homeostasis by promoting an anti-inflammatory status via regulation of ALDH activity specifically in CD103⁺CD11b⁺ DC. Interesting, the role of AMPK signaling in DC might be tissue-selective since in the lungs, CD11c^{ΔAMPKα1} mice seemed to present defective T cells-cytokine secretion.

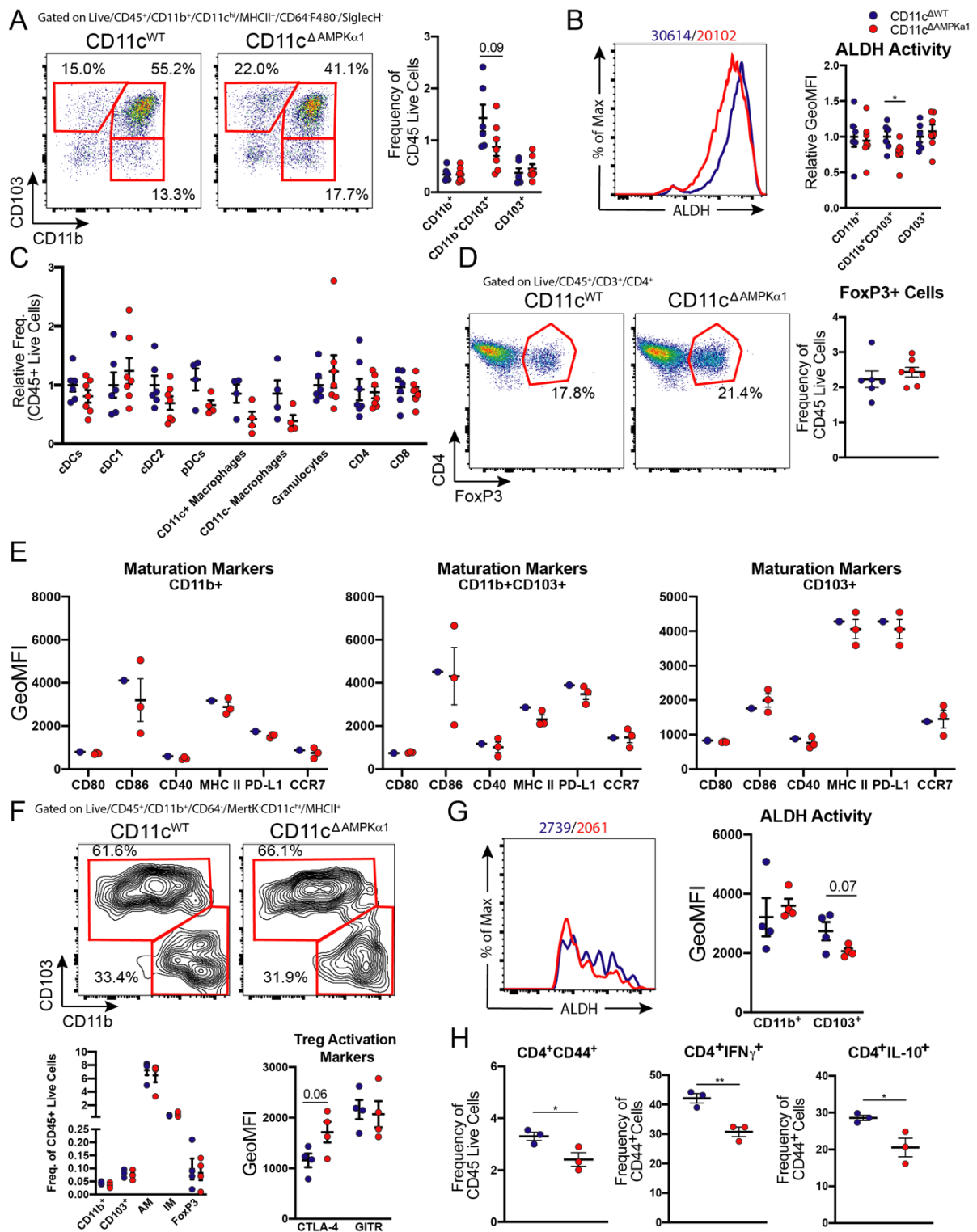


Figure 46: ALDH activity in gut CD11b+CD103+ DC is partially dependent of AMPK. (A-E) Cells from small intestine lamina propria (siLP) were isolated from CD11c^{WT} and CD11c^{ΔAMPKα1} mice and stained for flow cytometry analyzes. (A) Representative plot (left) and frequencies of CD45⁺ live cells (right) of the cDC found in the gut (see Supplementary Figure 1A for whole gating strategy). (B) representative plot of concatenated samples (left) and relative geometric median fluorescence intensity (GeoMFI) (right) of ALDH activity. (C) Frequencies of immune cells identified in the gut of CD11c^{WT} and CD11c^{ΔAMPKα1} mice. (D) Representative plot (left) and frequencies of CD45⁺ live cells (right) of CD4⁺FoxP3⁺ T cells found in the gut of CD11c^{WT} and CD11c^{ΔAMPKα1} mice (E) GeoMFI of indicated surface markers expressed by cDC found in the gut. (E-G) Lung cells were isolated from CD11c^{WT} and CD11c^{ΔAMPKα1} mice and stained for flow cytometry analysis. (A) Representative plot (upper) and frequencies of CD45⁺ live cells (lower left) of cDC, macrophages and CD4⁺FoxP3⁺ T cells found in the lungs of CD11c^{WT} and CD11c^{ΔAMPKα1} mice (see Supplementary Figure 1B for whole gating strategy) and expression of activation markers of CD4⁺FoxP3⁺ T cells

(lower right). Lung cells were stimulated with PMA/Ionomycin in the presence of Brefeldin A and CD4⁺ T cells were analyzed for expression of CD44 (H left) IFN- γ (H middle) and IL-10 (H right) as shown by frequencies of live cells. (A-E) Data are pooled from 2 independent experiments with 3/4 mice per genotype. (F-H). Data are from 1 experiment with 4 mice per genotype. Statistics are Unpaired T test. Data shown as mean \pm SEM; *p < 0.05, **p < 0.01, ***p < 0.001, ****p < 0.0001.

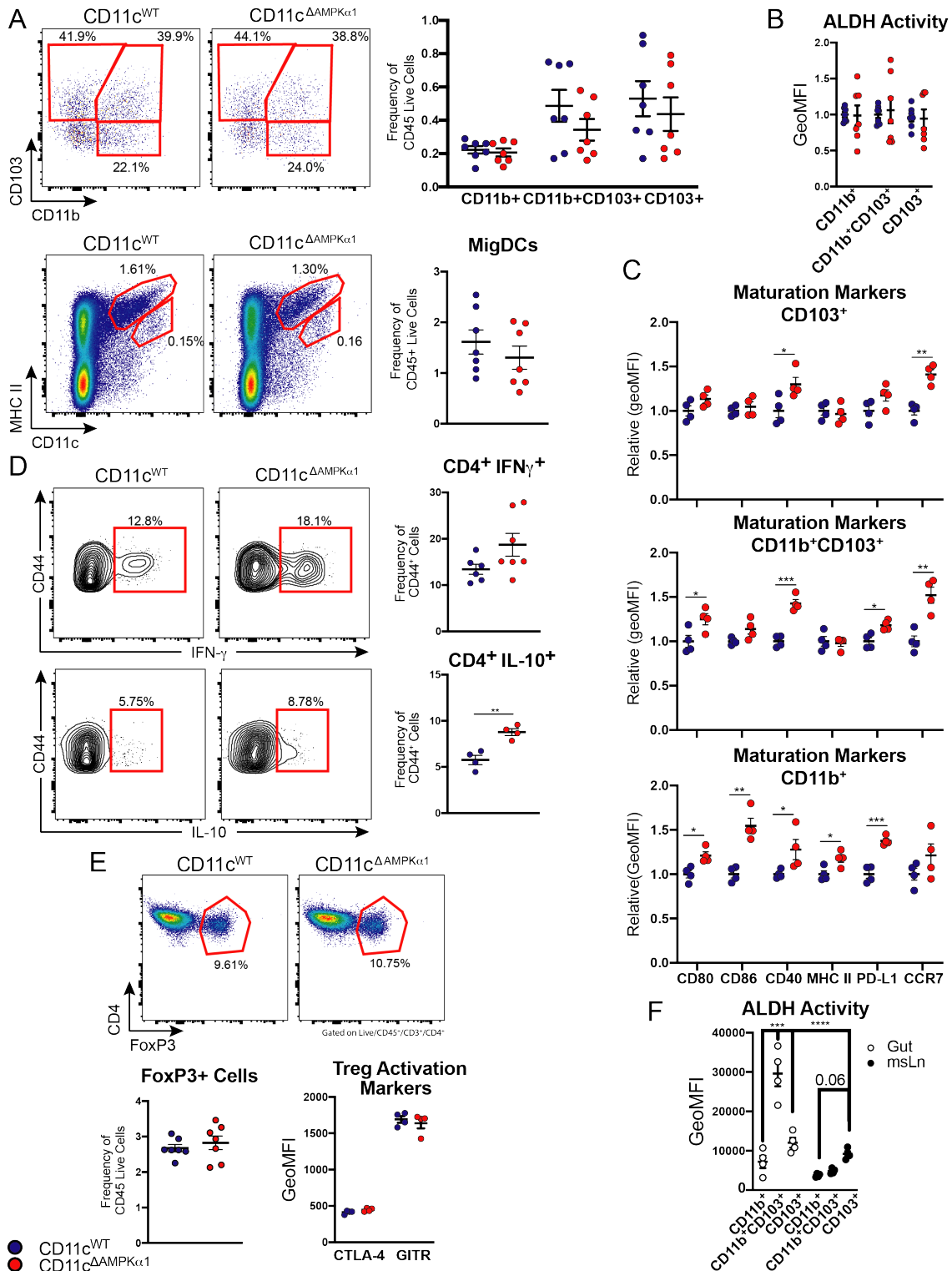


Figure 47: AMPK limits the expression of co-stimulatory molecules in cDC and helps to promote homeostasis in msLN. (A-E) Cells from mesenteric lymph node (msLN) were isolated from CD11c^{WT} and CD11c ^{Δ AMPK α 1} mice and stained for flow cytometry analyzes. (A) Representative plot (upper left) and frequencies of CD45⁺ live cells (upper

right) of the cDC found in the msLN (see Supplementary Figure 1A for whole gating strategy). Representative plot (bottom left) and frequencies of CD45⁺ live cells (bottom right) of migratory DC (MigDC) and resident DC (ResDC) found in the msLN. (B) Relative geometric median fluorescence intensity (GeoMFI) of ALDH activity in cDC found in the msLN. (C) Relative GeoMFI of indicated surface markers expressed by cDC found in the msLN. (D,E) cells from msLN were stimulated with PMA/Ionomycin in the presence of Brefeldin A and CD4⁺ T cells were analyzed for expression of IFN- γ (D) and IL-10 (E) as shown in representative flow cytometry plots (left) and frequencies of live cells (right). (F) ALDH activity in cDC in gut and msLN. Cells isolated from both gut and msLN were stained for the ALDH activity and the subtypes displaying higher ALDH activity are switched in the gut and msLN. (A-F) Data are pooled from 2 independent experiments with 3/4 mice per genotype. (F) Data are representative from 1 out of 2 independent experiment. Statistics are Unpaired T test. Data shown as mean \pm SEM; *p < 0.05, **p < 0.01, ***p < 0.001, ****p < 0.0001.

5. DISCUSSION

5. DISCUSSION

In the context of T1D, an autoimmune syndrome with a very complex pathophysiology, DC emerge as an important cell type because of their unique role in capturing, processing and presenting antigens to T cells. These cells, ultimately, will be responsible, directly or indirectly, for the destruction of islet beta cells. Interestingly, studying mo-DC from T1D patients, we observed reduced expression of CD80 followed by increases in IL-10 secretion. This would seem to contradict reports suggesting that DCs from NOD mice have a proinflammatory profile, with higher expression of costimulatory molecules and higher IL12p70 production (WHEAT et al., 2004). Nevertheless, other reports describe DCs with low CD86 expression and low ability to induce T lymphocyte proliferation in NOD mice compared to C57BL/6 and Balb/c mice (DAHLÉN; HEDLUND; DAWE, 2000). Consistent with our observation, low expression of costimulatory molecules, lower IL-12 secretion, followed by increases in IL-10 content, and poor ability to induce naïve T cell proliferation were observed in mo-DCs from T1D patients compared to mo-DC from healthy donors (ANGELINI et al., 2005). Suggesting a role for hyperglycemia in this phenomenon, serum from T2D patients or monocytes exposed to hyperglycemia displayed reduced expression of CD86, CD83 and failed to induce the proliferation of allogeneic T cells (MONTANI et al., 2016). Paradoxically, a low grade inflammation has been described in both NOD and mice treated with streptozotocin (a molecule able to induce beta cell destruction) associating this phenomena with increased levels of leukotriene-B4 (LT-B4) (FILGUEIRAS et al., 2015). To explain this apparent paradox of increased inflammatory response by deficient DC, it has been proposed that a deficiency in the maturation of patients' DC would lead to poor T lymphocyte stimulation, thus decreasing the stimulus for the generation of Tregs, facilitating the autoimmune process (ANGELINI et al., 2005; DAHLÉN et al., 1998; MOLLAH et al., 2008). Indeed, CD80/CD86 knockout NOD mice displayed severe insulinitis and reduced levels of Tregs (SALOMON et al., 2000) whereas CD11c^{ALKB1} mice, which display elevated levels of CD86, show increased Tregs counts in multiple organs (PELGROM et al., 2019). However, when we tested in our model, high glucose concentrations did not significantly affect the phenotype nor impaired the function of mo-DC from both patients and healthy donors. Interestingly, these mo-DC from patients, with lower CD80 expression and higher IL-10 production, are not mirrored by blood DC and CD14⁺ monocytes, which after LPS activation, secreted elevated levels of TNF- α . It is noteworthy, however, that under hyperglycemic conditions, mo-DC from diabetic

patients tended to secrete more TNF- α , IL-6 and IL-12p70 than mo-DC from healthy donors. This raises the question of how much the observed mo-DC phenotype and the increased ability of monocytes and blood DC from patients to secrete TNF are dependent on the same pathophysiological phenomena. Contributing to the complexity of the issue, it has been described that VitD3-treated mo-DC activated with LPS (but not CD40L) secreted elevated levels of TNF- α and the blocking of either membrane-bound TNF- α or soluble TNF- α impaired the capacity of these cells to induce Tregs (KLEIJWEGT et al., 2010).

We also investigated the role of VitD3 in both the “immunosuppressive” and metabolic properties of mo-DC from healthy donors and diabetic patients under different glucose concentrations. These two aspects of DC biology suffered coherent effects when the cells were obtained from healthy donors but seemed to dissociate when the cells were obtained from T1D patients. While VitD DC of diabetic patients maintained a similar metabolic profile, regardless of glucose concentration, VitD DC of healthy donors suffered significant variations in their glycolytic activity and oxidative metabolism, which were both partially inhibited at higher glucose concentrations. On the other hand, the immunophenotype of VitD DC from both patients and healthy donors was different from that of mo-DC, with reduced CD86 expression, lower TNF- α secretion (at higher glucose concentrations) and decreased ability to induce proliferation of T cells. Furthermore, VitD DC from healthy donors were even less efficient in inducing proliferation of allogeneic CD4⁺ T lymphocytes, when differentiated at higher glucose concentrations (25 mM), a phenomenon that was not observed in VitD DC from diabetic patients, since these cells were equally ineffective, regardless of glucose concentration. Interestingly, the reduced lymphostimulatory capacity observed in VitD DC from healthy donors differentiated at hyperglycemia was accompanied by reduction in glycolysis and oxidative profile, a feature displayed by diabetic patients’ VitD DC in both normo and hyperglycemia. This might suggest that VitD DC from healthy donors differentiated at high glucose concentration, tend to have a similar metabolic profile to VitD DC of diabetic patients and that VitD3-induced metabolic reprogramming might not rely as much on glycolysis in diabetic patients, as it seems to do in healthy donors.

In these experiments, where cells were exposed to glucose and their metabolism was evaluated, we noted that while VitD DC from healthy donors (differentiated under normoglycemic conditions) were able to increase intracellular glucose traffic, VitD DC

from diabetic patients (regardless of glucose concentration) were not. Interestingly, while increasing glucose concentration from 1 to 10mM was reported to be essential for the induction of the tolerogenic profile by VitD3 on healthy donors cells (FERREIRA et al., 2015), we noted that further increasing glucose concentration (25mM), inhibited glycolysis, but did not affect, in a similar degree, their lymphostimulatory deficit. Thus, although experiments with lower glucose concentrations suggest a causal relationship between tolerogenic profile and metabolic profile of mo-DC, the data we obtained with the higher dose of glucose on the cells of control subjects and the data obtained with patients' cells, regardless of glucose concentration, cast doubts upon such hypothesis.

The increase in glycolysis observed in VitD DC from healthy donors coincided with the increase in cell membrane GLUT1, when these cells were differentiated in the presence of 5.5 mM of glucose. Interestingly, VitD DC from diabetic patients differentiated in the presence of 5.5 mM of glucose also displayed increased surface GLUT1 expression without, however, increased glycolysis. Surface GLUT1 expression in diabetic patients was lower than that observed in healthy donors and this could, at least partially, explain why GLUT1 increase may not have been sufficient to increase glycolysis of these cells: the increased glucose available to the cell would be diverted to other metabolic pathways preventing the increased lactic acid production – the actual parameter we measure when we talk about “glycolysis”. When the cells were differentiated under hyperglycemia, VitD3 failed to increase expression of surface GLUT1 on both patients and healthy donors and glycolysis was reduced in VitD DC from healthy donors, resembling the metabolic profile of patients. This reinforces the hypothesis that VitD DC differentiated under high glucose concentrations tend to present the same metabolic reprogramming observed in diabetic patients. We cannot exclude the possibility that GLUT1-dependent metabolic modulations might have been biased by the time frame of our analysis. Increased GLUT3 and GLUT1 expression was observed 4 and 6 hours, respectively, after mo-DC received stimulus for differentiation (given by GM-CSF, IL-4 and VitD3) (FERREIRA et al., 2015) or after activation with LPS (KRAWCZYK et al., 2010). In our model, GLUT1 expression was evaluated 24 hours after LPS activation, a time when higher levels of expression might have been masked by GLUT1 internalization. In this scenario, since patients expressed lower levels of surface GLUT1, but similar to healthy donors' glucose uptake, one could hypothesize that, in order to maintain glucose homeostasis, patients' cells are actually constitutively expressing higher levels of GLUT1 and that after 24 hours of LPS activation, this

transporter would have been internalized leading to its reduction on the surface. In line with this observation, is the fact that at normoglycemic conditions mo-DC from diabetic patients were, actually more glycolytic than mo-DC from healthy donors (not considering VitD3 modulations). The same observation was true, here, for diabetic blood CD11c⁺CD123⁻ DC and diabetic alveolar macrophages (RAMALHO et al., 2019), with the first being accompanied by increased secretion of TNF- α , following LPS stimulation and dramatic reduction in glycolytic capacity, a metabolically feature already observed in LPS-activated DC (MALINARICH et al., 2015).

After activation by LPS, DC rapidly increase glucose consumption via the glycolytic pathway to fuel TCA (EVERTS et al., 2014b). Recently, it has been shown that glycogen-derived carbons are used during this initial increase of glycolytic pathway for citrate synthesis and that much of the extracellular glucose captured by DC is rapidly converted to glycogen (THWE et al., 2017). In hyperglycemic situations, this glycogen reserve may be lower than that of normoglycemia, which could potentially explain the fact that VitD DC of diabetic patients, although uptaking glucose in the same way as healthy cells, lack signs of consumption of this molecule in the glycolytic and oxidative pathways. This would be due to an even more immediate shift of glucose uptake to intracellular glycogen replacement, as suggested above.

Increases in OCR or even OCR/ECAR ratios may indicate greater mitochondrial function and the fission/fusion relationship of these organelles, since these phenomena have been described as associated in T lymphocytes (BUCK et al., 2016). In our model, though an increased OCR and OCR/ECAR was noted, we did not observe significant mitochondrial changes. Neither mitochondrial membrane potential nor mitochondrial mass were altered by treatment with VitD3 or by the pathological condition of the donor. However, we cannot discard that VitD3 induces alterations in the fission/fusion ratio of the cells. We performed a single preliminary experiment with VitD DC differentiated under low (1 mM) and medium (10 mM) glucose concentrations, and though it did not identify any changes in the shape of mitochondria (data not shown), it had a high cell mortality rate.

What seems to us to be the most interesting findings in relation to diabetic patients' experiments were the facts that (1) mo-DC from both diabetic patients and healthy donors were rendered "tolerogenic" by VitD3; (2) VitD DC from diabetic patients presented lower glycolytic rates than those of VitD DC from healthy donors and (3) VitD DC from patients were resistant to the higher extracellular glucose levels-induced

decrease in glycolysis and OXPHOS observed in VitD DC from healthy donors. These data suggest that although in healthy individuals VitD3 appears to rely on cellular metabolism modifications to induce a “tolerogenic” profile, linking metabolic to immunological alterations, monocytes from diabetic patients are resistant to VitD3-induced metabolic reprogramming but not to VitD3 ability to induce tolDC, a phenomenon that occurs without the evident metabolic changes.

We also aimed to investigate how blood monocytes and DC were affected in diabetic patients. Intriguingly, we observed an inverse association between circulating pDC frequency and duration of diabetes. This suggests that pDC might have a role in the onset and earlier phases of T1D. pDC are cells that secrete large amounts of IFN- α and are, therefore, believed to be important in virus innate immunity, since they express TLR-7 and TLR-9, which recognize viral nucleic acids (REYNOLDS; HANIFFA, 2015). Literature data are conflicting regarding the frequency of these cells in patients with T1D with both increased (ALLEN et al., 2009; KLOPPERK et al., 2019; PENG et al., 2003) and reduced (CHEN et al., 2008; VUCKOVIC et al., 2007) frequencies reported. Interestingly, two studies that used very similar numbers of patients (61 and 70) and newly diagnosed patients (between 1 and 2 months) had different outcomes. In one of them, an increase in the frequency of pDC in patients was reported (ALLEN et al., 2009), while the other reported decreased frequency of these cells (VUCKOVIC et al., 2007). It is noteworthy that virus infections have been associated with the development of T1D in experimental models (QAISAR et al., 2017) and humans (DOTTA et al., 2007) as well as increase in IFN- α secretion by pDC in the LNs (LI et al., 2008); this would explain the increased pDC population in newly diagnosed patients, as we observed. Furthermore, this hypothesis would predict that with time, pDC levels would decrease in the patients, what has been actually described in the same study mentioned above, where 2 years after diagnosis, 3 out of 5 patients had decreased frequency of pDC (ALLEN et al., 2009).

As already mentioned, classical monocytes and CD11c⁺ DC from diabetic patients secreted higher levels of TNF- α and displayed higher glycolytic features. Although any significant alteration in cDC1, cDC2, pDC or monocytes frequencies were observed, an increase in a CD123^{lo}CD11c⁺ DC population was observed in diabetic patients. Several efforts have recently been made to understand ontogeny, functions and the diversity of DC subpopulations, trying to correlate well-defined mouse populations with those present in peripheral blood (HANIFFA; COLLIN; GINHOUX, 2013; MERAD et al., 2013;

REYNOLDS; HANIFFA, 2015). Dzionek et al identified in 2000 (DZIOONEK et al., 2000) three antigens, called BDCA-2-4 (Blood Dendritic Cells Antigens) which, together with BDCA-1 (CD1c) are still used to identify blood populations of human DC. Genomics studies with emphasis on monocyte and DC subpopulations began with the idea of understanding ontogeny and homology of these cells (ROBBINS et al., 2008; WATCHMAKER et al., 2013). Based on these studies, it was possible to align the CD1c⁺ and CD141⁺ DC of human peripheral blood with the CD11b⁺ and CD8α⁺/CD103⁺ DC of mice, respectively.

Even with a limited number of colors, it was possible to identify the three main subpopulations of blood DC described in the literature in both healthy donors and diabetic patients. Also, it was possible to observe a population LIN(CD3/CD19/CD56)⁻HLA-DR⁺CD14⁻CD11c⁺CD123^{lo} expressing high levels of CD16 and that was more prevalent in diabetic patients. CD16⁺ DC have been described in the literature before (AUTISSIER et al., 2010; BACHEM et al., 2010; ROBBINS et al., 2008). However, in one study, the authors did not use CD123 to characterize pDC, but CD304, which makes impossible to draw any parallel since the present population expresses low/intermediate levels of CD123 (BACHEM et al., 2010). In another, they were characterized as CD11c⁺CD123⁻, without mentioning a population CD123^{lo} (AUTISSIER et al., 2010). The third work used public gene expression data to cluster known populations of DC by analyzing homology between humans and mice (ROBBINS et al., 2008).

Studies that identified cDC and pDC in diabetic patients either did not used CD16 or included this marker within the LIN⁻ (CHEN et al., 2008; PENG et al., 2003; SUMMERS et al., 2006; VUCKOVIC et al., 2007). Robbins et al. (ROBBINS et al., 2008), by analyzing public transcriptional data from healthy donors in CD16⁺ DC, compared this cells with others subpopulations of DC, monocytes, neutrophils and lymphocytes and they demonstrated that these cells clustered closer to neutrophils and monocytes than to DC, expressing genes more associated with these cells. Recent studies using single-cell RNA-seq have identified new subpopulations of DC in the blood. One of them was identified as a cDC precursor, expressing CD123, capable of inducing T lymphocyte proliferation, but not capable of secreting IFN-α (SEE et al., 2017). However, this population was selected based on a lineage that included CD16, making it difficult to hypothesize that diabetic patients have an increase in this precursor population of DC.

A second recent work also used single-cell RNA-seq to identify a new DC population and two new monocyte populations (VILLANI et al., 2017). Interestingly, in the first strategy to select cells for single-cell RNA-seq, authors used the same strategy used by us, identifying 6 types of DC named by the authors as follows: DC1 (corresponding to cDC1 and expressing CD141⁺), DC2 and DC3 (corresponding to divisions within the CD1c⁺ population, called by us cDC2), DC4 (population CD1c⁻CD141⁻), DC5 (new population expressing AXL and Siglec6) and DC6 (corresponding to pDC). According to the authors, the DC4 population expresses CD16 and, although it expresses many monocyte-like genes (a finding similar to that described by Robbins et al. in 2008 (ROBBINS et al., 2008)), formed a different cluster from the CD16⁺ monocyte cluster being characterized by expressing genes related to IFN type I secretion and antiviral response, while the monocyte population expressed immune process and leukocyte migration genes (VILLANI et al., 2017). Based on the literature and our finding that there is a CD123^{lo}CD11c⁺CD1c⁻CD141⁻ population expressing CD16, we can hypothesize that diabetic patients have a significant increase in this population, which could be the DC4 population, characterized by Villani et al.

Not only VitD3, but other compounds are able to induce tolDC when added to monocytes during the differentiation toward mo-DC (BAKDASH et al., 2015; MAGGI et al., 2016; TAI et al., 2011). In order to better understand how different compounds could induce tolDC and how these compounds could metabolically influence mo-DC, monocytes were treated with VitD3, RA and Dex. Largely consistent with the literature, we were able to efficiently induce tolDC with all the compounds, evidenced by the ability of T cells primed by all tol DC efficiently suppress the proliferation of bystander T cells without inducing the generation of FoxP3 Treg. Common features were observed among VitD DC and Dex DC, which shared a drastic reduction in co-stimulatory markers, increased secretion of IL-10 and reduced secretion of IL12p70. RA-induced mechanism did not alter co-stimulatory markers, neither IL-10 nor IL12p70 secretion by mo-DC, however T cells primed by RA DC secreted higher levels of IL-10 suggesting that RA DC is able to induce a subtype of Treg called Tr1, characterized by the low expression of FoxP3 and increased secretion of IL-10 (GROUX et al., 1997; ZENG et al., 2015). The induction of Tr1 had already been shown by RA-treated DC (BAKDASH et al., 2015) and also by butyrate-treated DC that induced RA secretion by DC with concomitant increased ALDH activity (KAISAR et al., 2017). Our data supports the idea that RA acts on mo-DC increasing their ability to differentiate Tr1 Treg.

One interesting find from the project, was that tolDC displayed an overall modulation of both LCFAs and ELOVL family genes, regardless if tolerogenic compounds were added to monocytes (at day 0) or to iDC (at day 5). ELOVL are enzymes enrolled during the first step of elongation of FA and, to date, seven different members, that can be ubiquitously or more tissue-related expressed, were identified (JAKOBSSON; WESTERBERG; JACOBSSON, 2006; TAMURA et al., 2009). The observed modulation of LCFA and ELOVL genes was not straightforward when analyzing the data from cells treated either at day 0 or at day 5. When cells were treated at day 0, increases in LCFAs were more prominent in tolDC than increases in ELOLV gene, whereas cells treated at day 5 displayed the opposite dynamics. This might reflect time-dependent discrepancies in which, in the first scenario (because cells were treated at earlier time points), the levels of LCFAs are increased due to a longer stimulation of the cells, allowing enough time for properly expression and activation of the enzymes. In contrast, in the second scenario, the enzymes' levels might not be as high as in the first situation and, as consequence, alterations in LCFAs are less evident. The same is true for the ELOVL genes, that might not be highly upregulated when cells were treated at day 0 but could have been 24 or 48 hours after the stimulus for differentiation. It is noteworthy, that we did not evaluate protein levels in neither of the situations and the possibility that gene upregulation did not actually correlates (or will be correlated) with increased expression of the enzymes cannot be excluded.

While VitD DC and Dex displayed higher levels of EPA, RA DC displayed an overall increase of low-grade inflammation LCFAs, particularly nervonic acid, erucic acid, 11-eicosenoic acid, EDA and DDA. Omega-3 α -linoleic acid and omega-6 linoleic acid are the most common PUFAs and they are both essentials FAs, which means they cannot be synthesized, and need to be acquired from diet (DOMINGUEZ; BARBAGALLO, 2017). Ultimately, these lipids give rise to their derivatives, especially EPA and AA, respectively (MEHTA; DWORKIN; SCHWID, 2009) that serves as substrates to two main types of enzymes: cyclooxygenase (COX) and lipoxygenases (LOX) which, in turn, generates eicosanoid like prostaglandins, leukotrienes, lipoxins and resolvins (NELSON; RASKIN, 2019). Generally, omega-3 FAs are associated with anti-inflammatory responses (GUTIÉRREZ; SVAHN; JOHANSSON, 2019) while omega-6 FAs are associated with pro-inflammatory responses (INNES; CALDER, 2018) and decrease in omega-6:omega-3 ratio has been suggested as essential for reducing risk of obesity and to reduce low-grade inflammation (DINICOLANTONIO; O'KEEFE, 2018;

SIMOPOULOS, 2016; 2003). EPA and AA give rise to different eicosanoids with AA's derivatives being classical mediators of inflammation like prostaglandin E₂ (PGE₂), leukotriene B₄ (LTB₄) and thromboxane A₂ (TXA₂) whereas EPA's derivatives are PGE₃, LTB₅ and TXB₃, which are less inflammatory eicosanoids than their AA-derivates counterparts (NAGY; TIUCA, 2017; NELSON; RASKIN, 2019).

With that being said, it is easy to understand how elevated levels of EPA in tolDC can contribute to their immunosuppressive capacity. DC treated with EPA displayed reduced expression of costimulatory markers and secretion of IL-12 (DRAPER et al., 2011; WANG et al., 2007; ZAPATA-GONZALEZ et al., 2008; ZEYDA et al., 2005). Interestingly, docosahexaenoic acid (DHA), a LC PUFA produced as consequence of EPA elongation, was even more potent in limiting DC functions (ZAPATA-GONZALEZ et al., 2008). Feeding either mice (TEAGUE et al., 2013) or rat (SANDERSON et al., 1997) with fish oil, which is rich in both DHA and EPA, also impaired the immunogenic function of DC, characterized by reduced expression of costimulatory markers and reduced T cell activation. Consistent, mice treated with resolvin E1 (RvE1), also a metabolite derived from EPA after 5-lipoxygenase (5-LOX) action, presented reduced migratory capacity from the skin to the draining LNs as well as reduced number of effector and memory T cells in a model of cutaneous hypersensitivity (SAWADA et al., 2015). EPA could also reduce the body weight and weight of adipose tissues, under steady state situation, which was accompanied by increased number of Tregs. Additionally, the ability of adipose tissue macrophages (ATM) to induce Tregs was also improved by EPA treatment (ONODERA et al., 2017).

Contrary to what we observe for VitD3 and Dex treatment, RA DC displayed reduced levels of EPA but an overall increase in LCFA. One of the LCFAs increased in RA DC was EDA, an omega-6 FAs that gives rise to AA. Contrary to AA, EDA is a less pro-inflammatory mediator with the capacity to inhibit inducible nitric oxide synthase (iNOS) and nitric oxide (NO) production in macrophages (HUANG et al., 2011; PEREIRA et al., 2014). It is noteworthy that 11-eicosenoic acid, also increased in RA DC, was also able to inhibit iNOS and NO production, although in less extent (PEREIRA et al., 2014). Consistently, higher EDA values in serum of patients with major depressive disorder (MDD), was significantly inversely correlated with circumference waist (MOCKING et al., 2013). Circumference waist is the primary risk factor for cardiovascular disease, which has been associated with mortality among patients with MDD (DHAR; BARTON, 2016). EDA levels in inflammatory bowel disease (IBD)

patients was demonstrated to be lower than those in healthy individuals and the elongation of linoleic acid to EDA, instead of γ -linoleic acid, has been suggested to be important in IBD because it could potentially decrease the AA:EDA ratio (SITKIN; POKROTNIKES, 2018), which was significantly increased in patients with ulcerative colitis (UC) (SITKIN et al., 2018). Interestingly, butyrate-producing bacteria (BPB) were depleted in UC patients and oral butyrate administration, not only enhanced BPB but also increased AA:EDA ratio (SITKIN et al., 2018). This is particularly interesting because butyrate has been demonstrated to induce tILD by inducing the secretion of RA and, consequently, increasing ALDH activity in DC (KAISAR et al., 2017), suggesting a possible link between RA and EDA.

Erucic acid, and the product of its elongation (nervonic acid), were also increased in RA DC and the anti-inflammatory properties of these LCFAs are particularly interesting in the context of neuroimmunological disorders, such as adrenoleukodystrophy (ALD), multiple sclerosis (MS) and Huntington's disease (extensively revised here (ALTINOZ et al., 2019; ALTINOZ; OZPINAR, 2019)), since nervonic acid is one of the lipids that compose myelin (SARGENT; COUPLAND; WILSON, 1994). Erucic acid is part of the Lorenzo's oil, which is the only available and partially efficient therapy for ALD, characterized by a progressive inflammatory demyelization in the brain and an abnormal accumulation of very long chain fatty acids (VLCFA) (ALTINOZ; OZPINAR, 2019). Patients with ADL displayed elevated levels of pro-inflammatory cytokines (MARCHETTI et al., 2017) and treatment with a mixture containing erucic acid decreased IL-6 in the cerebrospinal fluid 2 months after treatment, with also improvement in neurophysiologic parameters (CAPPA et al., 2011). Erucic acid has also been demonstrated to decrease the lytic activity of NK cells from ALD patients (SEDLMAYR et al., 1995) and was dramatically reduced in lungs from patients infected with H7N9 (SUN et al., 2018). Interestingly, in one of the patients, levels of erucic acid increased from day 9 to day 13 after disease onset, a time that reflects the window of resolution of lung inflammation and, in another patient, the levels of erucic acid decreased as lung inflammation became more severe (SUN et al., 2018). Another interestingly characteristic of erucic acid is its ability to decrease the activity of ELOVL1, responsible for the elongation of saturated and monounsaturated FAs C_{20} to C_{22} and C_{24} to C_{26} , such as the majority of LCFA presented in ALD (SASSA et al., 2014). In RA DC, ELOVL1 and ELOVL7, which also elongates FAs up to C_{24} , were the only two downregulated

ELOVL genes, suggesting that the downregulation of ELOVL1 (and potentially ELOVL7) might be a consequence of the increased levels of erucic acid in these cells.

When evaluating the metabolic profiles of tolDC, VitD DC were the most active tolDC, with increase glycolysis and OXPHOS. As already discussed, glycolysis seems to be important for suppressive functions of VitD DC (FERREIRA et al., 2015) by supporting the mitochondrial respiration (VANHERWEGEN et al., 2018). However, we demonstrated that even in low glucose concentrations, VitD DC were still able to induce functional suppressive T cells, upregulate ILT-3 and decrease co-stimulatory markers, suggesting that even in the absence of glucose, another metabolically pathway can be used to fuel mitochondrial respiration, perhaps glutaminolysis, since the block of FAO did not altered suppressive functions of VitD DC (FERREIRA et al., 2015). The fact that higher glucose concentrations was not indispensable for the induction of tolDC was consistent across data obtained from healthy donors both in Brazil and in The Netherlands and with different mo-DC generation methodology. In both situations, the glucose availability in the media had little effect in the differentiation of tolDC and, comparing with other tolerogenic compounds, with data pointing toward a selective effect in VitD DC, which is line with the highly glycolytic profile of these cells. Literature data points toward a more tolerogenic profile in high glucose concentration. However, T suppression assay performed in The Netherland suggested the opposite. We don't have a clear explanation why the results observed now are different from the literature, however it is worth to note that both the work from Ferreira et al. (FERREIRA et al., 2015) and the data obtained in Brazil were based on an experimental setup that was somewhat different from the one used by us now. Ferreira et al. and our data from Brazil were actually measuring the ability of mo-DC to induce the proliferation of T cells. The experiment we performed now was indeed measuring the ability of mo-DC to generate functional tolerogenic T cells. It can be that at low glucose levels the ability of mo-DC to induce the proliferation of T cells is not impaired, but the T cells that proliferate are more prone to become tolerogenic T cells. It is worth noting that the expression of both ILT-3 and PD-L1 were higher in VitD DC differentiated at low levels of glucose. Concordantly, mo-DC from poorly controlled type 1 diabetic patients with HbA1c around 10,2% (something around 13 mM of glycemia) differentiated in the presence of Vitamin D₂ and Dex were less tolerogenic than mo-DC from both healthy donors and well controlled type 1 diabetic patients (DÁŇOVÁ et al., 2017). This might suggest that actually, high glucose concentrations would impair the ability of mo-DC to become tolerogenic. On the other

hand, even having their tolerogenicity impaired, VitD DC still were able to efficiently generate functional suppressive T cells both in our work as well as from poorly controlled diabetic patients (DÁŇOVÁ et al., 2017).

The increase in OXPHOS observed after LPS treatment in tolDC is a strong suggestion of glucose oxidation, which has already been linked to VitD DC function (VANHERWEGEN et al., 2018). Previous data from the lab showed that tolDC had increase AMP/ATP ratio that together with glucose oxidation points toward an increase activation of AMPK, an important metabolic sensor in eukaryotic cells. AMPK is a heterotrimeric complex comprising a catalytic α -subunit and regulatory γ - and β - subunits (HARDIE; ROSS; HAWLEY, 2012). The activation of AMPK can be triggered by both canonical and non-canonical pathways, both of them having as final consequence the increase in ATP levels by activating catabolic and decreasing anabolic pathways (GARCIA; SHAW, 2017). We demonstrated here that VitD DC and RA DC had increased AMPK activity, once again indicating oxidative metabolism is important for the functions of tolDC. The VitD3-induced metabolic alterations were largely restored, especially glycolysis and basal levels of mitochondrial OCR, when tolDC were silenced for AMPK. On the other hand, the reduction in overall metabolic activity did not impair the suppressive functions of VitD DC. The dramatic reduction in glycolysis without affecting its function may seem surprising but may indicate that in the absence of enhanced glycolysis, another metabolic pathway is serving as a carbon source to fuel mitochondrial metabolism, allowing for maintenance of a mitochondrial driven suppressive capacity of these cells. Further studies would need to be performed to identify if/which compensatory metabolic pathways are operating in this scenario. Interestingly, we observed a reduced SRC in RA DC which suggests reduced mitochondrial activity, a characteristic that was shared with butyrate-conditioned DC capable of secreting RA (KAISAR et al., 2017). The reduction in SRC was restored when AMPK was silenced in RA DC, but to what extent the suppressive function of RA DC relies on reduced mitochondria activity is yet to be determined.

The main finding of our work was to demonstrate that AMPK is important for the suppressive functions of RA DC, both *in vivo* and *in vitro*. Interestingly, the absence of AMPK did not alter the expression of co-stimulatory markers in none of the human tolDC, but the ability to generate functional suppressive Tr1 Tregs was completely abolished in human RA DC silenced for AMPK. Likewise, murine RA-GMDC were able to efficiently induce the differentiation of Tregs, in this case FoxP3⁺ and this was not the

case for RA-GMDC derived from CD11c^{ΔAMPKα1}. The induction of Tregs by RA-treated DC was already demonstrated by both GMDC (FENG et al., 2010) and human mo-DC (BAKDASH et al., 2015), but we now for the first time show that this is dependent on AMPK signaling.

CD103⁺ DC has largely been associated with the induction of FoxP3⁺ Treg in the gut (COOMBES et al., 2007; DEL RIO et al., 2010), especially via the conversion of vitamin A into RA (LAMPEN et al., 2000) by the activity of ALDH enzymes (ILIEV et al., 2009). Here we have shown increased expression of CD103 in mo-DC and increased ALDH activity in both mo-DC GMDC treated with RA, observations that are largely in agreement with the literature (BAKDASH et al., 2015; FENG et al., 2010). Mostly, we were able to demonstrate that in human RA treated mo-DC, the increased activity of ALDH enzyme was largely lost when AMPK was silenced. Interestingly, although the suppressive effects of human RA DC could not be reversed when ALDH activity was blocked, possibly due to a technical limitation, we could demonstrate that this was true for RA GMDC, which suggests a direct link of AMPK, ALDH activity and the suppressive functions of RA DC. It has been demonstrated that TLR-MyD88 axis is required for the optimal function of RA DC (FENG et al., 2010) and in our human experiments we, indeed, did not observe any effect of AMPK silencing on ALDH activity when it was measured in immature DC, only when mo-DC were on a LPS background.

Intestinal cDC play an important role in maintaining intestinal homeostasis by keeping the balance between tolerance and immunity. The gut is a main source of RA and because of that cDC presented in this tissue, are more prone to acquire a suppressive phenotype (BEKIARIS; PERSSON; AGACE, 2014). It has been demonstrated that in msLN CD103⁺CD11b⁻ migratory DC are the main subset of cDC expressing *aldh1a2* gene with consequent higher ALDH activity and that this particular subset of cDC are most important to differentiation of FoxP3⁺ Tregs (ESTERHÁZY et al., 2016; 2019). We could observe that the relationship in ALDH activity, was actually switched between CD11b⁺CD103⁺ cDC and CD103⁺CD11b⁻ cDC (Figure 47F), which tempt us to speculate that in the siLP, perhaps the main suppressive subset of cDC would be the CD11b⁺CD103⁺ cDC instead of CD103⁺CD11b⁻ cDC. In fact, in both human (WATCHMAKER et al., 2013) and mouse (DENNING et al., 2011) siLP, CD11b⁺CD103⁺ cDC was the subset more prone to induce the differentiation of FoxP3⁺ Treg. Interestingly, while in human siLP CD103⁺CD11b⁻ cDC had lower ALDH activity and were unable to differentiate Treg, in mouse siLP the levels of ALDH activity were

similar between both subsets and CD103⁺CD11b⁻ cDC were also capable to differentiate Treg but a lesser extent than CD103⁺CD11b⁺ cDC. Our results are in agreement with this observation, since we found reduced frequencies and ALDH activity in CD103⁺CD11b⁺ cDC present in the lamina propria of CD11c^{ΔAMPKα1}, followed by increased expression of costimulatory markers, specially by CD103⁺CD11b⁺ cDC, and increased IFN-γ and IL-10 secretion by T cells, characterizing an overall inflammatory status in msLN.

Despite the fact that an overall increase in surface markers was observed in msLN cDC, the only marker that was increased in all subsets of CD11c^{ΔAMPKα1} mice was CD40. Interesting, the over expression of this co-stimulatory molecules in CD11c⁺ cells has been shown to impair the differentiation of pTreg and develop an spontaneous fatal colitis with reduced frequencies of both CD103⁺ cDC and CD103⁺CD11b⁺ cDC (BARTHELIS et al., 2017). Concordantly, AMPK deficiency BMDC, when stimulated with CD40L displayed a pro inflammatory status with increased secretion of IL-6 and decreased secretion of IL-10 (CARROLL; VIOLLET; SUTTLES, 2013). No differences were observed in the siLP cDC subsets regarding the expression of CD40. However, it can be hypothesized that the upregulation of the surface markers might occur during the migration of cDC from the siLP towards the msLN. In general, this data points toward an important role of AMPK in promoting the generation of Tregs by limiting the expression of CD40 in cDC specifically in the intestine/msLN. It is worth noting that we also analyzed liver from CD11c^{ΔAMPKα1} mice and no differences were observed regarding frequencies of cDC, ALDH activity, cytokine secretion by T cells.

Finally, to our surprise, despite the fact that CD103⁺ DC displayed a reduced ALDH activity in the lungs, we observed increased CTLA-4 expression by Tregs and reduced frequencies of effector T cells and IFN-γ-secreting T cells in CD11c^{ΔAMPKα1}. These results are not in agreement with previous data from the literature showing that CD11c^{ΔAMPKα1} actually had an impaired lung injury at baseline and followed by hookworm infection (NIEVES et al., 2016). Still, DC are not the only myeloid cells expressing CD11c and in the lungs and one of the most frequent myeloid cell population is the alveolar macrophages (AM), which express high levels of CD11c (MISHARIN et al., 2013). The importance of macrophages to control lung homeostasis seems to be higher than that promoted by DC (DUAN; CROFT, 2014) and *in vitro* experiments showed that interstitial macrophages (IM) were up to fourfold more efficient in inducing Tregs than DC (SOROOSH et al., 2013). AM also showed to be able to induce the differentiation of

FoxP3(COLEMAN et al., 2013) and AMPK might act differently in AM and DC. It is important to note that all *in vivo* data were performed under steady state and under inflammatory conditions the homeostasis' break could lead to differences not observed so far. Additional studies are needed determine the contribution of AMPK in macrophages vs DC in regulating lung and gut homeostasis both during steady state and following inflammation.

In conclusion, we demonstrate a role for AMPK in promoting the generation of DC rendered tolerogenic by RA. Although not completely illustrated, RA seems to induce increased ALDH in DC in an AMPK-dependent manner resulting in tolDC capable to instructs Tr1 regulatory T cells. These studies identify AMPK as a potential interesting target to regulate tolerance in autoimmune disease, especially in IBD since RA DC play an important role in gut homeostasis.

6. CONCLUSIONS

6. CONCLUSIONS

- Metabolic reprogramming induced by VitD3 in diabetic patients' monocytes is different from that induced in healthy donors' monocytes;
- Extracellular glucose levels had little effect upon VitD3-induction of functional tolDC in both T1D patients and healthy donors;
- Blood DC from T1D patients are more glycolytic and are characterized by higher secretion of TNF- α , which might indicate that these cells have a pro-inflammatory phenotype.
- VitD3, RA and Dex induce different metabolic changes in tolDC, which are, however, are equally capable to induce functional suppressive T cells;
- VitD3 treated DC were affected by extracellular glucose levels, which had no effect on RA- and Dex-induced DC;
- AMPK is required for various immunosuppression-related in vivo and in vitro activities of RA-DC, but not for VitD DC and Dex-DC, though its activity was also elevated on Vit DC;
- LCFA pathway might be a common feature for VitD3-, RA- and Dex-induced tolDC;

7. REFERENCES

7. REFERENCES

ADORINI, L. Tolerogenic dendritic cells induced by vitamin D receptor ligands enhance regulatory T cells inhibiting autoimmune diabetes. *v. 987*, p. 258–261, 1 abr. 2003.

ALLEN, J. S. et al. Plasmacytoid dendritic cells are proportionally expanded at diagnosis of type 1 diabetes and enhance islet autoantigen presentation to T-cells through immune complex capture. **Diabetes**, *v. 58*, n. 1, p. 138–145, jan. 2009.

ALONSO, D.; NUNGESTER, W. J. Comparative study of host resistance of guinea pigs and rats. V. The effect of pneumococcal products on glycolysis and oxygen uptake by polymorphonuclear leucocytes. **Journal of Infectious Diseases**, *v. 99*, n. 2, p. 174–181, set. 1956.

ALTINOZ, M. A. et al. Erucic acid, a nutritional PPAR δ -ligand may influence Huntington's disease pathogenesis. p. 1–9, 15 out. 2019.

ALTINOZ, M. A.; OZPINAR, A. PPAR- δ and erucic acid in multiple sclerosis and Alzheimer's Disease. Likely benefits in terms of immunity and metabolism. **International immunopharmacology**, *v. 69*, p. 245–256, 7 fev. 2019.

ALVAREZ, D.; VOLLMANN, E. H.; ANDRIAN, VON, U. H. Mechanisms and consequences of dendritic cell migration. **Immunity**, *v. 29*, n. 3, p. 325–342, 19 set. 2008.

ANGELIN, A. et al. Foxp3 Reprograms T Cell Metabolism to Function in Low-Glucose, High-Lactate Environments. **Cell Metabolism**, p. 1–20, 10 abr. 2017.

ANGELINI, F. et al. Altered phenotype and function of dendritic cells in children with type 1 diabetes. **Clinical and Experimental Immunology**, *v. 142*, n. 2, p. 341–346, 1 nov. 2005.

AUTISSIER, P. et al. Evaluation of a 12-color flow cytometry panel to study lymphocyte, monocyte, and dendritic cell subsets in humans. **Cytometry Part A**, *v. 9999A*, p. NA–NA, 2010.

BACHEM, A. et al. Superior antigen cross-presentation and XCR1 expression define human CD11c +CD141 +cells as homologues of mouse CD8 +dendritic cells. **Journal of Experimental Medicine**, *v. 207*, n. 6, p. 1273–1281, 7 jun. 2010.

BAKAY, M. et al. The Genetic Contribution to Type 1 Diabetes. **Current Diabetes Reports**, *v. 19*, n. 11, p. 55–14, 4 nov. 2019.

BAKDASH, G. et al. Vitamin D3 metabolite calcidiol primes human dendritic cells to promote the development of immunomodulatory IL-10-producing T cells. **Vaccine**, *v. 32*, n. 47, p. 6294–6302, 29 out. 2014.

BAKDASH, G. et al. Retinoic acid primes human dendritic cells to induce gut-homing, IL-10-producing regulatory T cells. **Mucosal Immunology**, *v. 8*, n. 2, p. 265–278, mar. 2015.

- BALASA, B. et al. CD40 ligand-CD40 interactions are necessary for the initiation of insulinitis and diabetes in nonobese diabetic mice. **Journal of immunology (Baltimore, Md. : 1950)**, v. 159, n. 9, p. 4620–4627, 1997.
- BANCHEREAU, J. et al. Immunobiology of dendritic cells. **Annual Review of Immunology**, v. 18, n. 1, p. 767–811, 2000.
- BARTHELIS, C. et al. CD40-signalling abrogates induction of ROR γ t⁺ Treg cells by intestinal CD103⁺ DCs and causes fatal colitis. p. 1–13, 2 mar. 2017.
- BASIT, F. et al. Human Dendritic Cell Subsets Undergo Distinct Metabolic Reprogramming for Immune Response. **Frontiers in immunology**, v. 9, p. 2489, 2018.
- BEKIARIS, V.; PERSSON, E. K.; AGACE, W. W. Intestinal dendritic cells in the regulation of mucosal immunity. **Immunological reviews**, v. 260, n. 1, p. 86–101, jul. 2014.
- BELL, G. M. et al. Autologous tolerogenic dendritic cells for rheumatoid and inflammatory arthritis. **Annals of the rheumatic diseases**, v. 76, n. 1, p. 227–234, jan. 2017.
- BENHAM, H. et al. Citrullinated peptide dendritic cell immunotherapy in HLA risk genotype-positive rheumatoid arthritis patients. **Science translational medicine**, v. 7, n. 290, p. 290ra87–290ra87, 3 jun. 2015.
- BHAGAVAN, N. V.; HA, C. E. **Chapter 25. Nucleotide Metabolism**. Traducao. [s.l.] Elsevier Inc, 2015. p. 465–488
- BHAGAVAN, N. V.; HA, C.-E. **Lipids I: Fatty Acids and Eicosanoids**. Traducao. First Edition ed. [s.l.] Elsevier Inc, 2010. p. 191–207
- BLANCO, B. 8. **Chapter 15 - Lipid Metabolism**. Traducao. [s.l.] Elsevier Inc, 2017. p. 325–365
- BOLTJES, A.; VAN WIJK, F. Human dendritic cell functional specialization in steady-state and inflammation. **Frontiers in immunology**, v. 5, p. 131, 2014.
- BROCKER, T.; RIEDINGER, M.; KARJALAINEN, K. Targeted Expression of Major Histocompatibility Complex (MHC) Class II Molecules Demonstrates that Dendritic Cells Can Induce Negative but Not Positive Selection of Thymocytes In Vivo. **Journal of Experimental Medicine**, v. 185, n. 3, p. 541–550, 3 fev. 1997.
- BUCK, M. D. et al. Mitochondrial Dynamics Controls T Cell Fate through Metabolic Programming. **Cell**, v. 166, n. 1, p. 63–76, 30 jun. 2016.
- BUCK, M. D. et al. Metabolic Instruction of Immunity. **Cell**, v. 169, n. 4, p. 570–586, 4 maio 2017.
- CALDERON, B.; CARRERO, J. A.; UNANUE, E. R. The central role of antigen presentation in islets of Langerhans in autoimmune diabetes. **Current opinion in immunology**, v. 26, p. 32–40, fev. 2014.

CANTOR, J.; HASKINS, K. Recruitment and Activation of Macrophages by Pathogenic CD4 T Cells in Type 1 Diabetes: Evidence for Involvement of CCR8 and CCL1. **Journal of immunology (Baltimore, Md. : 1950)**, v. 179, n. 9, p. 5760–5767, 18 out. 2007.

CAPPA, M. et al. A mixture of oleic, erucic and conjugated linoleic acids modulates cerebrospinal fluid inflammatory markers and improve somatosensorial evoked potential in X-linked adrenoleukodystrophy female carriers. **Journal of Inherited Metabolic Disease**, v. 35, n. 5, p. 899–907, 22 dez. 2011.

CARRENO, B. M.; BECKER-HAPAK, M.; LINETTE, G. P. CD40 regulates human dendritic cell-derived IL-7 production that, in turn, contributes to CD8⁺ T-cell antigen-specific expansion. **Immunology and Cell Biology**, v. 87, n. 2, p. 167–177, 11 nov. 2008.

CARRERO, J. A. et al. Defining the Transcriptional and Cellular Landscape of Type 1 Diabetes in the NOD Mouse. **PLoS ONE**, v. 8, n. 3, p. e59701–14, 26 mar. 2013.

CARRERO, J. A. et al. Resident macrophages of pancreatic islets have a seminal role in the initiation of autoimmune diabetes of NOD mice. **Proceedings of the National Academy of Sciences of the United States of America**, v. 114, n. 48, p. E10418–E10427, 28 nov. 2017.

CARROLL, K. C.; VIOLLET, B.; SUTTLES, J. AMPK α 1 deficiency amplifies proinflammatory myeloid APC activity and CD40 signaling. **Journal of leukocyte biology**, v. 94, n. 6, p. 1113–1121, dez. 2013.

CASTRO, L. F. C.; TOCHER, D. R.; MONROIG, O. Long-chain polyunsaturated fatty acid biosynthesis in chordates: Insights into the evolution of Fads and Elovl gene repertoire. **Progress in lipid research**, v. 62, p. 25–40, 1 abr. 2016.

CERBONI, S.; GENTILI, M.; MANEL, N. Diversity of pathogen sensors in dendritic cells. **Advances in immunology**, v. 120, p. 211–237, 2013.

CHEN, X. et al. Type 1 diabetes patients have significantly lower frequency of plasmacytoid dendritic cells in the peripheral blood. **Clinical Immunology**, v. 129, n. 3, p. 413–418, 1 dez. 2008.

CHEN, X. et al. Intercellular interplay between Sirt1 signalling and cell metabolism in immune cell biology. ... **immunology**, v. 145, n. 4, p. 455–467, 3 jun. 2015.

CHEUNG, P. C. et al. Characterization of AMP-activated protein kinase gamma-subunit isoforms and their role in AMP binding. **The Biochemical journal**, v. 346 Pt 3, n. Pt 3, p. 659–669, 15 mar. 2000.

COLEMAN, M. M. et al. Alveolar Macrophages Contribute to Respiratory Tolerance by Inducing FoxP3 Expression in Naive T Cells. **American journal of respiratory cell and molecular biology**, v. 48, n. 6, p. 773–780, 3 jun. 2013.

COOMBES, J. L. et al. A functionally specialized population of mucosal CD103⁺ DCs induces Foxp3⁺ regulatory T cells via a TGF-beta and retinoic acid-dependent mechanism. **Journal of Experimental Medicine**, v. 204, n. 8, p. 1757–1764, 6 ago. 2007.

COOPER, M. A. et al. Human natural killer cells: a unique innate immunoregulatory role for the CD56(bright) subset. **Blood**, v. 97, n. 10, p. 3146–3151, 15 maio 2001.

CROFT, M.; BRADLEY, L. M.; SWAIN, S. L. Naive versus memory CD4 T cell response to antigen. Memory cells are less dependent on accessory cell costimulation and can respond to many antigen-presenting cell types including resting B cells. **Journal of immunology (Baltimore, Md. : 1950)**, v. 152, n. 6, p. 2675–2685, 15 mar. 1994.

DAHLÉN, E. et al. Dendritic cells and macrophages are the first and major producers of TNF-alpha in pancreatic islets in the nonobese diabetic mouse. **Journal of immunology (Baltimore, Md. : 1950)**, v. 160, n. 7, p. 3585–3593, 1 abr. 1998.

DAHLÉN, E.; HEDLUND, G.; DAWE, K. Low CD86 Expression in the Nonobese Diabetic Mouse Results in the Impairment of Both T Cell Activation and CTLA-4 Up-Regulation. **Journal of immunology (Baltimore, Md. : 1950)**, v. 164, n. 5, p. 2444–2456, 1 mar. 2000.

DÁŇOVÁ, K. et al. NF- κ B, p38 MAPK, ERK1/2, mTOR, STAT3 and increased glycolysis regulate stability of paricalcitol/dexamethasone-generated tolerogenic dendritic cells in the inflammatory environment. **Oncotarget**, v. 6, n. 16, p. 14123–14138, 10 jun. 2015.

DÁŇOVÁ, K. et al. Tolerogenic Dendritic Cells from Poorly Compensated Type 1 Diabetes Patients Have Decreased Ability To Induce Stable Antigen-Specific T Cell Hyporesponsiveness and Generation of Suppressive Regulatory T Cells. **The Journal of Immunology**, v. 198, n. 2, p. 729–740, 15 jan. 2017.

DEL RIO, M.-L. et al. Development and functional specialization of CD103+ dendritic cells. **Immunological reviews**, v. 234, n. 1, p. 268–281, mar. 2010.

DENNING, T. L. et al. Functional Specializations of Intestinal Dendritic Cell and Macrophage Subsets That Control Th17 and Regulatory T Cell Responses Are Dependent on the T Cell/APC Ratio, Source of Mouse Strain, and Regional Localization. **Journal of immunology (Baltimore, Md. : 1950)**, v. 187, n. 2, p. 733–747, 6 jul. 2011.

DHAR, A. K.; BARTON, D. A. Depression and the Link with Cardiovascular Disease. **Frontiers in Psychiatry**, v. 7, n. 1, p. 130–9, 21 mar. 2016.

DINICOLANTONIO, J. J.; O'KEEFE, J. H. Importance of maintaining a low omega-6/omega-3 ratio for reducing inflammation. **Open Heart**, v. 5, n. 2, p. e000946–4, 26 nov. 2018.

DOGUSAN, Z. et al. Double-Stranded RNA Induces Pancreatic β -Cell Apoptosis by Activation of the Toll-Like Receptor 3 and Interferon Regulatory Factor 3 Pathways. **Diabetes**, v. 57, n. 5, p. 1236–1245, 1 maio 2008.

DOMINGUEZ, L. J.; BARBAGALLO, M. **Chapter 3. Not All Fats Are Unhealthy.** Tradução. [s.l.] Elsevier Inc, 2017. p. 35–58

DOMÍNGUEZ-AMOROCHO, O. et al. Immunometabolism: A target for the comprehension of immune response toward transplantation. **World Journal of Transplantation**, v. 9, n. 2, p. 27–34, 20 jun. 2019.

DONG, H.; BULLOCK, T. N. J. Metabolic influences that regulate dendritic cell function in tumors. **Frontiers in immunology**, v. 5, p. 24, 2014.

DOTTA, F. et al. Coxsackie B4 virus infection of beta cells and natural killer cell insulinitis in recent-onset type 1 diabetic patients. **PNAS**, v. 104, n. 12, p. 5115–5120, 20 mar. 2007.

DRAPER, E. et al. Omega-3 fatty acids attenuate dendritic cell function via NF- κ B independent of PPAR γ . **The Journal of Nutritional Biochemistry**, v. 22, n. 8, p. 784–790, 1 ago. 2011.

DUAN, W.; CROFT, M. Control of Regulatory T Cells and Airway Tolerance by Lung Macrophages and Dendritic Cells. **Annals of the American Thoracic Society**, v. 11, n. Supplement 5, p. S306–S313, dez. 2014.

DURAI, V. et al. Cryptic activation of an Irf8 enhancer governs cDC1 fate specification. **Nature immunology**, v. 462, p. 1–31, 17 ago. 2019.

DUTERTRE, C.-A. et al. Single-Cell Analysis of Human Mononuclear Phagocytes Reveals Subset-Defining Markers and Identifies Circulating Inflammatory Dendritic Cells. **Immunity**, v. 51, n. 3, p. 573–589.e8, 17 set. 2019.

DZIOŃEK, A. et al. BDCA-2, BDCA-3, and BDCA-4: three markers for distinct subsets of dendritic cells in human peripheral blood. **Am Assoc Immunol**, v. 165, n. 11, p. 6037–6046, 1 dez. 2000.

ESTERHÁZY, D. et al. Classical dendritic cells are required for dietary antigen-mediated induction of peripheral Treg cells and tolerance. **Nature immunology**, v. 17, n. 5, p. 545–555, maio 2016.

ESTERHÁZY, D. et al. Compartmentalized gut lymph node drainage dictates adaptive immune responses. **Nature Publishing Group**, v. 569, n. 7754, p. 126–130, maio 2019.

EVERTS, B. et al. Commitment to glycolysis sustains survival of NO-producing inflammatory dendritic cells. **Blood**, v. 120, n. 7, p. 1422–1431, 16 ago. 2012.

EVERTS, B. et al. TLR-driven early glycolytic reprogramming via the kinases TBK1-IKK ϵ supports the anabolic demands of dendritic cell activation. **Nature immunology**, v. 15, n. 4, p. 323–332, abr. 2014b.

EVERTS, B.; PEARCE, E. J. Metabolic control of dendritic cell activation and function: recent advances and clinical implications. **Frontiers in Immunology**, v. 5, p. 203, 2014.

EZZELARAB, M. B. et al. Regulatory Dendritic Cell Infusion Prolongs Kidney Allograft Survival in Nonhuman Primates. **American Journal of Transplantation**, v. 13, n. 8, p. 1989–2005, 11 jun. 2013.

FALLER, W. J. et al. mTORC1-mediated translational elongation limits intestinal tumour initiation and growth. **Nature Publishing Group**, p. 1–16, 5 nov. 2014.

FENG, T. et al. Generation of Mucosal Dendritic Cells from Bone Marrow Reveals a Critical Role of Retinoic Acid. **Journal of immunology (Baltimore, Md. : 1950)**, v. 185, n. 10, p. 5915–5925, 3 nov. 2010.

FERREIRA, G. B. et al. Differential protein pathways in 1,25-dihydroxyvitamin d(3) and dexamethasone modulated tolerogenic human dendritic cells. **Journal of proteome research**, v. 11, n. 2, p. 941–971, 3 fev. 2012.

FERREIRA, G. B. et al. 1,25-Dihydroxyvitamin D3 Promotes Tolerogenic Dendritic Cells with Functional Migratory Properties in NOD Mice. **Journal of immunology (Baltimore, Md. : 1950)**, v. 192, n. 9, p. 4210–4220, 18 abr. 2014.

FERREIRA, G. B. et al. Vitamin D3 Induces Tolerance in Human Dendritic Cells by Activation of Intracellular Metabolic Pathways. v. 10, n. 5, p. 711–725, 10 fev. 2015.

FERRIS, S. T. et al. A Minor Subset of Batf3-Dependent Antigen-Presenting Cells in Islets of Langerhans Is Essential for the Development of Autoimmune Diabetes. **Immunity**, v. 41, n. 4, p. 657–669, 16 out. 2014.

FILGUEIRAS, L. R. et al. Leukotriene B4-mediated sterile inflammation promotes susceptibility to sepsis in a mouse model of type 1 diabetes. **Science signaling**, v. 8, n. 361, p. ra10–ra10, 27 jan. 2015.

FISCHER, R. et al. Use of rapamycin in the induction of tolerogenic dendritic cells. **Handbook of experimental pharmacology**, v. 188, n. 188, p. 215–232, 2009.

FLIESSER, M. et al. Hypoxia-inducible factor 1 α modulates metabolic activity and cytokine release in anti-Aspergillus fumigatus immune responses initiated by human dendritic cells. **International journal of medical microbiology : IJMM**, v. 305, n. 8, p. 865–873, dez. 2015.

FORLENZA, G. P.; REWERS, M. The epidemic of type 1 diabetes. **Current Opinion in Endocrinology, Diabetes and Obesity**, v. 18, n. 4, p. 248–251, ago. 2011.

FÖRSTER, I.; LIEBERAM, I. Peripheral tolerance of CD4 T cells following local activation in adolescent mice. **European journal of immunology**, v. 26, n. 12, p. 3194–3202, dez. 1996.

FRIEDL, P.; GUNZER, M. Interaction of T cells with APCs: the serial encounter model. **Trends in Immunology**, v. 22, n. 4, p. 187–191, abr. 2001.

GARCIA, D.; SHAW, R. J. AMPK: Mechanisms of Cellular Energy Sensing and Restoration of Metabolic Balance. **Molecular Cell**, v. 66, n. 6, p. 789–800, 15 jun. 2017.

GEISSMANN, F. et al. Development of monocytes, macrophages, and dendritic cells. **Science (New York, N.Y.)**, 2010.

GIANNOUKAKIS et al. Phase I (Safety) Study of Autologous Tolerogenic Dendritic Cells in Type 1 Diabetic Patients. **Diabetes Care**, v. 34, n. 9, p. 2026–2032, 25 ago. 2011.

GOWANS, G. J. et al. AMP Is a True Physiological Regulator of AMP-Activated Protein Kinase by Both Allosteric Activation and Enhancing Net Phosphorylation. **Cell Metabolism**, v. 18, n. 4, p. 556–566, 1 out. 2013.

GRANOT, T. et al. Dendritic Cells Display Subset and Tissue-Specific Maturation Dynamics over Human Life. **Immunity**, v. 46, n. 3, p. 504–515, 21 mar. 2017.

GROHMANN, U. et al. CTLA-4-Ig regulates tryptophan catabolism in vivo. **Nature immunology**, v. 3, n. 11, p. 1097–1101, nov. 2002.

GROUX, H. et al. A CD4⁺ T-cell subset inhibits antigen-specific T-cell responses and prevents colitis. **Nature**, v. 389, n. 6652, p. 737–742, 16 out. 1997.

GUAK, H. et al. Glycolytic metabolism is essential for CCR7 oligomerization and dendritic cell migration. **Nature communications**, v. 9, n. 1, p. 1–12, 15 jun. 2018.

GUERMONPREZ, P. et al. Antigen presentation and T cell stimulation by dendritic cells. **Annual Review of Immunology**, v. 20, p. 621–667, 2002.

GUILLIAMS, M. et al. Dendritic cells, monocytes and macrophages: a unified nomenclature based on ontogeny. **Nature reviews. Immunology**, v. 14, n. 8, p. 571–578, ago. 2014.

GUILLIAMS, M. et al. Unsupervised High-Dimensional Analysis Aligns Dendritic Cells across Tissues and Species. **Immunity**, v. 45, n. 3, p. 669–684, 20 set. 2016.

GUTIÉRREZ, S.; SVAHN, S. L.; JOHANSSON, M. E. Effects of Omega-3 Fatty Acids on Immune Cells. **International Journal of Molecular Sciences**, v. 20, n. 20, p. 5028–21, out. 2019.

GWINN, D. M. et al. AMPK Phosphorylation of Raptor Mediates a Metabolic Checkpoint. **Molecular Cell**, v. 30, n. 2, p. 214–226, abr. 2008.

HANIFFA, M.; COLLIN, M.; GINHOUX, F. Ontogeny and functional specialization of dendritic cells in human and mouse. v. 120, p. 1–49, 2013.

HARDIE, D. G.; ROSS, F. A.; HAWLEY, S. A. AMPK: a nutrient and energy sensor that maintains energy homeostasis. **Nature reviews. Molecular cell biology**, v. 13, n. 4, p. 251–262, 22 mar. 2012.

HAWIGER, D. et al. Dendritic cells induce peripheral T cell unresponsiveness under steady state conditions in vivo. **Journal of Experimental Medicine**, v. 194, n. 6, p. 769–779, 17 set. 2001.

HAWLEY, S. A. et al. Complexes between the LKB1 tumor suppressor, STRAD alpha/beta and MO25 alpha/beta are upstream kinases in the AMP-activated protein kinase cascade. **Journal of biology**, v. 2, n. 4, p. 28–16, 2003.

HAWLEY, S. A. et al. Calmodulin-dependent protein kinase kinase-beta is an alternative upstream kinase for AMP-activated protein kinase. **Cell Metabolism**, v. 2, n. 1, p. 9–19, jul. 2005.

HEMMI, H.; AKIRA, S. TLR signalling and the function of dendritic cells. **Chemical immunology and allergy**, v. 86, p. 120–135, 2005.

HENDERSON, R. A.; WATKINS, S. C.; FLYNN, J. L. Activation of human dendritic cells following infection with Mycobacterium tuberculosis. **Journal of immunology (Baltimore, Md. : 1950)**, v. 159, n. 2, p. 635–643, 15 jul. 1997.

HOUSLEY, W. J. et al. PPARgamma regulates retinoic acid-mediated DC induction of Tregs. **Journal of leukocyte biology**, v. 86, n. 2, p. 293–301, ago. 2009.

HOVING, L. R. et al. GC-MS Analysis of Medium- and Long-Chain Fatty Acids in Blood Samples. In: **Toll-Like Receptors**. Methods and Protocols. Traducaao. New York, NY: Springer New York, 2018. v. 1730p. 257–265.

HUANG, Y. et al. Kidney-Derived Mesenchymal Stromal Cells Modulate Dendritic Cell Function to Suppress Alloimmune Responses and Delay Allograft Rejection. **Transplantation**, v. 90, n. 12, p. 1307–1311, dez. 2010.

HUANG, Y.-S. et al. Eicosadienoic acid differentially modulates production of pro-inflammatory modulators in murine macrophages. **Molecular and Cellular Biochemistry**, v. 358, n. 1-2, p. 85–94, 19 jun. 2011.

IDOYAGA, J. et al. Specialized role of migratory dendritic cells in peripheral tolerance induction. **Journal of Clinical Investigation**, v. 123, n. 2, p. 844–854, fev. 2013.

ILIEV, I. D. et al. Human intestinal epithelial cells promote the differentiation of tolerogenic dendritic cells. **Gut**, v. 58, n. 11, p. 1481–1489, nov. 2009.

IMAI, Y.; YAMAKAWA, M.; KASAJIMA, T. The lymphocyte-dendritic cell system. **Histology and histopathology**, v. 13, n. 2, p. 469–510, abr. 1998.

INAGAKI, K. et al. Identification and expression of a rat fatty acid elongase involved in the biosynthesis of C18 fatty acids. **Bioscience, biotechnology, and biochemistry**, v. 66, n. 3, p. 613–621, mar. 2002.

INNES, J. K.; CALDER, P. C. Omega-6 fatty acids and inflammation. **Prostaglandins, leukotrienes, and essential fatty acids**, v. 132, p. 41–48, maio 2018.

INOKI, K.; ZHU, T.; GUAN, K.-L. TSC2 mediates cellular energy response to control cell growth and survival. **Cell**, v. 115, n. 5, p. 577–590, 26 nov. 2003.

IP, W. K. E. et al. Anti-inflammatory effect of IL-10 mediated by metabolic reprogramming of macrophages. **Science (New York, N.Y.)**, v. 356, n. 6337, p. 513–519, 5 maio 2017.

ITANO, A. A.; JENKINS, M. K. Antigen presentation to naive CD4 T cells in the lymph node. **Nature immunology**, v. 4, n. 8, p. 733–739, ago. 2003.

JAKOBSSON, A.; WESTERBERG, R.; JACOBSSON, A. Fatty acid elongases in mammals: their regulation and roles in metabolism. **Progress in lipid research**, v. 45, n. 3, p. 237–249, maio 2006.

JANTSCH, J. et al. Hypoxia and Hypoxia-Inducible Factor-1 Modulate Lipopolysaccharide-Induced Dendritic Cell Activation and Function. **Journal of immunology (Baltimore, Md. : 1950)**, v. 180, n. 7, p. 4697–4705, 19 mar. 2008.

JAUREGUI-AMEZAGA, A. et al. Intraperitoneal Administration of Autologous Tolerogenic Dendritic Cells for Refractory Crohn's Disease: A Phase I Study. **Journal of Crohn's & colitis**, v. 9, n. 12, p. 1071–1078, 27 nov. 2015.

JONES, R. G.; PEARCE, E. J. MenTORing Immunity: mTOR Signaling in the Development and Function of Tissue-Resident Immune Cells. **Immunity**, v. 46, n. 5, p. 730–742, 16 maio 2017.

KAISAR, M. M. M. et al. Butyrate Conditions Human Dendritic Cells to Prime Type 1 Regulatory T Cells via both Histone Deacetylase Inhibition and G Protein-Coupled Receptor 109A Signaling. **Frontiers in immunology**, v. 8, p. 13–14, 30 out. 2017.

KHARE, A. et al. Cutting Edge: Dual Function of PPAR γ in CD11c +Cells Ensures Immune Tolerance in the Airways. **Journal of immunology (Baltimore, Md. : 1950)**, v. 195, n. 2, p. 431–435, 2 jul. 2015.

KLEIJWEGT, F. S. et al. Critical Role for TNF in the Induction of Human Antigen-Specific Regulatory T Cells by Tolerogenic Dendritic Cells. **Journal of immunology (Baltimore, Md. : 1950)**, v. 185, n. 3, p. 1412–1418, 21 jul. 2010.

KLEIJWEGT, F. S. et al. Tolerogenic dendritic cells impede priming of naïve CD8(+) T cells and deplete memory CD8(+) T cells. v. 43, n. 1, p. 85–92, 1 jan. 2013.

KLINKE, D. J. Extent of Beta Cell Destruction Is Important but Insufficient to Predict the Onset of Type 1 Diabetes Mellitus. **PLoS ONE**, v. 3, n. 1, p. e1374–10, 2 jan. 2008.

KLOPPERK, A. et al. Changes in innate and adaptive immunity over the first year after the onset of type 1 diabetes. **Acta Diabetologica**, p. 1–11, 27 set. 2019.

KNOTT, R. M.; FORRESTER, J. V. Role of glucose regulatory mechanisms in diabetic retinopathy. **The British journal of ophthalmology**, v. 79, n. 11, p. 1046–1049, nov. 1995.

KRAWCZYK, C. M. et al. Toll-like receptor-induced changes in glycolytic metabolism regulate dendritic cell activation. **Blood**, v. 115, n. 23, p. 4742–4749, 10 jun. 2010.

KURTS, C. Constitutive class I-restricted exogenous presentation of self antigens in vivo. **Journal of Experimental Medicine**, v. 184, n. 3, p. 923–930, 1 set. 1996.

LAMPEN, A. et al. Metabolism of vitamin A and its active metabolite all-trans-retinoic acid in small intestinal enterocytes. **Journal of Pharmacology and Experimental Therapeutics**, v. 295, n. 3, p. 979–985, dez. 2000.

LAMPROPOULOU, V. et al. Itaconate Links Inhibition of Succinate Dehydrogenase with Macrophage Metabolic Remodeling and Regulation of Inflammation. **Cell Metabolism**, v. 24, n. 1, p. 158–166, 12 jul. 2016.

LAN, Y. Y. et al. “Alternatively Activated” Dendritic Cells Preferentially Secrete IL-10, Expand Foxp3+CD4+ T Cells, and Induce Long-Term Organ Allograft Survival in Combination with CTLA4-Ig. **Journal of immunology (Baltimore, Md. : 1950)**, v. 177, n. 9, p. 5868–5877, 18 out. 2006.

LEHUEN, A. et al. Immune cell crosstalk in type 1 diabetes. v. 10, n. 7, p. 501–513, jul. 2010.

LEPRIVIER, G. et al. The eEF2 Kinase Confers Resistance to Nutrient Deprivation by Blocking Translation Elongation. **Cell**, v. 153, n. 5, p. 1064–1079, 23 maio 2013.

LI, Q. et al. Interferon-alpha initiates type 1 diabetes in nonobese diabetic mice. **Proceedings of the National Academy of Sciences of the United States of America**, v. 105, n. 34, p. 12439–12444, 26 ago. 2008.

LIU, D. Double-Stranded Ribonucleic Acid (RNA) Induces β -Cell Fas Messenger RNA Expression and Increases Cytokine-Induced β -Cell Apoptosis. **Endocrinology**, v. 142, n. 6, p. 2593–2599, 1 jun. 2001.

LIU, G. et al. Dendritic cell SIRT1-HIF1 α axis programs the differentiation of CD4⁺ T cells through IL-12 and TGF- β 1. v. 112, n. 9, p. E957–E965, 17 fev. 2015.

LUTZ, M. B.; SCHULER, G. Immature, semi-mature and fully mature dendritic cells: which signals induce tolerance or immunity? **Trends in Immunology**, v. 23, n. 9, p. 445–449, set. 2002.

MA, L. et al. Prevention of Diabetes in NOD Mice by Administration of Dendritic Cells Deficient in Nuclear Transcription Factor- κ B Activity. **Diabetes**, v. 52, n. 8, p. 1976–1985, 1 ago. 2003.

MACDOUGALL, C. E. et al. Visceral Adipose Tissue Immune Homeostasis Is Regulated by the Crosstalk between Adipocytes and Dendritic Cell Subsets. **Cell Metabolism**, v. 27, n. 3, p. 588–601.e4, 6 mar. 2018.

MADDUR, M. S. et al. Dendritic Cells in Autoimmune Diseases. v. 3, n. 1, p. 1–7, 12 jan. 2010.

MAGGI, J. et al. Dexamethasone and Monophosphoryl Lipid A-Modulated Dendritic Cells Promote Antigen-Specific Tolerogenic Properties on Naive and Memory CD4⁺ T Cells. **Frontiers in immunology**, v. 7, n. 8, p. 1473–12, 19 set. 2016.

MAHNKE, K. et al. Induction of CD4⁺/CD25⁺ regulatory T cells by targeting of antigens to immature dendritic cells. **Blood**, v. 101, n. 12, p. 4862–4869, 15 jun. 2003.

MALERBI, D. A.; FRANCO, L. J. Multicenter study of the prevalence of diabetes mellitus and impaired glucose tolerance in the urban Brazilian population aged 30-69 yr. The Brazilian Cooperative Group on the Study of Diabetes Prevalence. **Diabetes Care**, v. 15, n. 11, p. 1509–1516, nov. 1992.

MALINARICH, F. et al. High mitochondrial respiration and glycolytic capacity represent a metabolic phenotype of human tolerogenic dendritic cells. **The Journal of Immunology**, v. 194, n. 11, p. 5174–5186, 1 jun. 2015.

MANICASSAMY, S.; PULENDRAN, B. Dendritic cell control of tolerogenic responses. **Immunological reviews**, v. 241, n. 1, p. 206–227, maio 2011.

MARCHETTI, D. P. et al. Inflammatory profile in X-linked adrenoleukodystrophy patients: Understanding disease progression. **Journal of Cellular Biochemistry**, v. 119, n. 1, p. 1223–1233, 23 ago. 2017.

- MARTIN, A. P. et al. Increased expression of CCL2 in insulin-producing cells of transgenic mice promotes mobilization of myeloid cells from the bone marrow, marked insulinitis, and diabetes. **Diabetes**, v. 57, n. 11, p. 3025–3033, nov. 2008.
- MCGEE, S. L. et al. AMP-activated protein kinase regulates GLUT4 transcription by phosphorylating histone deacetylase 5. **Diabetes**, v. 57, n. 4, p. 860–867, abr. 2008.
- MCKEITHEN, D. N. et al. The emerging role of ASC in dendritic cell metabolism during Chlamydia infection. **PLoS ONE**, v. 12, n. 12, p. e0188643–18, 7 dez. 2017.
- MEHTA, L. R.; DWORKIN, R. H.; SCHWID, S. R. Polyunsaturated fatty acids and their potential therapeutic role in multiple sclerosis. **Nature Clinical Practice Neurology**, v. 5, n. 2, p. 82–92, fev. 2009.
- MERAD, M. et al. The Dendritic Cell Lineage: Ontogeny and Function of Dendritic Cells and Their Subsets in the Steady State and the Inflamed Setting. **Annual Review of Immunology**, v. 31, n. 1, p. 563–604, 21 mar. 2013.
- MILDNER, A.; JUNG, S. Development and function of dendritic cell subsets. **Immunity**, v. 40, n. 5, p. 642–656, 2014.
- MILLS, E. L. et al. Succinate Dehydrogenase Supports Metabolic Repurposing of Mitochondria to Drive Inflammatory Macrophages. **Cell**, v. 167, n. 2, p. 457–461.e14, 6 out. 2016.
- MISHARIN, A. V. et al. Flow Cytometric Analysis of Macrophages and Dendritic Cell Subsets in the Mouse Lung. **American journal of respiratory cell and molecular biology**, v. 49, n. 4, p. 503–510, out. 2013.
- MOCKING, R. J. T. et al. Ala54Thr Fatty Acid-Binding Protein 2 (FABP2) Polymorphism in Recurrent Depression: Associations with Fatty Acid Concentrations and Waist Circumference. **PLoS ONE**, v. 8, n. 12, p. e82980–10, 10 dez. 2013.
- MOLLAH, Z. U. A. et al. Abnormal NF-kappa B function characterizes human type 1 diabetes dendritic cells and monocytes. **Journal of immunology (Baltimore, Md. : 1950)**, v. 180, n. 5, p. 3166–3175, 1 mar. 2008.
- MONTANI, M. S. G. et al. High glucose and hyperglycemic sera from type 2 diabetic patients impair DC differentiation by inducing ROS and activating Wnt/ β -catenin and p38 MAPK. **BBA - Molecular Basis of Disease**, v. 1862, n. 4, p. 805–813, 1 abr. 2016.
- MOOKERJEE, S. A. et al. Quantifying intracellular rates of glycolytic and oxidative ATP production and consumption using extracellular flux measurements. **The Journal of biological chemistry**, v. 292, n. 17, p. 7189–7207, 28 abr. 2017.
- MOON, Y. A. et al. Identification of a mammalian long chain fatty acyl elongase regulated by sterol regulatory element-binding proteins. **The Journal of biological chemistry**, v. 276, n. 48, p. 45358–45366, 30 nov. 2001.
- MORAES, S. A.; FREITAS, I.; GIMENO, S. Diabetes mellitus prevalence and associated factors in adults in Ribeirão Preto, São Paulo, Brazil, 2006: OBEDIARP Project. **Cadernos de Saúde ...**, v. 26, n. 5, p. 929–941, 2010.

MORELLI, A. E.; THOMSON, A. W. Tolerogenic dendritic cells and the quest for transplant tolerance. **Nature Reviews Immunology**, v. 7, n. 8, p. 610–621, 13 jul. 2007.

NAGY, K.; TIUCA, I.-D. Importance of Fatty Acids in Physiopathology of Human Body. In: **Fatty Acids**. Traducao. [s.l.] InTech, 2017. p. 1–21.

NAVARRO-BARRIUSO, J. et al. Comparative transcriptomic profile of tolerogenic dendritic cells differentiated with vitamin D3, dexamethasone and rapamycin. **Scientific Reports**, v. 8, n. 1, p. 14985, 8 out. 2018.

NELSON, J. R.; RASKIN, S. The eicosapentaenoic acid:arachidonic acid ratio and its clinical utility in cardiovascular disease. **Postgraduate Medicine**, v. 131, n. 4, p. 268–277, 14 maio 2019.

NERUP, J. et al. HL-A antigens and diabetes mellitus. **Lancet (London, England)**, v. 2, n. 7885, p. 864–866, 12 out. 1974.

NIEVES, W. et al. Myeloid-Restricted AMPK α 1 Promotes Host Immunity and Protects against IL-12/23p40-Dependent Lung Injury during Hookworm Infection. **Journal of immunology (Baltimore, Md. : 1950)**, v. 196, n. 11, p. 4632–4640, 20 maio 2016.

O'NEILL, L. A. J.; KISHTON, R. J.; RATHMELL, J. A guide to immunometabolism for immunologists. **Nature reviews. Immunology**, v. 16, n. 9, p. 553–565, set. 2016.

OCHANDO, J. et al. Tolerogenic Dendritic Cells in Organ Transplantation. **Transplant International**, p. tri.13504–31, 31 ago. 2019.

OGURTSOVA, K. et al. IDF Diabetes Atlas: Global estimates for the prevalence of diabetes for 2015 and 2040. **Diabetes Research and Clinical Practice**, v. 128, p. 40–50, jun. 2017.

ONODERA, T. et al. Eicosapentaenoic acid and 5-HEPE enhance macrophage-mediated Treg induction in mice. **Scientific Reports**, v. 7, n. 1, p. 1821–11, 4 jul. 2017.

OREN, R. et al. Metabolic patterns in three types of phagocytizing cells. **The Journal of cell biology**, v. 17, n. 3, p. 487–501, jun. 1963.

O'KEEFFE, M.; MOK, W. H.; RADFORD, K. J. Human dendritic cell subsets and function in health and disease. **Cellular and Molecular Life Sciences**, v. 72, n. 22, p. 1–17, 4 ago. 2015.

PANTEL, A. et al. Direct type I IFN but not MDA5/TLR3 activation of dendritic cells is required for maturation and metabolic shift to glycolysis after poly IC stimulation. **PLoS biology**, v. 12, n. 1, p. e1001759, jan. 2014.

PASCHOU, S. A. et al. On type 1 diabetes mellitus pathogenesis. **Endocrine Connections**, v. 7, n. 1, p. R38–R46, 17 jan. 2018.

PATENTE, T. A. et al. Human Dendritic Cells: Their Heterogeneity and Clinical Application Potential in Cancer Immunotherapy. **Frontiers in immunology**, v. 9, p. 3176, 2018.

PEARCE, E. J.; EVERTS, B. Dendritic cell metabolism. **Nature Reviews Immunology**, v. 15, n. 1, p. 18–29, 1 jan. 2015.

PEARCE, E. J.; PEARCE, E. L. Immunometabolism in 2017: Driving immunity: all roads lead to metabolism. **Nature reviews. Immunology**, v. 18, n. 2, p. 1–2, 11 dez. 2017.

PEARCE, E. L.; PEARCE, E. J. Metabolic Pathways in Immune Cell Activation and Quiescence. **Immunity**, v. 38, n. 4, p. 633–643, 18 abr. 2013.

PEHMØLLER, C. et al. Genetic disruption of AMPK signaling abolishes both contraction- and insulin-stimulated TBC1D1 phosphorylation and 14-3-3 binding in mouse skeletal muscle. **American Journal of Physiology-Endocrinology and Metabolism**, v. 297, n. 3, p. E665–E675, set. 2009.

PELGROM, L. R. et al. LKB1 expressed in dendritic cells governs the development and expansion of thymus-derived regulatory T cells. **Cell research**, p. 1–14, 27 mar. 2019.

PENG, R. et al. Abnormal Peripheral Blood Dendritic Cell Populations in Type 1 Diabetes. **Annals of the New York Academy of Sciences**, v. 1005, n. 1, p. 222–225, 1 nov. 2003.

PEREIRA, D. M. et al. Anti-Inflammatory Effect of Unsaturated Fatty Acids and Ergosta-7,22-dien-3-ol from *Marthasterias glacialis*: Prevention of CHOP-Mediated ER-Stress and NF- κ B Activation. **PLoS ONE**, v. 9, n. 2, p. e88341–9, 13 fev. 2014.

PHILLIPS et al. Type 1 Diabetes Development Requires Both CD4+ and CD8+ T cells and Can Be Reversed by Non-Depleting Antibodies Targeting Both T Cell Populations. **The Review of Diabetic Studies**, v. 6, n. 2, p. 97–103, 2009.

QAISAR, N. et al. A Critical Role for the Type I Interferon Receptor in Virus-Induced Autoimmune Diabetes in Rats. **Diabetes**, v. 66, n. 1, p. 145–157, jan. 2017.

QUENTIN, T. et al. Different expression of the catalytic alpha subunits of the AMP activated protein kinase--an immunohistochemical study in human tissue. **Histology and histopathology**, v. 26, n. 5, p. 589–596, maio 2011.

RAMALHO, T. et al. Leukotriene-B4 modulates macrophage metabolism and fat loss in type 1 diabetic mice. **Journal of Leukocyte Biology**, v. 106, n. 3, p. 665–675, 22 jul. 2019.

RAMOS, R. N. et al. Monocyte-derived dendritic cells from breast cancer patients are biased to induce CD4+CD25+Foxp3+ regulatory T cells. **Journal of leukocyte biology**, v. 92, n. 3, p. 673–682, set. 2012.

RANDOLPH, G. J.; ANGELI, V.; SWARTZ, M. A. Dendritic-cell trafficking to lymph nodes through lymphatic vessels. **Nature Reviews Immunology**, v. 5, n. 8, p. 617–628, ago. 2005.

RASSCHAERT, J. et al. Global profiling of double stranded RNA- and IFN- γ -induced genes in rat pancreatic beta cells. **Diabetologia**, v. 46, n. 12, p. 1641–1657, 1 dez. 2003.

RASSCHAERT, J. et al. Toll-like receptor 3 and STAT-1 contribute to double-stranded RNA+ interferon-gamma-induced apoptosis in primary pancreatic beta-cells. *v. 280, n. 40, p. 33984–33991, 7 out. 2005.*

REDONDO, M. J. et al. Heterogeneity of type I diabetes: analysis of monozygotic twins in Great Britain and the United States. **Diabetologia**, *v. 44, n. 3, p. 354–362, mar. 2001.*

REWERS, M. J. et al. Assessment and monitoring of glycemic control in children and adolescents with diabetes. **Pediatric Diabetes**, *v. 15, n. S20, p. 102–114, 3 set. 2014.*

REYNOLDS, G.; HANIFFA, M. Human and Mouse Mononuclear Phagocyte Networks: A Tale of Two Species? **Frontiers in immunology**, *v. 6, p. 330, 2015.*

ROBBINS, S. H. et al. Novel insights into the relationships between dendritic cell subsets in human and mouse revealed by genome-wide expression profiling. **Genome biology**, *v. 9, n. 1, p. R17, 24 jan. 2008.*

RODRIGUES, C. P. et al. Tolerogenic IDO+ Dendritic Cells Are Induced by PD-1-Expressing Mast Cells. **Frontiers in immunology**, *v. 7, p. 111–17, 25 jan. 2016.*

RUDENSKY, A. Y. Regulatory T cells and Foxp3. **Immunological reviews**, *v. 241, n. 1, p. 260–268, 1 maio 2011.*

RYANS, K. et al. The immunoregulatory role of alpha enolase in dendritic cell function during Chlamydia infection. **BMC immunology**, *v. 18, n. 1, p. 27, 19 maio 2017.*

SAKAGUCHI, S. et al. FOXP3+ regulatory T cells in the human immune system. **Nature reviews. Immunology**, *v. 10, n. 7, p. 490–500, 18 jun. 2010.*

SALLUSTO, F.; LANZAVECCHIA, A. Efficient presentation of soluble antigen by cultured human dendritic cells is maintained by granulocyte/macrophage colony-stimulating factor plus interleukin 4 and downregulated by tumor necrosis factor alpha. **Journal of Experimental Medicine**, *v. 179, n. 4, p. 1109–1118, 1 abr. 1994.*

SALOMON, B. et al. B7/CD28 costimulation is essential for the homeostasis of the CD4+CD25+ immunoregulatory T cells that control autoimmune diabetes. **Immunity**, *v. 12, n. 4, p. 431–440, abr. 2000.*

SANDERSON, P. et al. Dietary fish oil diminishes the antigen presentation activity of rat dendritic cells. **Journal of Leukocyte Biology**, *v. 62, n. 6, p. 771–777, 1 dez. 1997.*

SARGENT, J. R.; COUPLAND, K.; WILSON, R. Nervonic acid and demyelinating disease. **Medical Hypotheses**, *v. 42, n. 4, p. 237–242, abr. 1994.*

SASSA, T. et al. Lorenzo's oil inhibits ELOVL1 and lowers the level of sphingomyelin with a saturated very long-chain fatty acid. **Journal of Lipid Research**, *v. 55, n. 3, p. 524–530, mar. 2014.*

SAWADA, Y. et al. Resolvin E1 inhibits dendritic cell migration in the skin and attenuates contact hypersensitivity responses. **Journal of Experimental Medicine**, *v. 212, n. 11, p. 1921–1930, 19 out. 2015.*

SAXENA, V. et al. The countervailing actions of myeloid and plasmacytoid dendritic cells control autoimmune diabetes in the nonobese diabetic mouse. **Journal of immunology (Baltimore, Md. : 1950)**, v. 179, n. 8, p. 5041–5053, 15 out. 2007.

SEDLMAYR, P. et al. Severely depressed natural killer cell activity of patients with adrenoleukodystrophy under treatment with Lorenzo's oil. **Journal of Inherited Metabolic Disease**, v. 18, n. 1, p. 101–102, 1995.

SEE, P. et al. Mapping the human DC lineage through the integration of high-dimensional techniques. **Science (New York, N.Y.)**, v. 66, p. eaag3009, 4 maio 2017.

SEGURA, E. et al. Human Inflammatory Dendritic Cells Induce Th17 Cell Differentiation. **Immunity**, v. 38, n. 2, p. 336–348, 21 fev. 2013.

SEO, M.; CROCHET, R. B.; LEE, Y.-H. **Chapter 14 – Targeting Altered Metabolism—Emerging Cancer Therapeutic Strategies**. Tradução. Second Edition ed. [s.l.] Elsevier, 2013. p. 427–448

SERBINA, N. V. et al. TNF/iNOS-Producing Dendritic Cells Mediate Innate Immune Defense against Bacterial Infection. **Immunity**, v. 19, n. 1, p. 59–70, jul. 2003.

SIMOPOULOS, A. An Increase in the Omega-6/Omega-3 Fatty Acid Ratio Increases the Risk for Obesity. **Nutrients**, v. 8, n. 3, p. 128–17, mar. 2016.

SIMOPOULOS, A. P. Importance of the ratio of omega-6/omega-3 essential fatty acids: evolutionary aspects. **World review of nutrition and dietetics**, v. 92, p. 1–22, 2003.

SITKIN, S. et al. P852 A metabolomics approach to discover biomarkers of chronic intestinal inflammation associated with gut microbiota dysbiosis in ulcerative colitis and Celiac. **Journal of Crohn's & colitis**, v. 12, n. supplement_1, p. S547–S548, 16 jan. 2018.

SITKIN, S.; POKROTNIKES, J. Alterations in Polyunsaturated Fatty Acid Metabolism and Reduced Serum Eicosadienoic Acid Level in Ulcerative Colitis: Is There a Place for Metabolomic Fatty Acid Biomarkers in IBD? **Digestive diseases and sciences**, p. 1–2, 5 jul. 2018.

SOROOSH, P. et al. Lung-resident tissue macrophages generate Foxp3+ regulatory T cells and promote airway tolerance. **Journal of Experimental Medicine**, v. 210, n. 4, p. 775–788, 8 abr. 2013.

STEINMAN, R. M. The dendritic cell system and its role in immunogenicity. **Annual Review of Immunology**, v. 9, n. 1, p. 271–296, 1991.

STEINMAN, R. M. et al. The induction of tolerance by dendritic cells that have captured apoptotic cells. **Journal of Experimental Medicine**, v. 191, n. 3, p. 411–416, 2000.

STEINMAN, R. M. et al. Dendritic cell function in vivo during the steady state: a role in peripheral tolerance. **Annals of the New York Academy of Sciences**, v. 987, p. 15–25, abr. 2003.

- STEINMAN, R. M.; WITMER, M. D. Lymphoid dendritic cells are potent stimulators of the primary mixed leukocyte reaction in mice. **PNAS**, v. 75, n. 10, p. 5132–5136, 1 out. 1978.
- SUMMERS, K. L. et al. Reduced IFN- α secretion by blood dendritic cells in human diabetes. **Clinical Immunology**, v. 121, n. 1, p. 81–89, out. 2006.
- SUN, G. et al. Adoptive Infusion of Tolerogenic Dendritic Cells Prolongs the Survival of Pancreatic Islet Allografts: A Systematic Review of 13 Mouse and Rat Studies. **PLoS ONE**, v. 7, n. 12, p. e2096, 18 dez. 2012.
- SUN, X. et al. Fatty Acid Metabolism is Associated With Disease Severity After H7N9 Infection. **EBioMedicine**, v. 33, n. C, p. 218–229, 1 jul. 2018.
- SUTHERLAND, A. P. R. et al. Interleukin-21 is required for the development of type 1 diabetes in NOD mice. **Diabetes**, v. 58, n. 5, p. 1144–1155, maio 2009.
- SVAJGER, U.; ROZMAN, P. Tolerogenic dendritic cells: molecular and cellular mechanisms in transplantation. **Journal of Leukocyte Biology**, v. 95, n. 1, p. 53–69, 2 jan. 2014.
- SWAIN, S. et al. CD103 (α E Integrin) Undergoes Endosomal Trafficking in Human Dendritic Cells, but Does Not Mediate Epithelial Adhesion. **Frontiers in immunology**, v. 9, p. 208–15, 21 dez. 2018.
- TAI, N. et al. IL-10-conditioned dendritic cells prevent autoimmune diabetes in NOD and humanized HLA-DQ8/RIP-B7.1 mice. **Clinical Immunology**, v. 139, n. 3, p. 336–349, 1 jun. 2011.
- TAMURA, K. et al. Novel lipogenic enzyme ELOVL7 is involved in prostate cancer growth through saturated long-chain fatty acid metabolism. **Cancer Research**, v. 69, n. 20, p. 8133–8140, 15 out. 2009.
- TEAGUE, H. et al. Dendritic cell activation, phagocytosis and CD69 expression on cognate T cells are suppressed by n-3 long-chain polyunsaturated fatty acids. ... **immunology**, v. 139, n. 3, p. 386–394, 13 jun. 2013.
- THOMAS, D. C. et al. Protection of Islet Grafts Through Transforming Growth Factor- β -Induced Tolerogenic Dendritic Cells. **Diabetes**, 2013.
- THORNTON, C.; SNOWDEN, M. A.; CARLING, D. Identification of a novel AMP-activated protein kinase beta subunit isoform that is highly expressed in skeletal muscle. **The Journal of biological chemistry**, v. 273, n. 20, p. 12443–12450, 15 maio 1998.
- THWE, P. M. et al. Cell-Intrinsic Glycogen Metabolism Supports Early Glycolytic Reprogramming Required for Dendritic Cell Immune Responses. **Cell Metabolism**, v. 26, n. 3, p. 558–567.e5, 5 set. 2017.
- TORQUATO, M. T. et al. Prevalence of diabetes mellitus and impaired glucose tolerance in the urban population aged 30–69 years in Ribeirão Preto (São Paulo), Brazil. **Sao Paulo medical journal = Revista paulista de medicina**, v. 121, n. 6, p. 224–230, 6 nov. 2003.

TORRES-AGUILAR, H. et al. IL-10/TGF-beta-treated dendritic cells, pulsed with insulin, specifically reduce the response to insulin of CD4+ effector/memory T cells from type 1 diabetic individuals. **Journal of Clinical Immunology**, v. 30, n. 5, p. 659–668, set. 2010.

TURLEY, S. et al. Physiological Cell Death Triggers Priming of Self-reactive T Cells by Dendritic Cells in a Type-1 Diabetes Model. **Journal of Experimental Medicine**, v. 198, n. 10, p. 1527–1537, 10 nov. 2003.

VANHERWEGEN, A.-S. et al. Vitamin D controls the capacity of human dendritic cells to induce functional regulatory T cells by regulation of glucose metabolism. **The Journal of steroid biochemistry and molecular biology**, v. 187, p. 134–145, 24 nov. 2018.

VILLANI, A.-C. et al. Single-cell RNA-seq reveals new types of human blood dendritic cells, monocytes, and progenitors. **Science (New York, N.Y.)**, v. 356, n. 6335, p. eaah4573–14, 20 abr. 2017.

VREMEC, D. The surface phenotype of dendritic cells purified from mouse thymus and spleen: investigation of the CD8 expression by a subpopulation of dendritic cells. **Journal of Experimental Medicine**, v. 176, n. 1, p. 47–58, 1 jul. 1992.

VUCKOVIC, S. et al. Decreased blood dendritic cell counts in type 1 diabetic children. **Clinical Immunology**, v. 123, n. 3, p. 281–288, jun. 2007.

WALLET, M. A.; TISCH, R. Type 1 diabetes, inflammation and dendritic cells. **Drug Discovery Today: Disease Mechanisms**, v. 3, n. 3, p. 373–379, set. 2006.

WANG, H. et al. ω -3 Polyunsaturated fatty acids affect lipopolysaccharide-induced maturation of dendritic cells through mitogen-activated protein kinases p38. **Nutrition**, v. 23, n. 6, p. 474–482, jun. 2007.

WANG, L. et al. The elevated glutaminolysis of bladder cancer and T cells in a simulated tumor microenvironment contributes to the up-regulation of PD-L1 expression by interferon- γ . **OncoTargets and Therapy**, v. Volume 11, p. 7229–7243, 2018.

WANG, M.-D. et al. HBx regulates fatty acid oxidation to promote hepatocellular carcinoma survival during metabolic stress. **Oncotarget**, v. 7, n. 6, p. 6711–6726, 9 fev. 2016.

WARBURG, O.; WIND, F.; NEGELEIN, E. THE METABOLISM OF TUMORS IN THE BODY. **The Journal of general physiology**, v. 8, n. 6, p. 519–530, 7 mar. 1927.

WATCHMAKER, P. B. et al. Comparative transcriptional and functional profiling defines conserved programs of intestinal DC differentiation in humans and mice. **Nature immunology**, v. 15, n. 1, p. 98–108, 1 dez. 2013.

WHEAT, W. et al. Increased NF-kappa B activity in B cells and bone marrow-derived dendritic cells from NOD mice. **European journal of immunology**, v. 34, n. 5, p. 1395–1404, maio 2004.

WILD, S. et al. Global prevalence of diabetes: estimates for the year 2000 and projections for 2030. **Diabetes Care**, v. 27, n. 5, p. 1047–1053, maio 2004.

WISE, D. R. et al. Myc regulates a transcriptional program that stimulates mitochondrial glutaminolysis and leads to glutamine addiction. **Proceedings of the National Academy of Sciences of the United States of America**, v. 105, n. 48, p. 18782–18787, 2 dez. 2008.

WOLLENBERG, A. et al. Immunomorphological and Ultrastructural Characterization of Langerhans Cells and a Novel, Inflammatory Dendritic Epidermal Cell (IDEC) Population in Lesional Skin of Atopic Eczema. **Journal of Investigative Dermatology**, v. 106, n. 3, p. 446–453, 1 jan. 1996.

WU, N. et al. AMPK-Dependent Degradation of TXNIP upon Energy Stress Leads to Enhanced Glucose Uptake via GLUT1. **Molecular Cell**, v. 49, n. 6, p. 1167–1175, 28 mar. 2013a.

WU, N. et al. AMPK-dependent degradation of TXNIP upon energy stress leads to enhanced glucose uptake via GLUT1. **Molecular Cell**, v. 49, n. 6, p. 1167–1175, 28 mar. 2013b.

XIAO, B. et al. Structure of mammalian AMPK and its regulation by ADP. **Nature Publishing Group**, v. 472, n. 7342, p. 230–233, 4 abr. 2011.

XU, G. et al. Prevalence of diagnosed type 1 and type 2 diabetes among US adults in 2016 and 2017: population based study. **BMJ**, v. 362, p. k1497, 4 set. 2018.

YANG, D.-F. et al. CTLA4-Ig-modified dendritic cells inhibit lymphocyte-mediated alloimmune responses and prolong the islet graft survival in mice. **Transplant Immunology**, v. 19, n. 3-4, p. 197–201, jul. 2008.

YANG, L.; VENNETI, S.; NAGRATH, D. Glutaminolysis: A Hallmark of Cancer Metabolism. **Annual Review of Biomedical Engineering**, v. 19, n. 1, p. 163–194, 21 jun. 2017.

YATES, S. F. et al. Induction of regulatory T cells and dominant tolerance by dendritic cells incapable of full activation. **Journal of immunology (Baltimore, Md. : 1950)**, v. 179, n. 2, p. 967–976, 15 jul. 2007.

YOGEV, N. et al. Dendritic cells ameliorate autoimmunity in the CNS by controlling the homeostasis of PD-1 receptor(+) regulatory T cells. **Immunity**, v. 37, n. 2, p. 264–275, 24 ago. 2012.

ZAPATA-GONZALEZ, F. et al. Human dendritic cell activities are modulated by the omega-3 fatty acid, docosahexaenoic acid, mainly through PPAR γ :RXR heterodimers: comparison with other polyunsaturated fatty acids. **Journal of Leukocyte Biology**, v. 84, n. 4, p. 1172–1182, 16 jul. 2008.

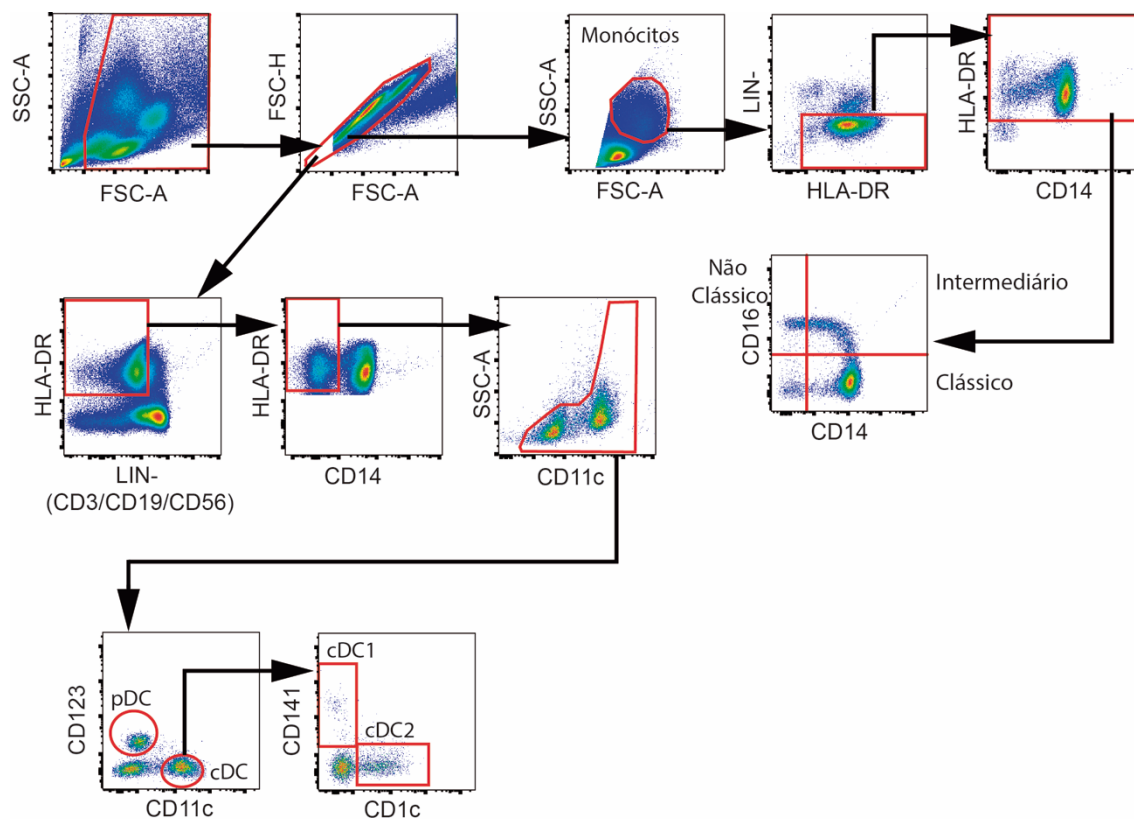
ZENG, H. et al. Type 1 regulatory T cells: a new mechanism of peripheral immune tolerance. **Cellular and Molecular Immunology**, v. 12, n. 5, p. 566–571, 8 jun. 2015.

ZEYDA, M. et al. Polyunsaturated Fatty Acids Block Dendritic Cell Activation and Function Independently of NF- κ B Activation. **The Journal of biological chemistry**, v. 280, n. 14, p. 14293–14301, 1 abr. 2005.

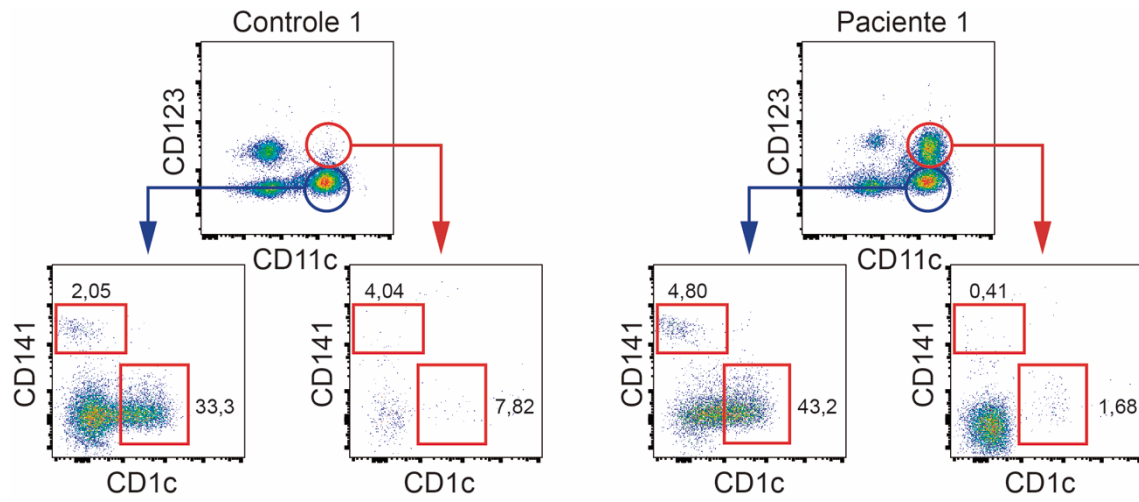
ZHAO, F. et al. Paracrine Wnt5a- β -Catenin Signaling Triggers a Metabolic Program that Drives Dendritic Cell Tolerization. **Immunity**, v. 48, n. 1, p. 147–160.e7, 16 jan. 2018.

8. APPENDIXES

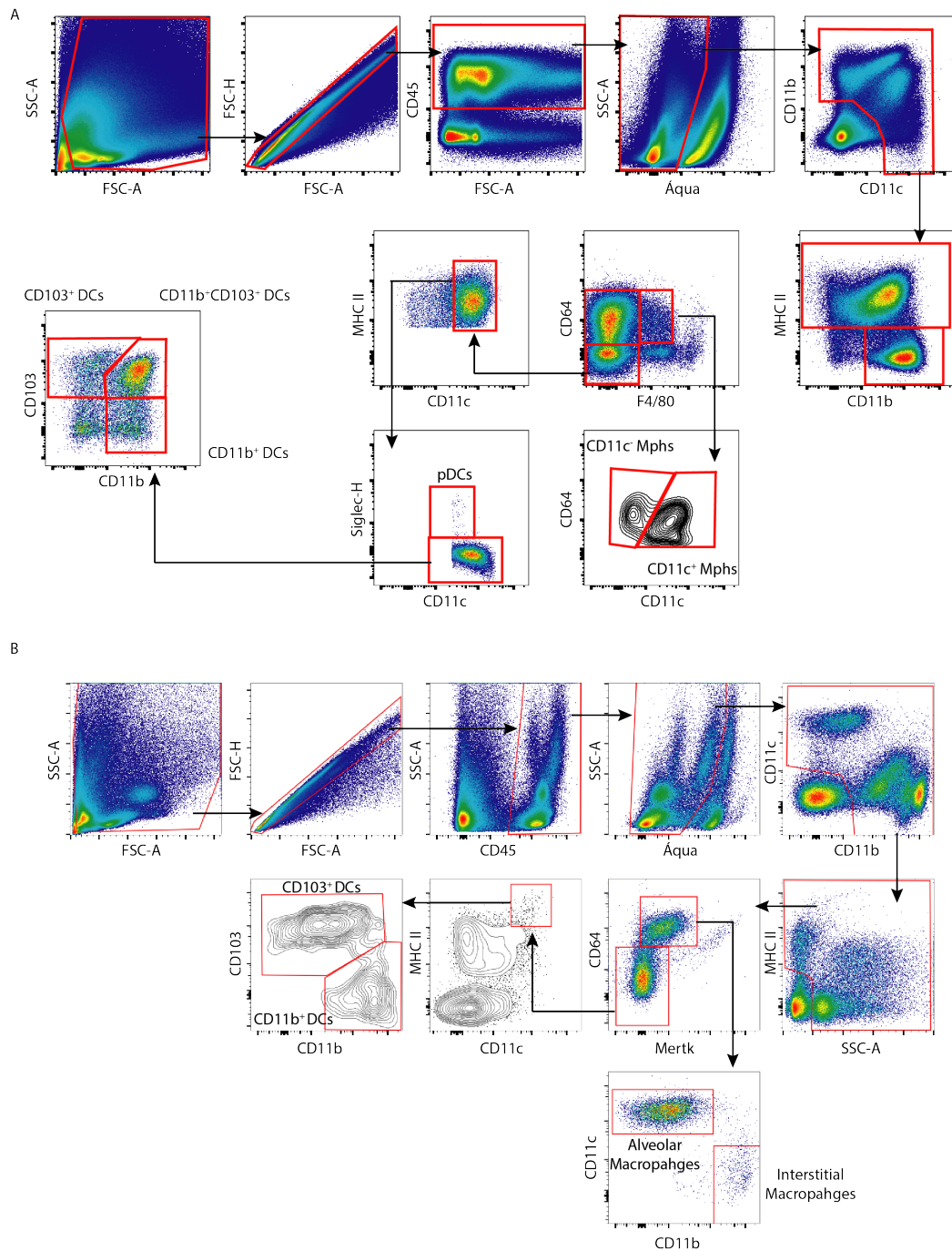
8. APPENDIXES



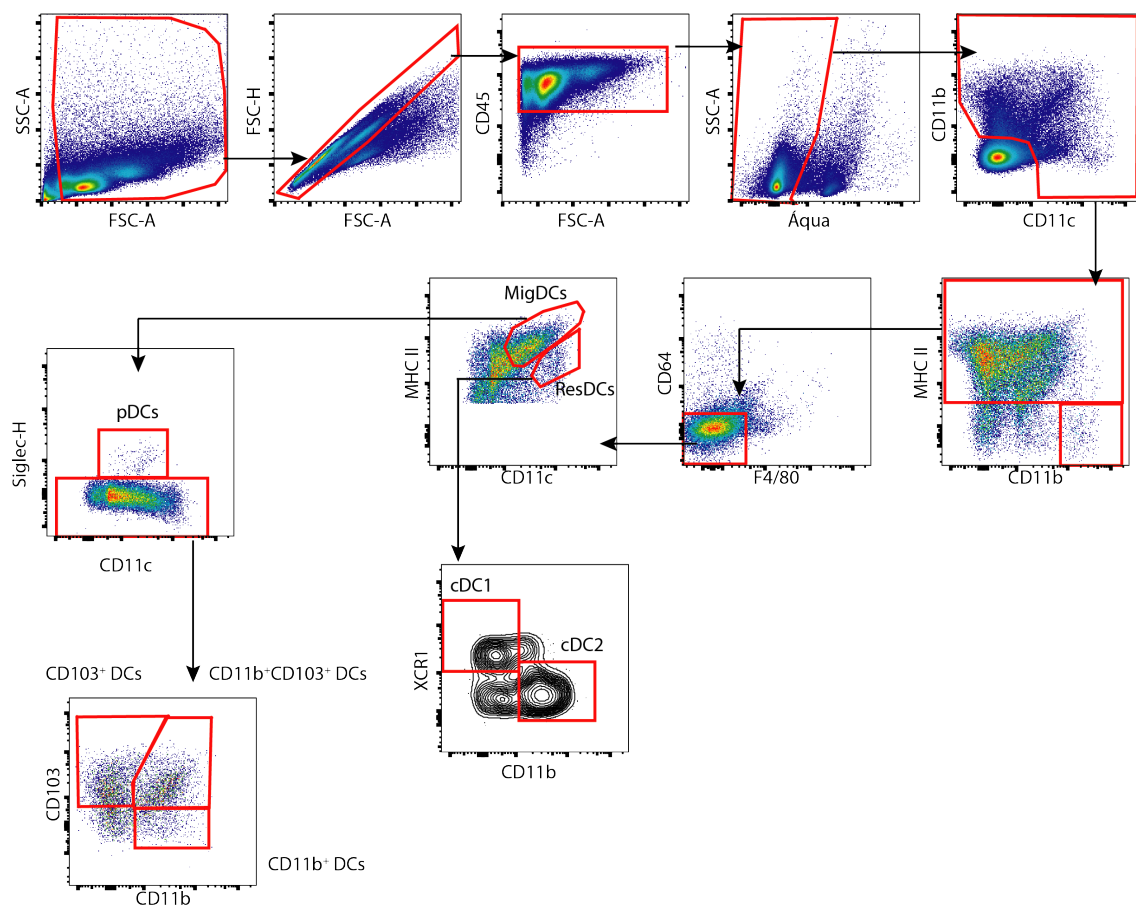
Supplementary Figure 1 – Gating strategy used for the analysis of blood and monocytes DC. After isolation PBMCs isolation, cells were washed with PBS and labeled with specific antibodies to CD3, CD19, CD56, CD11c, CD14, CD16, CD1c, CD141, CD123 and HLA-DR. Initially, the population with size and granularity compatible with PBMCs was selected; doublets were then excluded through the FSC-H vs FSC-A strategy; from then on, the analysis was divided for DC subpopulations and monocyte subpopulations. For DC subpopulations, CD3/CD19/CD56⁺ were excluded, then HLA-DR positive and CD14 negative cells are selected. From this population, CD123 x CD11c markers were analyzed to identify subpopulations of plasmacytoid DC (pDC) or classic DC (cDC). Within the cDC gate, CD141 vs CD1c expression was analyzed for identification of cDC1 and cDC2 subpopulations. For analysis of monocyte subpopulations, the population compatible with monocyte in size and granularity was selected and, to purify the analysis, cells positive for lineage and then cells negative for HLA-DR were excluded. From this population, monocyte subpopulations based on CD14 vs CD16 expression were analyzed.



Supplementary Figure 2 – Representative gates indicating that CD123^{lo}CD11c⁺ is mainly CD141⁻CD1c⁺ cells, being thus a subset of DC different from cDC1 and cDC2



Supplementary Figure 3 – Gating strategy for analysis of gut (A) and lung (B) myeloid cells. (A) Initially cells were gated base on size (FSC-A) and granularity (SSC-A) and doublets were excluded base on FSC-H vs FSC-A. Then, immune cells were selected base on CD45 expression and dead cells were excluded using SSC-A vs Aqua Live/Dead staining. Myeloid cells were selected base on CD11b and CD11c expression. Next, cells were analyzed for CD11b and MHC II expression and granulocytes were gated based on the lack of MHC II expression. The remaining cells were analyzed for CD64 and F4/80 expression and the double positive population (macrophages – Mphs) were gated as CD11c⁺ and CD11c⁻ population. The CD64⁺F4/80⁻ population were gated based on MHC II and CD11c population and the double positive population were further analyzed by Siglec-H and CD11c. The Siglec-H⁺CD11c^{int} population were gated as pDC and the remaining cells as cDC. Then cells were analyzed for the expression of CD11b and CD103 and cDC were gated in CD11b⁻CD103⁺ DC, CD11b⁺CD103⁺ DC and CD11b⁺CD103⁻ DC. (B) Until CD11b vs CD11c analysis, the gating strategy was the same for the gut. Next, cells were selected based on MHC II and SSC-A and then macrophages were gated based on Mertk vs CD64 expression. Next, within the CD64⁻Mertk⁻ population cDC were gated based on MHC II and CD11c. Next, cells were analyzed for CD103 and CD11b and gated for ALDH activity and frequency analysis.



Supplementary Figure 4 – Gating strategy for analysis of gut (A) and lung (B) myeloid cells. (A) Initially cells were gated base on size (FSC-A) and granularity (SSC-A) and doublets were excluded base on FSC-H vs FSC-A. Then, immune cells were selected base on CD45 expression and dead cells were excluded using SSC-A vs Aqua Live/Dead staining. Myeloid cells were selected base on CD11b and CD11c expression. Next, cells were analyzed for CD11b and MHC II expression and granulocytes were gated based on the lack of MHC II expression. The remaining cells were analyzed for CD64 and F4/80 expression and the double positive population (macrophages – Mphs) were gated as CD11c⁺ and CD11c⁻ population. The CD64⁺F4/80⁻ population were gated based on MHC II and CD11c in Migratory DC (MigDC - CD11c⁺MHCII^{hi}) and Resident DC (ResDC - CD11c⁺MHCII^{int}). MigDC were then gated as pDC (Siglec-H⁺CD11c^{int}) and cDC based on Siglec-H and CD11c expression and cDC were gated based in CD103 and CD11b expression in CD11b⁻CD103⁺ DC, CD11b⁺CD103⁺ DC and CD11b⁺CD103⁻ DC.



Human Dendritic Cells: Their Heterogeneity and Clinical Application Potential in Cancer Immunotherapy

Thiago A. Patente¹, Mariana P. Pinho¹, Aline A. Oliveira¹, Gabriela C. M. Evangelista¹,
Patrícia C. Bergami-Santos¹ and José A. M. Barbuto^{1,2*}

¹Laboratory of Tumor Immunology, Department of Immunology, Institute of Biomedical Sciences, University of São Paulo, São Paulo, Brazil, ²Discipline of Molecular Medicine, Department of Medicine, Faculty of Medicine, University of São Paulo, São Paulo, Brazil

OPEN ACCESS

Edited by:

Daniela Santoro Rosa,
Federal University of São Paulo, Brazil

Reviewed by:

Susan Kovats,
Oklahoma Medical Research
Foundation, United States
Laura Santambrogio,
Albert Einstein College of Medicine,
United States

*Correspondence:

José A. M. Barbuto
jbarbuto@icb.usp.br

Specialty section:

This article was submitted to
Antigen Presenting Cell Biology,
a section of the journal
Frontiers in Immunology

Received: 31 August 2018

Accepted: 24 December 2018

Published: 21 January 2019

Citation:

Patente TA, Pinho MP, Oliveira AA,
Evangelista GCM,
Bergami-Santos PC and Barbuto JAM
(2019) Human Dendritic Cells: Their
Heterogeneity and Clinical Application
Potential in Cancer Immunotherapy.
Front. Immunol. 9:3176.
doi: 10.3389/fimmu.2018.03176

Dendritic cells (DC) are professional antigen presenting cells, uniquely able to induce naïve T cell activation and effector differentiation. They are, likewise, involved in the induction and maintenance of immune tolerance in homeostatic conditions. Their phenotypic and functional heterogeneity points to their great plasticity and ability to modulate, according to their microenvironment, the acquired immune response and, at the same time, makes their precise classification complex and frequently subject to reviews and improvement. This review will present general aspects of the DC physiology and classification and will address their potential and actual uses in the management of human disease, more specifically cancer, as therapeutic and monitoring tools. New combination treatments with the participation of DC will be also discussed.

Keywords: human dendritic cells, DC, monocyte-derived dendritic cells, mo-DC, cancer vaccines, cancer combination therapies

INTRODUCTION

Identified in mouse spleen for their peculiar shape and capacity to activate naïve lymphocytes (1–3), dendritic cells (DC) are considered the most efficient antigen presenting cells (APC) (3, 4), uniquely able to initiate, coordinate, and regulate adaptive immune responses. Though their ability to capture, process and present antigens is considered their main characteristic, their phenotypic heterogeneity is striking and very different consequences can come from their action. This review will present an overview of the main subpopulations of human DC described and will focus on their potential translational use.

OVERVIEW OF DENDRITIC CELLS IN THE IMMUNE SYSTEM PHYSIOLOGY

Human DC are identified by their high expression of major histocompatibility complex (MHC) class II molecules (MHC-II) and of CD11c, both of which are found on other cells, like lymphocytes, monocytes and macrophages (5–12). DC express many other molecules which allow their classification into various subtypes (Table 1). Although some of the DC subtypes were originally described as macrophages, DC and macrophages have distinct characteristics (13–15) and ontogeny, so that, currently, little doubt remains that they belong to distinct lineages (16–24).

Available online at www.sciencedirect.com

ScienceDirect

Current Opinion in
Immunology

Dendritic cells are what they eat: how their metabolism shapes T helper cell polarization

 Thiago A Patente^{1,2}, Leonard R Pelgrom¹ and Bart Everts¹


Dendritic cells (DCs) are professional antigen-presenting cells that play a crucial role in the priming and differentiation of CD4⁺ T cells into several distinct subsets including effector T helper (Th) 1, Th17 and Th2 cells, as well as regulatory T cells (Tregs). It is becoming increasingly clear that cellular metabolism shapes the functional properties of DCs. Specifically, the ability of DCs to drive polarization of different Th cell subsets may be orchestrated by the engagement of distinct metabolic pathways. In this review, we will discuss the recent advances in the DC metabolism field, by focusing on how cellular metabolism of DCs shapes their priming and polarization of distinct Th cell responses.

Addresses

¹ Department of Parasitology, Leiden University Medical Center, Leiden, The Netherlands

² Laboratory of Tumor Immunology, Department of Immunology, Institute of Biomedical Sciences, University of São Paulo, SP, Brazil

Corresponding author: Everts, Bart (b.everts@lumc.nl)

It is becoming increasingly clear that immune cell activation and function, including that of DCs, are coupled to, and underpinned by, profound changes in cellular metabolism [2,3]. There is a growing body of literature showing that acquisition of an immunogenic phenotype by DCs, characterized by enhanced migratory-capacity and overall T cell priming-capacity, is accompanied by, and dependent on a switch from oxidative phosphorylation (OXPHOS) to glycolysis [4*,5,6**,7–13]. In addition, more recent studies show that the ability of DCs to drive polarization of different Th cell subsets may be underpinned by engagement of distinct metabolic pathways. In this review, we will discuss these recent advances in the DCs metabolism field, by specifically focusing on how DC metabolism shapes the priming and polarization of distinct CD4⁺ T cell responses. For a discussion of the metabolic requirements of DCs to shape CD8⁺ T cell responses please refer to the following recent studies/reviews [14*,15**,16–18].

Current Opinion in Immunology 2019, 58:16–23

This review comes from a themed issue on **Antigen processing**

Edited by **Jose Villadangos** and **Justine Mintern**

<https://doi.org/10.1016/j.coi.2019.02.003>

0952-7915/© 2018 Elsevier Ltd. All rights reserved.

Metabolic regulation of MHC II-mediated antigen presentation and costimulation

A prerequisite for priming of CD4⁺ T cell responses is antigen presentation in the context of MHC II. TLR-driven upregulation of surface expression of MHC II by murine DCs has been shown to depend on glycolysis [4*,6**,19]. DC activation involves acidification of the lysosomal compartment, which is required for efficient generation of peptides for loading into MHC II and that is dependent on activity of ATP-driven proton pumps [20]. In addition, TLR-driven surface expression of MHC II by DCs is primarily thought to arise from redistribution of molecules from endocytic compartments through an energy-dependent process called lysosome tubulation [21,22]. Therefore, it is conceivable that glycolysis is required for efficient upregulation of surface expression of MHC II because it serves as a key source of ATP to support these two steps in antigen presentation (Figure 1). Mammalian target of rapamycin complex 1 (mTORC1) is an important nutrient sensor that promotes glycolysis, anabolic metabolism and translation [23]. Consistent with a role for glycolysis in regulation of MHC II expression, mTORC1 is activated in DCs upon TLR stimulation [14*] and is implicated in TLR-induced MHC II surface expression by DCs [19,24], through its ability to promote lysosome acidification and tubulation [24,25]. However, constitutive activation of mTORC1 in murine DCs has been shown to result in impaired MHC II expression, via mTORC1-driven suppression expression of complex transactivator (CIITA), a

Introduction

Dendritic cells (DCs) are professional antigen-presenting cells that play a crucial role in the development of adaptive immune responses by governing the priming and maintenance of CD4⁺ and CD8⁺ T cell responses. Classically, DCs reside in a quiescent state in peripheral tissues acting as sentinels of the immune system. Upon capturing pathogen-derived antigens or detecting tissue-derived danger signals, DCs become activated and migrate to draining lymph nodes (LNs). Herein, processed antigens are presented to T cells to initiate an adaptive immune response. Depending on the DC subset involved and the nature of the activation signal received, DCs control the priming and differentiation of CD4⁺ T cells into several distinct subsets including effector T helper (Th) 1, Th17, and Th2 cells, as well as regulatory T cells (Tregs) [1].



ARTICLE

LKB1 expressed in dendritic cells governs the development and expansion of thymus-derived regulatory T cells

Leonard R. Pelgrom¹, Thiago A. Patente¹, Alexey Sergushichev², Ekaterina Esaulova³, Frank Otto¹, Arifa Ozir-Fazalikhhan¹, Hendrik J. P. van der Zande¹, Alwin J. van der Ham¹, Stefan van der Stel¹, Maxim N. Artyomov³ and Bart Everts¹

Liver Kinase B1 (LKB1) plays a key role in cellular metabolism by controlling AMPK activation. However, its function in dendritic cell (DC) biology has not been addressed. Here, we find that LKB1 functions as a critical brake on DC immunogenicity, and when lost, leads to reduced mitochondrial fitness and increased maturation, migration, and T cell priming of peripheral DCs. Concurrently, loss of LKB1 in DCs enhances their capacity to promote output of regulatory T cells (Tregs) from the thymus, which dominates the outcome of peripheral immune responses, as suggested by increased resistance to asthma and higher susceptibility to cancer in CD11c^{ΔLKB1} mice. Mechanistically, we find that loss of LKB1 specifically primes thymic CD11b⁺ DCs to facilitate thymic Treg development and expansion, which is independent from AMPK signalling, but dependent on mTOR and enhanced phospholipase C β1-driven CD86 expression. Together, our results identify LKB1 as a critical regulator of DC-driven effector T cell and Treg responses both in the periphery and the thymus.

Cell Research (2019) 0:1–14; <https://doi.org/10.1038/s41422-019-0161-8>

INTRODUCTION

Dendritic cells (DCs) form a central link between innate and adaptive immunity and are crucial for initiation and regulation of T cell responses both under inflammatory conditions as well as during steady state. DCs are also key regulators of immune homeostasis and maintenance of immune tolerance by governing the development of regulatory T cells (Tregs). Tregs can be induced in the thymus, referred to as thymic-derived Tregs (tTregs), as well as in the periphery (pTregs) from naive T cells.¹ tTregs are characterized by a TCR repertoire that predominantly recognizes self-antigens and are important to maintain self-tolerance and to prevent auto-immunity.² pTregs, on the other hand, are thought to primarily govern tolerogenic responses against foreign antigens and microbes.³ Whereas the mechanisms through which pTregs are induced in the periphery by DCs are fairly well characterized,⁴ the pathways through which DCs control tTreg development and homeostasis are still poorly defined.

There is a growing appreciation that activation and effector function of immune cells, including that of DCs, are dependent on reprogramming of intracellular metabolic pathways.^{5,6} Primarily in vitro studies have shown that an immunogenic phenotype of DCs induced by Toll-like receptor (TLR) activation depends on a glycolysis-driven anabolic program,^{7,8} while a more catabolic type of metabolism is linked to quiescent and tolerogenic DCs, characterized by increased fatty acid oxidation and mitochondrial oxidative phosphorylation (OXPHOS).^{7,9,10} However, to what extent catabolic vs. anabolic metabolism of DCs regulates the balance between tolerogenic and immunogenic properties of DCs under physiological conditions, remains to be determined.

The tumor suppressor liver kinase B1 (LKB1, encoded by *Stk11*) is a bioenergetic sensor that controls cell metabolism and growth.

LKB1 has several downstream targets, but it is most well known for being a key upstream activator of AMP-activated Kinase (AMPK). Under low intracellular ATP levels, as a result of insufficient oxygen and/or nutrient availability to fuel mitochondrial OXPHOS and glycolysis to generate ATP, LKB1 phosphorylates AMPK. This allows AMPK to activate catabolic mitochondrial metabolism and to suppress anabolic sugar and lipid metabolic pathways to conserve energy and restore cellular bioenergetic homeostasis.¹¹ The role of LKB1 as a tumor suppressor has been well appreciated as germline mutations in *Stk11* are responsible for the inherited cancer disorder Peutz-Jeghers Syndrome¹² and as LKB1 is commonly mutated in various types of cancer.¹³ More recently a picture is emerging that LKB1 also plays a key role in regulation of the immune system. For example, LKB1 was shown to be required for haematopoietic stem cell maintenance^{14,15} and T cell development in the thymus.¹⁶ It is also crucial for metabolic and functional fitness of Tregs^{17,18} and can dampen pro-inflammatory responses in macrophages.¹⁹ However, the physiological role of LKB1 in regulating metabolic and functional properties of DCs has not yet been explored.

We here report that loss of LKB1 in DCs results in disruption of mitochondrial fitness and enhanced immunogenic properties of these cells in vivo. Surprisingly, however, loss of LKB1 also greatly enhances the capacity of CD11b⁺ DCs in the thymus to promote the generation of functional Tregs, through enhanced mTOR signalling and phospholipase C β1-driven CD86 expression. Our findings reveal a central role for LKB1 in DC metabolism and immune homeostasis, as it — depending on the context — acts as a critical brake on the immunogenic and tolerogenic properties of DCs.

¹Department of Parasitology, Leiden University Medical Center, Leiden, The Netherlands; ²Computer Technologies Department, ITMO University, Saint Petersburg, Russia and ³Department of Pathology and Immunology, Washington University School of Medicine, St. Louis, USA





Correspondence: Bart Everts (b.everts@lumc.nl)

Received: 8 November 2018 Accepted: 8 March 2019
Published online: 02 April 2019

ORIGINAL RESEARCH



Frequency determination of breast tumor-reactive CD4 and CD8 T cells in humans: unveiling the antitumor immune response

Mariana Pereira Pinho ^a, Thiago Andrade Patente ^a, Elizabeth Alexandra Flatow ^a, Federica Sallusto^{b,c}, and José Alexandre Marzagão Barbuto ^a

^aDepartment of Immunology, Institute of Biomedical Sciences of the University of Sao Paulo, Sao Paulo, Brazil; ^bInstitute for Research in Biomedicine, Faculty of Biomedical Sciences, Università della Svizzera italiana, Bellinzona, Switzerland; ^cInstitute of Microbiology, ETH Zurich, Zurich, Switzerland

ABSTRACT

As cancer immunotherapy gains importance, the determination of a patient's ability to react to his/her tumor is unquestionably relevant. Though the presence of T cells that recognize specific tumor antigens is well established, the total frequency of tumor-reactive T cells in humans is difficult to assess, especially due to the lack of broad analysis techniques. Here, we describe a strategy that allows this determination, in both CD4 and CD8 compartments, using T cell proliferation induced by tumor cell-lysate pulsed dendritic cells as the readout. All 12 healthy donor tested had circulating CD4 and CD8 tumor cell-reactive T cells. The detection of these T cells, not only in the naïve but also in the memory compartment, can be seen as an evidence of tumor immunosurveillance in humans. As expected, breast cancer patients had higher frequencies of blood tumor-reactive T cells, but with differences among breast cancer subtypes. Interestingly, the frequency of blood tumor-reactive T cells in patients did not correlate to the frequency of infiltrating tumor-reactive T cells, highlighting the danger of implying a local tumor response from blood obtained data. In conclusion, these data add T cell evidence to immunosurveillance in humans, confirm that immune parameters in blood may be misleading and describe a tool to follow the tumor-specific immune response in patients and, thus, to design better immunotherapeutic approaches.

ARTICLE HISTORY

Received 15 January 2019
Revised 21 March 2019
Accepted 7 April 2019

KEYWORDS

Cancer Immunosurveillance;
Tumor-specific
T lymphocytes; Tumor-
infiltrating lymphocytes;
T cell repertoire; Dendritic
cell



Introduction

Cancer is a disease of one's own cells that acquire characteristics that allow tumor progression, due to the accumulation of mutations and protein expression changes.¹ These protein modifications give rise to a number of different antigens that have the potential to be recognized by T cells,² a phenomenon that is central to the development of specific immune responses. Today, the ability of the immune system to recognize tumor cells through the presence of T cells that are specific for different tumor antigens is well acknowledged, and is a fundamental concept used in the development of new immunotherapeutic approaches.³ Indeed, a number of studies have shown, in humans, the existence of both CD4 and CD8 T cells specific for mutated and non-mutated tumor-associated antigens.^{4,5} Not surprisingly, since T cell receptor (TCR) generation is random and independent of presence or exposure to antigens,⁶ tumor-specific T cells are found also in healthy individuals.⁷

The presence of tumor-specific T cells has been shown to affect patient prognosis and the response to therapy, even for non-immunological treatments.⁸ Thus, tracking the T cell response against the tumor during the course of the disease and therapy is becoming an urgent need, since

it can be a powerful tool to improve personalized approaches to treatment. However, although the presence of T cells that recognize certain tumor antigens can be measured using multimers of major histocompatibility complex (MHC) molecules, the construction of multimers for all possible antigens in a tumor is not possible. Broader methods usually used consist of tumor-specific T cell cytotoxicity evaluation or cytokine production (like IFN- γ ELISPOT) as readouts of specificity. Although valid specially for the CD8 compartment, these strategies restrict the evaluation to T cells that have specific cytokine-secretion patterns or that are able to kill tumor cells.

Thus, considering these challenges to assess the total frequency of tumor-reactive T cells in humans,⁹ we developed a strategy to determine the frequency of tumor-reactive CD4 and CD8 T cells. Sallusto's group has described a technique that allows the quantification of antigen-specific T lymphocytes, by generating T cell libraries through non-specifically expanding and challenging T cells with antigen-presenting cells (APC) loaded with the antigens of interest.¹⁰ Here, we include modifications that would allow this quantification in the cancer setting, where antigen-specific T cells may have low antigen affinity due to their resemblance to self-antigens,¹¹ and/or may be exhausted,¹² thus, decreasing their ability to proliferate. Accordingly, we chose monocyte-derived

CONTACT José Barbuto  jbarbuto@icb.usp.br  Immunology Department of the Institute of Biomedical Sciences, University of Sao Paulo, Avenida Prof. Lineu Prestes, 1730. CEP05508-000, Sao Paulo, SP, Brazil

© 2019 Taylor & Francis Group, LLC